UNIVERSITY OF THE WITWATERSRAND

JOHANNESBURG

UNIVERSITY OF THE WITWATERSRAND, JOHANNESBURG

FACULTY OF BUILT AND ENVIRONMENT

A thesis submitted to the Faculty of the Built and Environment, University of the Witwatersrand, Johannesburg, in fulfilment of the requirements for the degree of Doctor of Philosophy

Discrimination between Nearby and Direct Lightning Strikes to a Long Operational Medium Voltage line to Assist in the Determination of the Basic Insulation Level (BIL)

Willem Jacobus Dirkse van Schalkwyk

Johannesburg 2022

DECLARATION

.'

I declare that this thesis is my own, unaided work. It is being submitted for the Degree of Doctor of Philosophy at the University of the Witwatersrand, Johannesburg. It has not been submitted before for any degree or examination at any other University.

____

(Signature of candidate)

___15____________day of __November____2022__________at__Bloemfontein_

CONFERENCES AND JOURNAL PAPERS

Papers presented and published as journal papers:

W. J. Dirkse van Schalkwyk, C. Gomes and J. Van Coller, "A New Method to Measure the Lightning Performance of a Long Medium Voltage Line," in *Proceedings of IEEE Africon 2021*, Arusha, Tanzania, September 2021. Not journal

Papers presented:

W. J. Dirkse van Schalkwyk, C. Gomes, J. M. van Coller and A. A. Beutel, "Discrimination between Nearby and Direct Lightning Strikes to a Long Operational Medium Voltage line to Assist in the Determination of the Basic Insulation Level (BIL)," in *The 8th EPPEI Annual Student Workshop Virtual Conference*, Durban, South Africa, 11 - 12 November 2021.

Journal papers re-submitted:

W. J. Dirkse van Schalkwyk, C. Gomes and J. M. van Coller, "A New Method to Distinguish between Nearby and Direct Lightning Strikes on Long Operational Medium Voltage Lines" to SAIEE Africa Research Journal. Did received reviewer reports and submitted an updated Journal paper

Papers were submitted but the conference was cancelled due to Covid 19:

W. J. Dirkse van Schalkwyk, C. Gomes and J. M. van Coller, "Distinguishing between Indirect Lightning Faults, Direct Lightning Faults and Weather-Related Faults on an Operational Medium Voltage Line in South Africa" 35th International Conference on Lightning Protection, Colombo, Sri Lanka, 30th August to 4th September 2020.

Papers and journal papers submitted and awaiting conference and journal paper publication:

W. J. Dirkse van Schalkwyk, C. Gomes and J. M. van Coller, "A Reduction in the lightning-induced overvoltage amplitude for an energized MV power line with attached line equipment", South African Universities Power Engineering Conference Durban, South Africa, 25 -27 January 2022. Not journal paper

ABSTRACT

The lightning performance of a Medium Voltage (MV) line needs to be divided into two categories: lightning performance due to nearby lightning and direct lightning strikes. A better nearby lightning performance requires a higher Basic Insulation Level (BIL) while the direct lightning performance requires a lower BIL to minimize equipment failure. The electromagnetic coupling models for calculating the Lightning Induced Overvoltage (LIOV) on a line are complicated and reliant on accurate input data. Therefore, short floating lines (< 3 km) were used to calculate the line's lightning performance. The models were then verified with LIOV measurements on these short floating lines and the results were normalized to estimate the lightning performance of long operational lines. These estimations for long lines could never be verified due to the complexity of calculations and the cost and logistics of equipment to do measurements on long operational lines.

A new methodology to measure the lightning performance of a long operational line was developed and verified. The obstacles such as the long line length, the changing soil resistivity, the lightning channel properties and the rapid attenuation of the LIOV along the energized line have been used as an advantage in the new method. The finite soil conductivity was used as an advantage to distinguish between nearby lightning and direct lightning strikes while the power frequency current was used to determine whether the LIOV exceeded the line BIL and caused a line fault.

An existing electromagnetic coupling computer model, the ATP-EMTP, was verified with the existing ERM using the same input data. The ATP-EMTP model was then extended to include the equipped long MV line. There was no existing model or measurements to which the results could be compared to. Actual nearby lightning and direct lightning strikes of which the termination point was known were used to verify the new methodology. A significant size database (consisting of 38 675 lightning flashes and 1 155 line faults over two years) was used to evaluate the IEEE Std 1410-2010 estimated lightning performance of the long line.

ACKNOWLEDGEMENTS

I would like to express my gratitude to the Faculty of Engineering and the Built Environment, University of the Witwatersrand, Johannesburg for providing me with the scholarship to undertake this PhD program and also for the research facilities

I am grateful to ESKOM Power Plant Engineering Institute (EPPEI)-HVAC for financial support

I wish to acknowledge my study leaders Prof Chandima Gomes and Dr John van Coller, who gave me enormous support and provided valuable guidance during my research. They also made it possible for me to present my work at several international conferences.

I am very grateful to my colleagues at Eskom Holdings SOC for their contribution to conducting experiments and retrieving data.

I would also like to thank the local power utility – Eskom Holdings SOC for the research opportunity and funding of my studies.

I would like to thank the Journal of Geophysical Research, IEEJ Transactions, Elsevier and IEEE Transactions for Permission obtained to use pictures published by them.

I also thank specific paper owners that permitted me to use pictures in their papers as references.

CONTENTS

LIST OF FIGURES

LIST OF TABLES

GLOSSARY

AC	Alternating Current
ATP	Alternative Transient Program
BIL	Basic Insulation Level
BG	Bruce Golde (model)
C	Capacitance
CSIR	Council of Scientific and Industrial Research
CFO	Critical flashover voltage
DE	Detection efficiency
DNUTL	Dynamic Non-Uniform Transmission Line
E	Electric field
EID	Engineering Investigation Department
EMTP	Electromagnetic Transients Program
EPRI	Electric Power Research Institute
ERM	Extended Rusck Model
ESO	Elevated Strike Object
FALLS	Fault Analysis and Lightning Location System
FSOU	Free State Operating Unit
GFD	Ground Flash Density
GPS	Global Positioning System
GLD	Ground lead disconnect (of a surge arrester)
GWh	Gigawatt hour
H	Magnetic field strength
HV	High Voltage
HEM	Hybrid Electromagnetic Model
I	Current
ICLRT	International Centre for Lightning Research and Testing
IEEE	Institute of Electrical and Electronics Engineers
IEC	International Electrotechnical Commission
kWh	Kilowatt-hour
L	Inductance
LDN	Lightning Detection Network
LGC	lightning generated current
LGV	lightning generated voltage (due to a direct lightning strike)
LIOV	lightning-induced overvoltage (due to a nearby lightning strike)

LLS	Lightning Location System
LPF	Lightning Proof Fuse
LSP	Lightning strike point
MULS	Master, Uman, Lin and Standler (model)
MOV	Metal Oxide Varistor
MTLE	Modified Transmission Line model with Exponential current decay with height
MTLL	Modified Transmission Line model with Linear current decay with height
NEC	Neutral earthing compensator
NETFA	National Electrical Test Facility
OGW	Overhead ground wire
PQ	Power Quality
R	Resistance
RVZ	Rouxville Zastron
SALDN	South African Lightning Detection Network
SANS	South African National Standard
SCADA	Supervisory Control and Data Acquisition
TL	Transmission Line
MTLL	Modified Transmission Line with Linear current decay model
MTLE	Modified Transmission Line with Exponential current decay model
TCS	Travelling Wave Current Source (model)
V	Voltage
ZnO	Zinc Oxide (surge arrester)

1 INTRODUCTION

Lightning can cause between 50% and 80% [1] [2] [3] [4] of equipment failures as well as disturbances of the voltage and current as shown in Figure 1.1. An unscreened MV line's lightning performance is compromised by lightning nearby and direct to the line. The higher the line's BIL is, the more lightning energy (charge) is contained in the resultant LIOV that travels along the line to the equipment connected to the line. Except for MV equipment failures [5] due to voltage surges as shown in Figure 1.2 and Figure 1.3, line faults caused by lightning flashovers result in voltage dips [6] [7] [8] that can also damage equipment on the low voltage network [9]. On the contrary, the lower the BIL is, the more faults caused by LIOVs due to nearby lightning strikes that exceed the BIL could occur as shown in Figure 1.4. To find an optimal BIL for the line, it is therefore necessary to clearly distinguish between faults caused by nearby lightning and direct lightning strikes when evaluating the line's lightning performance.

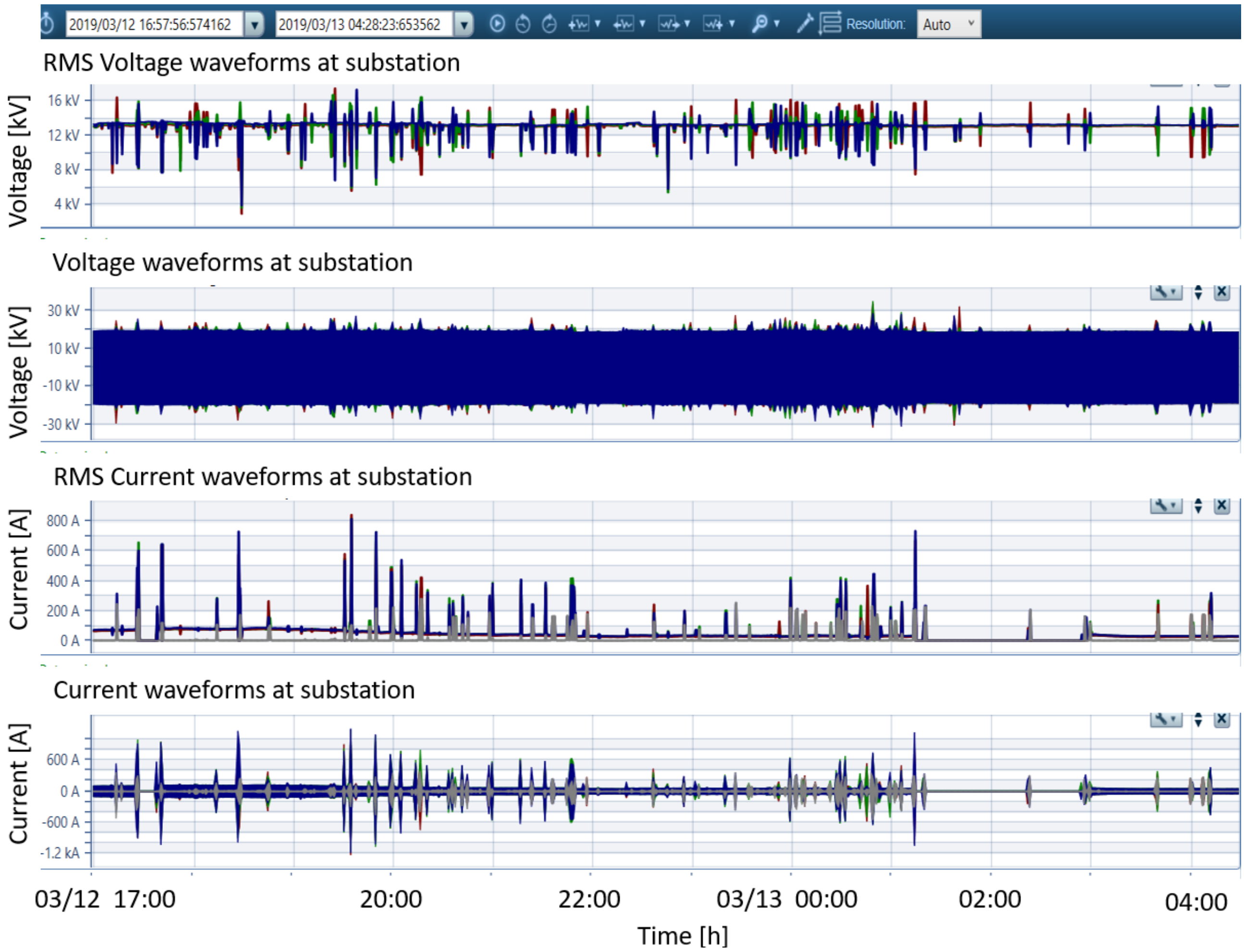

Figure 1.1 A recording of the voltage and current at the feeder substation. The recording at the top shows numerous voltage disturbances and the bottom recording several faults caused during a lightning storm that lasted for 11 hours.

Figure 1.2 Lightning either ignites or splinters (if the lightning strike exceeds 7 kA [10]) the wood. The insulators of the charcoaled pole were tested to be in perfect order.

The Lightning Generated Voltage (LGV) on the line due to direct lightning strikes exceeds the BIL in 98% of the cases [11] [12] [13], causing line faults and possible equipment failure. LIOV amplitudes due to nearby lightning strikes depend on many factors, mainly the lightning channel and lightning strike current parameters, the distance between the nearby lightning strike and the line, the line characteristics, equipment connected to the line and line geometry, the soil parameters and the environment. The LIOV amplitude due to nearby lightning strikes can either be calculated or measured to determine whether it exceeds the line's BIL. Previous research mostly used short (< 3 km) floating lines to increase accuracy, simplify measurements and calculation of LIOVs. The results were then normalized to derive the lightning performance of a long operational line.

Figure 1.3 Surge arrester failures resulted in transformer failures at one of the customer Network Centres.

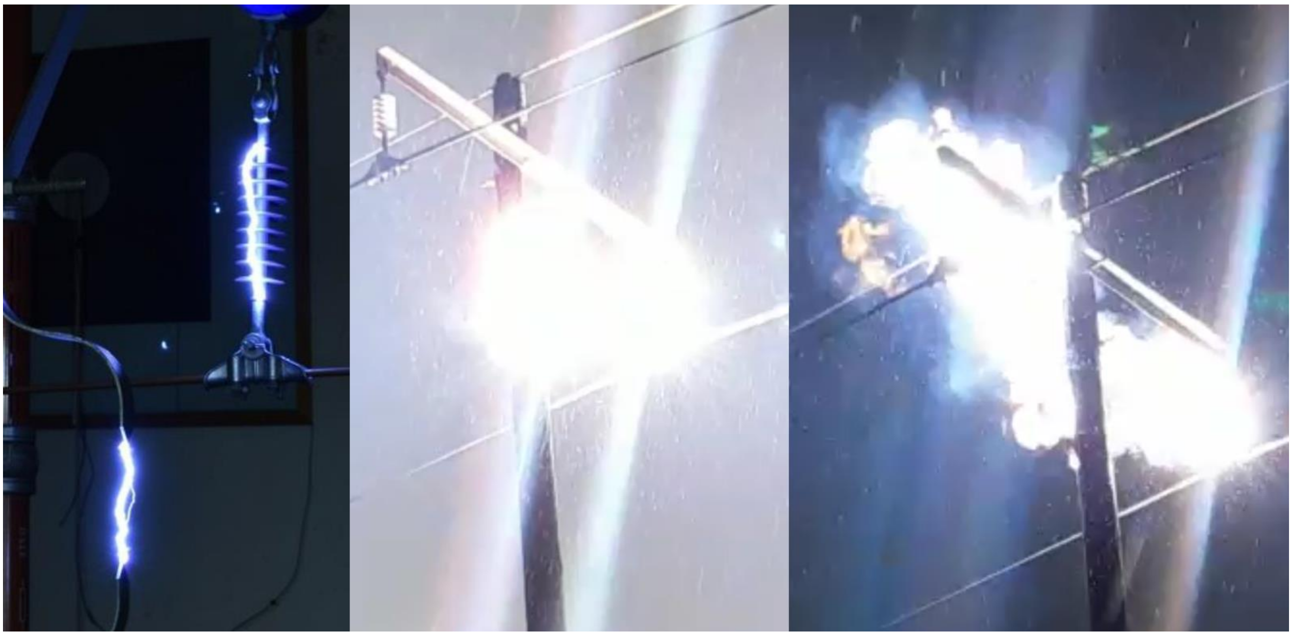

Figure 1.4 A LIOV that exceeds the BIL will flash over to earth (left). A power frequency fault will then follow (middle) along the spark caused by lightning and if not isolated in time can be developed into a three-phase fault (right).

Calculation and simulations to determine the LIOV on the line are very complex and lengthy, even if the section of line is short and sometimes numerous assumptions and approximations had to be made. These assumptions and approximations will compromise the accuracy of this research significantly. The energized line in this research is 714 km long, had many branches, had 234 transformers with sets of arresters and the line geometry and soil conductivity changed significantly along the line. Other input data parameters to the models such as the distance between the nearby lightning strike termination point and the line were not known reliably enough and some of the lightning channel parameters (tortuosity and inclination) were unknown. The LIOV amplitude and so the nearby lightning performance of the line in this research can therefore not be determined reliably by calculation or simulation.

Cameras [14] [15] and the position of lightning-triggering rocket launchers [16] were used in previous research to determine the lightning strike earth termination point. Rogowski coils, as well as a capacitor and resistor dividers connected to high sampling rate recorders that were triggered by the LIOV, were installed on these test lines at the points closest to the nearby lightning strike earth termination point. The LIOV amplitude on the line is the highest at the point closest to the nearby lightning strike and it is therefore the point with the highest probability of the LIOV exceeding the line BIL, causing a line flashover that results in a power frequency fault. As the amplitude and the shape of the LIOV attenuate rapidly over a short distance, it is of utmost importance to do the measurement as close as possible to the point on the line closest to the nearby lightning strike. Due to the length of the line in this research, the cost and logistics of the number of measuring equipment needed would be too high and were also not available.

Previous research [17] on the lightning performance due to nearby lightning strikes to an MV line in operation used three different methods (different combinations of protection operation, LDN data and the LIOV-EMTP software) that delivered three significant different answers and it could not be compared to the IEEE standard 1410-2010 estimations. It was an indication that the current approach to calculation and measurements of the LIOV to determine the nearby lightning performance of long operational lines was not possible due to the complexity and lack of accurate input data.

A new approach to measure the actual lightning performance that distinguishes reliably between nearby lightning and direct lightning strikes to long operational lines was followed. A new methodology and model, where it was only necessary to compare the polarity of the LIOV and Lightning Generated Current (LGC) on the line with the lightning current polarity obtained from the

LDN to distinguish between nearby lightning and direct lightning strikes to the line. The rigorous verified model proves that the polarity of the LIOV on the line change after about 250 m due to the finite soil conductivity and becomes opposite to the lightning channel current polarity. To determine whether the LIOV exceeded the BIL, the power frequency fault current was used to determine a line flashover (which does not always result in breaker operation). The line length that would have made the research impossible, the changing soil conductivity and the complexity that the power frequency energization would have added to the LIOV amplitude, were then used to the advantage of this research. Faults during a storm could then easily be categorized as faults due to nearby lightning, direct lightning strikes or weather-related faults where the moisture content in the lightning storm caused insulation breakdown.

The new methodology consisted of measuring the LIOV and LGC polarities on the line at the feeder substation and comparing it to the corresponding lightning return stoke polarity as captured in the LDN. A direct lightning strike will inject a charge into the line of the same polarity as that of the cloud (and the lightning channel current) because there was no soil directly involved between the lightning strike termination point and the line. The charge will dissipate to earth through flashovers, surge arresters, other equipment and a portion will dissipate to earth through the Neutral Earthing Compensator (NEC) at the feeder substation. As the LIOV attenuate about 40% of the time to an amplitude that cannot trigger an instrument anymore, the resultant LGC due to the charge that dissipates to earth through the NEC are measured by a continuous high sampling rate (400 kHz) specially configured Quality of Supply (QoS) recorder (logger). If the LGC polarity was the same as the corresponding lightning return-stroke current polarity captured by the LDN, it will indicate that it was a direct lightning strike to the line.

The ATP-EMTP model [18] was then extended to include the energized long RVZ line and it proved that at a distance further than 250 m from a nearby lightning strike the polarity of the resultant LIOV was of opposite polarity to the lightning channel if the ground conductivity was finite. Traditionally the LIOV was measured to detect lightning activity, but the LIOV measurement was difficult to see as it was superimposed on the 22 kV Alternating Current (AC), However, the LGC on the NEC zero-sequence current (with a nominal voltage of zero Ampere) recording was much easier to notice. If the polarity of the LGC superimposed on the zero-sequence (common mode) current was opposite to the polarity of the lightning return-stroke current recorded by the LDN, it indicated that the lightning strike was nearby to the line. An AC fault current at the same time would indicate that the LIOV exceeded the line BIL and caused a line fault. An AC fault current during a storm without the LDN recording a lightning strike (within ± 10 ms) was categorized as a fault due to insulation failure caused by other elements of the storm (wind or moisture). An accurate lightning performance database over two years was then normalized and compared to the IEEE Std 1410-2010 lightning performance estimation [12].

1.1 Problem statement

The following problem statements were identified:

1. The methods to detect and record LIVs and the lightning termination point used for short lines cannot be used for long lines because it is not practical to install a large number of cameras, recorders and current sensors as well as resistor dividers.
2. The location accuracy of lightning detection networks is not consistent and varies between zero and 500 m. Thus, the data it provides cannot be used to determine whether the lightning was nearby or was a direct lightning strike to the line.
3. The LIOV that is key in measuring lightning activity on short lines cannot be used on long lines as the LIOV is attenuated as it propagates along the line to such an extent that it is no longer measurable.
4. The earth conductivity, environmental conditions and BIL vary along the line and therefore a long line's lightning performance prediction cannot be extrapolated from a short line's lightning performance.
5. With the above in mind, a new method which is independent of the requirements mentioned in PS 1 and the locational inaccuracy of the LDN is needed.

1.2 Objectives of the research

To address the above problem statements, the following objectives are proposed:

1. To develop a model that can support measurements of zero-sequence currents to distinguish between nearby and direct lightning strikes to a long MV line
2. To develop a measurement method to verify the model in Objective 1
3. To develop a statistically significant lightning performance database of an MV line using the model in Objective 1 and the measurement method in Objective 2
4. To use the database to compare the actual lightning performance of a long operational MV line with the IEEE standard 1410-2010 predicted lightning performance for that line

1.3 Research questions

1. Extending the existing theoretical models of the lightning-induced voltages on MV lines, can a model be developed and verified that uses the polarity of the lightning channel current obtained from the LDN and the polarity of the LGC superimposed on the zero-sequence current to discriminate between nearby lightning and direct lightning strikes to a long MV line?

2. Using the measured lightning performance data and the developed theoretical model, can the deficiencies of the IEEE standard 1410-2010 estimation method applied to a given long MV line be checked?

2 LIGHTNING PERFORMANCE OF MV LINES: A LITERATURE SURVEY

The lightning performance of a line is negatively affected when either nearby lightning strikes or direct lightning strikes to the line cause an insulation failure on a line that results in a power frequency flashover. There are also line faults due to other factors such as wind and moister present in a lightning storm that can be by mistake attributed to lightning-initiated faults. A literature survey of existing models to describe the lightning properties along the return-stroke channel and the coupling between the return-stroke current and the line was done. The purpose will be to determine the probability of these lightning strikes inducing a voltage on the line that exceeds the line BIL and whether these methods are also applicable to long operational power lines. A survey on modelling the lightning channel and the coupling between the lightning channel and the power line was done. The accuracy, assumptions and applicable limits of each model were studied. Limitations on actual measurements of magnetic fields, electric fields and induced voltages to verify the models were part of the survey. The success of attempts of previous research to apply these modelling and measurements to long operational lines were evaluated. Existing standards that estimate the lightning performance of an MV power line were surveyed as well.

A lightning discharge produces an electric field and a magnetic field. These fields in turn induce voltages and currents on nearby power lines. Figure 2.1 shows measured values [19] of the electric field, E, and the magnetic field strength, H, on a line two km from an 8 kA lightning strike.

The two most important models needed are a return-stroke model which specifies the current along the channel during the return-stroke phase and a coupling model to calculate the electromagnetic coupling between the lightning return-stroke channel and the line. The line construction (configuration) is modelled with many assumptions and approximations of the environment. Monte Carlo methods [20] [21] [22] [23] [24] [25] can be used to model the probability, point of termination and lightning parameters (amplitude, waveform).

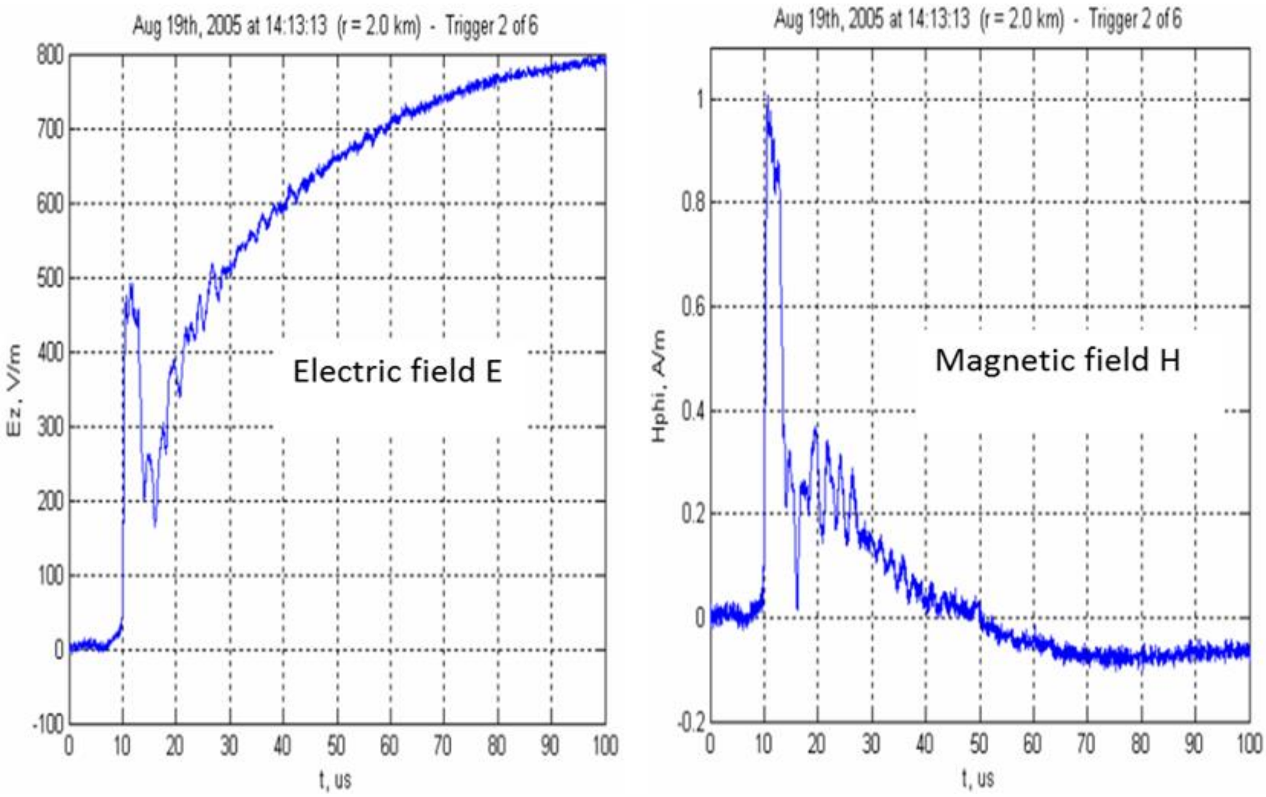

Figure 2.1 Electric and magnetic fields experienced by a line 2 km away from an 8 kA lightning strike [26]. *Permission obtained from the Journal of Geophysical Research 2007.*

Simulation of lightning in laboratories, triggered lightning and actual lightning experiments have been performed to verify the models and approximations. Laboratory lightning and triggered lightning experiments are best for deriving theoretical formulas for specific line configurations. Many of these experiments are done on de-energized lines to simplify and protect the measuring equipment. Although this can be used as a very necessary base for line design, it is practically influenced by a large number of different line and equipment configurations as well as environmental factors.

2.1 Definition of lightning current parameters

A definition of all the lightning parameters is given by SANS 62305-1 [27]. SANS adopted the IEC values. The lightning parameters of interest is shown in

Table 2.1 and in **Error! Reference source not found.**. The peak value and the rise time of the lightning surge current are important input parameters to electromagnetic coupling models for analysis purposes to determine the resultant LIOV on the line for a given line surge impedance.

Table 2.1 Lightning parameters of interest.

Parameter in Figure 2.2	Description
I_{10}	10% intercept along the stroke current waveshape
I_{30}	30% intercept along the stroke current waveshape
I_{90}	90% intercept along the stroke current waveshape
I_{100}	100% intercept along the stroke current waveshape
S_{30}	Instantaneous rate-of-rise of current at I_{30}
$S_{10/90}$	Average steepness through I_{10} and I_{90} intercepts
S_m	Maximum rate-of-rise of current along the wavefront
T_1	Front time
T_2	Time to half value
$T_{10/90}$	Equivalent linear wavefront duration derived from I_{100} /$S_{10/90}$

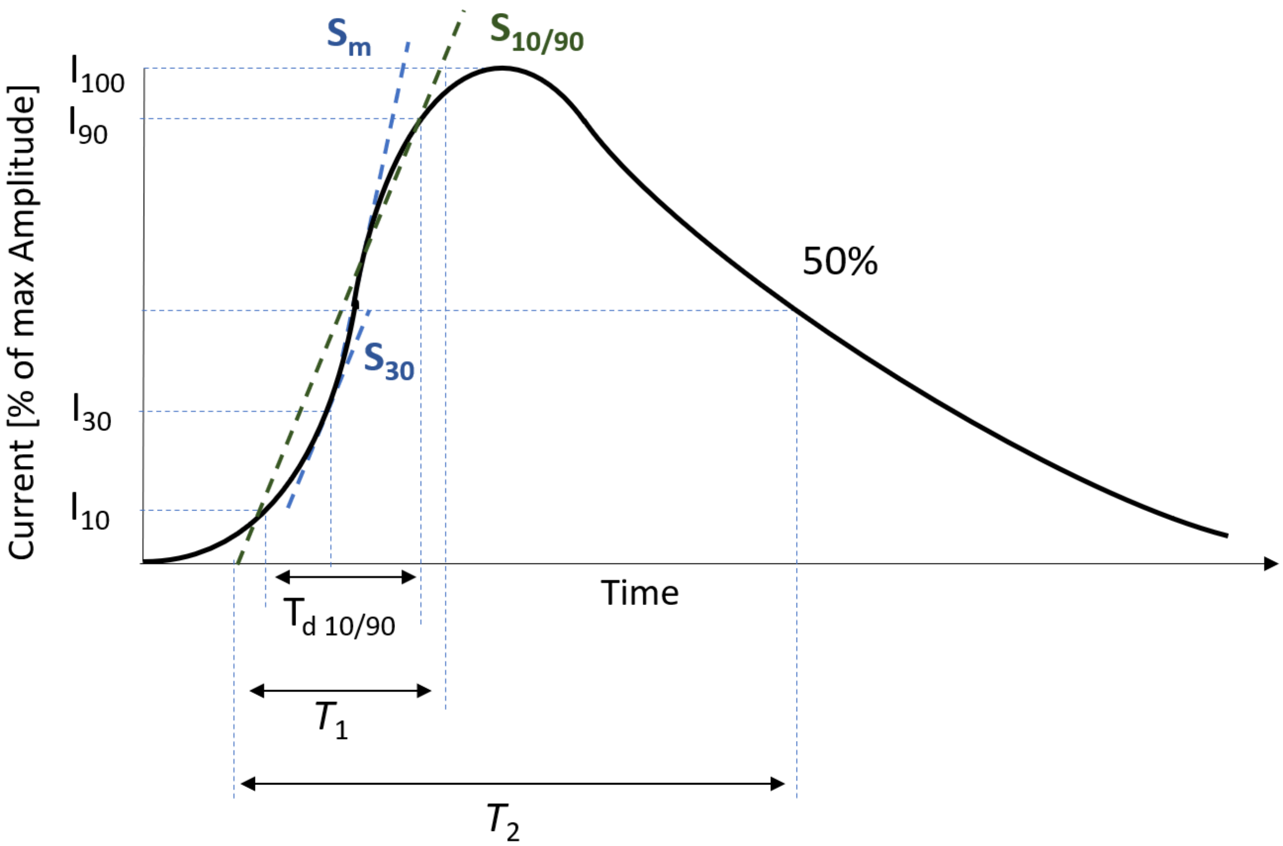

Figure 2.2 Important parameters of the lightning surge current.

According to SANS 62305-1, typical values for T_1 and T_2 of the current wave shapes are:

– for the first positive stroke: 10/350 µs,

– for the first negative stroke: 1/200 µs,

– for the subsequent negative stroke: 0,25/100 µs

Some authors [28] [29] added a factor to describe a nearby lightning strike and concluded that the mean rise-time of a subsequent stroke can be taken as 0.67 µs.

Anderson and Eriksson [30] did a study comparing their measurements with those of other researchers. They derived a formula to calculate the average rise-time for the first stroke as:

$$S_{30} = 3.2 I^{0.25} \qquad (1)$$

And for subsequent strokes as:

$$S_{30} = 6.9 I^{0.42} \qquad (2)$$

where, S_{30} = the wave front rise-time in kA/µs

I = the peak current amplitude in kA.

Calculations to determine the induced voltage amplitude of a lightning stroke are very dependent on the rise-time. For the worst-case scenario, the maximum rise-time for the first strokes in a flash can be determined as shown in Figure 2.3 [30]:

$$S_m = 3.9 I^{0.55} \qquad (3)$$

And for subsequent strokes:

$$S_m = 3.8 I^{0.95} \qquad (4)$$

A lightning flash consists of either one or more strokes. A lightning flash is defined [17] as a group of strokes that terminate on the ground within 1 second and are within a radius of fewer than 10 km. Furthermore, strokes with the same flash may not be further apart than 500 ms. Research done by Le Vine [31] shows that the lightning frequency spectrum ranges between 1 kHz and 1 GHz. The frequencies 124 kHz (mean value of 31.1 kA and 24.3 kA/μs first stroke) and 516 kHz (mean value of 12.7 kA and 39.9 kA/μs subsequent stroke) are recommended for first and subsequent strokes respectively [32] in cases where a single frequency is used for estimates. Power lines have a high surge impedance (about 350 Ω) that results in high surge voltage amplitudes when lightning currents are injected into the line. To do proper calculations, it is necessary to know the lightning return-stroke current parameters as well as the surge impedance of the line.

Usually, three steps are taken when calculating induced voltages on overhead lines, namely:

- the estimation of the spatial and temporal distribution of the current along the lightning channel,
- the calculation of the generated electromagnetic fields
- the coupling of the obtained fields with overhead conductors located near the lightning channel.

2.2 Propagation of current along the lightning channel

The lightning channel between the cloud and an Elevated Strike Object (ESO) on the ground can normally be seen during the return-stroke phase. The propagation of current along the channel depends on the channel conductance. Conductance is normally dynamic as the current propagates between the cloud and the ESO. Measuring points along the channel are defined as the distance from the earth – zero metres being on top of the ESO. According to [33] the current amplitude and its rise-time decrease closer to the cloud as shown in Figure 2.3. The lower the rise-time, the lower the current amplitude and the further the current dipole is from the line segment, the less the electric field strength and LIOV amplitude on the line become. This means that the coupling between the top of the lightning channel and the line is much less than the coupling between the lightning channel termination point on earth and the line.

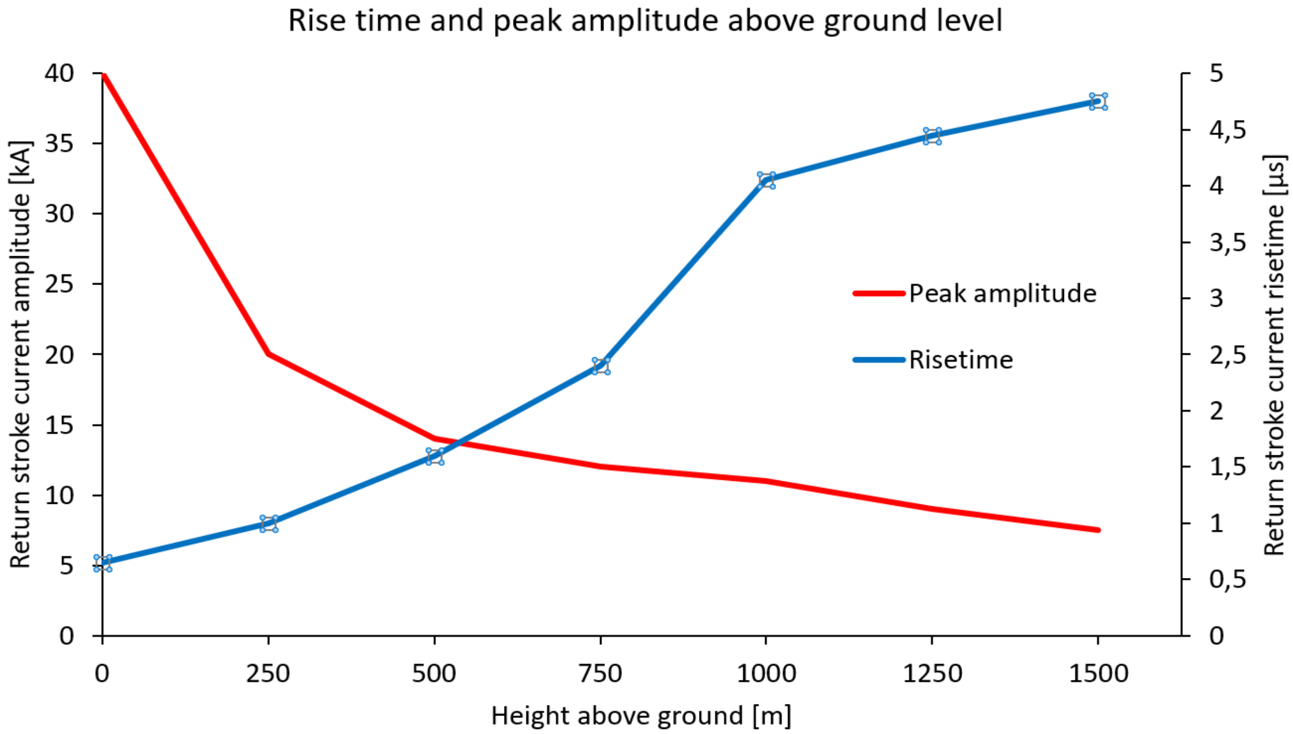

Figure 2.3 The current characteristics along the lightning channel. The return-stroke current amplitude and rise-time decrease as the height above ground increases.

Figure 2.4 shows a lightning strike nearby a line. Some models describing the lightning channel are listed on the right. The lightning strike channel is not straight and each segment or current dipole has a different coupling strength to each line segment. Most models assume the lightning strike to be straight and vertical to the ground to simplify calculations. Some electromagnetic coupling models between the lightning return-stroke and the line (Rusck, Chowdhuri, Agrawal and ERM) or computer coupling models (LIOV-EMTP, ATP-EMTP, Rusck-EMTP and LIV-ATP) that will be analysed later are also shown. It is important for this research that the electromagnetic coupling model includes the coupling between lossy ground and the line as the horizontal electric field component due to the ground becoming significant at some distance from the nearby lightning strike termination point. Most coupling models assume that the line is floating and some that the line is lossless to simplify the calculations. The line in this research was not floating and lossless and the ground had a finite conductivity, therefore an electromagnetic coupling model that included the electric field component due to the ground resistivity was chosen and was extended to include the ATP model of the research line.

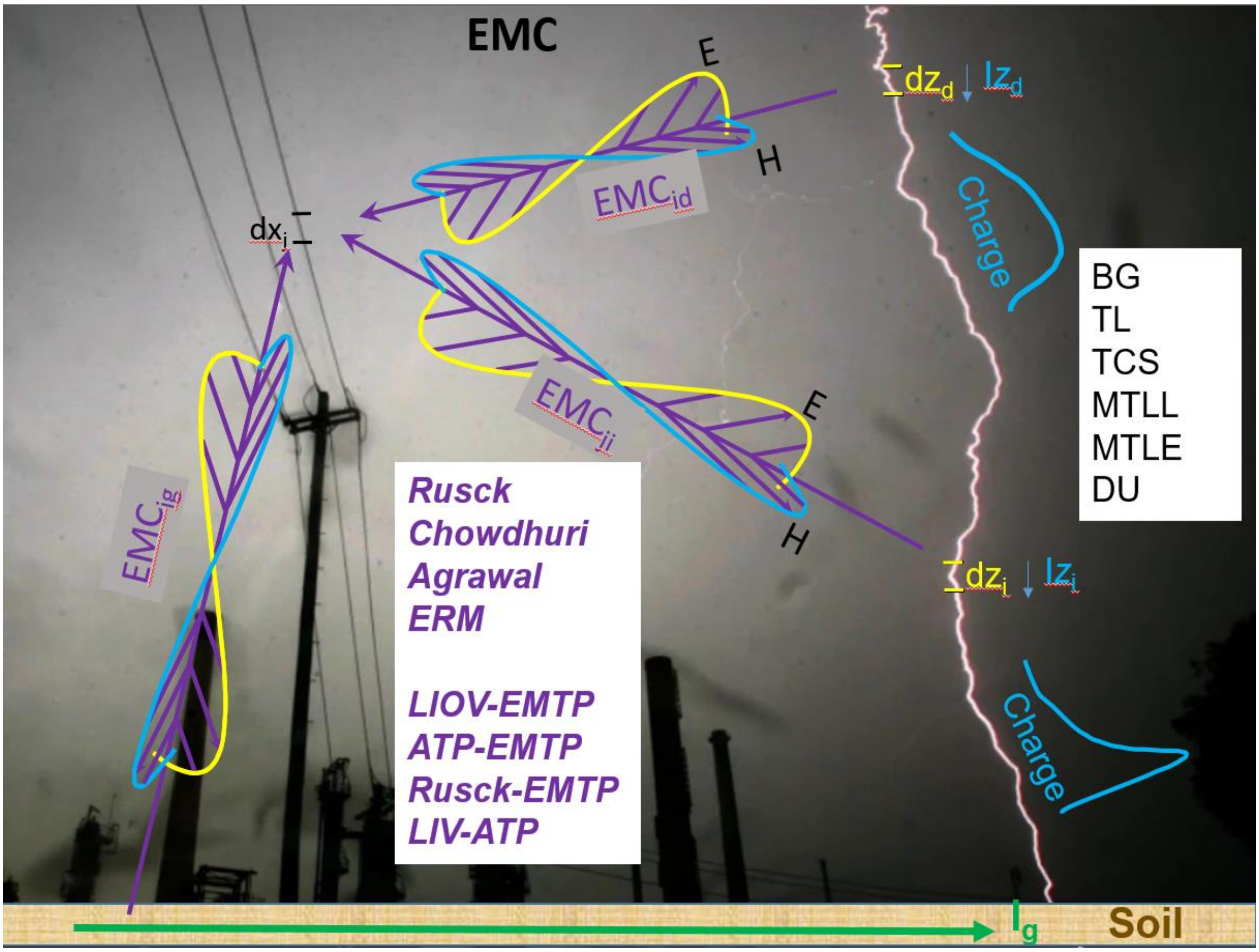

Figure 2.4 The coupling between a nearby line and a lightning return-stroke channel. Note that the lightning channel of the return-stroke is not straight in any way. On the right side is different return-stroke channel models, in the middle coupling models and below computer models that are based on the coupling models and returns stroke current models.

The propagation velocity of the current along the current channel is given by [34]:

$$V_f = \frac{c}{\sqrt{1+(W/I_p)}} \tag{5}$$

where Ip is the current peak value (in kA) and W is an empirical constant. According to Wagner [35], W = 230 kA. According to [36], the propagation speed of the current along the channel does not influence the current peak. The choice between these hypotheses will be important in a methodology where the LIOV was calculated to determine whether the LIOV exceeded the line BIL. The measured fault current at the substation will reveal whether the LIOV exceeded the line BIL in this research.

Knowledge regarding the lightning current propagation along the lightning channel is important to accurately model the coupling between the return-stroke and the ESO. Lightning channel models can be grouped into four different models [37]. These four models are Gas Dynamic models (mostly physical models), Engineering models, Distributed Parameter models (Transmission line models) and Electromagnetic models.

2.2.1 Gas Dynamic models for calculating the current along the channel

Different Gas dynamic models were created by Braginski [38], Hill [39], Krider [40], Plooster [41] and Borovsky [42] to mention some. These models are based on the radial evolution of a short segment of the lightning channel and its associated shock wave [43]. Some of these Gas Dynamic models were developed to be used in a laboratory to simulate spark discharges in the air [44]. Gas Dynamic models are useful to better understand the lightning energy balance and thunder generation mechanisms. These models do not include the longitudinal evolution of the lightning channel and usually ignore heating of the air around the lightning channel, the corona sheath and the electromagnetic skin effect and will therefore not be further investigated for this research.

2.2.2 Electromagnetic models

Existing electromagnetic models created by Moini [45], Baba [46] and Chen [47] to name some simulated the electromagnetic fields produced by the lightning current and induced voltages and currents on other objects. They are based on Maxwell's equations which are solved using numerical techniques such as the method of moments or the finite-difference method. The basic model consists of a perfectly conducting ground, a vertical wire with a 30 mm radius and a 10 m current source between the wire and ground [48]. Figure 2.5 is an illustration of the model configuration.

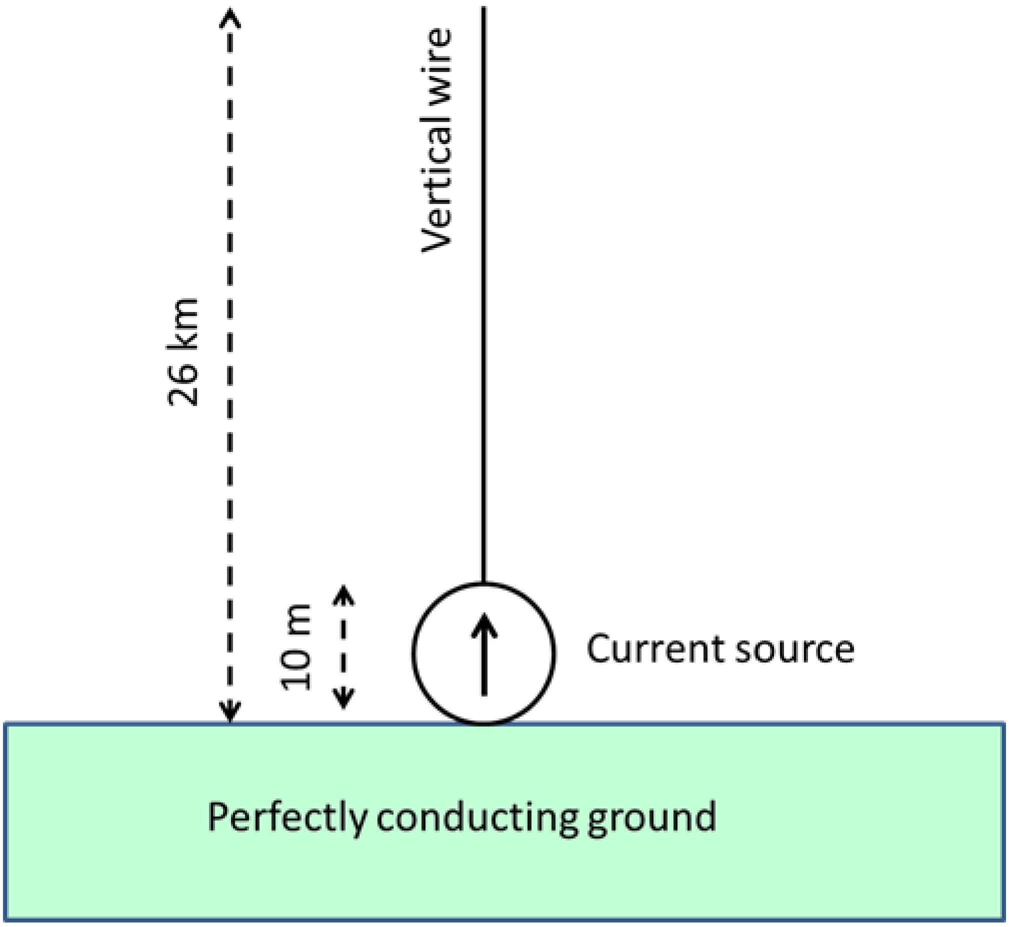

Figure 2.5 The basic Electromagnetic model [48].

There are generally six types [48] or different sets of values for the speed of the current, the vertical wire (inductance and resistance) and the dielectric medium (permittivity and permeability) surrounding the wire. The configuration of type six differs from the other types as it consists of two vertical wires with a radius of 20 mm each and that is 30 m apart.

It is not necessary to employ a model for the field propagation effects (such as the Cooray-Rubenstein formula), nor a model for the field to conductor coupling (such as the Agrawal et al formula) when using the Electromagnetic model - which is an advantage. However, the calculations are more difficult.

In conclusion, for practical application, all the models are very dependent on accurate assumptions of the soil conductivity, lightning parameters and their actual geographical position, dielectric properties of the surrounding media and other objects close to the object of interest.

2.2.3 Engineering models for calculating the current along the channel

Engineering models [49] [50] relate the current propagation along the vertical channel to the electromagnetic field at various distances for an assumed spatial-temporal distribution of the current along the channel. The line has been considered grounded on one end. These models also make use of the strengths of the electromagnetic, gas dynamic and distributed circuit models. Some inputs to these models are dependent on experimental data.

The Engineering models can further be categorized into three types namely the current propagation, current generation and current dissipation models. The current propagation model is used by many researchers to construct different transmission line models. It considers the steamer as a current from earth to the cloud through a lossless path that is created by the stepped leader. The current generation models take the effect of corona into account. It is observed in the current dissipation model that if the travel current pulse magnitude through the transmission line is lesser than the corona threshold value, the propagation is assumed to be lossless.

One of the current propagation models, the Transmission Line model, was used in the research. The lightning channel is considered to be a transmission line with distributed R-L-C parameters in this model. Each of the line parameters representing the return channel is a function of both space and time [51] [52]. This approach is representable in EMTP.

There are several transmission line return-stroke models. Some of them are:

- lossless transmission line (TL) [53],
- modified transmission line model with linear current decay with height (MTLL) [54]
- modified transmission line model with exponential current decay with height (MTLE) [55].

The TL and the Bruce Golde (BG) [56] models are similar and assume that the lightning channel current has the same amplitude along the channel. The TL, MTL and MTLL models are classified as the transmission line type models while the TCL, BG and Diendorfer and Uman (DU) [57] models are classified as travelling current source type models. The return-stroke current beneath the wavefront in the lightning channel can be described as:

BG model:

$$I(z,t) = i(0,t) \tag{6}$$

TL model [53]:

$$I(z,t) = i(0, t - z'/v) \quad (7)$$

MTLE model [58] [59]:

$$I(z,t) = i(0, t - z'/v) exp(-z'/\lambda) \quad (8)$$

MTLL model [60]

$$I(z,t) = i(0, t - z'/v)(1 - z'/H_{sol}) \quad (9)$$

TCL model [61]:

$$I(z,t) = i(0, t + z'/v) \quad (10)$$

DU model [57]:

$$I(z,t) = i(0, t + z'/c) - I\left(0, z'/V_f/\left(1 + V_f/c\right)\right)e^{-\left(t - z'/V_f\right)/\tau_D} \quad (11)$$

where

$I(z,t)$ = the current along the return-stroke channel at a certain height z and time t

$i(0,t)$ = the current at the bottom of the return-stroke channel

z' = the high from ground level

v = the return-stroke speed V_f

λ = the return-stroke current decay constant

H = the lightning channel height

c = speed of light

τ_D = rise-time

Figure 2.6 shows the lightning return-stroke current amplitude attenuation along the lightning return stroke channel for the TL, MTLL and MTLE models. The lightning return-stroke current amplitude does not attenuate along the lightning channel for the TL model but attenuated linear and exponential for the MTLL and MTLE models along the lightning channel respectively. Figure 2.6d shows a comparison of the return-stroke current amplitudes for the TL, MTLL and MTLE models at a height of 4000 m.

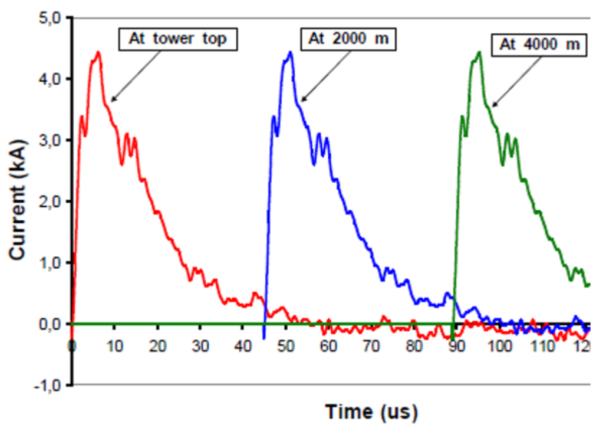

a. The lightning current profile along the lightning channel using the TL model

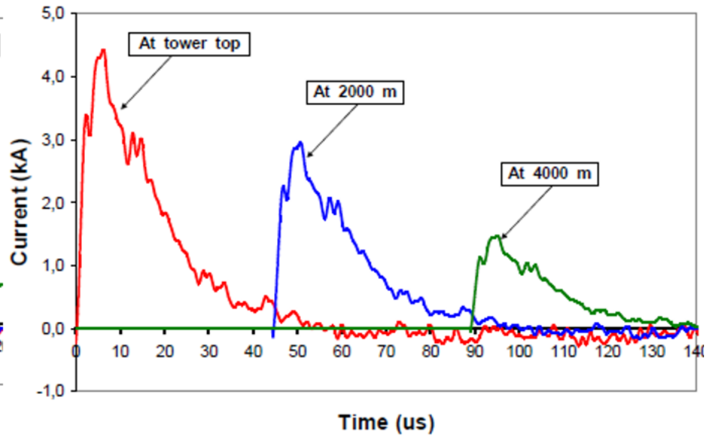

b. The lightning current profile along the lightning channel using the MTLL model

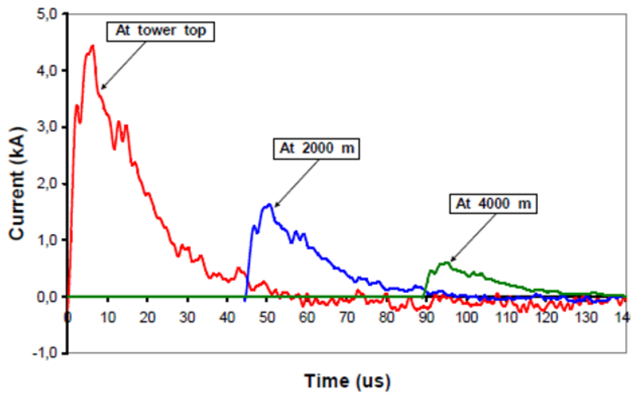

c. The lightning current profile along the lightning channel using the MTLE model

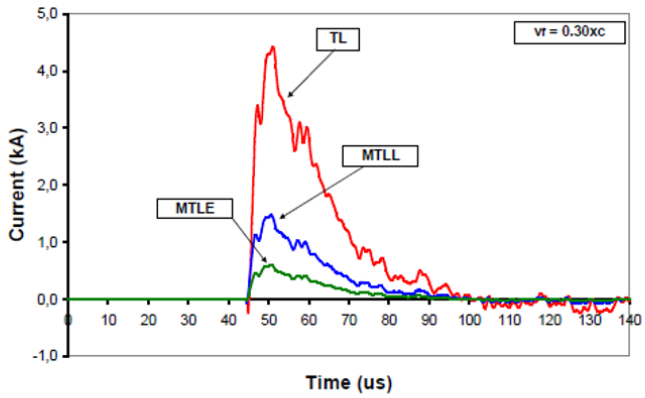

d. Comparison of the 3 models at 4000 m (at the top of the lightning channel)

Figure 2.6 The current along the lightning channel for TL, MTLL and MTLE models at distances of 0 m, 2000 m and 4000 m from ground level [34]. The last panel shows a comparison between the TL, MTLL and MTLE models at 4000 m. Permission obtained from Alexandre Piantini.

Of importance for this research was that the model that was used to calculate the electric field generated by the returns stroke needed to be valid nearby as well as far from the lightning termination point. Figure 2.7 shows a recording of the electric field due to flash S9721 [62] 110 m and 50 m from the lightning channel. Figure 2.8 shows the predicted electric field 50 m [63] from Flash S9721. All the relevant models predicted the maximum electric field very similar to the measured value. Some models [64] also include the effect of non-vertical lightning strikes and non-flat terrain [65], but it did not influence the results of this research.

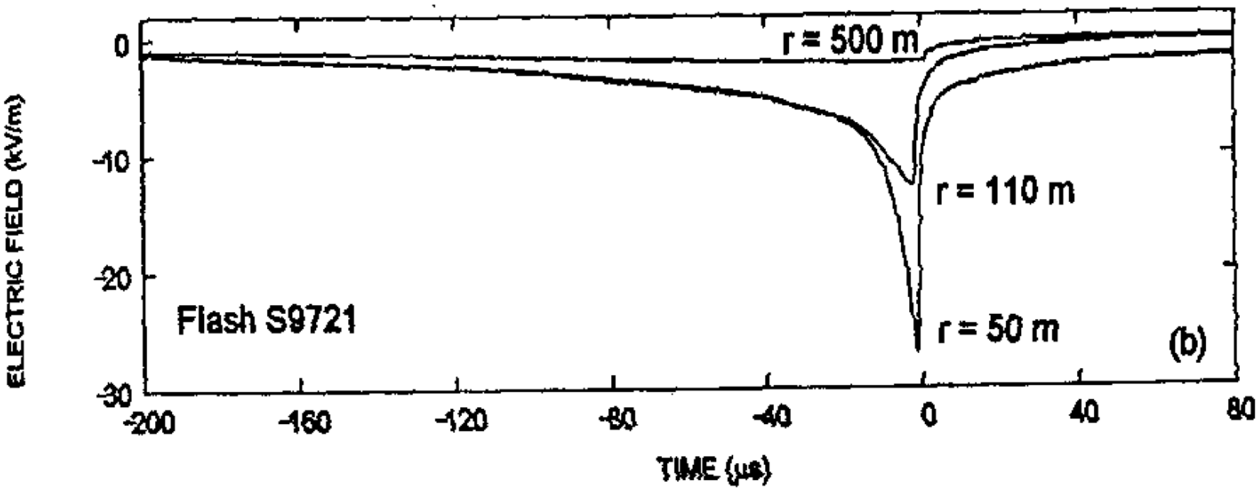

Figure 2.7 A recording of the electric field generated by Flash S9721. Note that the maximum electric field was recorded as 26 kV/m 50 m away from this flash [62]. Permission obtained from the Journal of Geophysical Research 2001

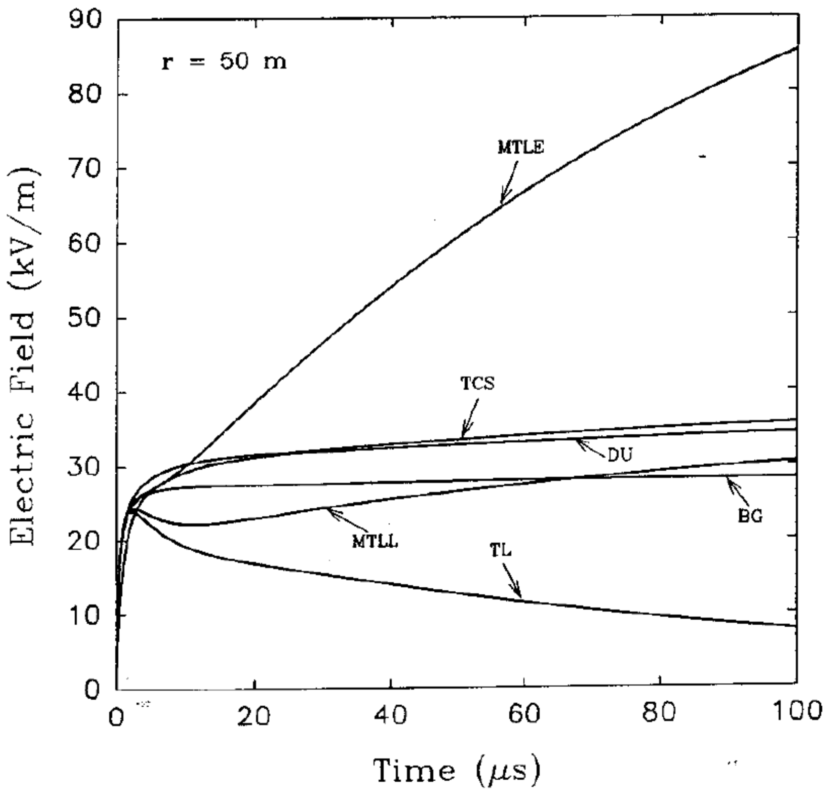

Figure 2.8 A simulation of the electric field generated by Flash S9721 50 m from the lightning channel termination point using several different lightning channel models [63]. *Note that all the models except for the MTLE predicts an electric field of between 25 and 30 kV/m which is very close to the measured value of 27 kV/m. Permission obtained from Rajeev Thottappillil.*

An accurate prediction of the electric field far away from the lightning channel was also important for this research. Figure 2.9 shows the electric field calculated by the TL, MTLE, BG and TCS models at 5 km and 100 km from a lightning flash [66]. There was very little difference between the results. The TL model can be selected for this research as it is mathematically the simplest model and the results will be more than adequate. The TL model was employed by many electromagnetic coupling models as it will not underestimate the electric field within the Transmission line model assumptions [67].

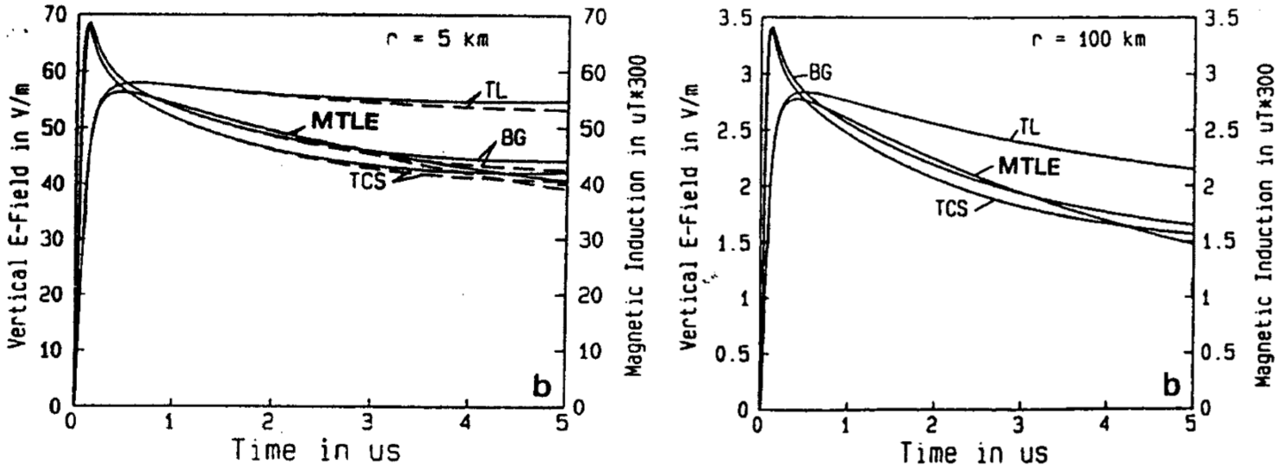

Figure 2.9 The electric field calculated by the TL, MTLE, BG and TCS models at distances of 5 km (solid lines on the left) and 100 km (right) [66]. Permission obtained from the Journal of Geophysical Research.

2.2.4 Distributed Parameter models of the current along the channel

The Distributed Circuit Models simulated the lightning channel as being a vertical transmission line with specific values of shunt capacitance, resistance and series inductance per unit length. The voltages and currents were then calculated along the lightning channel. It also took the effects of the leader into account [68]. It is further divided into Discharge Models that assumed the transmission line to be charged, Lumped Excitation Models that assumed that the transmission line is not charged and Parameter Estimation Models where the streamer current and the transmission pulse current are used to estimate the physical lightning properties. The properties of the return-stroke current were not important for this research as only the polarity of the return-stroke current was needed.

2.3 Coupling models between the lightning channel and the line

There are several models [69] [20] [16] that were used to calculate the coupling between the return-stroke current and the line. The best-known basic coupling models are the models derived by Rusck (1957) [70], Chowdhuri (1969) [71] and Agrawal (1980) [20]. Piantini derived the Extended Rusck

Model (ERM) [72]. The Rusck model did not take the contribution of the vector potential into account and therefore makes the model source dependent [73]. The Chowdhuri model does not include the magnetic induction contribution of the incident field [74]. Some researchers investigated the transient response of multiconductor lines [20] [75] [76]. These models can be verified by comparing them to models that were already verified and proved to be rigorous. A model can also be verified by measurements on experimental lines. Longer operational test lines involved more complexities of which some elements were not known accurately. In this research, the operational line was 714 km long (that includes the branches), was running along a changing environment and natural lightning (captured by the LDN) was used as a source for the induced voltages. In such cases there may be a bigger difference between the model and measurement results.

To compare models more accurately, some assumptions were made. The most common assumptions were that the lightning channel was straight and terminate perpendicular to the ground, the line was floating, short and lossless, the exact distance between the nearby lightning strike termination point and the line was known and defined the soil conductivity as infinite. These assumptions can also be simulated in laboratories for model verification, but cannot be made when doing line designs as it can result in some errors in line performance that may be significant and will be quantified later [73].

The Rusck model was the simplest equation where all the above assumptions were made as shown in Equation 12.

$$U_m = 30\left(1 + \frac{v/c}{\sqrt{2-(v/c)^2}}\right)\left(\frac{h \times I_p}{d}\right) \qquad (12)$$

where

U_m= the LIOV on the line

v = the speed of the current propagation

c = the speed of light

h = the height of the conductor above the ground

I_p = the return-stroke current

d = the distance between the lightning strike termination point and the line

As for this research, at least the soil conductivity had to be considered. The Rusck model was then improved to the Extended Rusck Model (ERM) [72] to include the soil properties. An induced voltage on the line as a result of a horizontal electric field due to the finite conducting soil was added to the

LIOV generated by the horizontal and vertical electric field over infinite conduction soil. It can be written as [72]:

$$U(x,t)_{p>0} = U(x,t)_{p=0} + VExI(x,t) \quad (13)$$

Where

U = the induced voltage on the line

$VExI$ = the voltage induced due to the horizontal electric field as a result of the lossy ground.

As proposed by [77], the horizontal component of the incident electric field can be written as [72]:

$$Ex(x,h,t) = \frac{\partial V^{s}(x,t)}{\partial x} + V'_{g}(x,t) + L\frac{\partial I(x,t)}{\partial t} \quad (14)$$

and the unit length volt drop due to the ground transient resistance is [77]:

$$V'_{g}(x,t) = \int_{0}^{t} \xi'_{g}(t-\tau)\frac{\partial}{\partial \tau}I(x,\tau)d\tau \quad (15)$$

Where

Ex = horizontal electric field

V^{s} = scattered voltage

V'_{g} = volt-drop due to the ground transient resistance

L = inductance of the line

ξ'_{g} = ground transient resistance

Figure 2.10 shows the ERM equivalent circuit of a single line that was used to calculate the induced voltage on the line that was excited by the electromagnetic field due to a return-stroke. Of importance is that the induced voltage (V_g) due to the horizontal electric field component as a result of lossy ground was included in the ERM model.

.

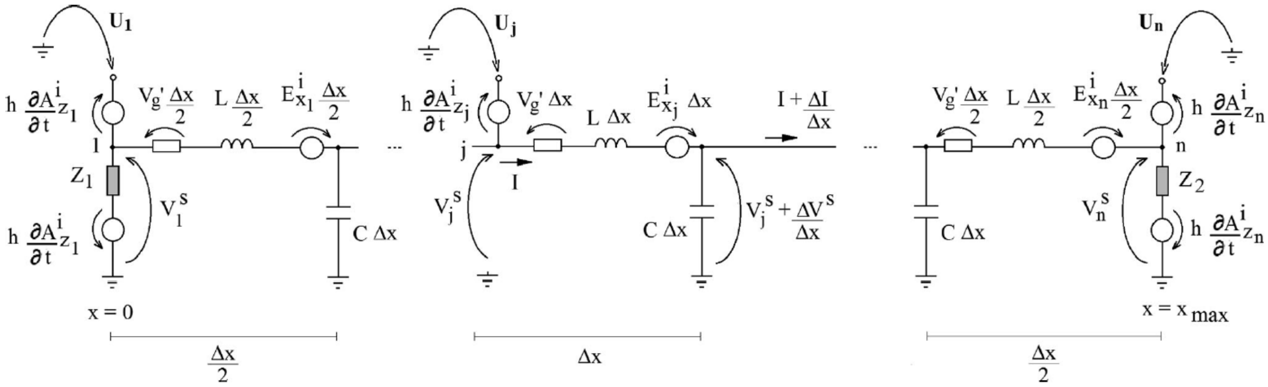

Figure 2.10 The ERM equivalent circuit of a single line [72]. Permission obtained from Alexandre Piantini.

The Chowdhuri model does not take the effect of finite soil conductivity into account [71] and will therefore not be considered for this research. The CR model [78] took the soil conductivity into account in the horizontal electric field calculation and was used as part of the computer model that was used for this research. It can be described by:

$$E_r(z = h, r) = -H_{\emptyset}(z = 0, r)\frac{\sqrt{\mu_0}}{\sqrt{\epsilon + \sigma / j\omega}} + E_{rp}(z = h, r) \quad (16)$$

Where

$E_r(z = h, r)$ = horizontal electric field

$H_{\emptyset}(z = 0, r)$ = the ideal azimuthal magnetic field that is at ground level

$E_{rp}(z = h, r)$ = the horizontal field when soil conductivity is infinite

μ_0= magnetic permeability of space

ϵ = ground electric permittivity

σ = ground conductivity

ω = angular frequency

The Agrawal model expresses the coupling equations in terms of the scattered voltage on the conductor, the inductance of the conductor and the ground impedance to calculate the incident electric field along the *x-axis* at the conductor's height. Equations 17, and 18 are the TL coupling equations of the Agrawal model that is expressed in the time domain and the total voltage is given by equation 19 [75] [79].

$$E_x^e(x,h,t) = \frac{\partial v^s(x,t)}{\partial x} + \xi'_g \otimes \frac{\partial i_i(x,t)}{\partial x} + L\frac{\partial i(x,t)}{\partial t} \quad (17)$$

$$\frac{\partial i(x,t)}{\partial x} + G'v^s(x,t) + C'\frac{\partial v^s(x,t)}{\partial t} = 0 \quad (18)$$

$$v(x,t) = v^s\,(x,t) + v^i(x,t) \quad (19)$$

where

$E_x^e(x,h,t)$ = the horizontal component of the incident electric field along the *x-axis* at the conductor's height (in V/m)

$i(x,t)$ = the current induced along the line (in A)

ξ'_g = the inverse Fourier transform of the ground impedance (in Ω)

$\otimes$ = denotes the convolution product

L', *C'*, *G'* = the line inductance, capacitance and conductance per unit length respectively

$\mathrm{i}_\mathrm{i}(x,t)$ = multi-conductor line induced current vector along the line (in A)

$v^s(\mathrm{x},\mathrm{t})$ = single-conductor line scattered voltage along the line (in V)

$v^i(x,t)$ = single-conductor line incident voltage along the line (in V)

$v(x,t)$ = single-conductor line total voltage along the line (in V)

Figure 2.11 shows a schematic layout of the Agrawal formulation [75].

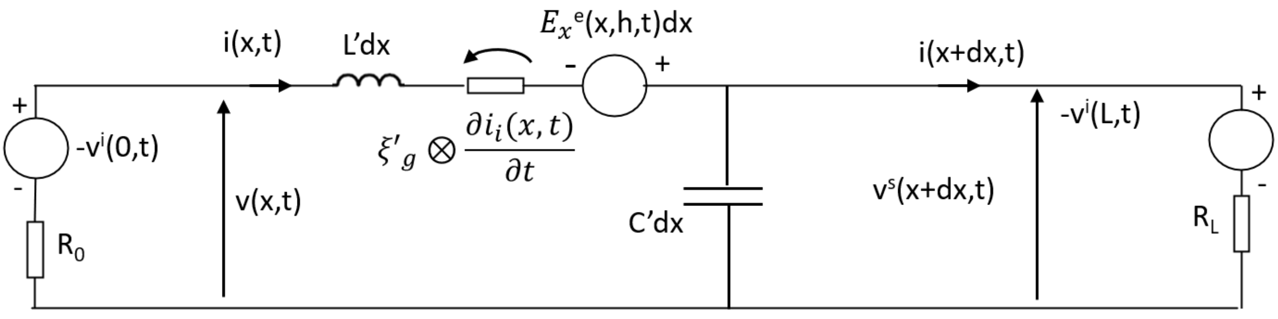

Figure 2.11 A differential coupling circuit redrawn for a lossless single wire overhead line according to the Agrawal formulation [75].

Piantini [80] also confirmed that the modelling accuracy of the lightning channel does not have much influence on the peak amplitude of the induced voltage. However, it does influence the amplitude of the surge tail.

2.4 The effect of coupling between the line and the ground on the LGC

The methodology in this research mainly used the LGC along the line to distinguish between nearby and direct lightning strikes to the line as the LIOV was in most cases not visible due to the low substation source impedance. The amplitude of the LGC was reduced due to the ground transient resistance and was dependent on the relative permittivity of the ground and the line geometry.

Carson derived an expression to calculate the transient ground impedance for frequencies up to a few MHz [81]. Timotin [82] derived an expression that assumed that the conduction current density in the ground with a poor conductivity was negligibly small. The ground transient impedance increased indefinitely at very high frequencies due to this assumption. Sunde [83] derived an expression that seems to be accurate within the TL limits. At lower frequencies, the Sunde expressions reduced to the Carson expression.

A new expression which was non-singular and analytic, was proposed by [77] to describe the soil impedance behaviour accurate at both late-time and early-time within the TL limits. The validity of the expression compared well with an inverse Fast Fourier Transform algorithm of the Sunde expression when calculating the volt-drop per unit length due to the soil transient resistance. The Timotin expression resulted in higher volt-drop values (0.29 V/m versus 0.26 V/m for both the Sunde and the Rachidi et al new expression) [77] for a 5 mm conductor 10 m above the ground (conductivity of 0.001 s/m and relative permittivity of 10). The risetime was 0.5 μs and the current 1 A. current.

The LGC amplitude for this research was measured at the substation that was between 500 m and 70 km from the closest point on the line where the nearby lightning strike terminated. The LGC on the line closest to the nearby lightning strike was less than 350 A and attenuated to be in the order of 40 A at the substation where the current was terminated to ground through an NEC. For this research, the amplitude was not of importance as only the polarity of the LGC superimposed on the power frequency zero-sequence current was measured to distinguish between nearby and direct lightning strikes.

2.5 Computer models

Several computer models based on electromagnetic coupling models and lightning channel models were developed to calculate the LIOV on the line. The EMTP-RUSCK model was tested against measurements [84] and was found to correlate better than 10%. It was also compared with the

Agrawal model [85] and was found to correlate better than 5%. However, nothing was mentioned about the soil resistivity and it is not sure whether this was considered, which was crucial for this research.

The LIOV-EMTP model [17] was based on the MTLE lightning channel model and the Cooray-Rubenstein coupling model. It took the effect of lossy ground into account. This model was used to calculate the LIOV on the line closest to the nearby lightning strike. The input data to this model was compromised by the LDN geographical accuracy and would have been difficult to use for this research.

The ATP-EMTP model [18] used the Transmission Line model for the return-stroke channel, the Cooray-Rubinstein model for the horizontal electric field over lossy ground and the Agrawal coupling model to calculate the LIOV on the line. This model was accurate for calculating the LIOV due to a nearby strike that is between 100 m and 10 km from the line and for line lengths up to 2 km. The ATP-EMTP model was suitable to be include as part of the ATP model of the line in this research. The ATP-EMTP model was also extended to include line protection such as overhead screening wires (that was not applicable in this research) and surge arresters and the extended model was known as the LIV-ATP computer model [86].

2.6 Electromagnetic coupling model dependencies on input data

The electromagnetic coupling and computer models are theoretical accurate and were verified by actual measurements in controlled areas with certain assumptions. However, the input data to the models on lines in operation was not always available or accurate. This was typical data such as the lightning tortuosity, an accurate distance between the lightning channel termination point on earth and the line and the changing soil properties,

Figure 2.12 shows that the electric field due to a different lightning channel tortuosity can vary up to 29% from what is predicted due to a straight lightning return-stroke channel. The angle between the lightning return-stroke channel and the line can result in an even bigger difference in the LIOV as shown in Figure 2.13. The lightning tortuosity as well as the angle between the line and the lightning return-stroke channel are most of the time not available and will result in an unacceptable inaccuracy even when using the most accurate lightning channel model.

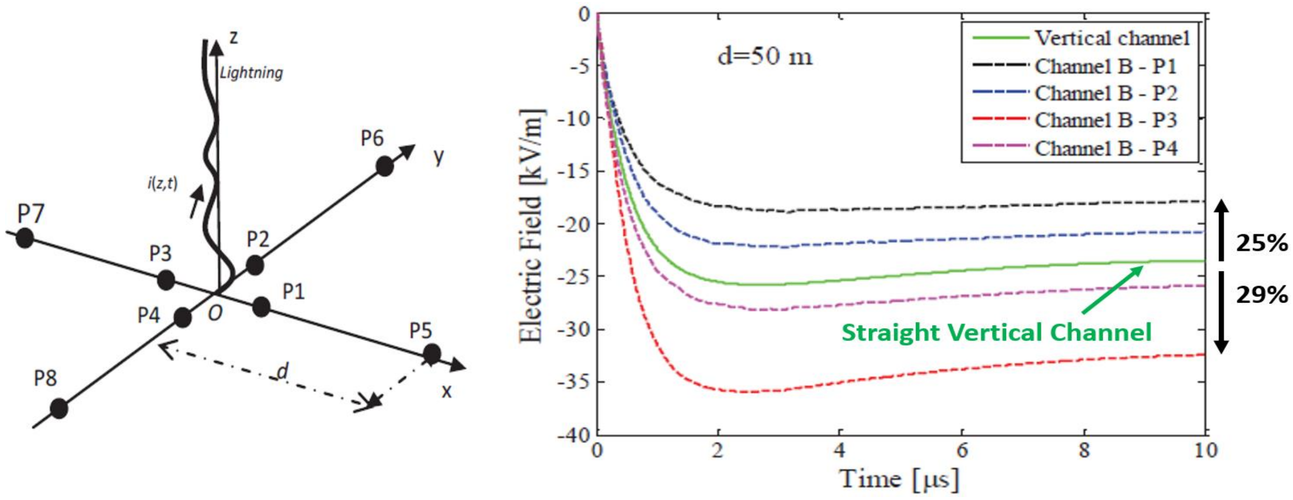

Figure 2.12 The effect of the lightning channel tortuosity on the electric field around the lightning return-stroke. It shows the sensitivity of the electric field to the lightning channel tortuosity[87]. Permission obtained from the IEEE 2013

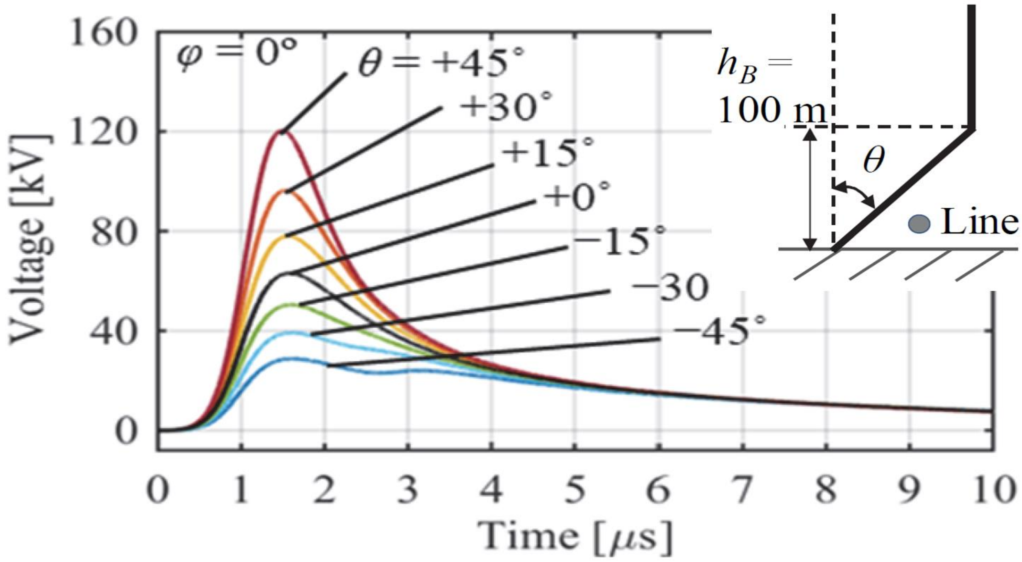

Figure 2.13 The sensitivity of the LIOV to the lightning channel angle in relation to the line [88]. Permission obtained from the ScienceDirect Elsevier Electric Power System Research.

The current rise-time [89] of the lightning return-stroke was also an important input needed for the electromagnetic coupling models and it can make a 35% difference in the LIOV amplitude between a 1 μs and 9 μs rise-time as shown in Figure 2.14. A lightning stroke induced a voltage of 420 kV and 160 kV if it terminates 50 m and 200 m [90] from the line. A significant deviation in the calculation of the LIOV can be expected due to this input parameter as the LDN accuracy was specified as better than 500 m. Should the soil resistivity [90] worsen from zero to 1000 Ω.m the LIOV amplitude will increase from 240 kV to 480 kV for this specific case. The line height [89] above the ground (which can differ due to the terrain) also resulted in a significant difference in the LIOV amplitude calculation. It can therefore be concluded that LIOV were very sensitive to these input parameters, which were not always available in uncontrolled areas, even though the most accurate coupling model was used.

The lower the soil resistivity (higher soil conductivity), the lower the induced voltage on the line due to nearby flashes [12] [17]. This is due to a larger coupling between the ground and the conductor as the return-stroke current does not penetrate deep into the ground. Darveniza [91] suggests that the Extended Rusck Model can be simplified by increasing the line height to simulate a higher soil resistivity. Figure 2.15 shows the dependency of the number of flashovers per 100 km per year on the Critical Flashover Voltage (CFO) of the line and the soil (ground) conductivity.

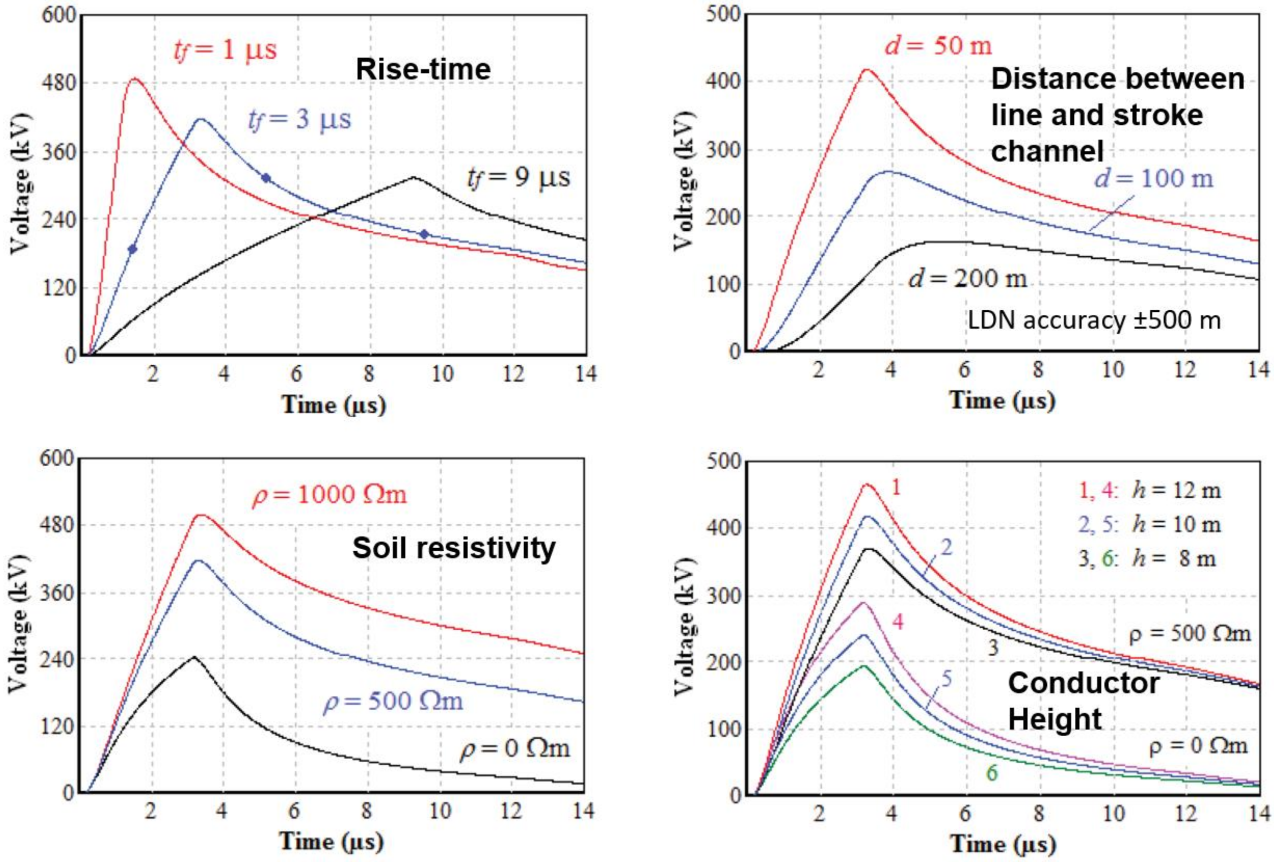

Figure 2.14 The LIOV is very sensitive to inaccuracies of the return-stroke rise time [89], the distance between the line and return-stroke [90], the height of the conductor [89] and the soil resistivity [90] was possible. Permission obtained from the IEEE 2016.

Nucci et al [17] used the Monte Carlo method [52] [53] [54], in conjunction with the LIOV-EMTP program to determine the effect of ground conductivity on the LIOVs on a typical Italian 15 kV network. Soil conductivities of 0.001 S/m and ideal ground were compared for a ground-flash density of 1 ground flash/km^2/year as shown in Figure 2.16. In both the mentioned cases the flashover rate of the line increased as the ground conductivity decreased.

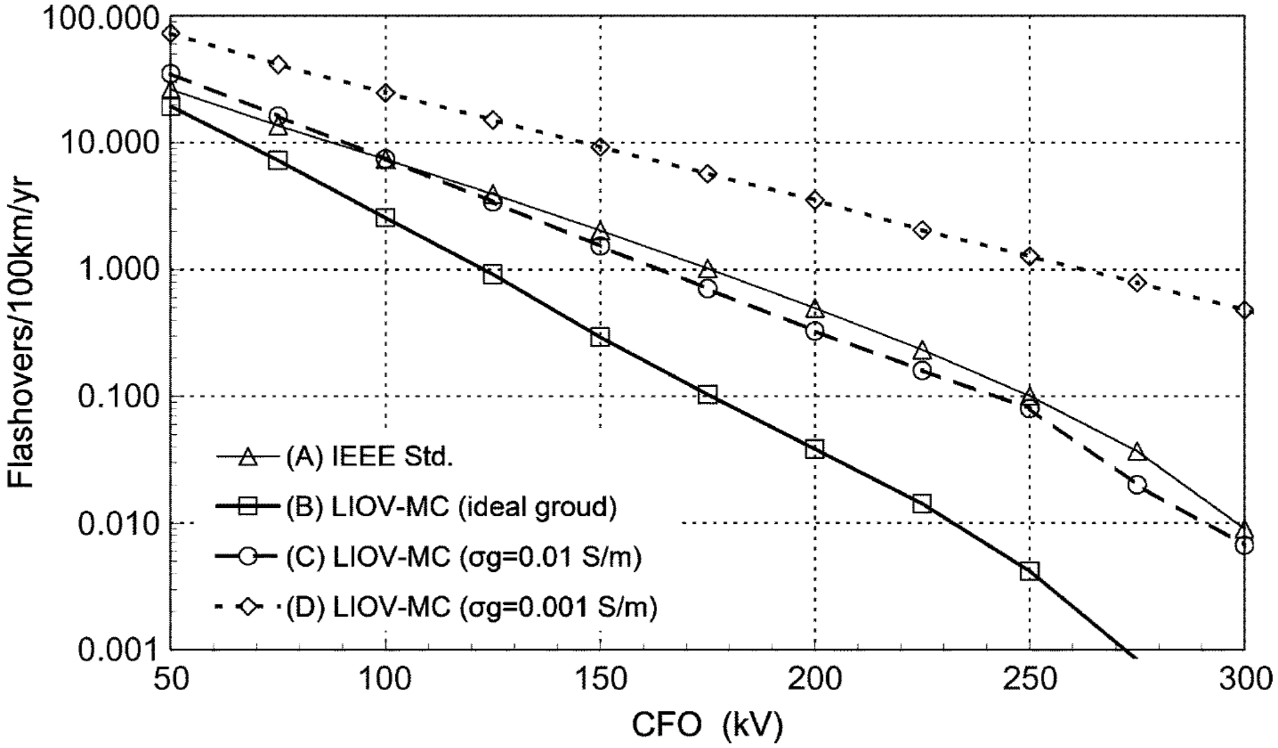

Figure 2.15 The dependency of the number of flashovers per 100 km per year as a function of the Critical Flashover Voltage (CFO) and the ground (soil) conductivity [92]. Permission obtained from the IEEE 2007.

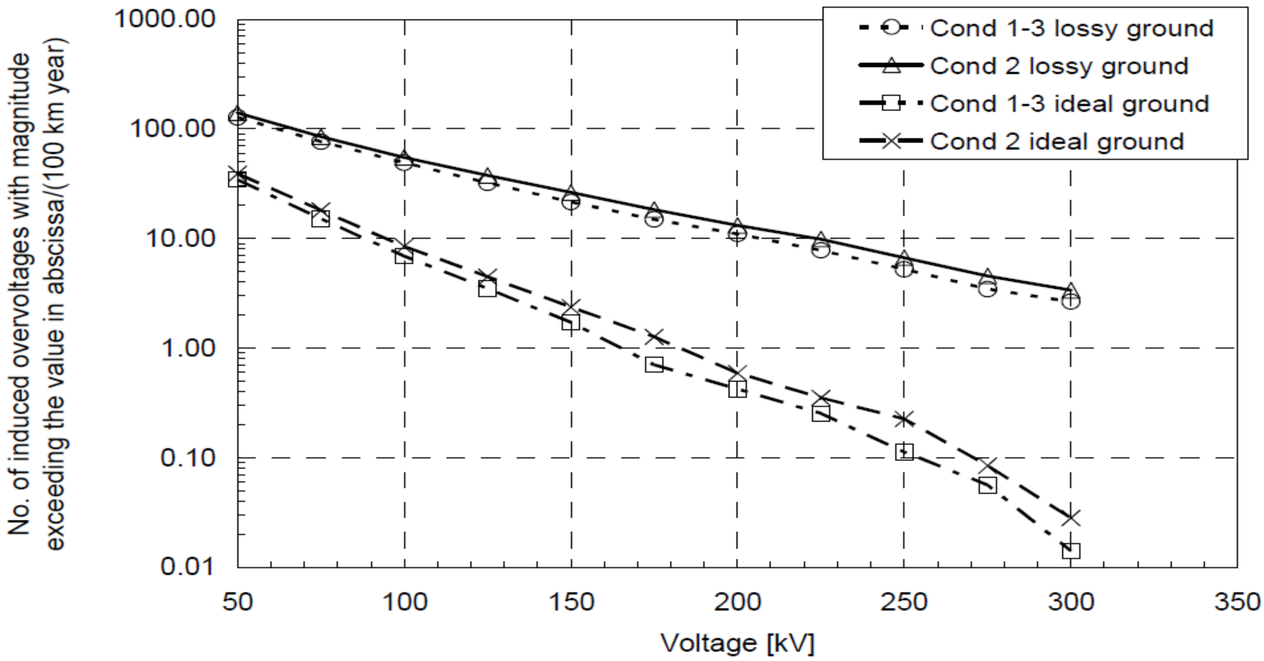

Figure 2.16 LIOVs on a 15 kV line with soil conductivity of 0.001 S/m and ideal ground, for a ground-flash density of 1 ground flash/km^2/year. Conductors 1 and 3 are lower than conductor 2 [92]. Permission obtained from the IEEE 2007.

Figure 2.17 shows that the higher the ground conductivity, the lower the induced voltage. In this case there were 10.5 times more incidents where the LIOV on the line exceeds 150 kV when the ground conductivity is 0.001 S/m instead of ideal ground. The result corresponds well with [29] [93].

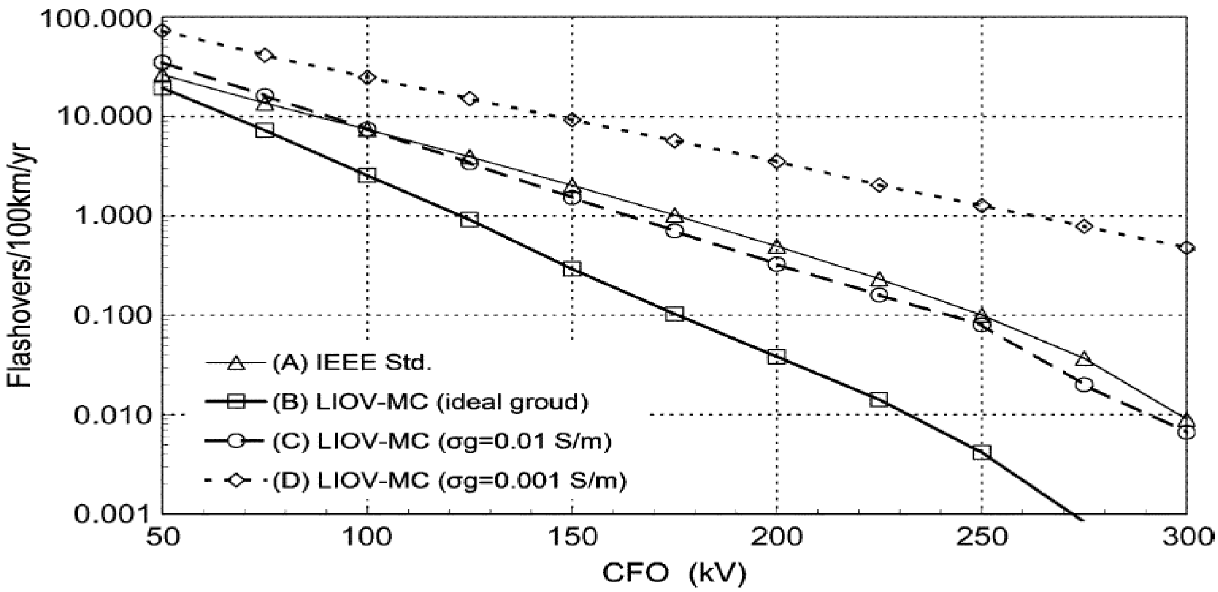

Figure 2.17 An improved model of the dependency of the number of flashovers per 100 km per year as a function of the Critical Flashover Voltage (CFO) and the ground (soil) conductivity [92]. Permission obtained from the IEEE 2007.

It can be seen that the soil conductivity can contribute significantly to errors in calculating the LIOV. However, this research was not dependent on accurate values of the soil resistivity to calculate an accurate value for the LIOV to determine whether the LIOV amplitude exceeded the line BIL.

2.7 Accuracy of the LDN

The LDN is an important tool to be used for lightning research. The LDN GPS time stamping of a lightning strike, the geographical position of the lightning strike termination point or both can be used to correlate a specific lightning strike with a point of interest. Both these parameters were used in this research. The time correlation between the recorder (logger) at the feeder substation was within 10 ms and was the primary source for correlating lightning strikes with line faults. The geographical position of the lightning strike point was mainly used to establish in which section of the line the lightning strike terminated. In events where there was more than one lightning strike at the same time along the 714 km line, the pole-mount breaker operations could then be correlated with the relevant lightning strike to establish which lightning strike caused a line fault. Some of the nearby lightning strikes terminated on trees which were about 15 m from the line. If the GPS coordinates of the lightning termination point were accurate (±10 m) this research was not necessary to determine whether the lightning strike terminated on the line or nearby the line. However, the specification for the geographical accuracy of most LDNs is < 500 m.

The Detection Efficiency (DE) of the LDN which is an indication of how many lightning strikes were not missed but detected by the LDN is also an important parameter for this research. One of the LDN suppliers (that also supplied the South African LDN) indicated that the global accuracy of the LDN is on average 1 km [94]. The DE depends on the lightning stroke amplitude as shown in Figure 2.18 [95]. Note that the average DE for negative 20 kA lightning strikes (which was average in that research), was 95%.

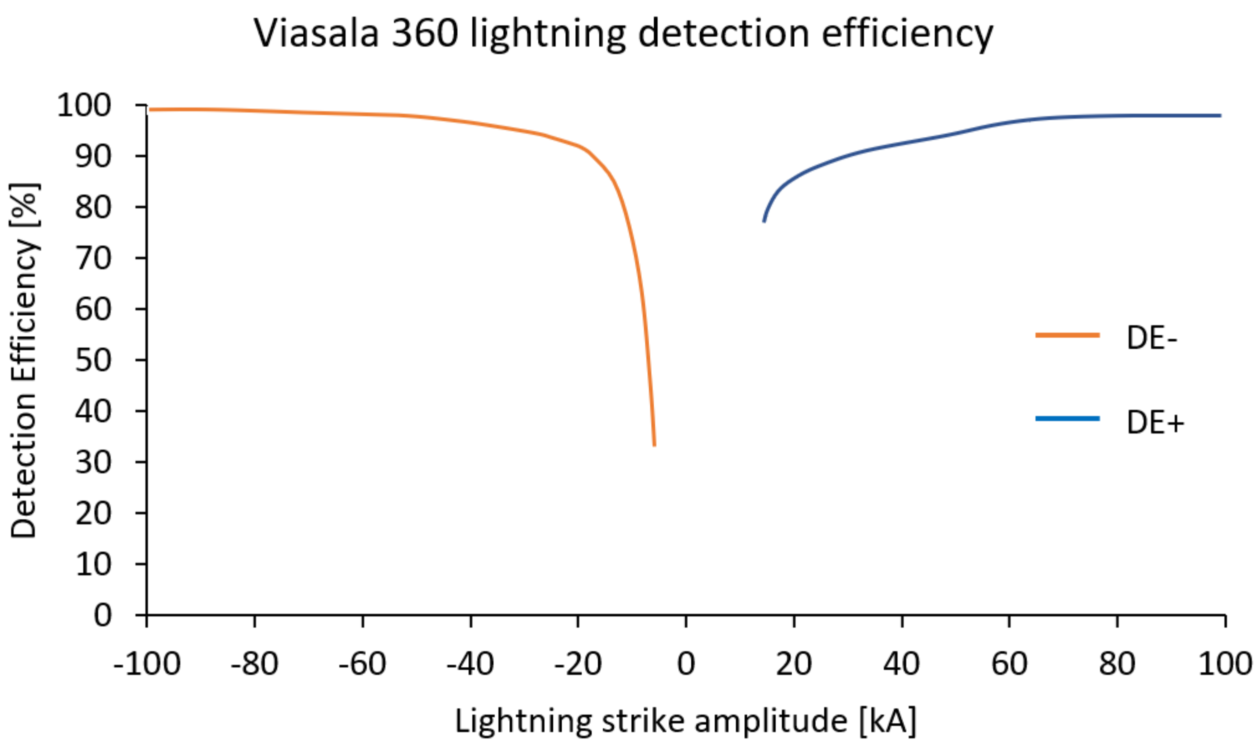

Figure 2.18 The Detection Efficiency of the Vaisala GLD360 LDN. The DE increased as the lightning return-stroke amplitude increased.

The Austrian LDN geographical accuracy was measured [96] using cameras as a reference and the median deviation was 95 m, 130 m and 90 m in 2015, 2018 and 2018 respectively. The maximum distance deviation was 3.5 km, 2.6 km and 2.7 km for 2015, 2017 and 2018 respectively. A lightning flash DE between 96.08% and 98.62% and a lightning stroke DE between 76.36% and 85.6% were measured. The US NLDN [97] geographical accuracy median deviation was measured using Elevated Strike Objects (ESO) as a reference and was found to be 308 m and the maximum distance deviation was 4.2 km. These findings would result in significant errors when calculating the LIOV.

A similar test was done using the Slovenian Lightning Locating System [98]. In this study lightning that caused line faults were matched to strikes in a 500 m, 1000 m or 2000 m corridor or buffer along the line. It was not clear whether GPS time stamping was used and whether the lightning strikes were direct or nearby to the line. It seems as if 56% of the LDN results had more than a 500 m error. Table 2.2 shows the results.

Table 2.2 Correlation of 865 lightning strikes in different corridor widths with line faults.

Width of corridor [m]	Correlated events [%]
0 – 500	44
500 – 1000	27.5
1000 – 2000	28.5

Studies to determine the geographical accuracy error of the International Centre for Lightning Research and Testing (ICLRT) site at Camp Blanding, Florida, are summarized in Figure 2.19. The LDN geographical accuracy varied significantly even with the lightning strikes seen by the same number of sensors.

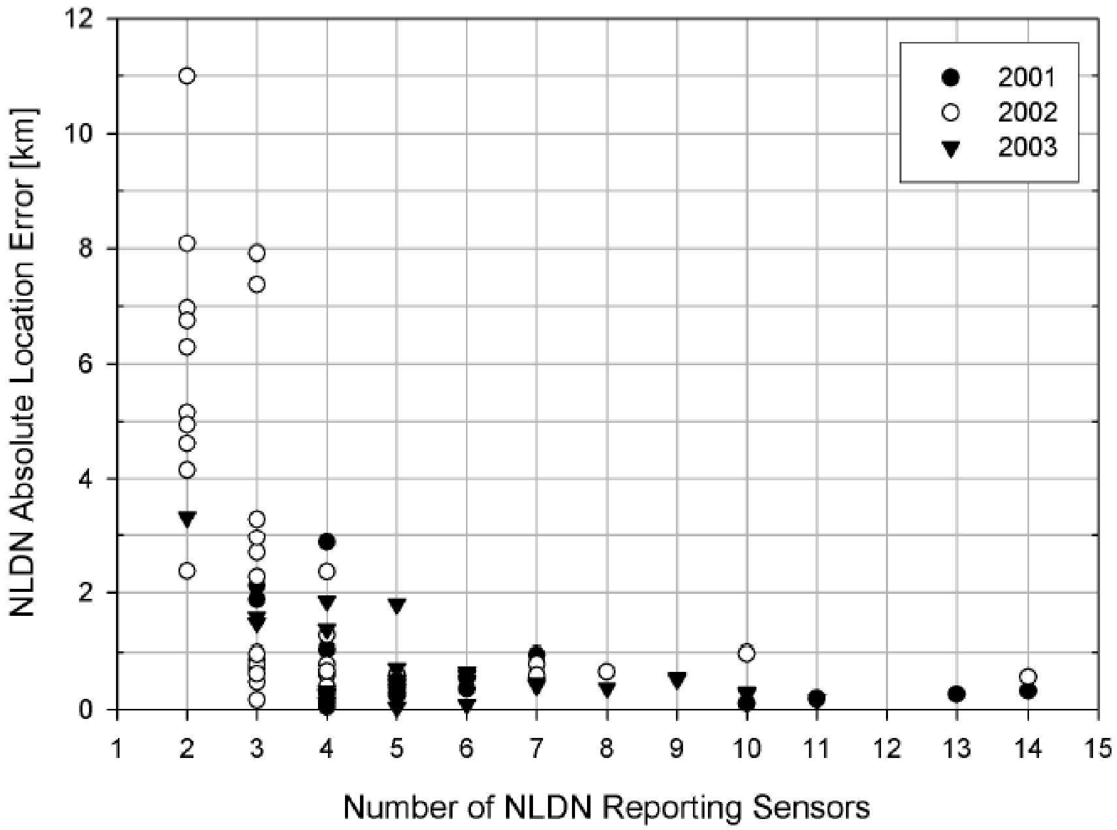

Figure 2.19 The NLDN absolute location error versus the number of reporting NLDN sensors, for 95 strikes in 31 triggered flashes during 2001-2003 [99]. Permission obtained from the Journal of Geophysical Research.

Before this research was started the South African LDN was also tested. A 24 Vaisala LS7000 sensor LDN was used for the study in this research. The geographical accuracy was specified to be < 500 m and the flash detection efficiency was > 90%. A camera that was triggered by movement caused by lightning [100] was used in research at the University of the Witwatersrand to determine the SALDN DE and to verify the geographical accuracy between 2009 and 2013. The camera was installed 1.88 km from the Brixton tower in Johannesburg to measure the location accuracy of flashes captured by the SALDN against the ground-truth photographs and was found to be 280 m. The maximum capturing speed of the camera was limited to 30 Frames Per Second (FPS) [101]. The time correlation between the photographs and the corresponding lightning flashes captured by the LDN was 12 ms. An important finding of the research in [102] [103] was that only 40% of the median error ellipses included the tower. During these four years, the SALDN flash DE increased from 50% to 76% due to extra sensors that were added to the network. The 10% confidence ellipses included the tower in 10% of the lightning flash events while the 99% confidence ellipses included the tower between 90% and 100% of the lightning flashes. In 2015 two new Phantom cameras were installed, one with a 5000 FPS capability and the other one's speed was 15 000 FPS [104].

The confidence ellipse in the LDN geographical display is an indication of the deviation between the displayed lightning termination point by the LDN and the ground-truth termination point of the lightning strike. A small ellipse is an indication that the displayed lightning termination point is closer to the ground-truth termination point. The size of the ellipse is determined by the difference between each sensor location point. A method to discard the outlier sensor positions was investigated by comparing the Gaussian distribution, the Cauchy function and the Students t-distribution [105]. The length of the 95th confidence ellipse decreased from 1.25 km to 350 m in an example where the Students t-distribution was used. [106]

Research done between February 2017 and February 2018 [107] by the University of the Witwatersrand on the geographical accuracy of lightning strikes to the same tall towers indicated a median location error of 68.5 m. The maximum location errors were 1.7 km and 11.6 km for the two towers respectively. The LDN geographical accuracy needs to be less than 10 m for all the lightning ground-termination points in this research to distinguish between nearby lightning and direct lightning strikes to the line.

Analysing results from Jooste et al [108] showed two strikes (-120 kA and -19 kA) measured by the South African LDN that were located within 20 m (detected by 11 sensors) and 200 m (6 sensors) respectively.

The South African LDN accuracy was further investigated for this research by analysing the direct strikes to the line. The exact location of the strike termination on the line was unknown. It was then assumed that the lightning strike terminated on the point closest to the midpoint of the ellipse on the line as illustrated in Figure 2.20. The best possible geographical accuracy of the LDN is shown in Figure 2.21. The average geographical inaccuracy of the LDN per number of sensors that detected the lightning strike is shown in Figure 2.22 which shows that the geographical distance deviation is not consistent with the number of sensors that detected the stroke.

The accuracy of the LDN was very random (see Figure 2.22) and it seems like the number of sensors that detected the lightning strike is not directly related to the geographical accuracy. The geographical data of the LDN should therefore be validated and verified with additional measurements.

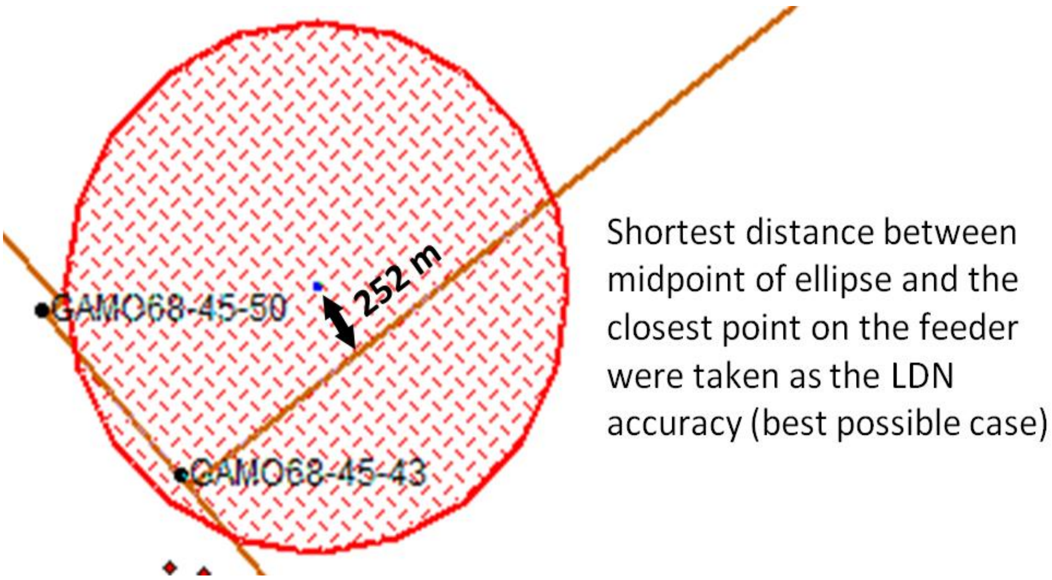

Figure 2.20 A drawing illustrating how the SALDN geographical lightning stroke position deviated from the ground-truth position of the stroke which was assumed to be a point on the line closest to the ellipse centre. A direct lightning strike to the line was plotted 252 m from the line.

In this research, the SALDN average geographical distance error was measured as 231 m and the flash DE was 95%. A summary of research that has been done at the University of the Witwatersrand [109] published a flash DE of 93% for downward flashes and 56% for upward flashes to the towers that were used to determine the DE. These towers were very high and would result in much more upward flashes than from the 10 m line that was used in this research.

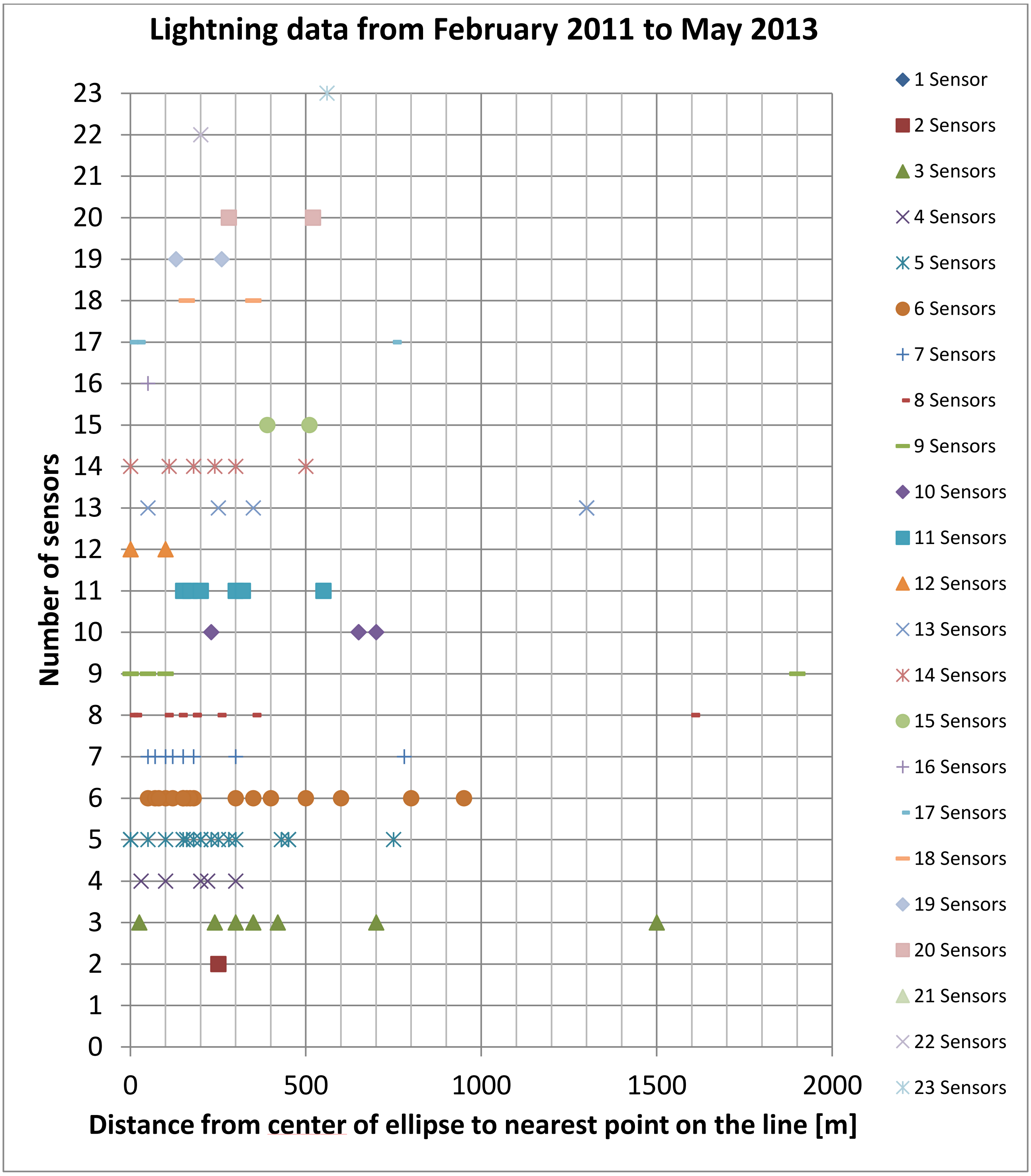

Figure 2.21.The South African LDN geographical accuracy.

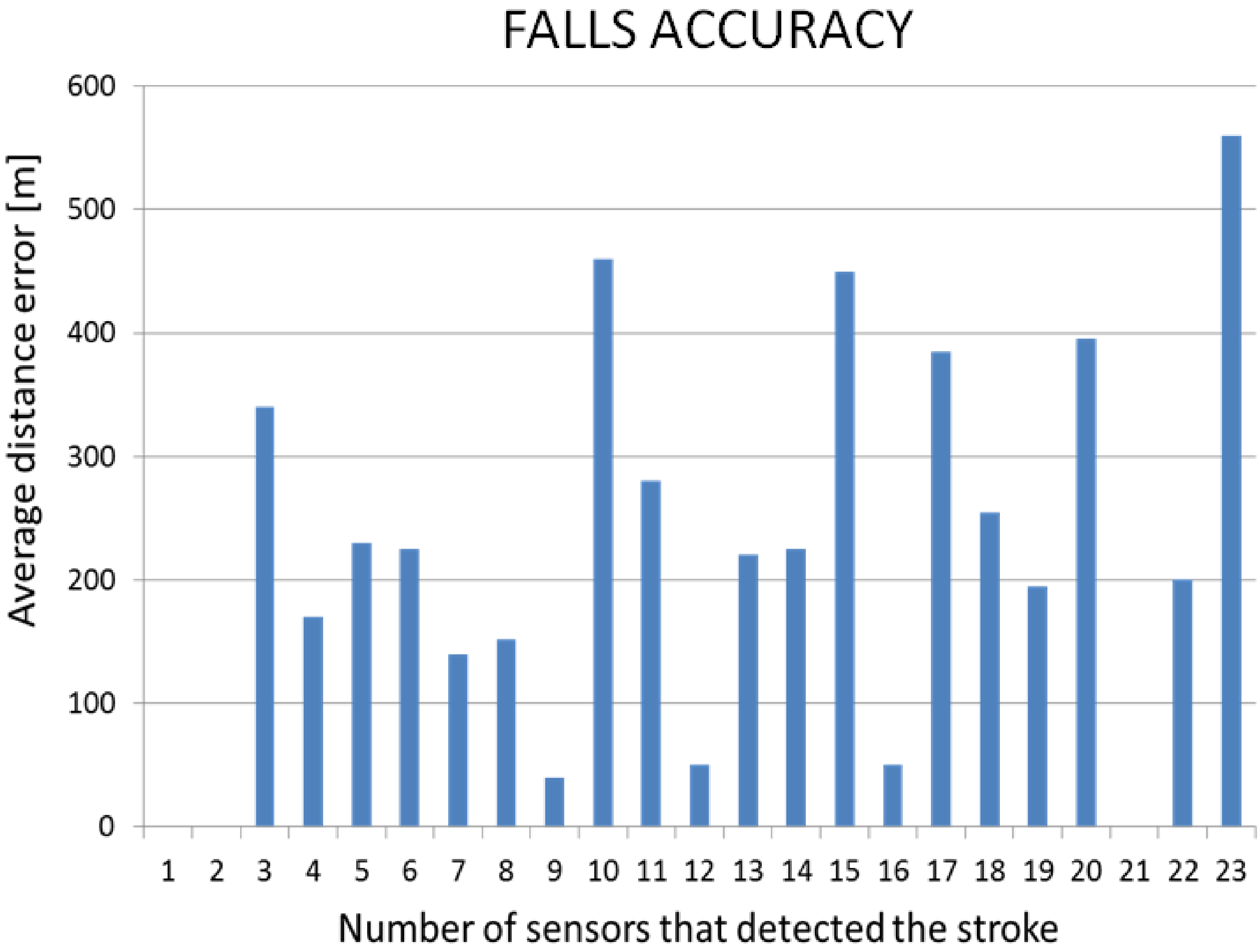

Figure 2.22 The average accuracy of the South African LDN per number of sensors that detected the lightning strike. The graph shows that the geographical distance deviation is not consistent with the number of sensors that detected the stroke. There was only one lightning strike that was detected by 23 sensors simultaneously.

A relatively high geographical inaccuracy that was much higher than the required 10 m was noted on all the LDNs that were studied. An average geographical inaccuracy of 231 m (South African LDN) is much higher than the required 10 m, hence this research. Otherwise, the LDN alone could be used to determine whether a lightning strike was nearby or direct to the line. The geographical data alone can therefore not be used to determine whether the lightning strike was direct or nearby to the line. GPS time stamping, circuit breaker operations and PQ loggers need to be used in conjunction with the LDN geographical data to determine whether the lightning strike was direct or nearby to the line. The recorded LDN distance from the line can also not be used to calculate the induced voltage on the line.

2.8 Measurements done in previous research

Many different methods were used to do lightning measurements on lines, mostly to verify models. Measurements were also used as a source for average model input data parameters. As lightning-induced voltage amplitude and waveform shape attenuate significantly over a short distance along the line, it is important to install a measurement instrument at the location or very close to the location where the LIOV need to be verified or measured.

Small scale networks [65] [110] that fit into the laboratory were a popular method to verify models and derive constants in equations. The advantages of small-scale models are that the induced voltages were of much lower amplitude and the environment parameters were known and could be well controlled. Models of networks [111] [112] [113] were built inside the laboratory and an impulse generator was then used to simulate the lightning strike. The output parameters of the impulse generator could also be well controlled. This was a reliable and safe method to do measurements and where models could be reliably verified.

A second measurement method was to use a rocket launcher [114] [16] [115] [116] [117] [118] to trigger the discharge from the cloud. The position of the lightning strike termination point (the rocket launcher) was known and proper instruments could be installed at the rocket launcher to measure the lightning strike properties reliable. Instruments could also be installed on the test line at the optimal locations. The line properties and the soil properties were known reliably. Although more expensive, this method offered an accurate experimental configuration to verify electromagnetic coupling models.

A third method was to use natural lightning activity to a known high building [119] or high mast (ESO) next to the line to do these measurements [120]. Instruments to measure the lightning parameters were installed in the ESO. In these cases, the tall object close to the line where lightning terminated was used as a known point of termination. This method could be timeous (need to wait for lightning activity), but it rendered more realistic results due to a natural lightning channel tortuosity.

A fourth method was to use natural lightning [121] and cameras [122] [15] [123] [124] to determine the actual point of termination. The lightning flash parameters as captured by the LDN were used in conjunction with the photos captured by the camera to calculate the LIOV on the nearby line [14]

[125]. This method was closest to reality. One of the challenges experienced with the cameras was that the visibility was hampered by heavy rain and mist.

Measurements to capture induced voltage oscillations [126] showed that in 67% of the cases the LIOV tend to oscillate around the zero voltage axis. This was also the case in numerous other measurements. Only the polarity of the first half cycle of the oscillation was of interest in this research.

There was a well-known research site in South Africa [125] [127] [128] [129] [130] between 1978 and 1989. Only lightning parameters of direct lightning strikes to the line were available as there were no LDNs available at that time. The 10 km 11 kV line that was built at a high altitude (1500 m) was floating for the first half of the research. Thereafter the line was equipped and energized. A significant finding of this research was that the LIOV amplitudes declined from 160 kV to 40 kV after the line was equipped and energized as shown in Figure 2.23. It shows that a much lower LIOV amplitude can be expected on energized lines than on floating lines.

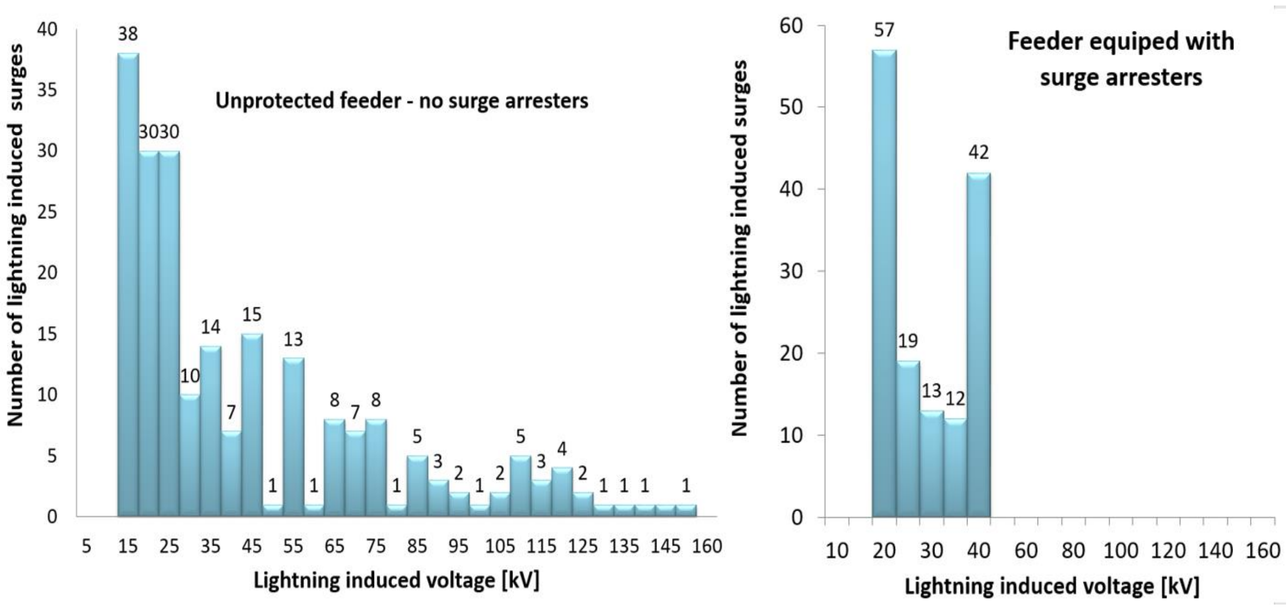

Figure 2.23 Measured LIOV before the line was equipped and energized (left) and after the line was equipped and energized (right).

Most of the induced voltages of 47 nearby lightning strikes close to the test line were less than 100 kV [130]. It was not sure whether surge arresters were installed during all the incidents at the time of the research.

The research inputs from the CSIR, Eskom's research division and municipalities together with the test line findings were then used to determine the most optimal BIL of an MV line. Although the highest LIOV measured on the floating line was 160 kV and the author's comment that the LIOV due to nearby lightning should rarely exceed 200 kV, it was decided to standardise on a 300 kV BIL. An assumption was made that the number of flashovers due to indirect lightning strikes will be negligible should the BIL be 300 kV.

From a practical point of view, insulators with a BIL of 150 kV were used in series with a wood gap in the bonding wire down the pole, totalling a 300 kV BIL. A 300 kV BIL line design will result in a good PQ performance as there is very little chance of a line flashover due to nearby lightning flashes. An insulation over-design in favour of PQ results in compromising SAIDI due to equipment failure. Evidence of this was found on the 10 km test line as 76 wood-poles were damaged by lightning between 1978 and 1982 [130].

One shortcoming of all the South African research was the absence of a Lightning Detection Network (LDN) before 1996 that could provide details of lightning strokes. Secondly, there were no surge arresters installed on the test line when the highest induced voltages were recorded. At a later stage, surge arresters were installed on the test line with the main objective being to study the surge arrester characteristics. No recording could be found of nearby lightning-induced surges that exceeded the 10% rating of arresters [125]. There was therefore a high probability that all lightning-related equipment failures on a well-maintained line could be attributed to direct lightning strikes to the line or equipment connected to the line. The research results were not in a format that could provide a measured flashover rate per year per 100 km

It was also noted in the research on the RVZ line [131] that LIOVs on an energized line due to nearby lightning had a much lower amplitude than on floating lines. Figure 2.24 shows a nearby lightning strike of -12 kA that terminated 800 m from an energized line and 5 km from a floating line. Figure 2.25 shows that the accumulated charge on the floating line resulted in a 40 kV LIOV lasting for about 500 ms on the line where no equipment was installed – except for the 5 MΩ three-phase resistor divider. The charge on the energized line was consumed by surge arresters, equipment, load and coupling between the line and the environment. There was no trace of a LIOV or LGC on the waveform measurement at the feeder substation due to this nearby lightning stroke as shown in Figure 2.26.

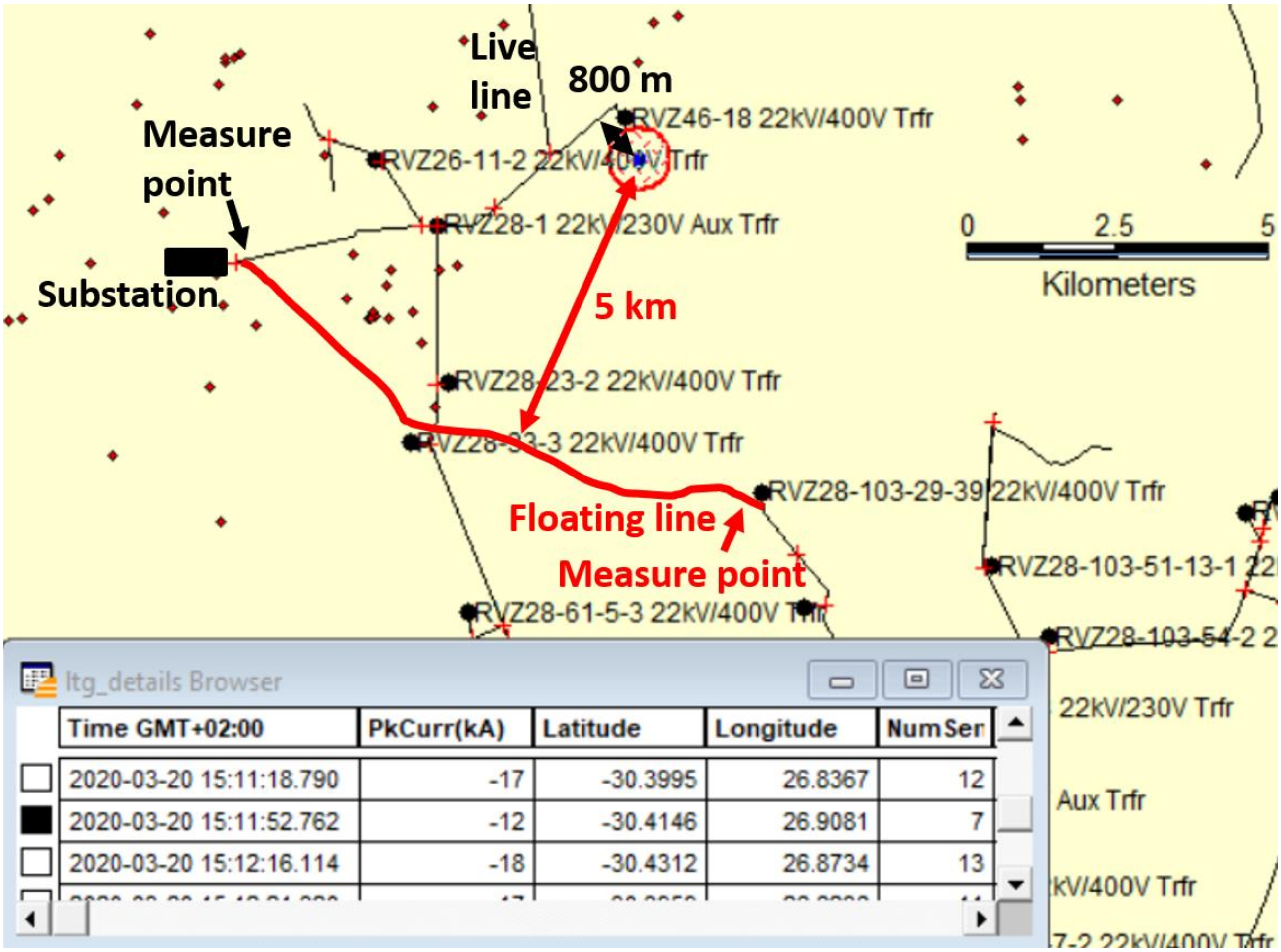

Figure 2.24 A -12 kA nearby lightning strike terminated 800 m from the energized line and 5 km from the floating line.

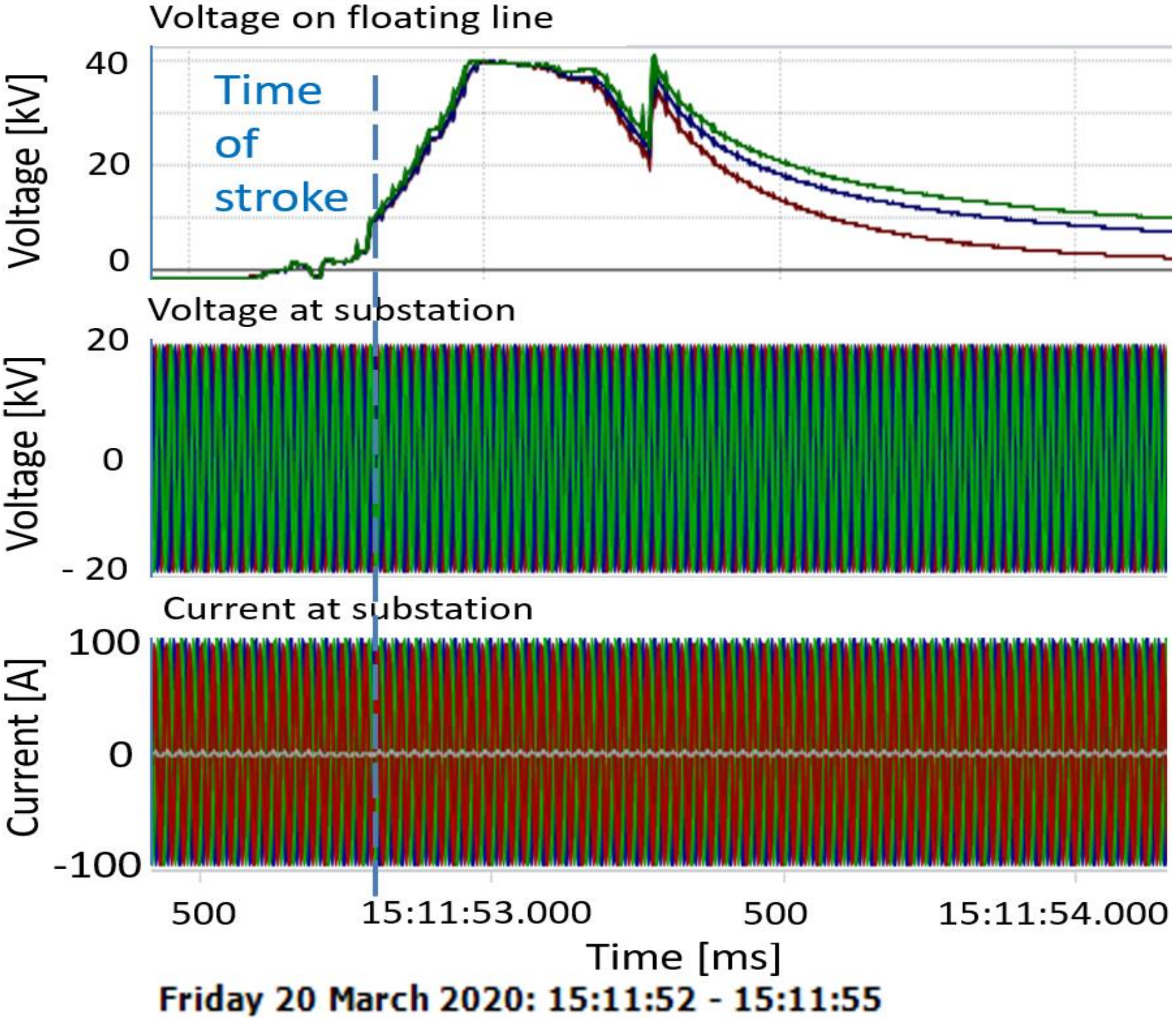

Figure 2.25 The waveform measured on the floating line (top) and at the substation (bottom) measured at the same time as the -12 kA nearby lightning stroke shown in Figure 2.24. The time scale at the bottom is valid for all three panels.

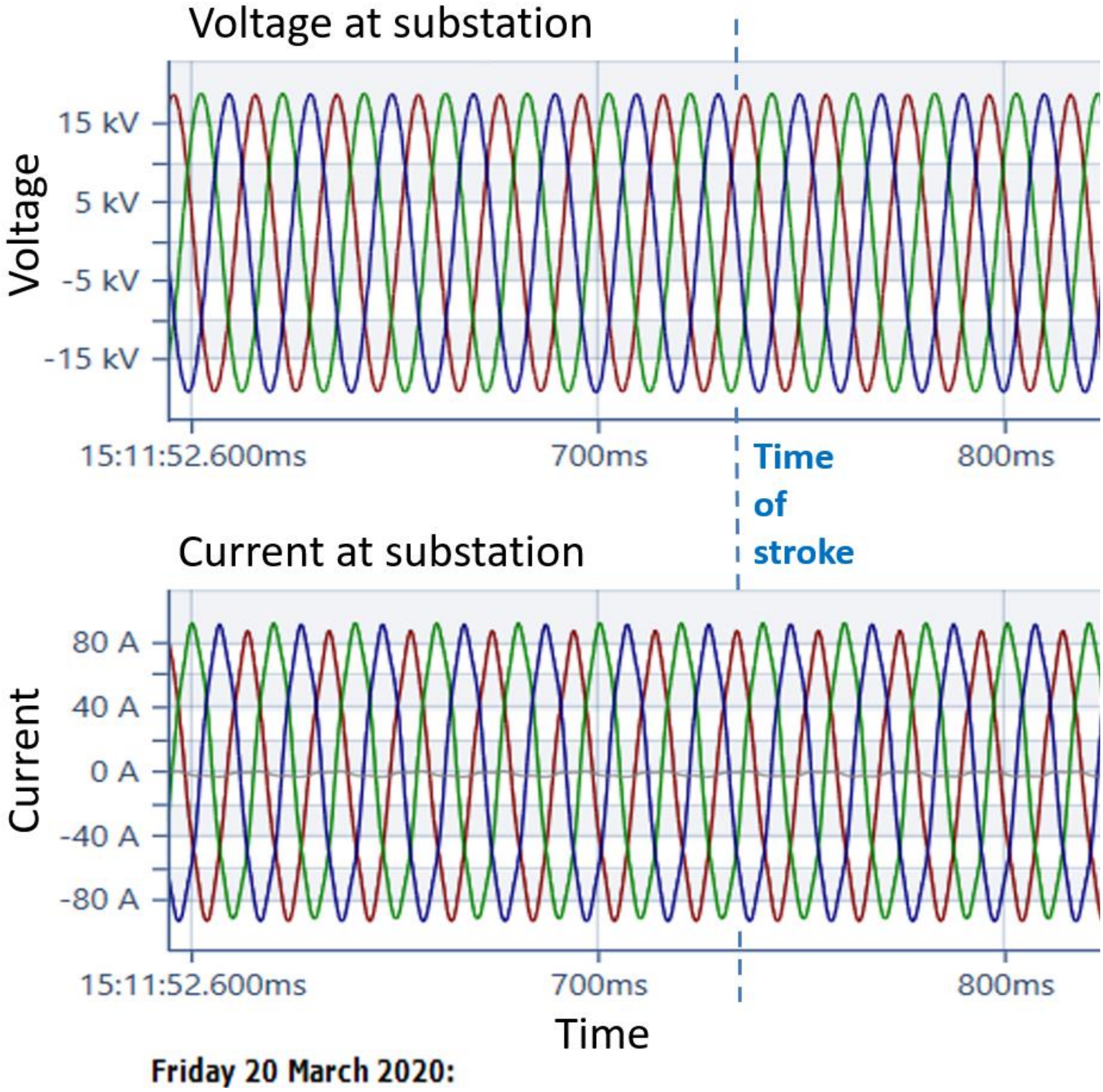

Figure 2.26 There was no trace of any LIOV or LGC due to the -12 kA nearby lightning stroke on the waveform recordings at the feeder substation.

Lightning research in Italy [17] where a live MV line was monitored using the Italian Lightning Location System CESI [132] [133] (geographical accuracy <500 m and detection accuracy >90%) to link the lightning captured by the Italian monitoring system and protection relay operations CESI-SAM [6].

The first criterion for linking lightning to line faults was if there was a protection relay operation as well as lightning strikes in the vicinity of the line that correlate within 1 second. If this criterion was met, it was seen as a possible fault due to lightning. These flashes and the line were then modelled using a computer simulation program, Lightning Induced Over Voltage – Electromagnetic Transients Program code (LIOV-EMTP) [134] [135] [136], to calculate the LIOV along the line for each of those flashes. The LIOV-EMTP code was a result of merging the LIOV code [25] [137] [75] [81] [138] [139] and the EMTP [140] [141].

The second criterion used was to find strikes that could be linked to protection operation and could induce a high enough voltage (using LIOV-EMTP) to exceed the BIL of 125 kV. A third criterion was to identify strikes that comply with both the first and second criteria. The result is shown in Table 2.3. There were big differences in the results of the three criteria.

Table 2.3 A summary of the number of lightning strikes that comply with the three different criteria that linked lightning activity to line faults.

	Fault events correlated to lightning according to criterion 1	Candidate faults events determined by using criterion 2 (LIOV-EMTP correlation)	Candidate fault events determined by using criterion 3 (time and LIOV-EMTP correlation)
Number of single-phase fault events	14	11 (6)	4
Number of multi-phase fault events	16	21 (13)	4

Some comments on this study would be that there might be doubt whether it was a direct or nearby lightning strike to the line that caused the fault. This was due to the inaccuracy of the LDN. No surge waveforms were shown to determine whether it was a direct or nearby lightning strike.

Uncertainties with this work were the exact position (<500 m) of the detected flash which would have a large influence on the coupling between the flash and the line. The one-second time deviation may also cause uncertainty as to which lightning strike caused the protection relay operation. In cases where the protection relay operated due to a phase-to-phase fault, the voltage dip (due to the fault current) could indicate where the fault possibly was along the line. This would help with identifying the lightning strike.

It was also challenging to link the actual lightning strike with the relevant measured induced voltage in other research. A one-second time difference in time-stamping between the strike and measured induced voltage was acceptable for *[142] [143] [144] [145] [7] [6]*. Napolitano et al *[146]* studied a 26 km MV network in Italy and reported a time correlation of tens of milliseconds between the

LDN and recording equipment on the line. They studied 6 out of the 569 flashes as shown in Figure 2.27. Table 2.4 shows the strike and protection detail that was studied by Napolitano et al *[146]*. Figure 2.28 shows the measured voltage waveform of the first strike of flash 62676 and Figure 2.29 for the second strike. It is visible that the first strike was negative, but the first cycle of the surge voltage is positive. The second strike was also negative and so was the voltage polarity. The author did not mention an important finding that the first strike was nearby to the line while the second one was direct to the line.

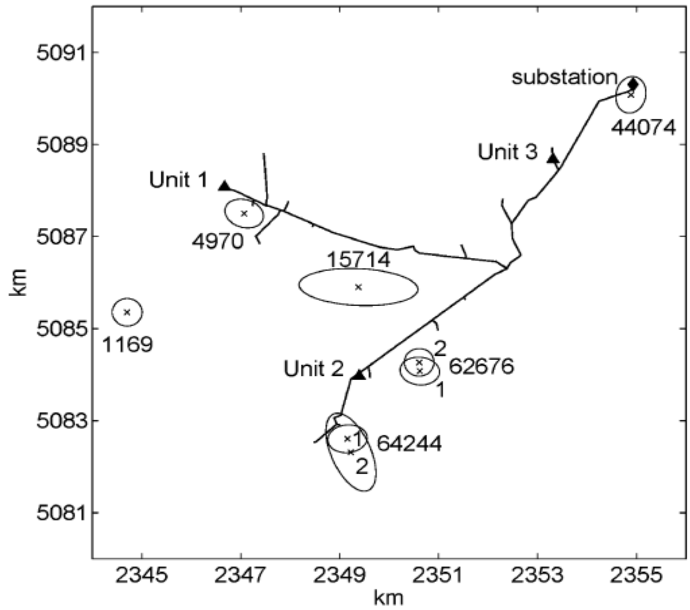

Figure 2.27 An Italian network that was studied where Units 1 to 3 are voltage recorders. The cross and ellipse are the lightning strike location with the accuracy probability [146]. Permission obtained from the ScienceDirect Elsevier Electric Power System Research.

Table 2.4 Details of the strike and the protection operation. Permission obtained from the ScienceDirect Elsevier Electric Power System Research.

Flash event number	15714	62676	64244
Date	May 15, 2007	June 15, 2007	June 15, 2007
Stroke1			
LLS time stamp	14:30:20. 627983052	16:30:20. 511131173	16:41:49. 626720476
Peak current (kA)	8.7	– 10.3	– 11.2
Error ellipse axes (m)	1200 and 400	400 and 300	400 and 300
Related voltage transient	Fig. 6	Fig. 7	Fig. 11
Trigger time delay (μs)	9.9 (Unit 1) 39.2 (Unit 2)	40.6 (Unit 1) 2.8 (Unit 2) 18.2 (Unit 3)	42.8 (Unit 1) −37.7 (Unit 2) 29.9 (Unit 3)
Stroke 2			
LLS time stamp	–	16:30:20. 566098022	16:41:49. 670654962
Peak current (kA)	–	−11.5	−10.4
Error ellipse axes (m)	–	300 and 300	900 and 400
Related voltage transient	–	Fig. 8	Fig. 12
Trigger time delay (μs)	–	31.6 (Unit 1) 3.6 (Unit 2) 15.7 (Unit 3)	23.7 (Unit 1) −0.6 (Unit 2) 43.5 (Unit 3)
Directional relay activation	–	16:30:20.57	16:41:49.64
Overcurrent relay activation	14:30:20.74	16:30:20.54	16:41:49.65
Circuit breaker tripping	–	16:30:20.66	16:41:49.73
Directional relay deactivation	–	16:30:20.74	16:41:49.79
Overcurrent relay deactivation	14:30:20:74	16:30:20.74	16:41:49.80
Circuit breaker reclosing	–	16:30:21.13	16:41:50.20
Circuit breaker opening transient	–	Fig. 9	Fig. 13
Circuit breaker closing transient	–	Fig. 10	Fig. 14

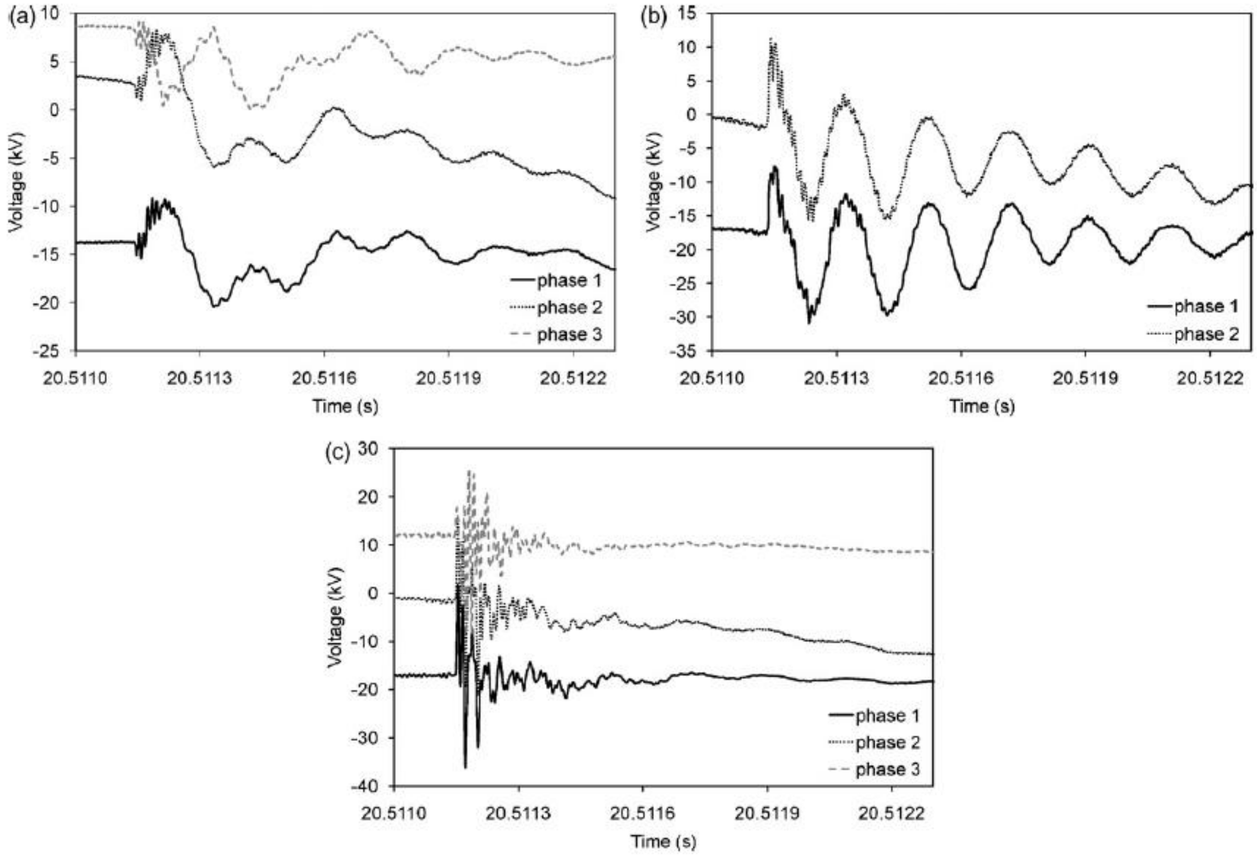

Figure 2.28 The voltage waveforms in graphs a to c were recorded on units 1 to 3 respectively for flash 62676 strike 1 [146]. Permission obtained from Fabio Napolitano.

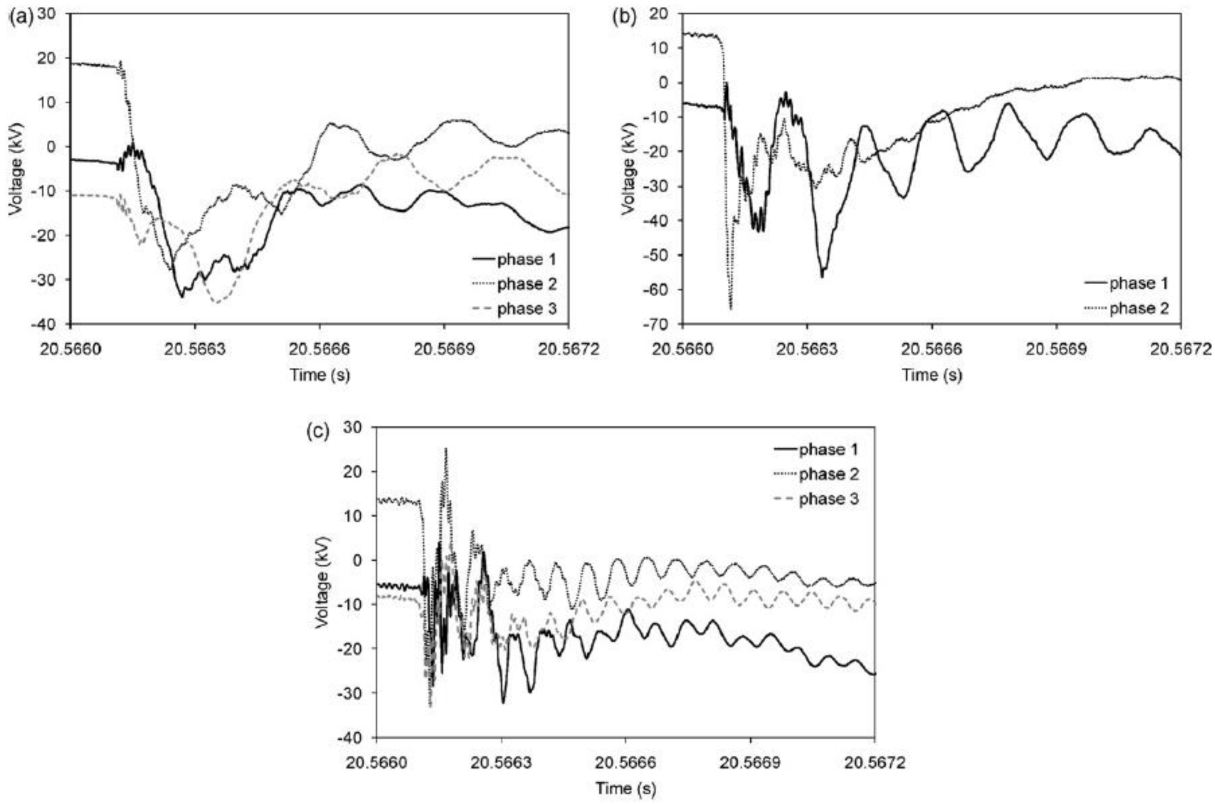

Figure 2.29 The voltage waveforms in graphs a to c were recorded on units 1 to 3 respectively for flash 62676 second strike [146]. *Permission obtained from Fabio Napolitano.*

2.9 The effect of arc quenching on lightning performance measurements

Protection operation was normally used to determine if lightning caused a line flashover. It was necessary to do actual recordings of the voltage and current on the test feeder as some of the faults may quench before the protection operation was activated. Actual measurements on live lines using natural lightning required special measurement equipment with proper surge protection as well as fast sampling rates. Fast sampling rates over long periods will result in a need for huge data storage capabilities.

Power frequency arc-quenching can take place [108] [2] after a lightning strike (direct or nearby to the line) caused a line flashover which might be followed most of the time by a power frequency fault current. Figure 2.30 shows an example of such an event. This would underestimate the actual lightning performance (shows fewer faults) of a line should the protection operation be used to determine line faults due to lightning.

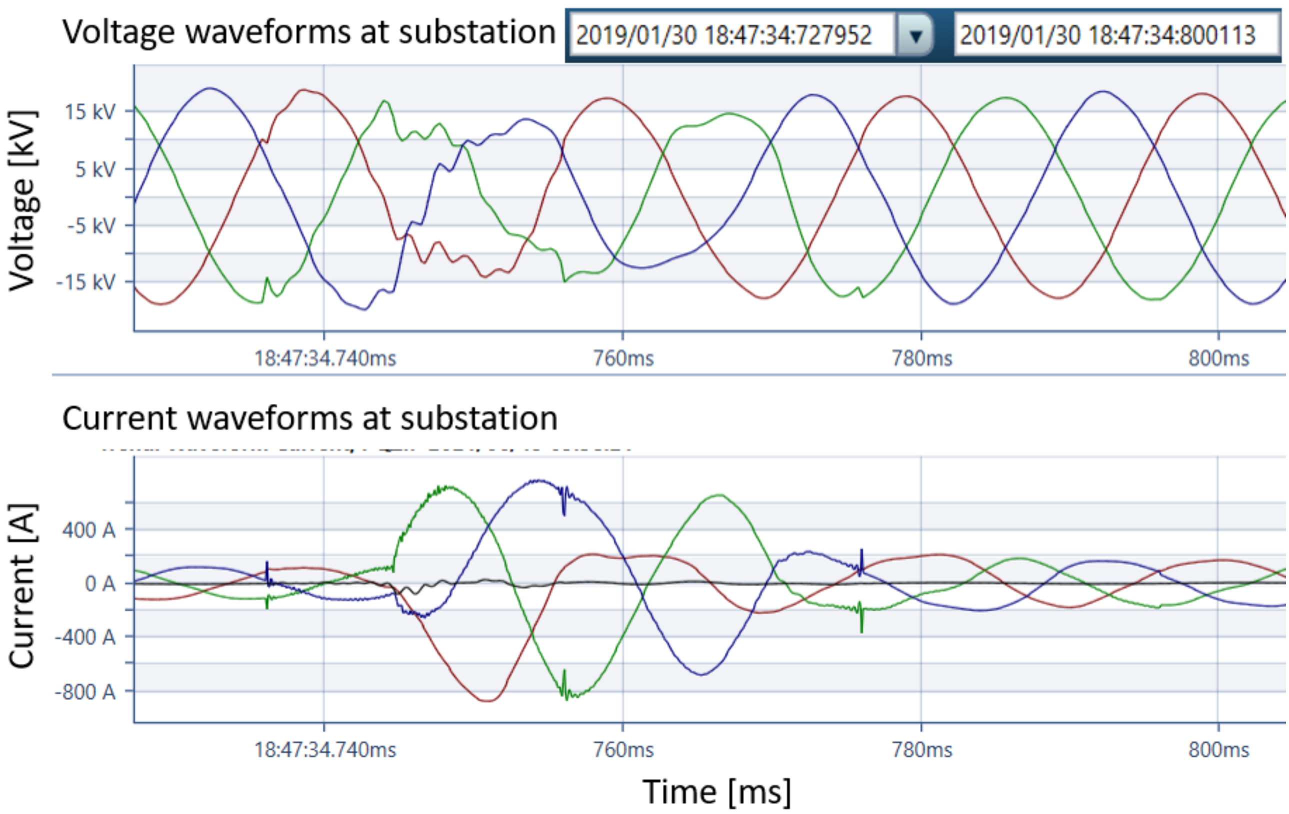

Figure 2.30 Example of arc-quenching of a power frequency 3 phase fault caused by a direct lightning strike as shown in Figure 2.31. The fault was quenched before the breaker operated.

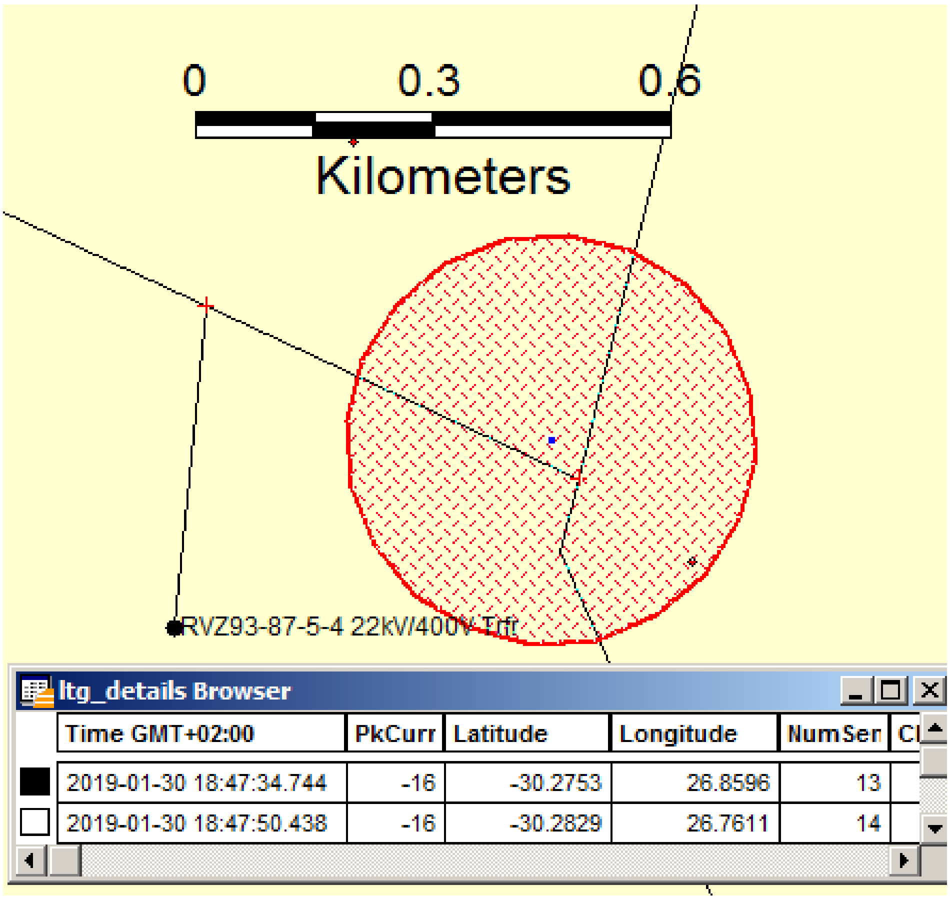

Figure 2.31 The direct lightning strike to the feeder that caused a line flashover shown in Figure 2.30.

Table 2.5 shows the number of lightning-related faults on an 11 kV line where the power frequency arc was quenched [108]. Of the 52 power frequency faults, 31 were quenched. A large number of nearby lightning strikes were present in comparison to the direct lightning strikes to the line as was also found by Rusck [147]. Table 2.6 shows a lightning investigation on a 22 kV line over eight years involving 12195 lightning flashes [148] causing 266 lightning-related which 42% of the faults quenched were before breaker operation. Similar work was done by Miyazaki et al [123] as shown in Table 2.7 where some of the fault currents also were quenched before circuit breaker operation. Figure 2.32 shows a summary of the work done by Miyazaki [123]. It was noted that several direct lightning strikes to the pole-top resulted in a line fault which caused the upstream circuit breaker to trip. One fault was initiated by a direct lightning strike to a pole-top fitted with a surge arrester. It was also noted that the author acknowledges that in some cases the exact termination point of the lightning strike captured by the camera, was difficult to establish due to bad weather.

Table 2.5 Number of trips and arc-quenching due to direct and nearby lightning on an 11 kV line [108].

TBP 11 kV feeder faults due to lightning March 2008 to February 2009					
Direct Flashes: 52			Nearby Flashes: 2078		
Phase to Phase faults	Single-phase to earth faults	No breaker trip	phase-to-phase faults	Single-phase to earth faults	No trip
15	6	31	0	0	2078

Table 2.6 A summary of the circuit breaker operations caused by lightning on the GAKG line. All nearby lightning flashes within 1 km of the line were tabled [2].

	Direct lightning			Nearby lightning (11929 flashes)		
Year ending February	Phase-phase faults (breaker operation)	Single-phase faults (breaker operation)	Faults quenched before breaker operation	Phase-phase faults	Single-phase faults	Did not cause a flashover
2009	15	0	18	0	0	1603
2010	34	9	9	0	0	2062
2011	30	2	28	0	0	1983
2012	26	3	14	0	0	2471
2013	14	0	22	0	0	1091
2014	7	1	11	0	0	887
2015	4	0	6	0	0	1087
2016	9	0	4	0	0	745
Annual average	17.4	1.9	14	0	0	1491.1
	Direct lightning faults = 33.3			Nearby lightning = 1491.1		

Table 2.7 Observations of specific lightning strikes that caused flashovers but not necessarily a circuit breaker operation due to arc quenching.

Case N0	Lightning phenomena				Relay operations in substations	Estimated current by LPATS	Remarks
	Lightning strike point	Number of flashover phases	Number of following current phases	Maximum insulator voltage (absolute value)			
1	Phase conductor	1 (R-phase)	0	150 kV (over range)	(no operation)	-41.5 kA	One phase flashover did not cause the line faults in this case
2	Pole head	0	0	50 kV	(no operation)	-43.32 kA	ZnO elements equipped with the struck pole probably prevented the flashover generation
3	Pole head	2 (R-,T-phases)	0	116 kV	(no operation)	-21.66 kA	This case suggested that AC following current spontaneously extinguished after flashover
4	Pole head	3	2 (R-,T-phases)	134 kV	OCR	-54.55 kA	
5	Pole head	3		67 kV	OCR	-35.35 kA	This case suggests that distribution line faults were caused by following strokes in a flash

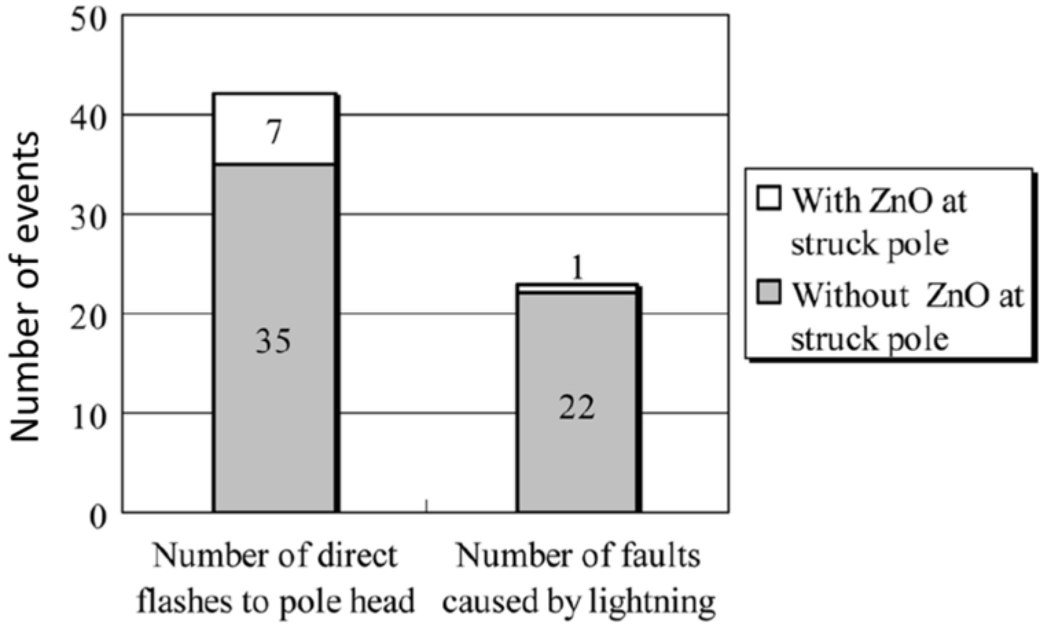

Figure 2.32 A summary of the work done by [123] showed that several faults were quenched before breaker operation. Permission obtained from the IEEE 2009.

2.10 The effect of line construction on the line flashover rate

The BIL in the midspan of the line is much higher than at the pole-tops. It is therefore relevant to know whether the lightning strike terminated midspan or on the pole-top. Oguchi et al [14] measured lightning surges and used cameras to record lightning strikes to the line. One of the findings was that lightning tends to terminate on the pole rather than on the shield wire (57% and 95% of lightning strikes terminate on the pole-tops with and without shield wires respectively as shown in Figure 2.46). However, if the shield wire cap (450 mm high) is left on the pole, 100% of the strikes terminate on the pole. Although poles with earthed points that extend higher than 450 mm above the phase conductors can replace the effect of shield wires (have a positive effect), surges due to nearby flashes will be of higher amplitude when the shield wire is removed [32] [149]

Pattern	Lightning flash to	No. of lightning flashes	
①	Pole head	31	(57%)
②	Ground wire	18	(33%)
③	Power line	2	(4%)
	Others	3	(6%)
	Total	54	(100%)

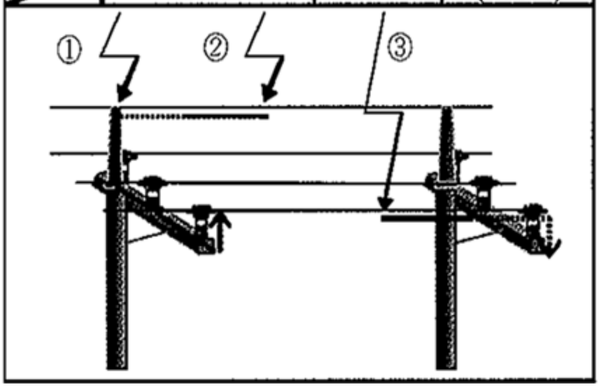

Pattern	Lightning flash to	No. of lightning flashes	
④	Pole head	18	(95%)
⑤	Power line	1	(5%)
	Others	0	(0%)
	Total	19	(100%)

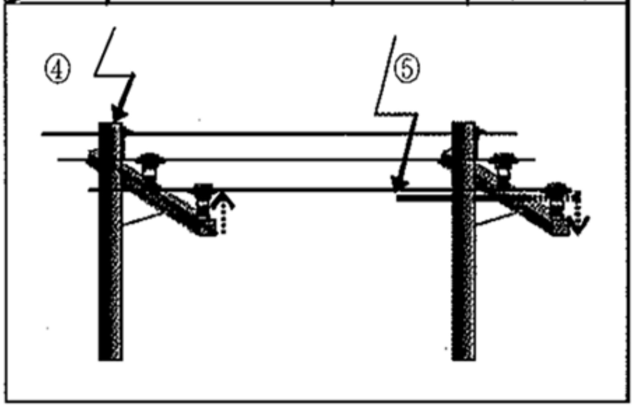

Figure 2.33 Lightning strike terminations on the line [14]. Permission obtained from the IEEE 2012.

Due to the distances along the shielding wire from the midspan to the pole and down the pole with some earth resistance as well, a midspan flashover might take place. In this case the pole BIL had not much effect. However, should a ground wire cap be left sticking out on top of the pole (and with no ground shielding wire), all lightning flashes terminated on top of the pole. In this study, it was found that only 7 out of 248 nearby (indirect) lightning strikes caused line faults as seen in Figure 2.34. Oguchi concluded that this 6.6 kV line with only the insulators contributing to the BIL, is resistant to nearby strikes. The BIL of the insulators was not mentioned.

It can therefore be concluded that the literature with regards to measured lightning events and resultant effects on distribution networks has inaccuracies. These inaccuracies can be ascribed to the fact that no accurate distinction was made between direct and nearby lightning strikes to long lines in the absence of cameras. The shortfall will be addressed in this thesis.

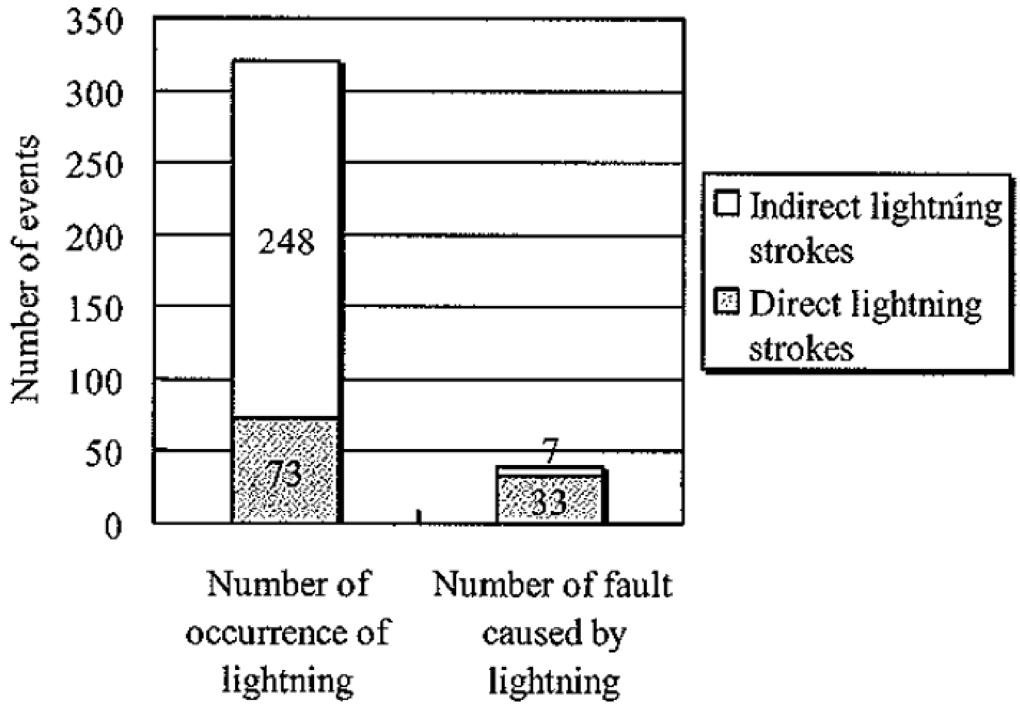

Figure 2.34 Results of Oguchi's research [14]: Lightning events that are related to line faults. A small number of faults were due to nearby lightning strikes. Permission obtained from the IEEE 2012.

2.11 Line construction and insulation levels

HV lines (44 kV and above) with overhead shield wires are designed to withstand nearby lightning strikes as well as low amplitude direct lightning strikes should the tower footing resistance values be low enough. The design objective is for the lightning to terminate on the overhead shield wires and not directly on the phase conductors. If low earth resistances cannot be achieved, line surge arresters can be used to prevent flashover to the phase conductors.

The insulation level of an unshielded MV line will not be sufficient to prevent a line flashover due to a direct lightning strike should there be no surge arrester in close proximity. Flashovers might occur at multiple poles until the remaining LIOV amplitude is less than the line's BIL [11]. The higher the earth resistance, the more flashovers will take place.

The lower the BIL, the lower will be the amplitude of the remaining LIOV that propagates to equipment (mainly surge arresters, fuses and transformers) installed on the line. Secondly, less energy will be dissipated in the surge arresters as most of the lightning current will be diverted to the ground at the points where flashovers occurred. It is therefore advantageous from this point of view to ensure that the line's BIL is as low as possible. The ideal will be to install surge arresters on each pole, but this will result in high capital and maintenance costs.

A balance needs to be found between lowering the BIL, the acceptable flashover rate due to nearby lightning strikes and damage to equipment due to direct lightning strikes. The weakest point of the line insulation is at the poles. Several factors influence the line's pole design to satisfy the required BIL to minimise flashover due to indirect lightning strikes.

Objects such as trees, buildings, telecommunication structures, high ground, and other tall objects along the line have both a negative and a positive influence on the flashover rate of the line [12]. Other design parameters such as surge arrester installation, phase conductor height above the ground, overhead shield wire, and low ground resistivity reduce the induced lightning surge amplitude [32]. The lightning flash parameters (mainly rise time, lightning channel tortuosity and the angle between the lightning channel and the line) also influence the LIOV amplitude along the.

2.12 Pole construction of the research line

The intention was to design the RVZ line according to a 300 kV philosophy which was implemented on most of the line suspension poles as shown in Figure 2.35. The reason for using wood as part of the insulation was to increase the line BIL at a low cost to improve the nearby lightning performance of the line during lightning storms [150]. A flashover (due to high LIOV) along a wood path is characterized by a relatively high residual arc voltage which gives the wood some arc-quenching properties [150]. Strain poles with stays had a BIL of 150 kV (only the insulator BIL) as shown in Figure 2.36. The strain poles also effectively lower the suspension poles' BIL.

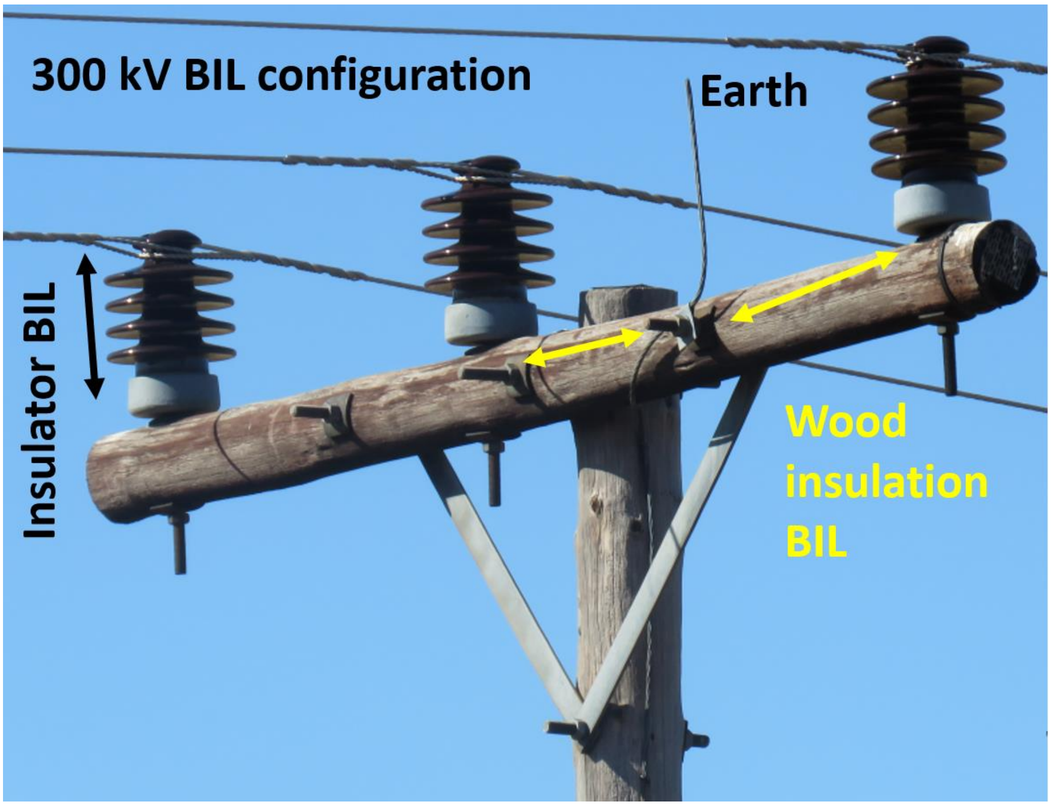

Figure 2.35 A suspension pole-top with a 300 kV BIL configuration. Wood was used to increase the pole-top BIL to 300 kV.

Figure 2.36 A pole-top configuration of a strain pole with stays. The BIL was limited to the insulator BIL of 150 kV. The contribution of the stay insulator to the BIL was negligible.

2.13 Design philosophy

Measurements done by Geldenhuys [11] showed that induced voltages on 8 – 10 m unshielded distribution lines occasionally exceed 200 kV but seldom exceed 250 kV. A 300 kV BIL line should therefore be able to withstand most of the nearby lightning-induced voltages.

As there are many more lightning strikes adjacent to the line compared with direct strikes to the line, the focus was mostly to ensure that as few as possible line trips occurred due to nearby lightning strikes. The biggest challenge was to model the line correctly. The model was influenced by the number of surge arresters, insulation level, soil resistivity [92] (which is also weather dependent), earthing configuration, screening by other objects [32] and the construction of the line. These factors vary along the line and the design along the line often changes due to practical reasons. Several field and theoretical studies [151] [120] [138] [152] [122] [15] were done to determine the optimal line configurations and use of protective devices.

2.13.1 Shielding by adjacent objects

Figure 2.37 shows the effect of tall objects along the line as presented in the IEEE standard. The further away the object, the lower the shielding factor. The shielding factor can be defined as the lightning protection that an object next to the line gives to the line itself.

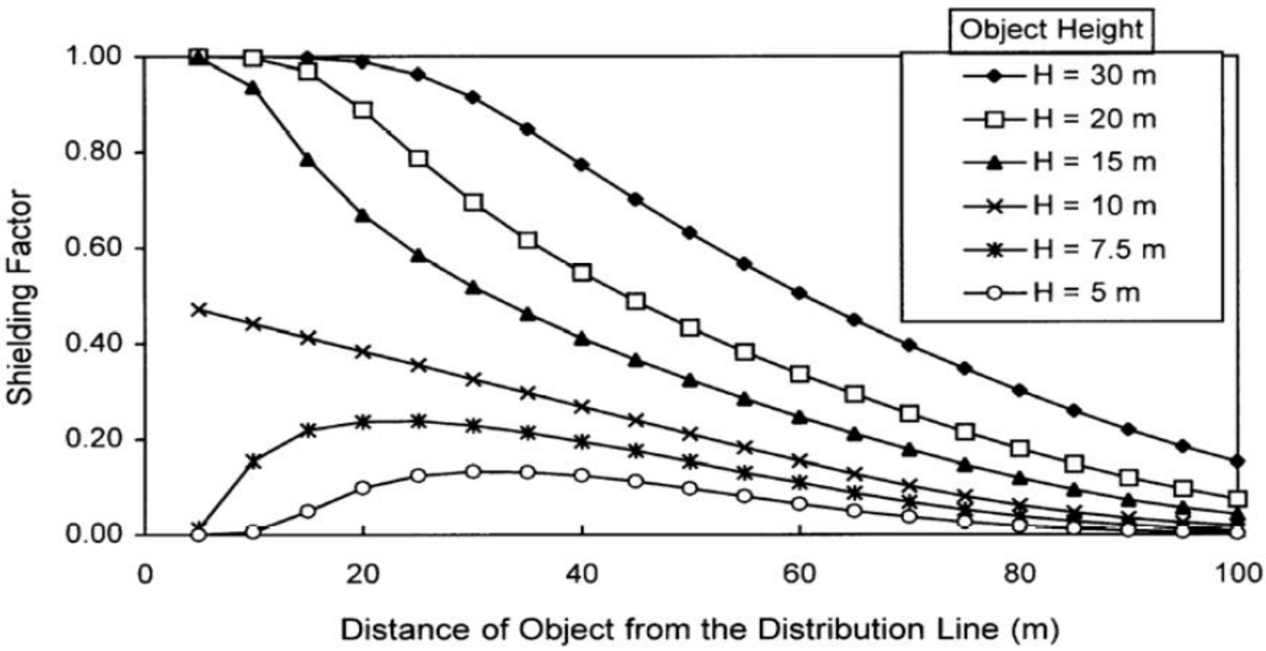

Figure 2.37 Shielding factor due to objects of different heights along the line [12]. Permission obtained from the IEEE 2010. Adjacent objects also attract lightning closer to the line.

The environment along the RVZ research line consisted mostly of flat grasslands and very few high trees and high ESOs were found close to the line.

2.13.2 Influence of the Overhead Ground Wire

The Overhead Ground Wire (OGW) on MV lines has three basic functions. One is to protect the line by ensuring that the lightning current terminates on the OGW. Another is to conduct the lightning current to earth and the third is to reduce the LIOV on the line due to the electric field caused by nearby lightning. As shown by Jooste et al [153] and Mafatle et al [154], the choice of shield wire material is very important. Copper and aluminium conduct lightning current with a volt drop up to 100 times lower than steel (due to the skin effect) [153]. Steel overhead ground wires may flash over to the phase conductors for midspan lightning current terminations [154]. The effectiveness of the Overhead Ground Wire (OGW) is very dependent on the number of grounding points and the value of the pole footing earth resistance. Should there be only one earth point on the OGW, the formula for describing the voltage U_G on the phase conductor is given [155] [156] as:

$$U_G(t) = I_G \times \left({}^{Z_G}/_{2} + R \right) \tag{20}$$

- where I_G is the current through the earth point (in A), Z_G the surge impedance of the OGW (in Ω) and R is the pole footing earth resistance (in Ω).

Figure 2.38 shows the effect of the shield wire on the induced voltage due to nearby lightning on the line. For the condition considered in [149], the shielding factor, which is the ratio between the induced voltage on the line with and without the shield wire, is between 55% and 70%.

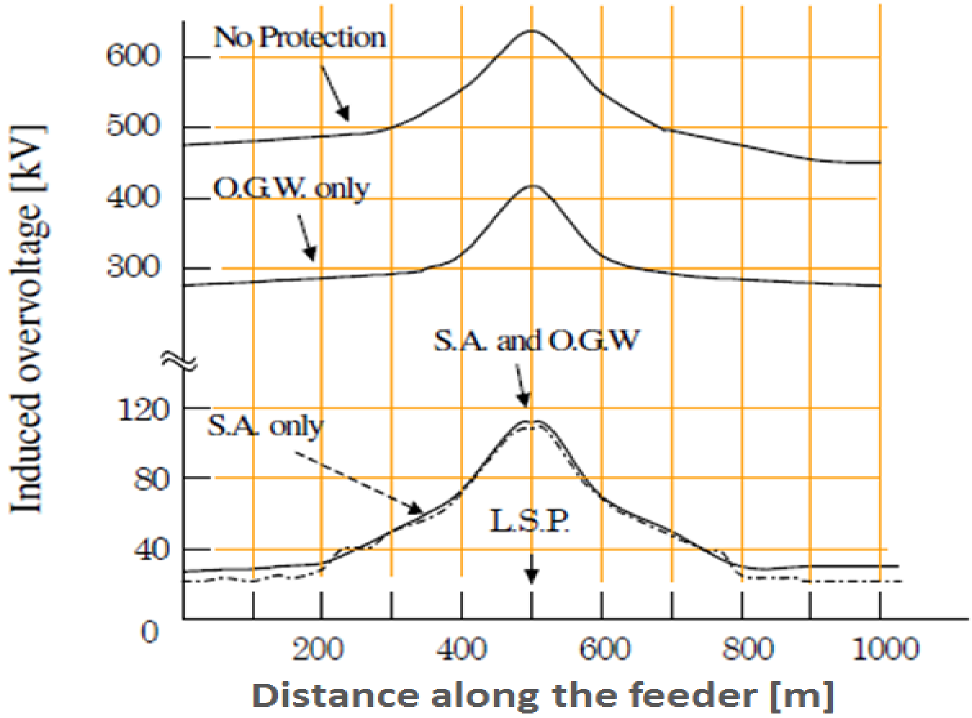

Figure 2.38 The effect of OGW on induced voltages for a nearby lightning flash. LSP is the Lightning Strike Point, SA indicates the presence of surge arresters. The distance between the LSP and the line was 50 m [149]. Permission obtained from IEEJ Trans 2007.

The overhead ground wire contributed significantly to a floating line in reducing induced surge amplitudes on the phase conductors due to nearby lightning strikes.

2.13.3 Surge arresters

Line surge arresters are the component that contributes most to an improved lightning performance of a line. It reduces the induced overvoltages on the line if the induced voltage exceeds the surge arrester protective level. The shorter the distances between the surge arresters the lower the induced surge voltages. Figure 2.39 shows a significant reduction in the induced surge voltages on the line if there are surge arresters close to the lightning termination point [149].

Piantini et al [157] [158] used a simulation model [110] to calculate the voltage on an MV line induced by a 38 kA stroke 70 m away with and without surge arresters. The result is shown in Figure 2.40. It can be seen that line surge arresters placed 300 m apart caused a reduction in surge voltage of more than 50%. However, should the surge arresters be further apart (600 m) the effect on the induced voltage became much less.

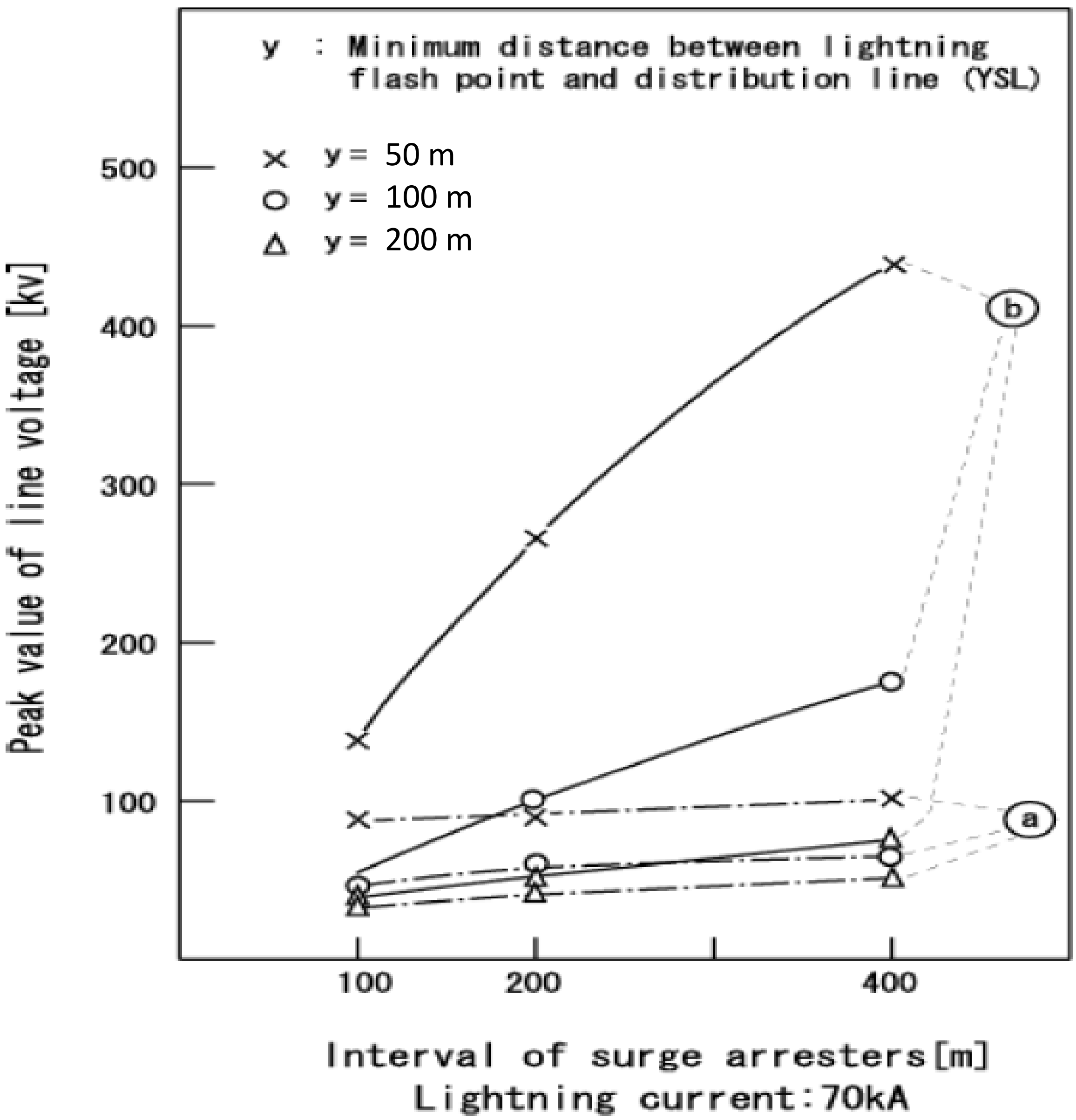

Figure 2.39 The effect of line surge arresters on the lightning-induced voltages on the line where a is where the lightning strike point is closest to a pole fitted with surge arresters and b is where the lightning strike point is closest to the midpoint between surge arresters [149]. Permission obtained from IEEJ Trans.

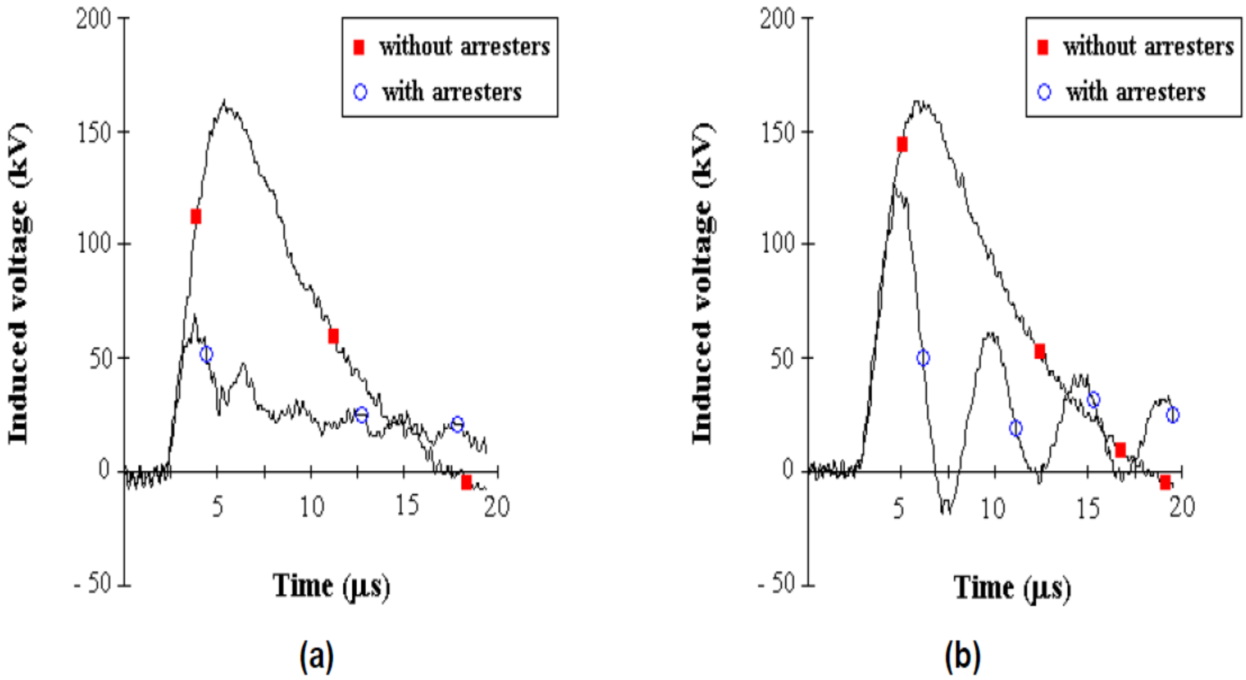

Figure 2.40 The induced voltage on a line with and without a surge arrester due to a lightning strike 70 m from the line with surge arresters spaced every 300 m (a) and every 600 m (b) [157]. Permission obtained from Alexandre Piantini.

Borghetti et al [159] did a comparison between lightning-induced overvoltages on a line with and without surge arresters. The line configuration used is shown in Figure 2.41. Strike location 2 was taken for the illustration. Should surge arresters be installed at each transformer, the induced voltages at the transformers were reduced. Figure 2.42 shows voltage peaks at the T-offs and the transformer points without any surge arresters installed. This was due to wave reflections from the transformers that were seen as a high impedance to the ground for voltage surges. After surge arresters were added, the induced surge voltage amplitude was reduced significantly as shown in Figure 2.43. The surge voltage amplitude reduced from 133 kV to 61 kV at transformer 1 (comparing Figure 2.42 and Figure 2.43). However, there were no changes in induced voltage on the line closest to the strike. This was due to the relatively high impedance (in the high-frequency range) between the point of termination and the closest surge arrester. Figure 2.44 shows the voltage at the point in the line closest to the nearby lightning strike termination point with and without surge arresters. The surge arresters reduced the induced voltage significantly to safe values. Should surge arresters be installed at the T-offs as well, the highest induced voltage was 73 kV (at T_0) which was a significant reduction from 167 kV (at the point in the line that was closest to the nearby lightning strike) as shown in Figure 2.45.

Surge arresters do make a significant contribution to reducing the LIOVs on the line. However, in practice one would have to make sure that surge arresters are well earthed and soil ionization and pole footing earth resistance need to be considered to calculate the LIOV more reliable.

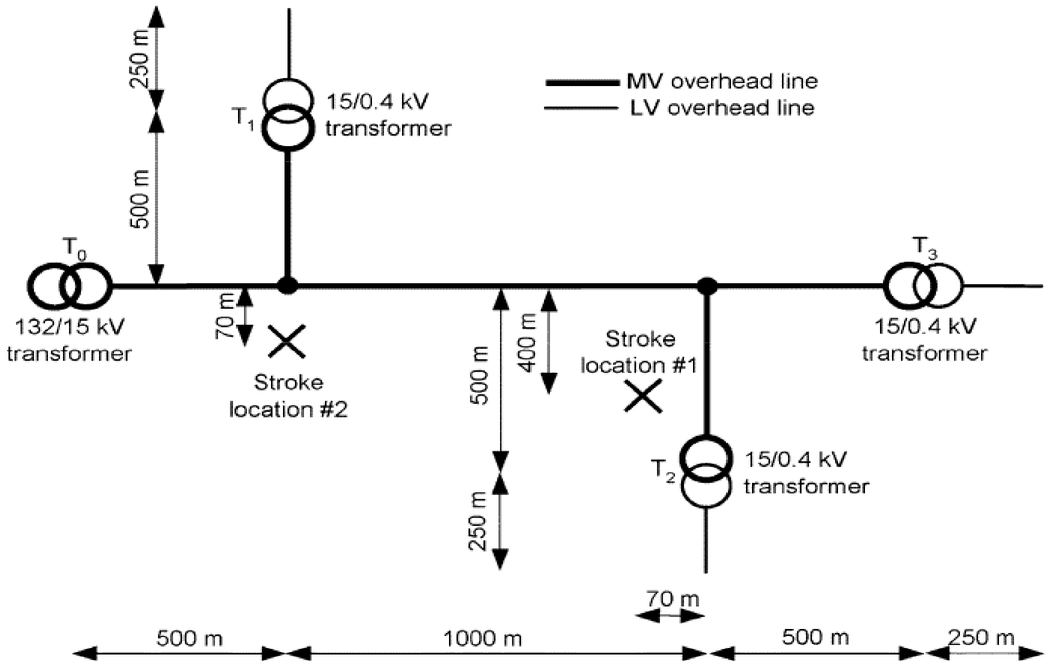

Figure 2.41 Line configuration studied by Borghetti et al to show the effect of surge arresters. The strike at location 2 will be used for the calculations [159]. Permission obtained from the IEEE 2009.

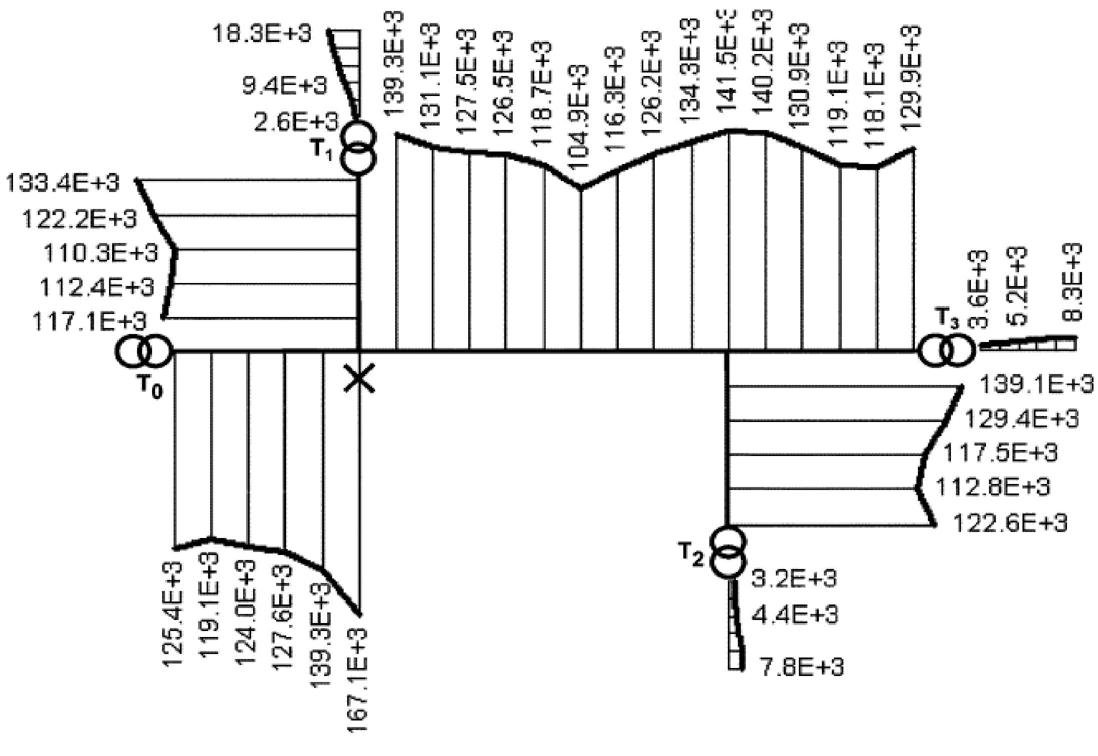

Figure 2.42 The induced overvoltage along the line without any surge arresters [159]. Permission obtained from the IEEE 2009.

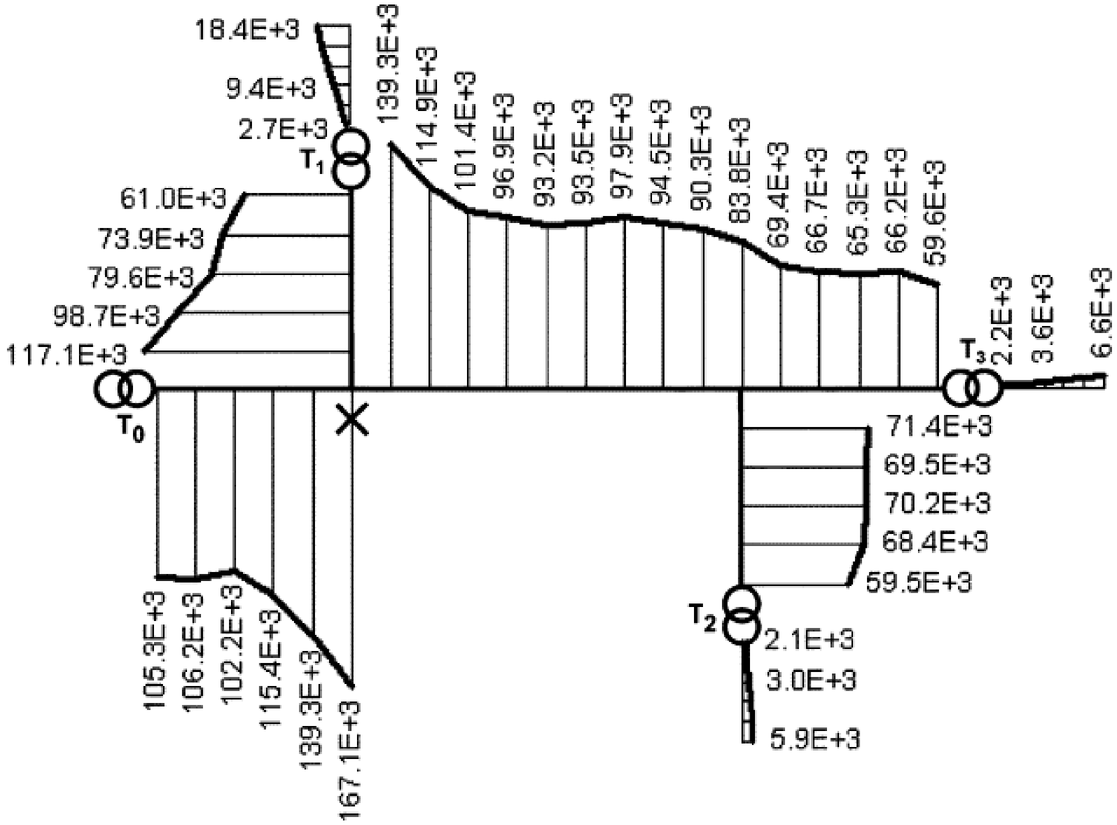

Figure 2.43 Induced voltages along the line with surge arresters installed at all the transformers [159]. Permission obtained from the IEEE copyright 2009.

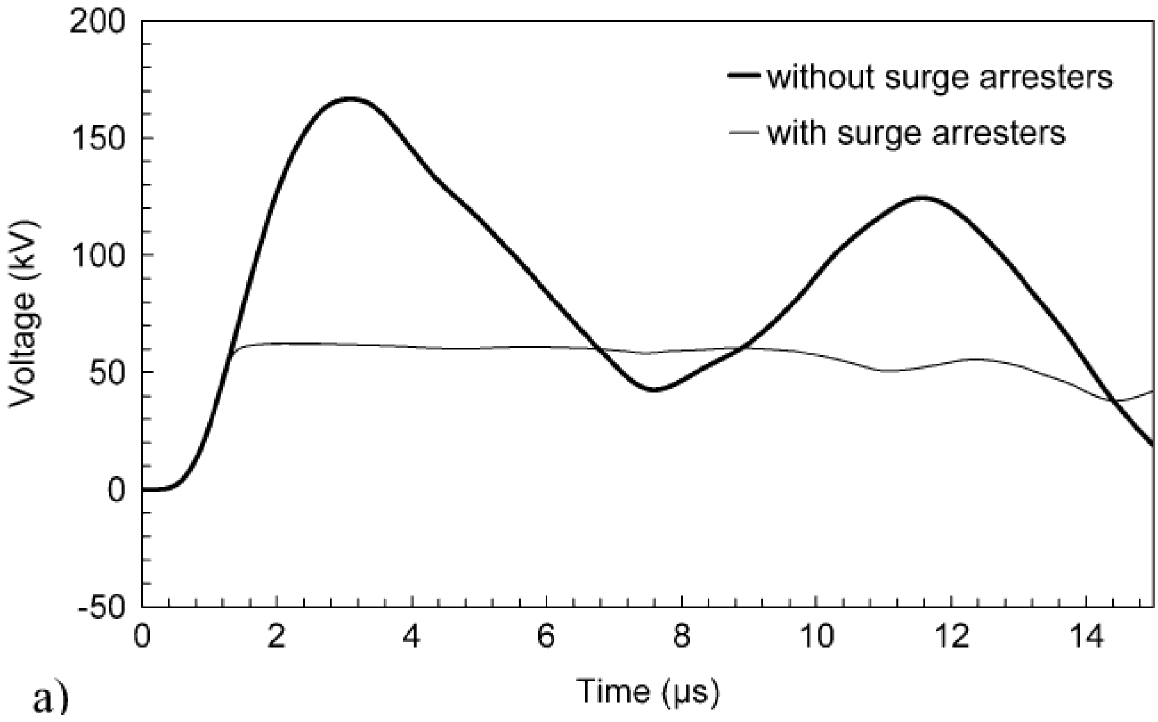

Figure 2.44 LIOV at the point in the line that is closest to the nearby lightning strike with and without surge arresters [159]. Permission obtained from the IEEE 2009.

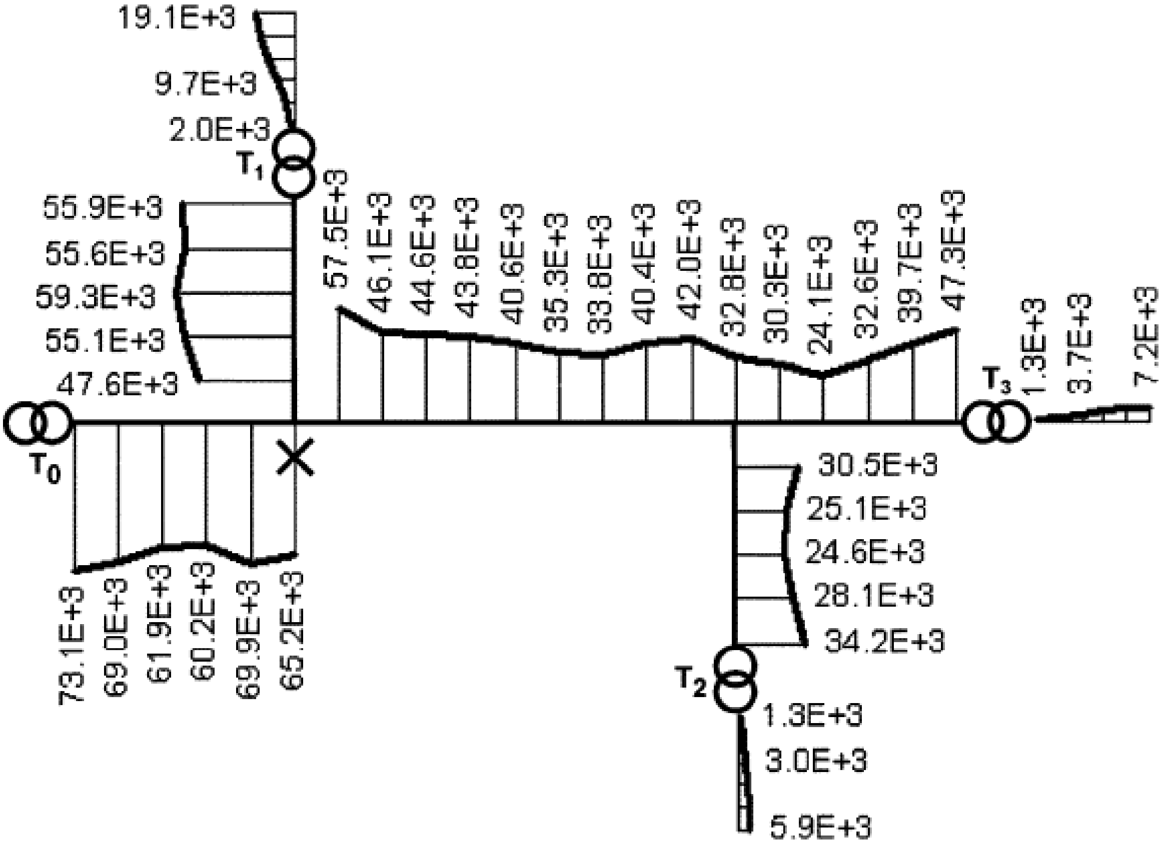

Figure 2.45 Surge arresters installed on the transformers as well as on the T-offs [159]. Permission obtained from the IEEE 2009.

Nucci et al [17] used the Monte Carlo method to generate random strikes and varied the peak value of the lightning current I_f, its front time t_f, the strike location and the value of the voltage for each phase. These strikes were uniformly placed around a 1.8 km line in lossy ground. Surge arresters were placed at different locations along the line. Figure 2.46 shows that there are about 160 times more incidents where the induced voltage exceeded 150 kV should the surge arrester spacing be 1800 m instead of 150 m in ideal ground conditions.

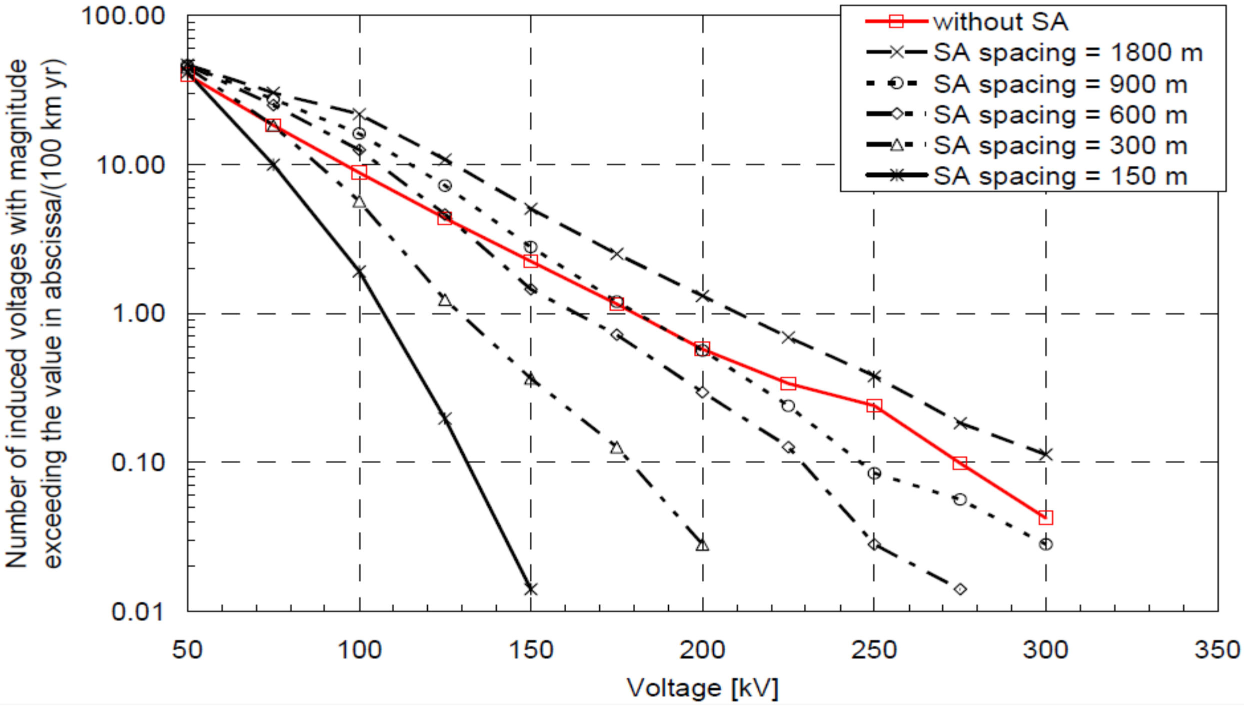

Figure 2.46 The effect of the lightning-induced overvoltage on an MV line at different line surge arrester intervals for a ground- flash density of 1 ground flash/km^2/year [17]. Permission obtained from the IEEE 2010.

Figure 2.47 shows the influence of the line surge arrester spacing on the lightning-induced overvoltage on an MV line according to IEEE Std 1410 2010 [12].

IEEE Std 1410-2010
IEEE Guide for Improving the Lightning Performance of Electric Power Overhead Distribution Lines

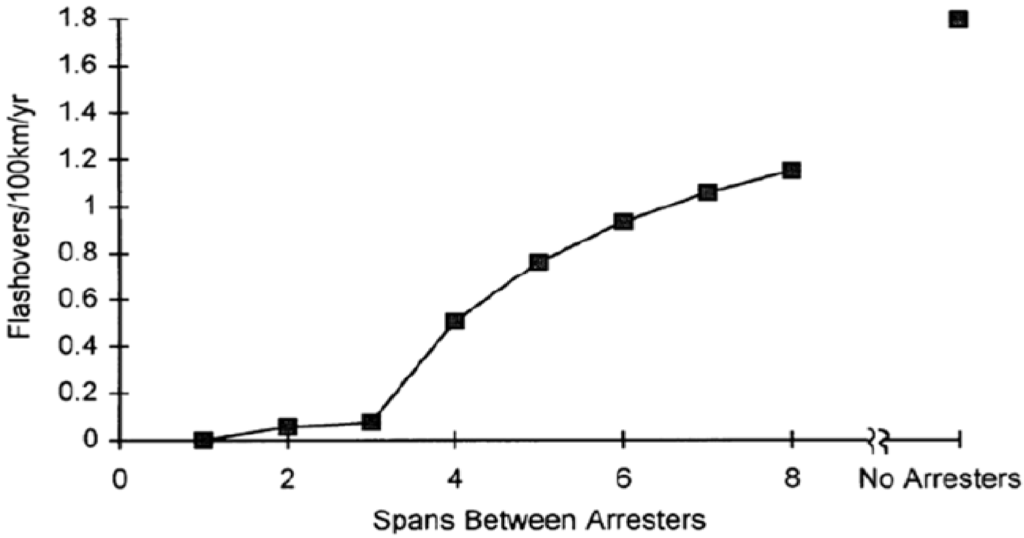

NOTE—CFO=150 kV, h=10 m, N_g = 1 flash/km^2/yr, span length = 75 m

Figure 2.47 Typical influence of the surge arrester spacing on the lightning-induced overvoltage [12]. Permission obtained from the IEEE 2010.

All the work mentioned in this section indicated that especially with surge arresters placed at intervals less than 200 m apart, there was a significant reduction in the lightning-induced overvoltage on the line.

2.14 Summary of relevant findings of literature survey

Lightning activity on MV lines was measured by several researchers. Several parameters were not available reliably to distinguish between nearby lightning and direct lightning strikes to the line and also to configure the data in a format that could be compared to the IEEE 1410-2010. Although the lightning return-stroke models as well as the electromagnetic coupling models between the return-stroke and the line were accurate, many assumptions had to be made to simulate cases where natural lightning was used for simulation (not all the relevant lightning channel data and accurate distance between the ground-termination point and the line was always available). However, the lightning performance estimation for long operational lines based on the existing methods and models could not be successfully verified by measurement due to cost and logistical support.

The geographical inaccuracy of the LDN was the main reason why the existing methods could not be used to model or measure the lightning performance of long operational lines. The number of cameras needed to capture the position and tortuosity of the lightning return-stroke reliably was also not feasible on long lines. Furthermore, the LIOV attenuated to such an extent that it could not be used to trigger instruments to start recording. No research could be found where the LGC was measured (neither the amplitude nor the polarity) or used to trigger an instrument. A lack of reasonable accurate field data to be used in existing lightning return-stroke models and electromagnetic coupling models yielded inaccurate results.

A very useful measurement in previous research was that the LIOV on the line changed polarity at about 250 m from the nearby lightning return-stroke as shown in Figure 2.48 [120] and models (Figure 2.49 [160]). This principle was used to analyse measurements at the substation (further than 250 m from the return-stroke point of ground termination) to distinguish between nearby lightning strikes and direct lightning strikes to the line.

The changing environment and line parameters along a long operational line made it difficult to determine whether a nearby lightning return-stroke would result in a LIOV that exceeded the BIL of the line. Some previous research used the protection operation to determine whether the LIOV exceeded the BIL of the line, but it could result in an error of between 38% and 40% due to arc quenching (the fault current was independently quenched before protection or breaker operation). However, this principle was refined in this research by continuous measurement (not using the LIOV to trigger the instruments) and it could be used to overcome the error due to arc quenching.

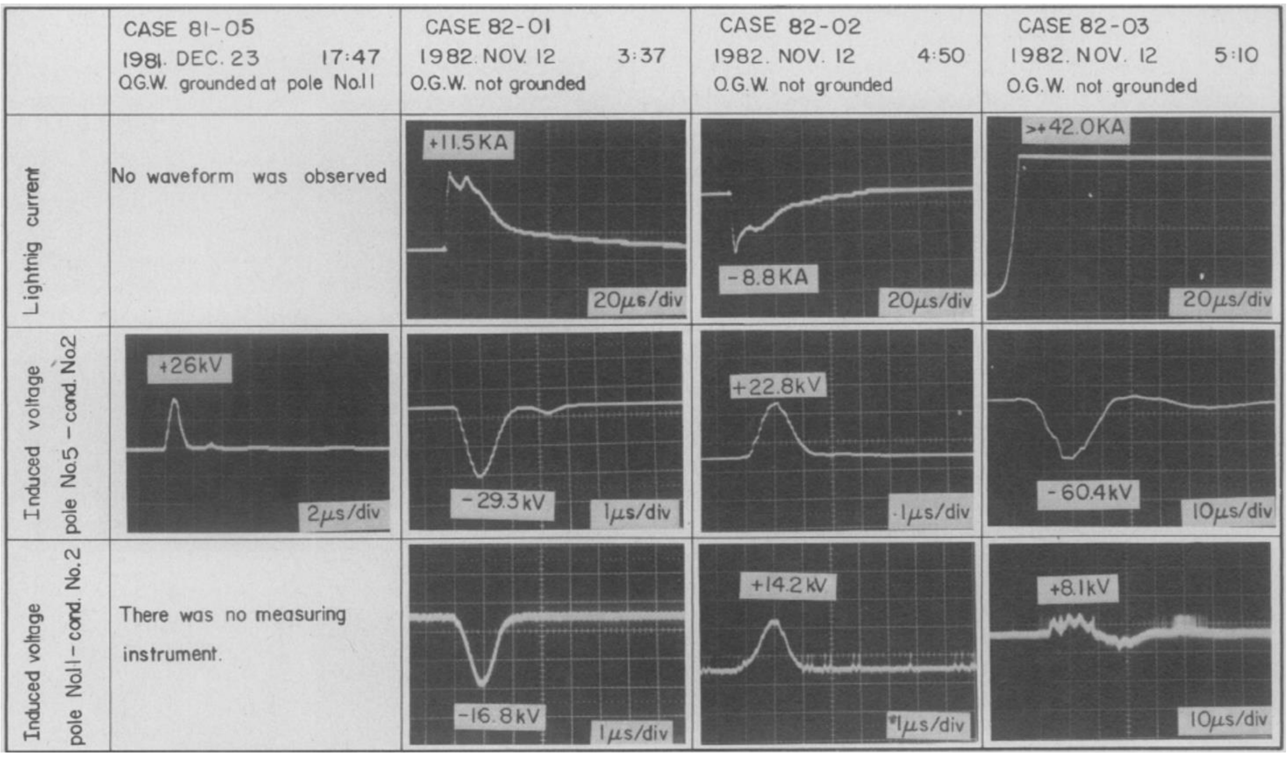

Figure 2.48 Recordings on an MV line of lightning terminated on an ESO that was 200 m from the line [120]. Permission obtained from the IEEE 1986.

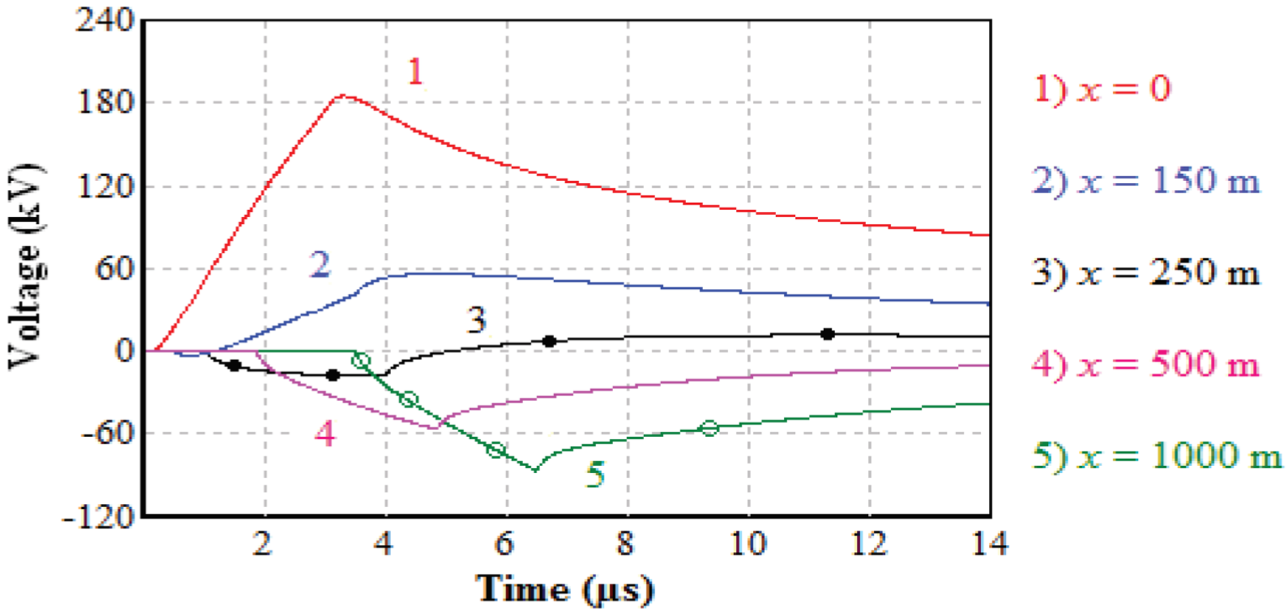

Figure 2.49 The ERM shows that the LIOV on the line change polarity at about 250 m from the nearby lightning return-stroke due to the finite ground conductivity [160]. Permission obtained from Alexandre Piantini.

Previous research concluded that surge arresters improved the lightning performance of MV lines significantly. Surge arresters will contribute best to low LIOVs if the surge impedance of the surge arrester earth leads as well as the earth resistance (of the earth configuration and soil) is low. The uneven spread of surge arresters and different earthing resistances of the surge arresters such as in long operational lines made accurate modelling of these long lines difficult.

3 THE RESEARCH METHODOLOGY

3.1 Area of study

An area with a high lightning Ground Flash Density (GFD) was chosen to create a significant lightning incident database with a high confidence level. The RVZ 22 kV line in the Free State, South Africa was used for data collection. The GPS coordinates in the middle of the line were -30.2732º south and 27.1558º east. The GFD along this line varied between 3 and 24 flashes per km² per year while the average soil conductivity for the area was between 0.01 S/m and 0.003 S/m.

3.2 Tools, equipment and software

The available tools consisted of the South African Weather Service's (LDN), the Alternative Transient Program (ATP) software, an advanced Quality of Supply (QoS) data logger and a fully equipped 714 km (including the branches) 22 kV operational MV line. Protection data, breaker operation information and Supervisory Control and Data Acquisition (SCADA) data were also available.

The ATP-EMTP simulation model that was developed by Høidalen [18] was used for simulating the coupling between nearby lightning and the line. The ATP-EMTP simulation model made use of the TL model for the lightning channel, the propagation effect of the electromagnetic field was modelled using the CR approximation and the Agrawal model was used for calculating the LIOV. The MV line was modelled using the JMarti model. The lightning parameters were adjusted to the information from the LDN for the lightning event that was measured or recorded.

The sampling speed of the ELSPEC recorders that were used was 400 kHz. The resistor dividers that were used as a backup VT, were exclusive non-inductive resistors with a voltage coefficient < 0.003ppm/V. A capacitor divider was also used to supply another backup recorder but was unreliable during wet weather.

The LDN information has two uses, one being live lightning data which is used by the Utility Control Centre for operational purposes and the other being Fault Analysis Lightning Locating System (FALLS) software that provided lightning flash detail that was used for this research. The ATP software is an interface to the Electromagnetic Transient Program (EMTP) to model LIOVs, LGCs, 50 Hz power supply and the operational line with all its equipment and loads. High-level protection operation information was available from the SCADA system while detailed protection operation was downloaded directly from the breakers.

3.3 Coordination of the instruments and the measurements

To obtain a statistically significant dataset of voltages, currents, LIOVs and LGCs on the line, a long (714 km that includes the branches) operational radial MV line in a high lightning density area was selected for studying lightning events. The lightning-induced voltages and currents were recorded with an advanced QoS data logger installed on the line at the substation. A second QoS recorder was installed in the middle of the line (as a reference when needed).

The QoS data recorders (loggers) were configured to:

- Continuously record the voltage and current on the line with a high sampling rate (400 kHz) to ensure that no lightning activity on or near the line will be missed. There was no need for a LIOV to trigger the recordings
- Calculate the zero sequence (common mode) current using the phase currents to monitor the LGC polarity
- Ensure that the data memory capacity was not exceeded by compressing the data while measurement was in progress

Data from the LDN was obtained to compare the lightning return-stroke information with the QoS logger recordings on the line. Should the recorded lightning strike polarity obtained from the LDN be opposite to the related measured LGC and LIOV, it was classified as a nearby lightning strike. Details of this process will be discussed in the Data analysis section. Incidents where the LIOV or LGV (due to either a nearby or direct lightning strike respectively) exceeded the BIL of the line were identified by a 50 Hz fault current due to the line flashover. Cases where nearby lightning caused a line flashover were identified and investigated to verify the BIL at that point of interest and to note any abnormalities on the line or equipment.

The results of the new methodology were then compared to the IEEE standard 1410-2010 by normalizing the average GFD in a 2 km buffer along the line as well as the number of lightning-related faults over the two years to the number of faults per year for a GFD of one flash per km² per year. This comparison will reveal the difference in the estimated lightning performance (according to the IEEE Std 1410-2010 for floating lines) and the real lightning performance of the operational line.

The result will be an indication to insulation coordination designers of the expected level of insulation overdesign should they use the IEEE Std 1410-2010 for floating lines (worst case scenario) as a base for their design.

3.4 Application of the tools, equipment and software

The amplitude of the LIOV on short floating lines (no equipment connected) could be accurately measured to determine whether it exceeded the BIL of the line by using high sampling rate recorders that were triggered by the LIOV. As the line was extended and energized (equipment connected), the LIOV attenuated to such an extent in relation to the 50 Hz voltage component that it cannot be used to trigger data loggers. Both the simulations and the measurements showed that in some cases the LIOV become invisible when superimposed on the 22 kV waveform. Simulations could be used in these cases to omit the 22 kV waveform and to reduce the voltage scale for the LIOV to become visible. This was the reason why the LGC was used to verify the polarity as it was superimposed on the zero-sequence current that was normally zero Ampere. Calculations to determine whether the LIOV exceeded the BIL of the line could also no longer be used as the actual point where the lightning terminated was unknown due to the LDN geographical error margin.

Traditionally the LIOV was measured to determine whether the LIOV exceeded the line BIL. Due to the distance (kilometres) between the lightning termination point and the measurement equipment, the LIOV amplitude attenuated in some cases to such an extent that it could not indicate if it exceeded the line BIL. A new approach whereby the LGC on the zero-sequence current was used to give the required information about the polarity of the lightning-generated charge on the line. One recorder at the feeder substation was sufficient to satisfy the need for the required power frequency and lightning data. The recorder was set to sample continuously to ensure that the required power frequency and lightning activity on the line could be captured. Data storage space was optimized by varying the recorder sampling speed and compressing the data while recording. This made it possible to capture data for months before it was necessary to download the recorder.

A new methodology to distinguish between nearby and direct lightning flashes was employed whereby the polarity of the LGC component that flowed through the NEC was measured. Under ideal conditions, the 50 Hz current component through the NEC was zero and the LGC superimposed on the zero-sequence power frequency current could easily be identified. A 50 Hz fault current on the line indicated that the LIOV exceeded the BIL of the line.

A cloud can be discharged to the ground along a lightning return stroke channel with a ground-termination point that is either on the line (direct lightning strike to the line) or nearby to the line as shown in Figure 3.1. In a case of a direct lightning strike to the line, the return-stroke current injected into the line will cause an LGV amplitude that has a 98% [12] probability of being higher than the line BIL at that point. There is a good chance that the LGV amplitude can be clamped at a voltage that is less than the line BIL and will prevent a flashover if there are well earthed surge arresters at that point in the line. The resultant LGV and LGC will flow along the line and attenuate due to surge arresters, the line surge impedance and other equipment impedances. The polarity of this LGV and the LGC injected into the line will be the same as the polarity of the lightning return-stroke [125] [120]**.** Part of the lightning-injected current will flow to earth through the NEC at the feeder substation. Due to the attenuation of the LGV along the line and the low source impedance at the substation, the LGV superimposed on the voltage of the 22 kV line may not be visible at the feeder substation in some cases. As the zero-sequence power frequency current was mostly less than 2 A, the component of the LGC superimposed on the zero-sequence current at the substation could easily be seen and was measured continuously with an advanced QoS recorder at a high sampling frequency rate (400 kHz) to determine the polarity of the LGC.

In the case of a nearby lightning strike, the current in the stroke generated a magnetic and electric field. The electric field could be divided into two components, namely a horizontal electric field and a vertical electric field (as shown in Figure 3.1) to determine the total electric field. The polarity of the LGC and LIOV due to the nearby lightning strike needed to be interpreted correctly for this research. The amplitude of the LIOV was mainly dependent on the lightning return-stroke current amplitude, soil conductivity, the channel tortuosity, channel inclination, the line height and the distance between the nearby lightning strike and the line. The polarity of the LIOV on the line very close to the nearby lightning strike was the same polarity as the return-stroke current. At some distance along the line, the polarity of the LIOV change to be opposite to the lightning return stroke if the soil conductivity is finite. Several models [12] showed that if a lightning strike terminates closer than 60 m to the line, it was normally attracted to the line and rather terminated direct to the line while LIOVs on the line due to nearby lightning strikes further than 1 km from the line were insignificant compared to the BIL of the line.

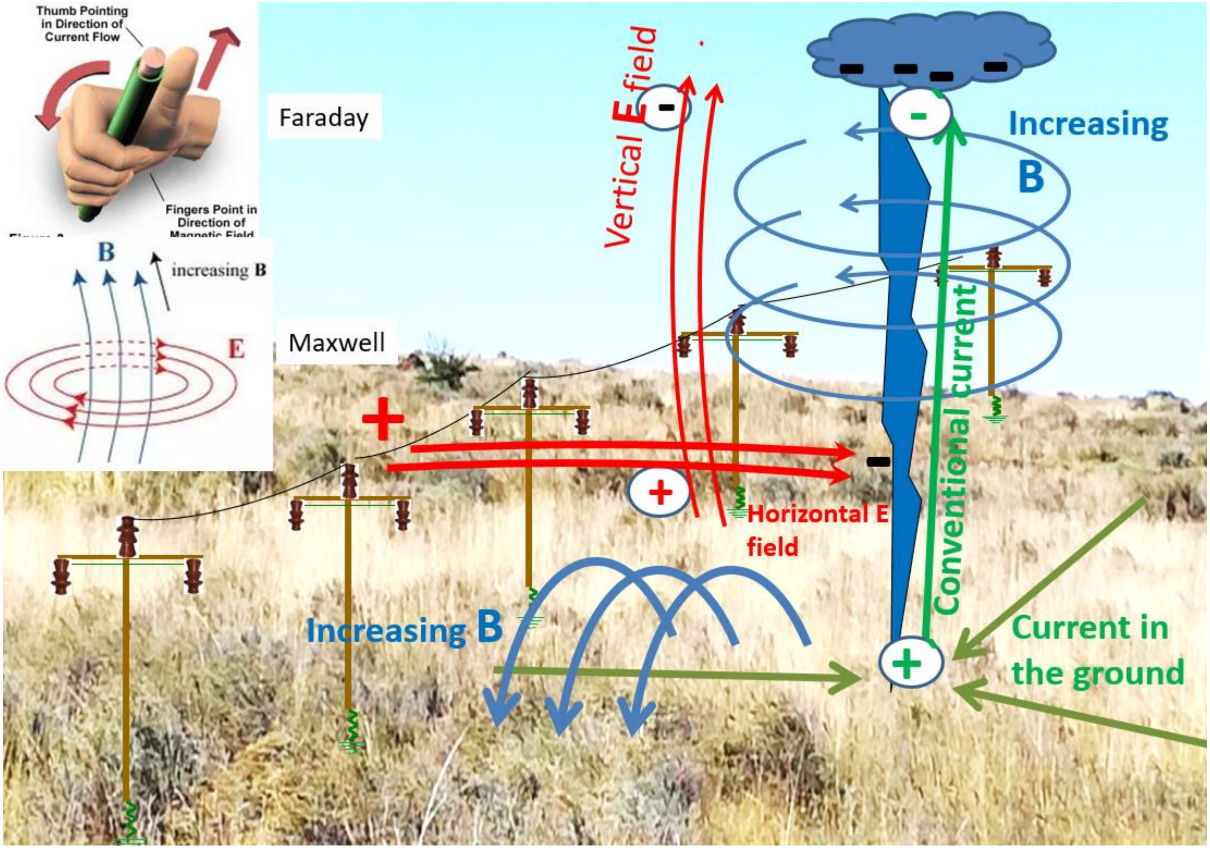

Figure 3.1 The electric and magnetic fields due to a nearby lightning return-stroke.

As pointed out in the literature review and verified in this research, the polarity of the LIOV and then LGC in areas with finite soil conductivity changed to be opposite to the polarity of the lightning return-stroke at about 250 m from the nearby lightning return-stroke ground-termination. This was not the case for a direct lightning strike to the line as there was no soil directly involved between the lightning termination point to the line and the point of measurement at the feeder substation. On average 99.96% of nearby lightning strikes to the 714 km line used in this research were therefore further than 250 m from the substation. The chances that a LIOV due to a nearby lightning strike closer than 250 m to the substation exceeded the line BIL was further minimized by the well earthed surge arresters at the feeder substation. Should the polarity of the LGC be the same as the return-stroke polarity (obtained from the LDN), it was classified as a lightning strike direct to the line while opposite polarities will indicate a nearby lightning strike to the line.

This new measurement methodology was able to distinguish between nearby lightning strikes and direct lightning strikes to a long line in operation without being dependent on the accuracy of the distance between the lightning strike termination point and the line, the lightning return-stroke inclination and tortuosity, accurate line parameters and soil properties, protection operation, triggering of instruments by the LIOV and having instruments connected at the position on the line closest to the lightning strike termination point. As the LIOV amplitude could not be measured on a long operational line, the current waveform recording at the feeder substation was used to detect a fault current, which indicated that the LIOV amplitude exceeded the line BIL.

3.5 Methodology used

The methodology used in this research to distinguish between the nearby lightning and direct lightning strikes to the line was to:

- print the recordings on the logger at the substation that contains fault current flow to a file (PowerPoint). This was an indication that the line insulation level was exceeded.
- search the LDN database for lightning events at the same time as the fault recordings.
- print the matching LDN geographical display, the lightning return-stroke polarity, GPS coordinates and the confidence ellipse to a file (PowerPoint).
- compare the LGC polarity in the recording to the lightning return-stroke polarity
- use the breaker operations report to assist in rare cases where there were more than one lightning return-strokes that could cause the line fault.
- Classify lightning return-strokes with the same polarity as the LGC as direct lightning strikes to the line and opposite polarity events as nearby lightning.
- Normalize the measured data on the operational line and compare it to the IEEE Std 1410-2010 lightning performance estimation.

3.6 Comparison between existing and new methodology

The flowcharts in Figure 3.2 shows the process that was followed when existing electromagnetic coupling models were used to distinguish between nearby lightning and direct lightning strikes to the line and to determine the lightning performance of short floating MV lines. The input parameters in the red dotted blocks were usually not adequately accurate to distinguish between nearby lightning and direct lightning strikes to the line for determining the lightning performance of a long operational MV line.

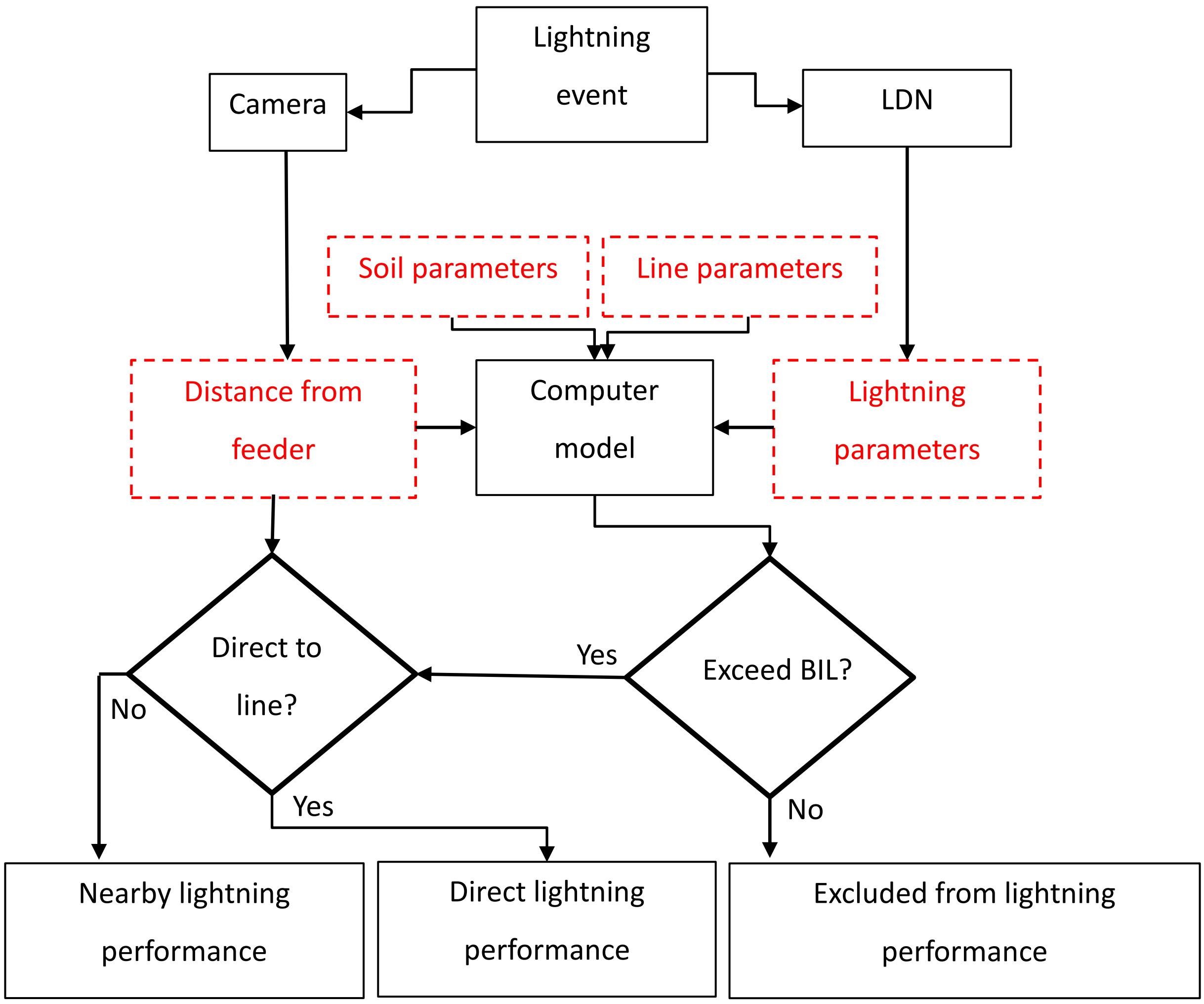

Figure 3.2 A flowchart of the method used in conjunction with existing electromagnetic coupling models to determine the lightning performance of short floating MV lines. The blocks with the red dotted lines are the parameters that lack adequate accuracy in the case where the line is long and in operation.

Figure 3.3 shows the process for measuring the lightning performance of short floating lines. The purpose of the measurements was to verify the models and therefore the soil and line parameters (in the red dotted blocks) were also needed. The soil conductivity changes along a long line and are generally not accurately available. The cost became high and logistics difficult for data analysis of a high number of cameras (in the red dotted block) to verify the lightning return-stroke termination point.

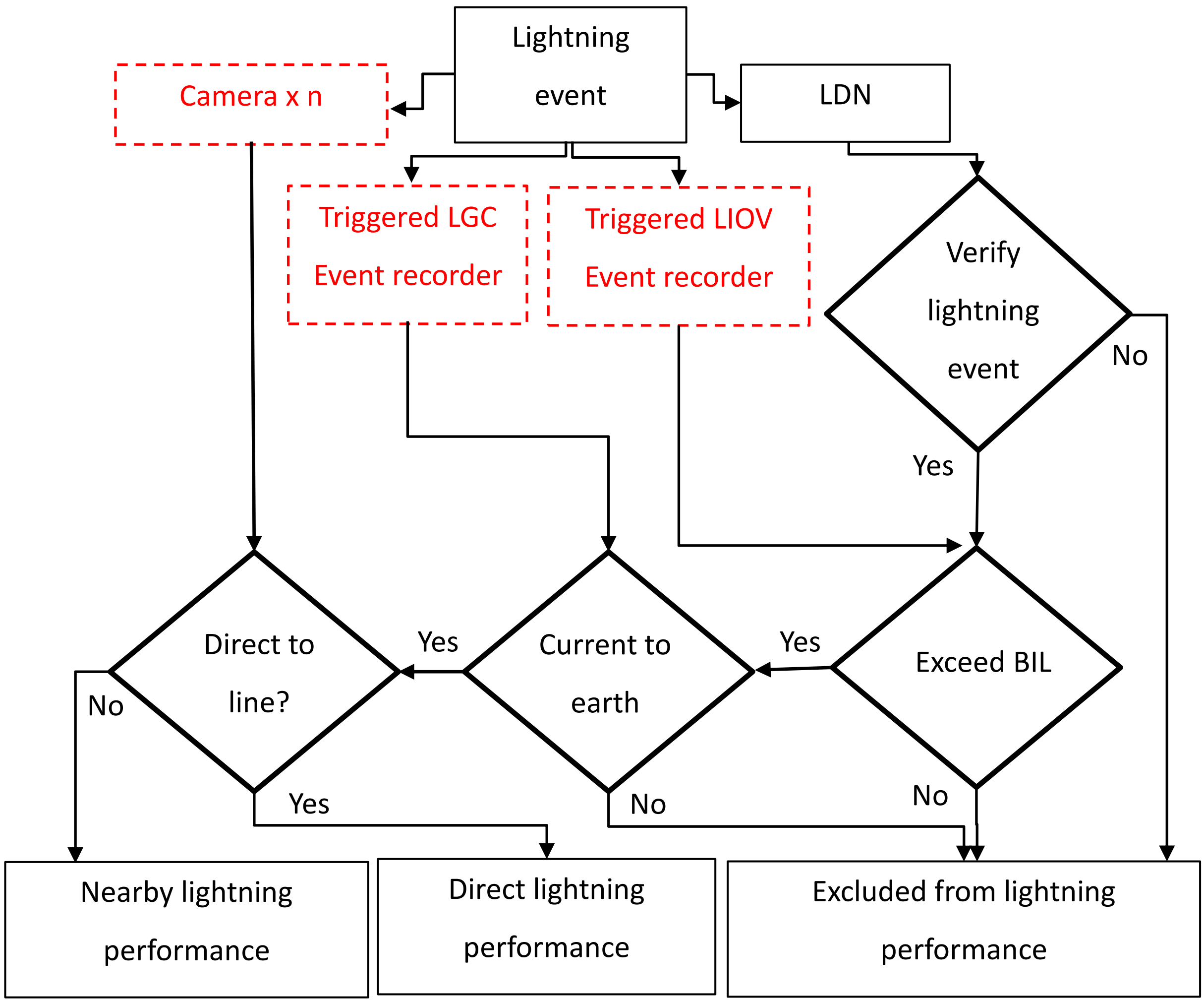

Figure 3.3 A flowchart of the method used in conjunction with existing measurement configurations to determine the lightning performance of short floating MV lines. The blocks with the red dotted lines were the parameters that lack adequate accuracy in the case where the line was long and in operation.

Figure 3.4 shows the new process to distinguish between nearby lightning and direct lightning strikes to the line and measure the lightning performance of long MV lines in operation. The new methodology complemented the existing methods because the existing electromagnetic coupling models and measurement methods could only be used to determine the lightning performance for short floating lines whereas the new method could only be used for long lines in operation. There was an overlapping line length where both methods could be used. Floating lines between a few meters and 3 km were used in most existing electromagnetic coupling models and measurement processes. If a section of the line was more than 250 m from the nearby lightning strike termination point, was energized and the neutral point of the NEC or transformer was earthed at the supply point, the new measurement method could also be used to measure the lightning performance of this section of the line.

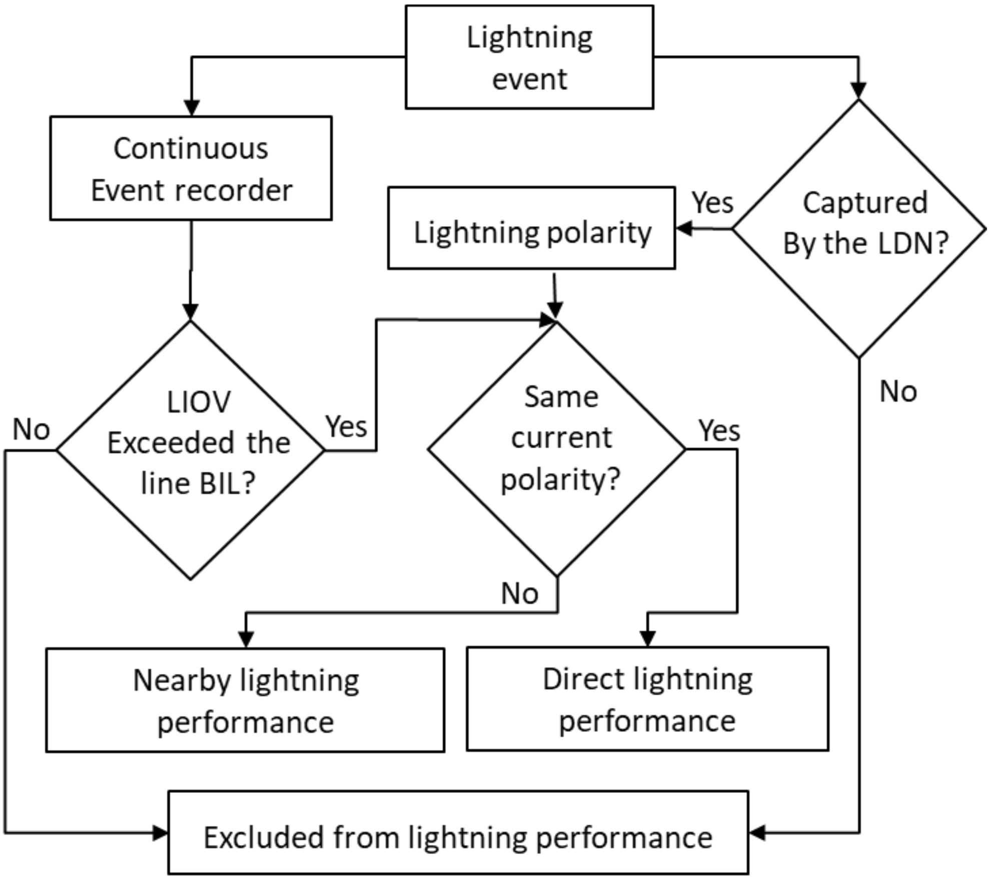

Figure 3.4 A flowchart for the new measurement methodology to distinguish between nearby lightning and direct lightning strikes to a long MV line in operation.

3.7 Justification of the new methodology

An ATP model as shown in Figure 3.5 was used to calculate the BIL along the MV line. An LGC was simulated on the line using a Heidler impulse current model. The LGC amplitude was increased up to a point where the LIOV would exceed the lowest BIL of the line in the vicinity of the nearby lightning strike termination point. The amplitude of the LIOV on the line closest to the nearby lightning return-stroke termination point was then taken as the BIL of the line at that point. An average BIL of the line as well as the BIL at these specific points on the line where line flashovers occurred due to nearby lightning strikes was modelled. A database consisting of 38 675 lightning flashes (126 311 lightning return-strokes) within a 2 km buffer around the line that distinguishes between line flashovers due to nearby lightning, direct lightning strikes, weather-related faults and other faults were created. The database was normalized in a format to compare the results with the IEEE standard 1410-2010 estimation of the lightning performance of the line.

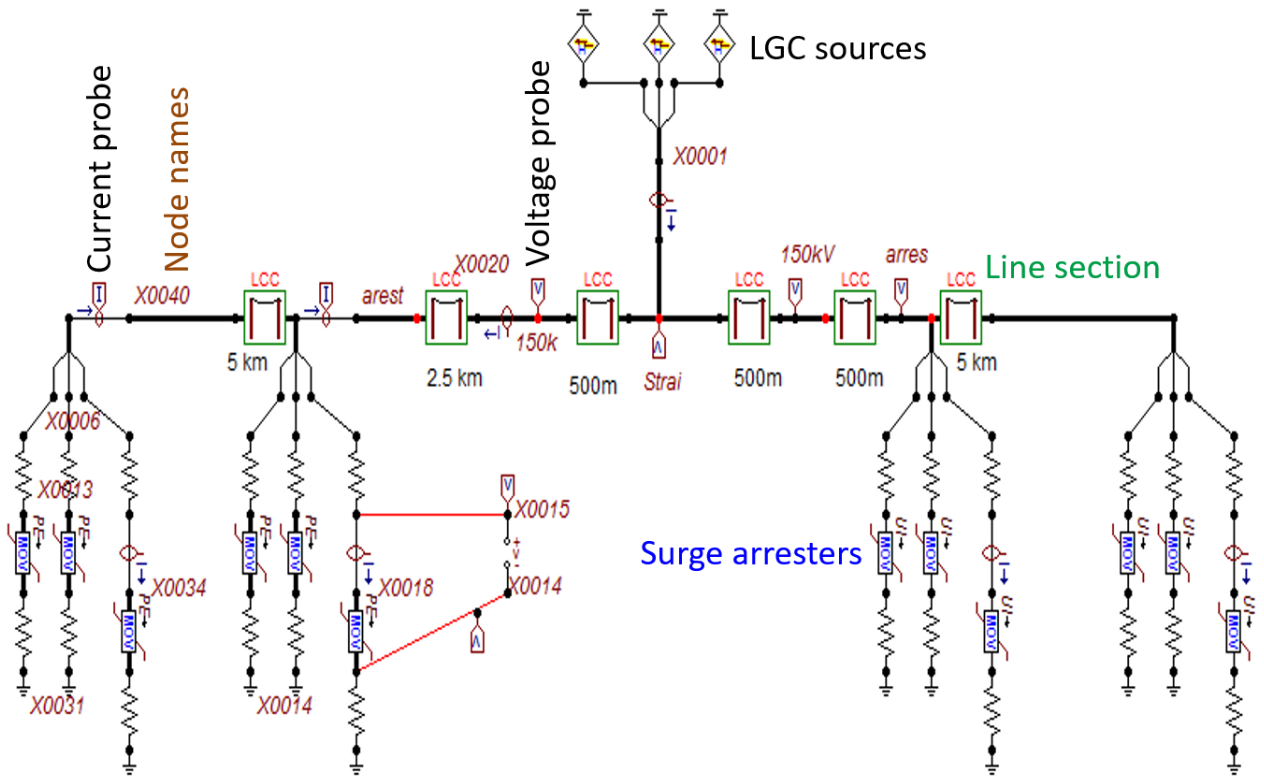

Figure 3.5 An example of the ATP model to determine the line's local BIL.

The ATP-EMTP computer model [161] was employed as it was easy to extend this model by including the ATP model of the long line in operation that was used in this research. This computer model is based on a TL return-stroke model, the CR model to simulate the horizontal electric field and the Agrawal model for the electromagnetic coupling between the return-stroke and the line. A +50 kA lightning strike 50 m from a 1 km line and soil resistivity of 500 Ω.m. was modelled and the LIOV was then compared with the ERM [160] that used the same parameters. Figure 3.6 shows a simulation with the ATP-EMTP model [161] as well as the ERM [160]. Of importance was that beyond 250 m along the line, the LIOV on the line changes from being the same polarity as the lightning return-stroke to opposite polarities. The distance where the LIOV polarity changed depended on the soil resistivity. The higher the soil resistivity, the quicker a polarity change was experienced. For example, if the soil resistivity was 2000 Ωm, the polarity of the LIOV changed at approximately 150 m from the point in the line closest to the nearby lightning strike. The LIOV polarity change occurred at approximately 500 m when the soil resistivity was 100 Ωm. The methodology can therefore be used for soil resistivity of between 100 Ωm and 2000 Ωm.

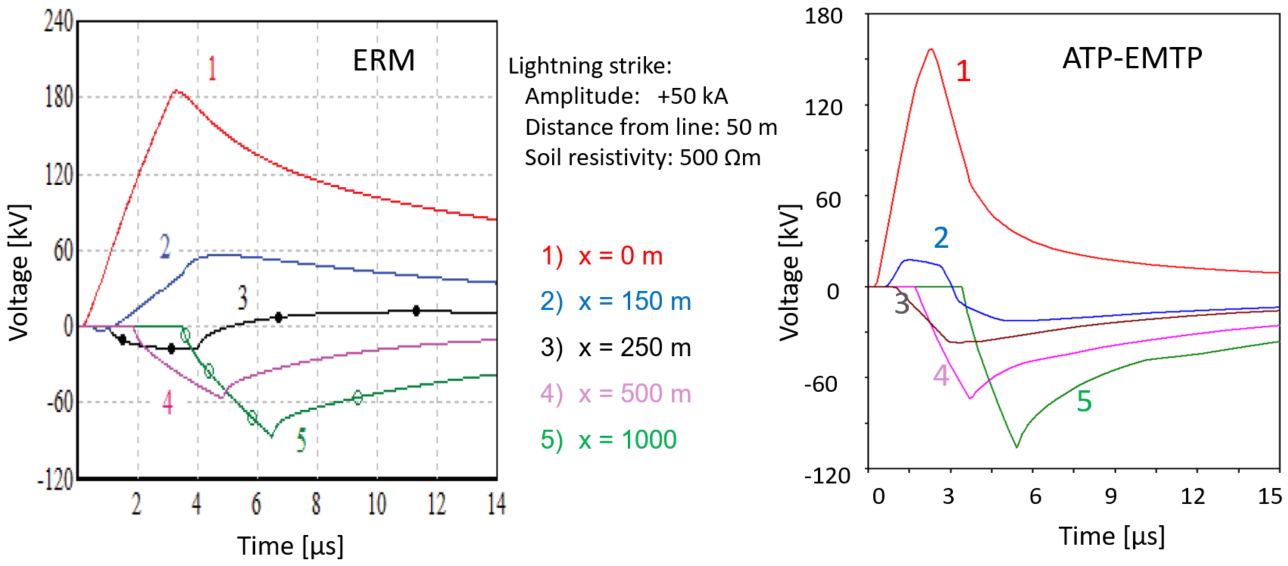

Figure 3.6 A direct comparison between the ERM (Permission obtained from Alexandre Piantini) [160]) and the ATP-EMTP model using the same input parameters. Of importance is the change in polarity of the LIOV after about 250 m from the nearby lightning strike.

The LIOV amplitude was normally peaking closest to the nearby lightning strike (red curve in Figure 3.6) and is of most interest. The maximum amplitude of the LIOV should not exceed the BIL of the line. In this research, the LIOV amplitude peak on the line closest to the nearby lightning point of termination could not be measured or calculated because of the lack of equipment and the uncertainty of the LDN geographical distance between the nearby lightning strike and the line. For this reason, the power frequency fault current was measured to detect whether the LIOV amplitude exceeded the BIL of the line.

The ATP-EMTP model was then extended to include part of the three-phase floating line towards the feeder substation with no equipment connected to the line. As shown in Figure 3.7, the LIOV attenuated significantly towards the feeder substation, but of importance was that the polarity of the first cycle of the LIOV oscillation 15 km from the nearby lightning strike was opposite to the polarity of the lightning return-stroke polarity. Figure 3.8 shows the current along the line after the equipment was connected. Although some oscillations in the LGC could be seen, the first cycle of the LGC oscillations at the substation was of opposite polarity in comparison to the lightning return-stroke polarity.

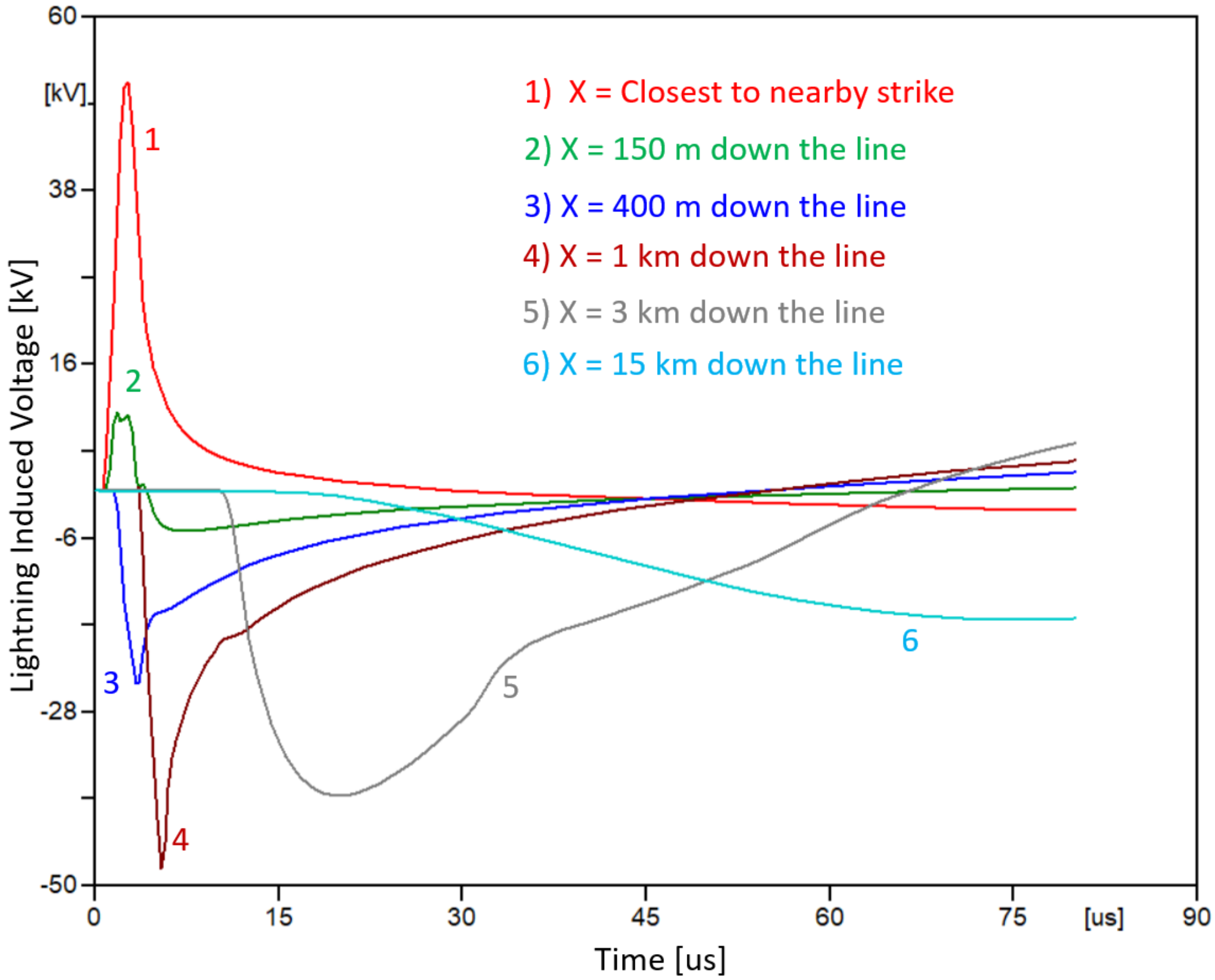

Figure 3.7 The ATP-EMTP model included the Høidalen model for nearby lightning as well as a 15 km three-phase line that was floating and with no equipment connected. There was a close correlation between the 3 phases and therefore only one phase was shown. The polarity of the LIOV changed after about 250 m and was of opposite polarity (negative) at the feeder substation (curve no. 6) in comparison with the lightning return-stroke polarity (positive) that was used for this simulation.

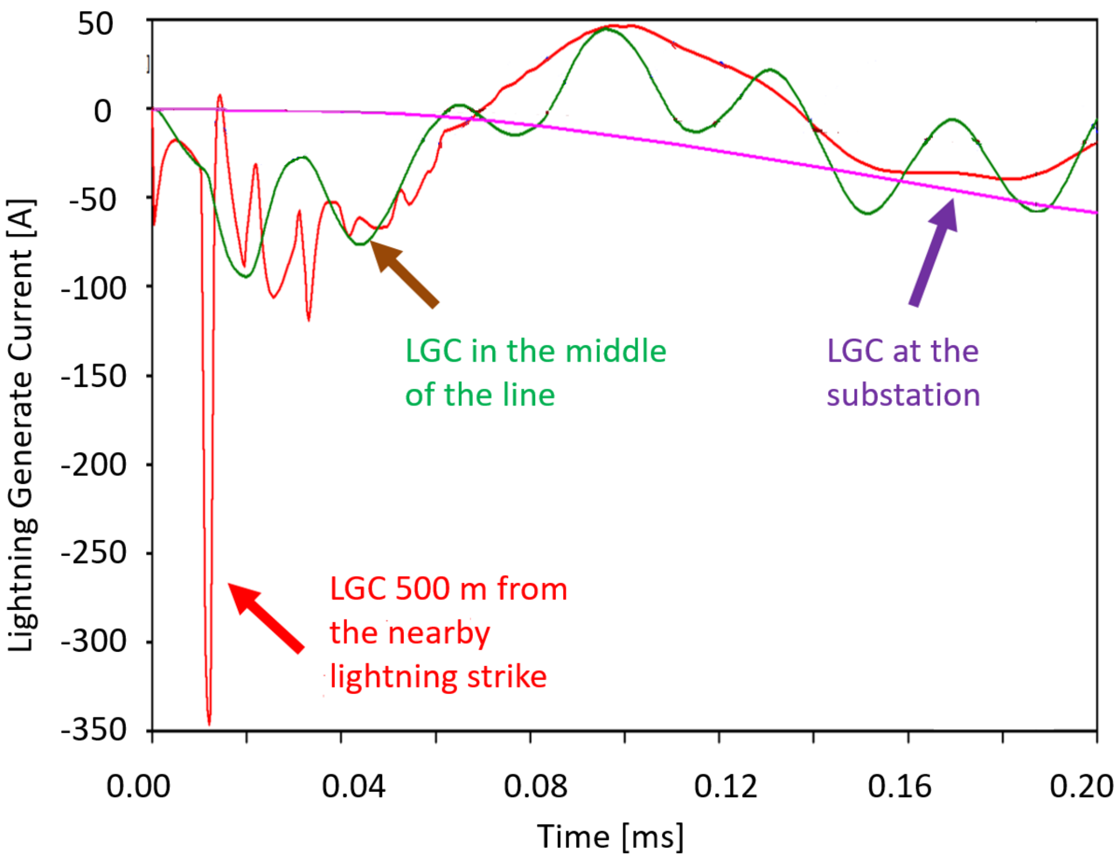

Figure 3.8 The ATP model shows the reflections (of LGC) caused by the line configuration and equipment that was connected to the line. The amplitude of the oscillations due to the reflections became lower as it progressed along the line. The first cycle of the LGC oscillation was still of opposite polarity (negative) in comparison with the lightning return-stroke polarity (positive) used in the simulation.

There were no existing models and measurements that this new methodology could be verified with. A basic validation of a short floating line in the ATP-EMTP model was verified with the same input data on the same short line in the ERM and the result was similar. This comparison validated the basic principle of the new methodology – that the LIOV polarity as a result of nearby lightning change polarity after about 250 m due to the finite soil conductivity. This is not the case for a direct lightning strike to the line as there is no soil directly involved.

The extended ATP-EMTP model (that includes an ATP model for the long equipped and energized line) had to be verified as being rigorous using actual measurements. Eight nearby lightning and four direct lightning return-strokes of which there was no uncertainty of being nearby or direct to the line, with different polarities and different distances from the feeder substation were used for verification of the measurements and the model. Lightning strikes with different polarities, amplitudes, both sides of the line, beyond the end of the line and different distances from the feeder substation were analysed and compared to simulations using the extended ATP-EMTP. Both the measurements and the extended ATP-EMTP model verified that the methodology was rigorous. This methodology was also verified with other lightning events in this research as documented in journal papers and conference papers [131] [162].

The actual distance between the nearby lightning return-stroke ground-termination point and the line was unknown (due to the LDN geographical distance error). A distance of 50 m between the line and the nearby lightning return-stroke ground-termination point was assumed for simulation purposes (if the lightning strike was closer to the line, the line would have attracted it to be a direct lightning strike to the line [12]). Uncertainty in the distance between the line and the nearby lightning strike termination point would compromise the amplitude accuracy of the LIOV and LGC. The new methodology did not require an accurate amplitude of the LIOV and the LGC as a power frequency fault current will reveal whether the LIOV exceeded the BIL of the line. The surge impedance of the line was 350 Ω. Should a lightning strike terminate direct to the line, the lightning current would therefore detect an effective impedance of 175 Ω.

For direct lightning strikes to the line:

- there will be wood splintering damage (that could only be caused by lightning > 7 kA).
- low amplitude direct lightning strikes that would not have caused a line fault if it was a nearby lightning strike, were used in the case studies.
- Using the Rusck formula for a floating line, a nearby lightning strike of more than 20.161 kA, 50 m from the line is needed to cause a flashover on a line with a 150 kV BIL (minimum BIL of the line in this research). In the case of an operational line, this nearby lightning strike amplitude necessary to cause a flashover will be much higher (mainly due to surge arresters connected to the line). A low amplitude direct lightning strike will be < 20.161 kA.
- The measurements in the case studies were verified using the extended ATP-EMTP model and the measured LGC was in all cases of the same polarity compared to the relevant lightning return-stroke polarity.

For nearby lightning:

- The minimum line BIL on the line was 150 kV, with a line surge impedance of 350 Ω (resultant surge impedance of 175 Ω as the LGC flows to both sides on the line), a lightning-generated current of 857 A will exceed the line BIL and cause a flashover on the line. Therefore, nearby lightning strikes with high amplitudes (several times higher than the required direct lightning return-stroke amplitude needed to exceed the line BIL) were used.

There was no power frequency fault current measured at the time of that theses nearby lightning strikes. This indicated that it must have been nearby lightning strikes.

- As high amplitude (>7 kA) nearby lightning return-strokes were used in cases to prove the methodology, there was a high probability that wood damage would occur if it was misinterpreted as a direct lightning strike, which was not found in the nearby lightning cases.
- The measurements in the case studies were verified using the extended ATP-EMTP model and the measured LGC was in all cases of opposite polarity compared to the relevant lightning return-stroke polarity.

The above criteria seem to be adequate to distinguish between nearby lightning and direct lightning to the line. However, unevenly spread surge arresters and other equipment attached to the line as well as compromised line equipment insulation, may cause unexpected flashovers due to nearby lightning. There were 10 incidents where nearby lightning-caused flashovers due to other insulation shortcomings. There were cases where much higher amplitude direct lightning strikes to the line did not cause flashovers (6 in this research). There were surge arresters close by in these cases. Therefore, a new methodology had to be used. Table 3.1 shows a summary of the verification of the methodology.

Table 3.1 A summary of the simulated and measured verification of the methodology

	Nearby lightning	Direct lightning	Flashover (Yes / No)	Distance from the recorder [km]	Polarity comparison	Comments
Case 1	-18 kA on the right side of the line		No	12	The strike polarity was opposite to the recorded LGC	An 18 kA direct lightning strike would have caused a flashover
Case 2	+59 kA on left side of the line		No	44	The strike polarity was opposite to the recorded LGC	A 59 kA direct lightning strike would have caused a flashover
Case 3	+140 kA on the right side of the line		No	44	The strike polarity was opposite to the recorded LGC	A 140 kA direct lightning strike would have caused a flashover
Case 4	-61 kA on the right side of the line		No	49	The strike polarity was opposite to the recorded LGC	A 61 kA direct lightning strike would have caused a flashover
Case 5	-69 kA on the left side of the line		No	50	The strike polarity was opposite to the recorded LGC	A 69 kA direct lightning strike would have caused a flashover

Case 6	+118 kA on the left side of the line and a +19 kA on the right side of the line		No	9	Both the strike polarities were opposite to the recorded LGCs	A 118 kA and a 19 kA direct lightning strike would have caused a flashover
Case 7	+101 kA beyond the end of the line		No	38	The strike polarity was opposite to the recorded LGC	A 101 kA direct lightning strike would have caused a flashover
Case 8		-9 kA	Yes	31	The strike polarity and the recorded LGC had the same polarity	A 9 kA nearby lightning strike would not have caused a flashover. There was also wood damage that confirms that it was a direct lightning strike
Case 9		-14 kA and -13 kA	Yes	18	The strike polarity and the recorded LGC had the same polarity	A 14 kA and a 13 kA nearby lightning strike would not have caused a flashover. There was also wood damage that confirms that it was a direct lightning strike
Case 10		+81 kA	Yes	31	The strike polarity and the recorded LGC had the same polarity	A 81 kA nearby lightning strike could have caused a flashover, but there was wood damage that confirms that it was a direct lightning strike

Case 1 in Figure 3.9 shows the LDN geographical presentation of a -18 kA nearby lightning strike that was at the right side of the feeder and 12 km from the feeder substation. There was no fault current on the feeder which was an indication that the LIOV did not exceed the line BIL at any point.

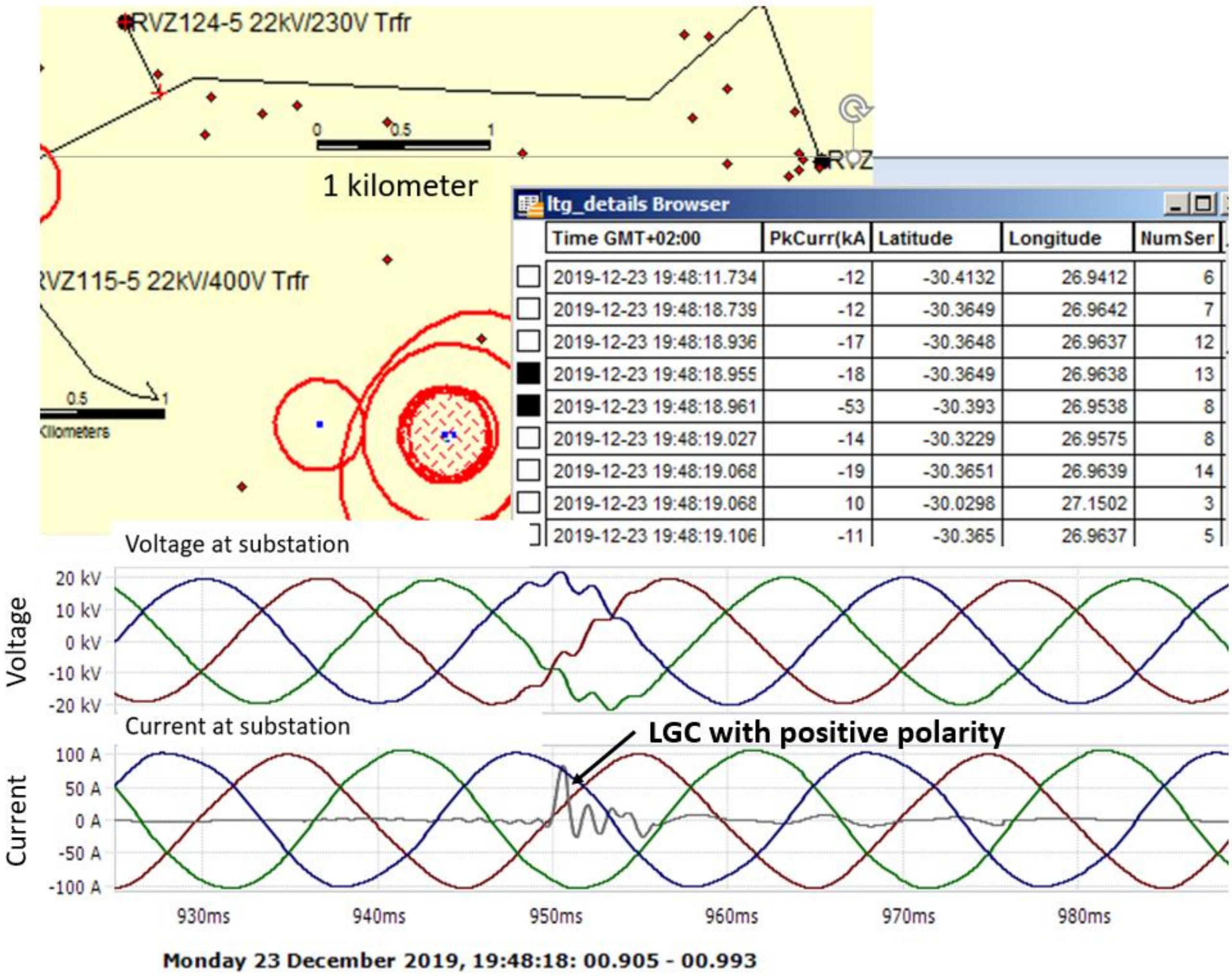

	Time GMT+02:00	PkCurr(kA	Latitude	Longitude	NumSer
☐	2019-12-23 19:48:11.734	-12	-30.4132	26.9412	6
☐	2019-12-23 19:48:18.739	-12	-30.3649	26.9642	7
☐	2019-12-23 19:48:18.936	-17	-30.3648	26.9637	12
■	2019-12-23 19:48:18.955	-18	-30.3649	26.9638	13
■	2019-12-23 19:48:18.961	-53	-30.393	26.9538	8
☐	2019-12-23 19:48:19.027	-14	-30.3229	26.9575	8
☐	2019-12-23 19:48:19.068	-19	-30.3651	26.9639	14
☐	2019-12-23 19:48:19.068	10	-30.0298	27.1502	3
☐	2019-12-23 19:48:19.106	-11	-30.365	26.9637	5

Figure 3.9 Case 1. A -18 kA nearby lightning strike at the right side of the line, 12 km from the feeder substation caused a positive LGC on the zero-sequence current recording. The amplitude of the LIOV was too small to make a reliable conclusion on the polarity of the LIOV.

Figure 3.10 shows the extended ATP-EMTP model simulation results for the LGC and LIOV as from 1 km from the nearby lightning stroke ground-termination point up to the feeder substation. In both the measurement and the simulation, the LGC had a positive polarity due to the -18 kA nearby lightning strike. The LIOV measured at the substation was negligibly small in both the simulation and the measurement. This was mainly due to the line surge impedance, surge arresters, other equipment and the source impedance at the feeder substation. The difference in the measured and simulated amplitude of the LGC could be attributed to the different actual line and lightning channel parameters used in the simulation.

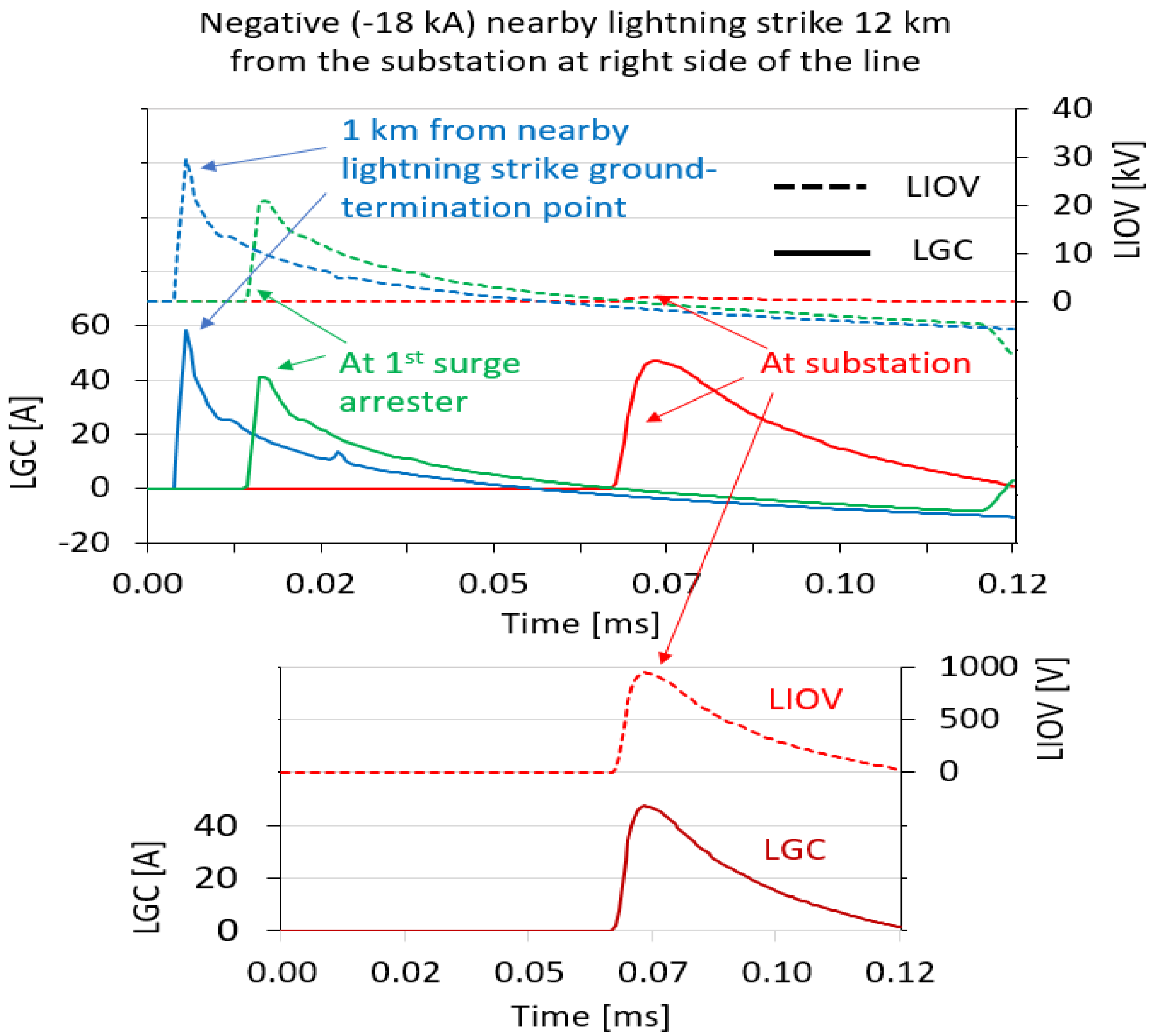

Figure 3.10 An ATP-EMTP simulation of a -18 kA nearby lightning strike (Figure 3.9) that was 12 km from the feeder substation. The exact distance between the nearby lightning strike and the line was unknown and 50 m was used in the simulation. The simulation shows the resultant LGC and LIOV both had a positive polarity at 1 km from the nearby lightning strike where the closest surge arresters were installed and at the feeder substation.

Figure 3.11 shows the LDN geographical display of a +59 kA nearby lightning strike on the right side of the feeder and 42 km from the feeder substation. The LIOV attenuated to such an extent that it was not visible when superimposed on the power frequency voltage waveform while the polarity of the LGC was clearly visible and had a negative polarity. The +59 kA lightning return-stroke was modelled using the extended ATP-EMTP model and the result is shown in Figure 3.12.

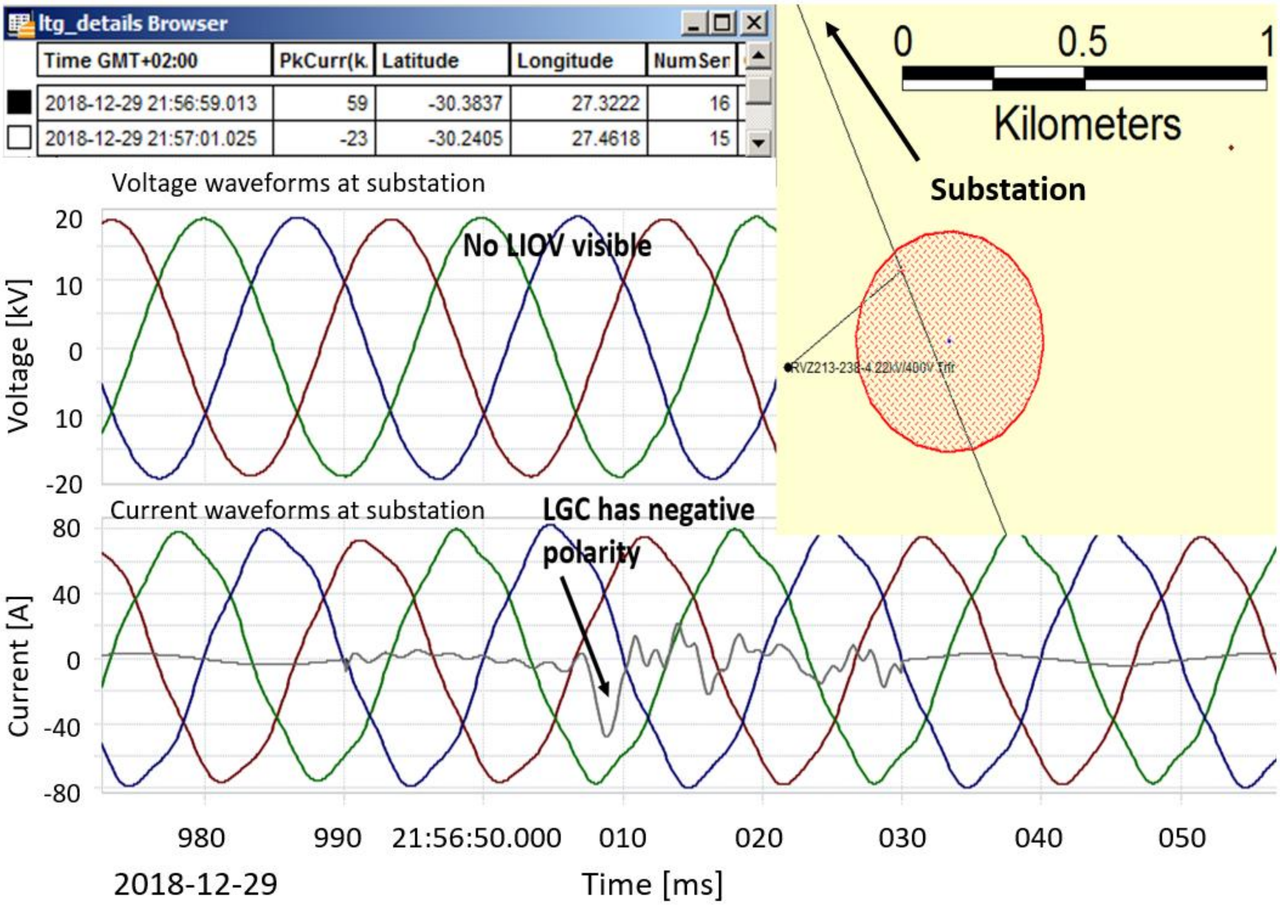

Figure 3.11 Case 2. A +59 kA nearby lightning strike at the left side of the line, 44 km from the substation caused a negative LGC on the zero-sequence current recording. The LIOV was not visible on the recording.

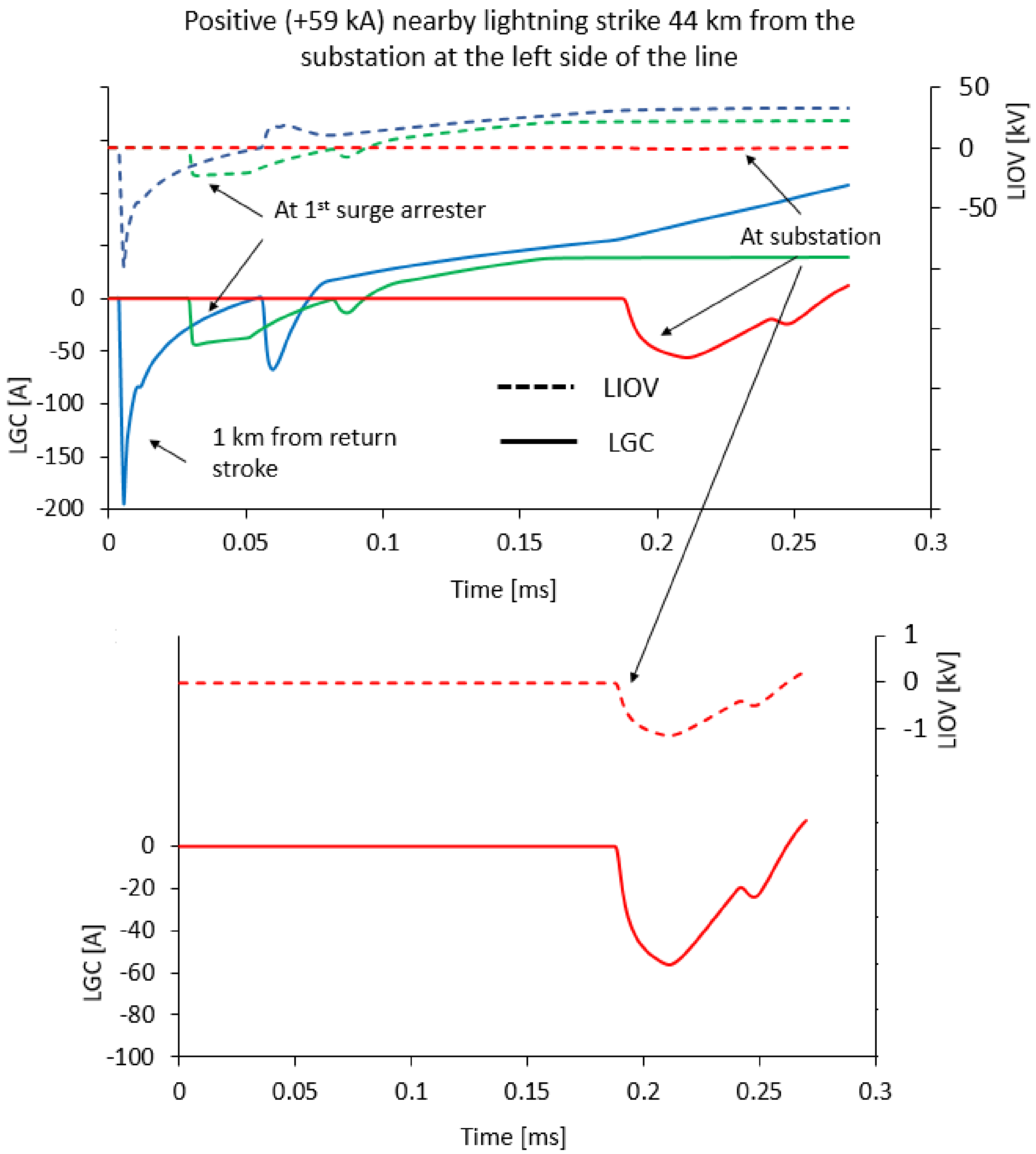

Figure 3.12 A simulation of the LIOV and LGC along the line as from 1 km from the nearby lightning return-stroke point of termination up to the feeder substation that was 44 km from the nearby lightning return-stroke point of ground termination. The LIOV at the substation was not visible before it was amplified in the bottom graph.

Figure 3.13 shows positive (+140 kA) nearby lightning strike that terminated on the right side of the line at a point 44 km from the feeder substation.

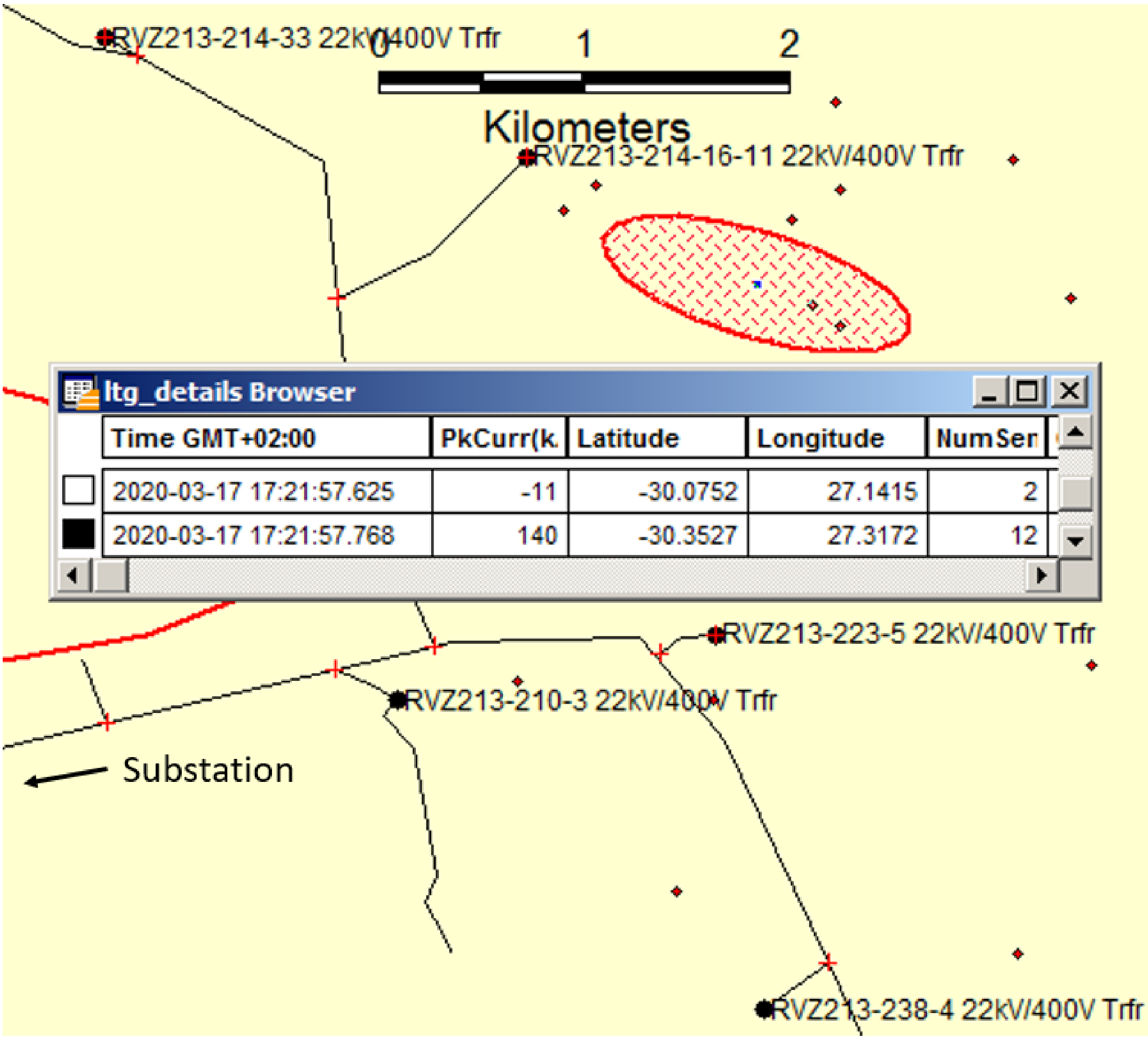

Figure 3.13 Case 3The LDN geographical presentation of a +140 kA nearby lightning strike 44 km from the feeder substation at the right side of the line.

Figure 3.14 shows a recording of the LIOV and LGC. A small disturbance could be seen on the LIOV and it is difficult to identify the polarity of the LIOV. The LGC had a negative polarity due to a positive nearby lightning strike. There was no indication of a fault current on the recording at the substation.

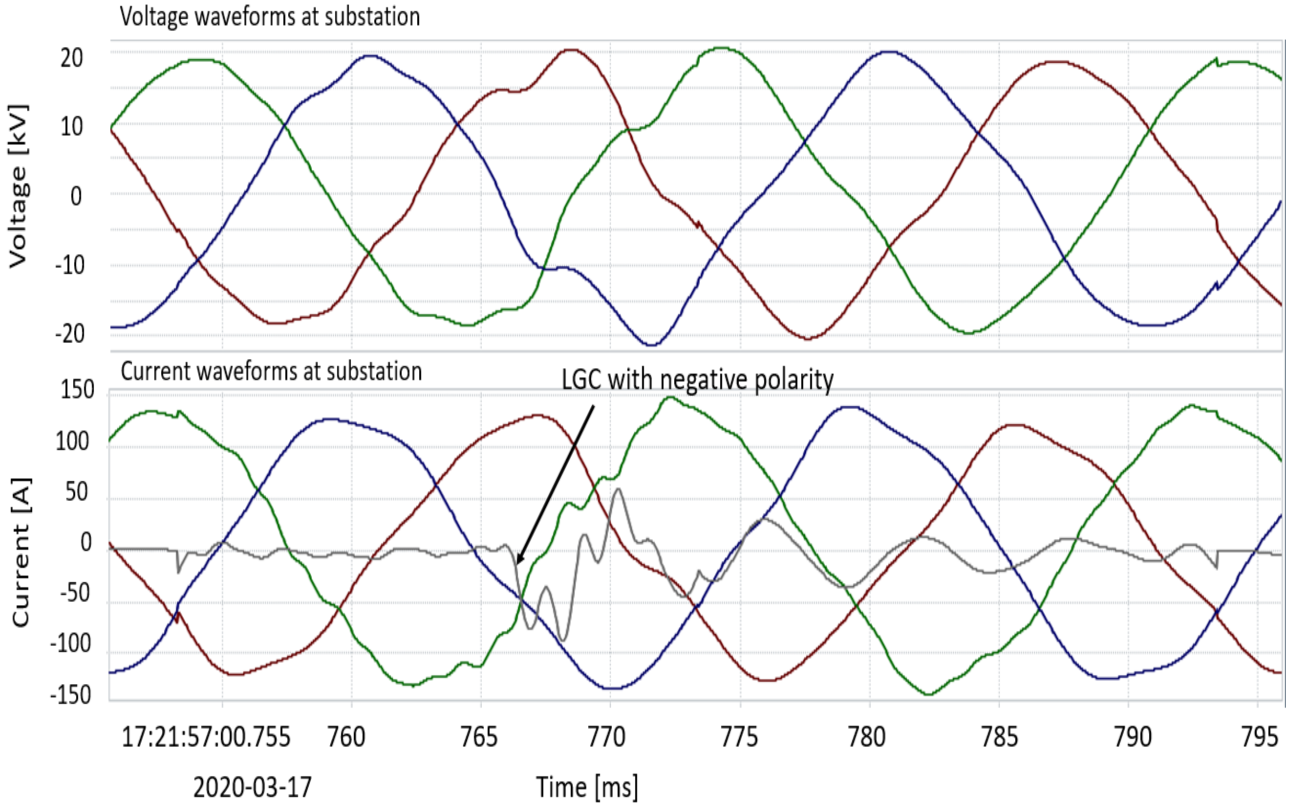

Figure 3.14 A recording at the feeder substation of the LGC (negative polarity) due to a positive nearby lightning stroke shown in Figure 3.13.

Figure 3.15 shows an ATP-EMTP simulation of the nearby lightning strike in Figure 3.13 and as recorded at the feeder substation in Figure 3.14. Both the LIOV and LGC had a negative polarity due to a positive nearby lightning strike at the right side of the feeder.

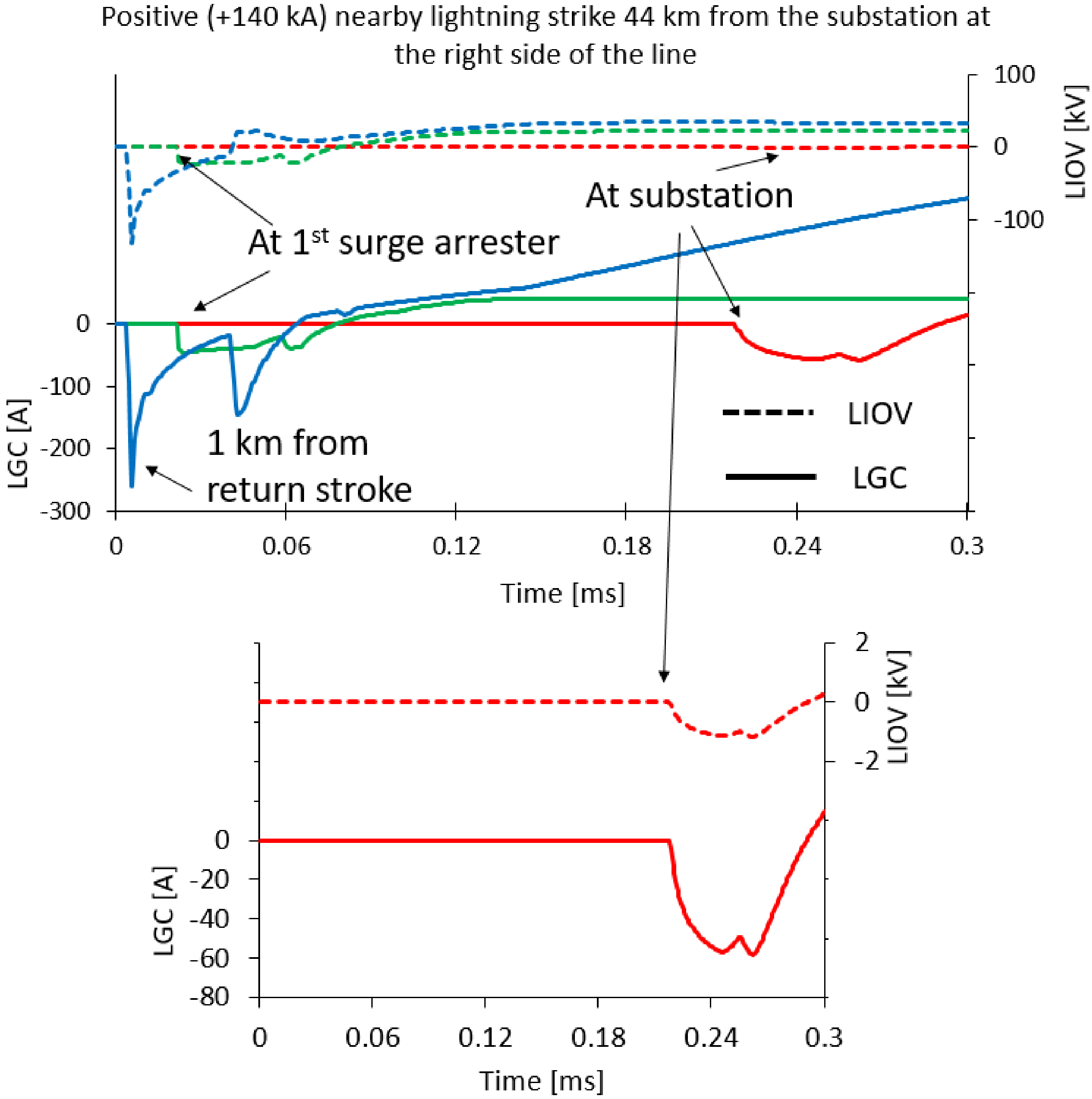

Figure 3.15 An extended ATP-EMTP simulation of the LGC and LIOV on the line due to the nearby lightning strike as recorded in Figure 3.14. The LGC amplitude in the simulation is less than the recorded LGC due to unknown parameters of the changing soil conductivity along the line and the distance between the line and the nearby lightning strike ground termination point.

Figure 3.16 shows the LDN geographical display of a negative (-61 kA) nearby lightning strike on the right side of the feeder. The incident occurred 49 km from the substation.

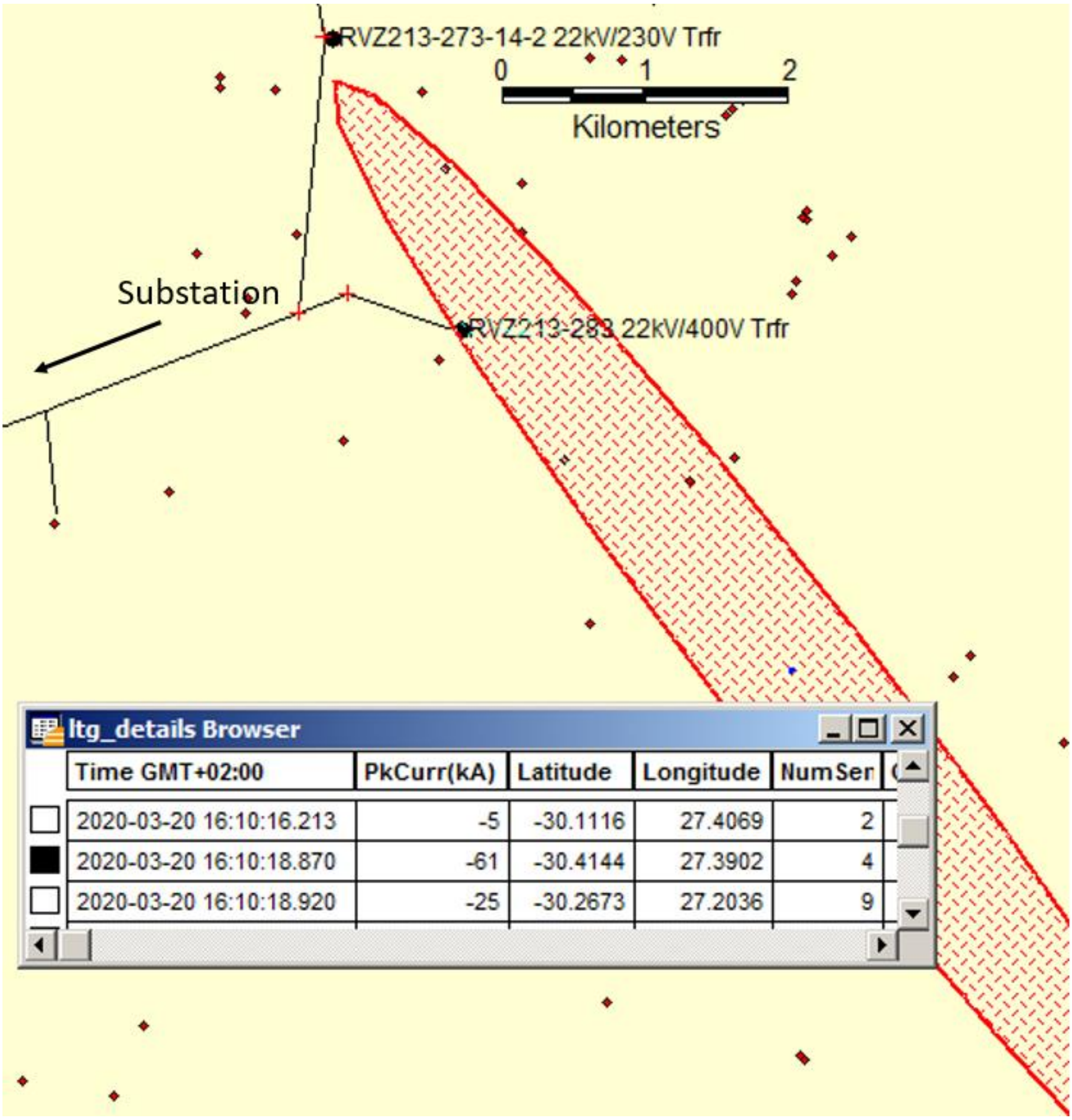

Figure 3.16 Case 4. The LDN geographical presentation of -61 kA nearby lightning strike at the right side of the line 49 km from the substation.

Figure 3.17 shows the voltage and current recording at the feeder substation at the time of the nearby lightning strike in Figure 3.16. No LIOV superimposed on the 22 kV voltage waveform can be noticed. The LGC had a positive polarity due to the negative nearby lightning strike. There was no fault current measured at the substation which was an indication that the LIOV did not exceed the line BIL.

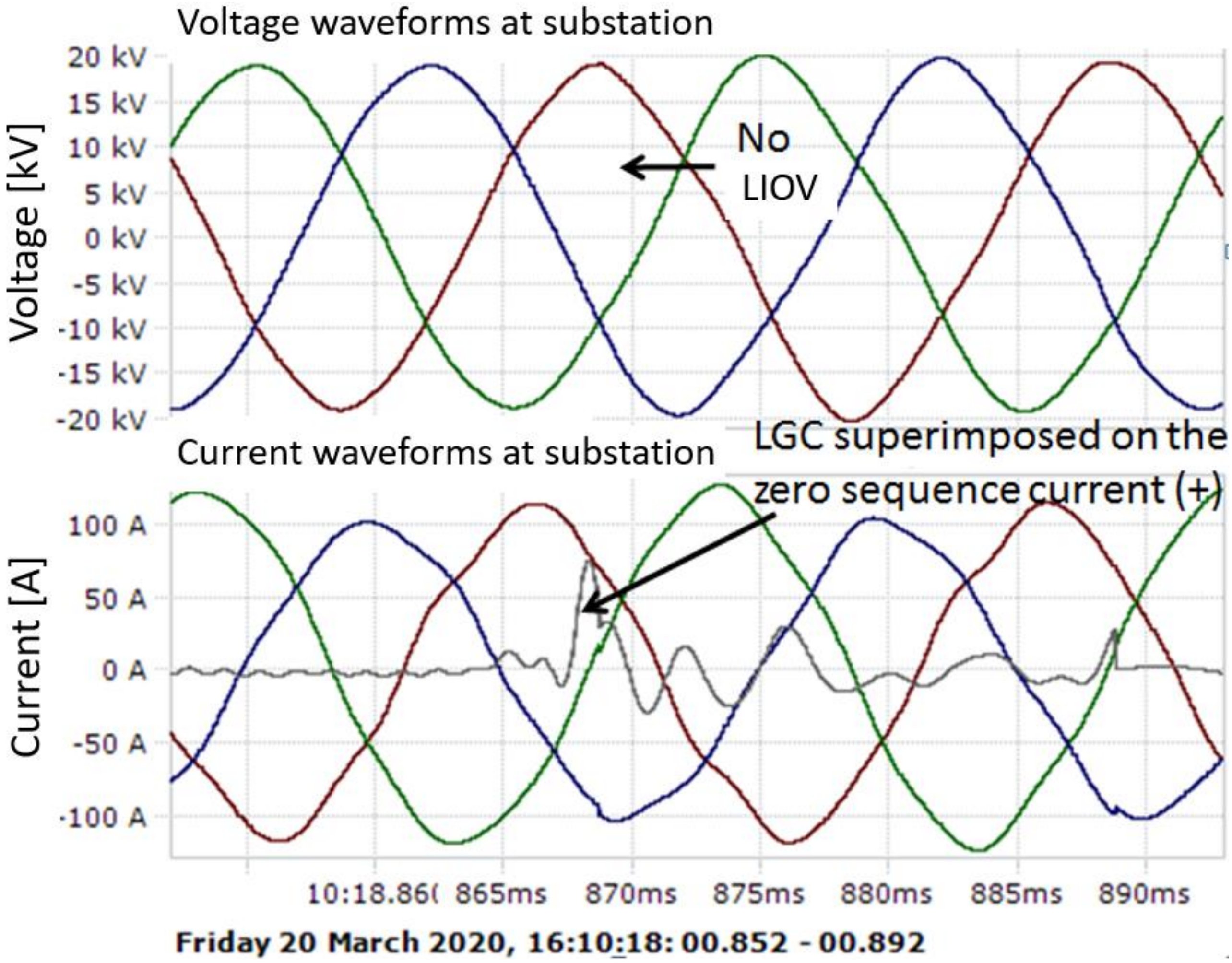

Figure 3.17 A recording of the LGC with positive polarity due to a negative nearby lightning strike shown in Figure 3.16.

Figure 3.18 shows an ATP-EMTP simulation of the -61 kA nearby lightning strike which caused a positive LIOV and LGC.

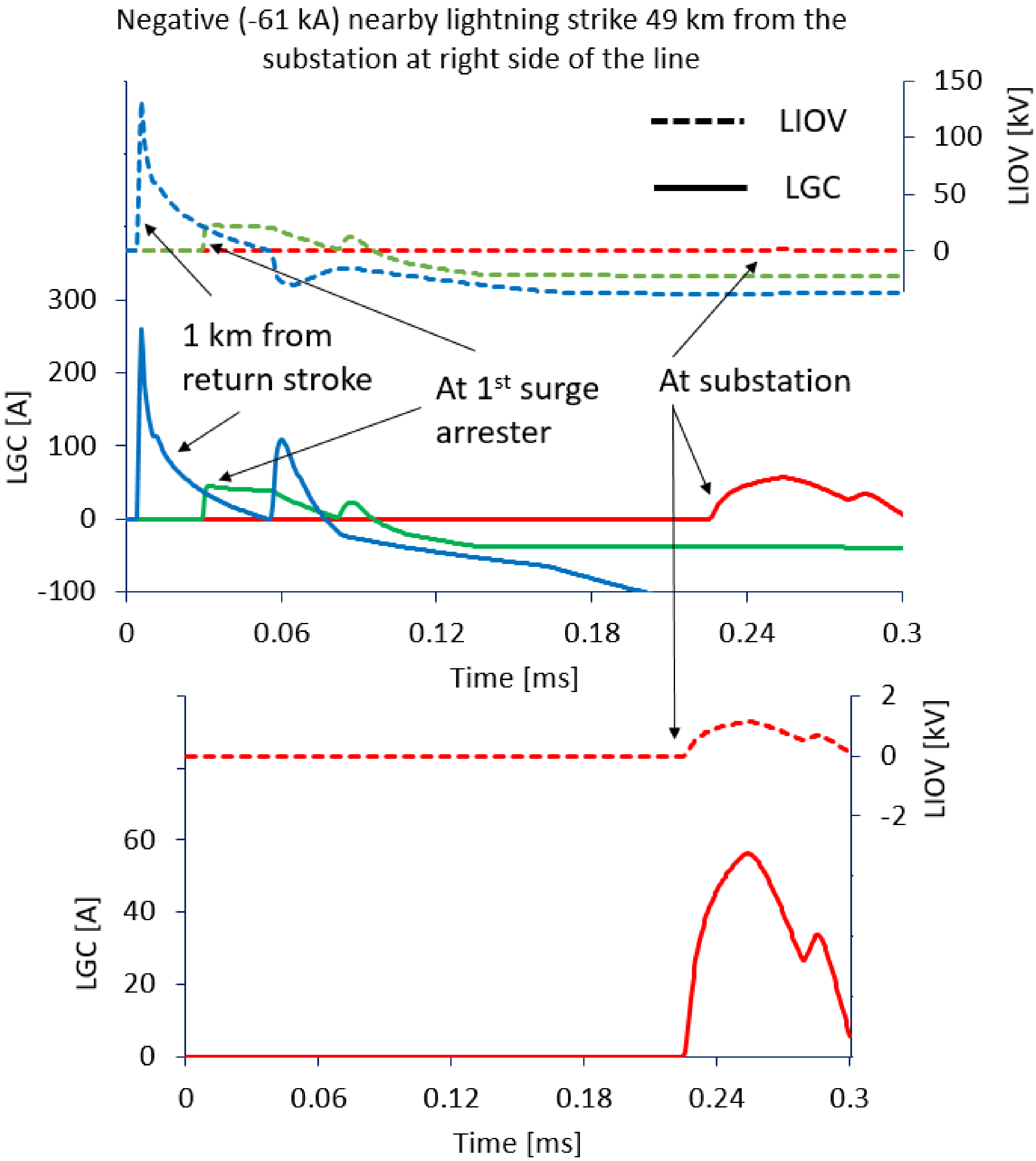

Figure 3.18 A simulation done using the extended ATP-EMTP model due to a negative nearby lightning strike shown in Figure 3.16. Both the LGC and the LIOV polarity are opposite to the lightning return stroke current polarity of the nearby lightning strike.

Figure 3.19 shows a geographical display of a -69 kA nearby lightning strike that terminated on the left side of the line at a point 50 km from the substation.

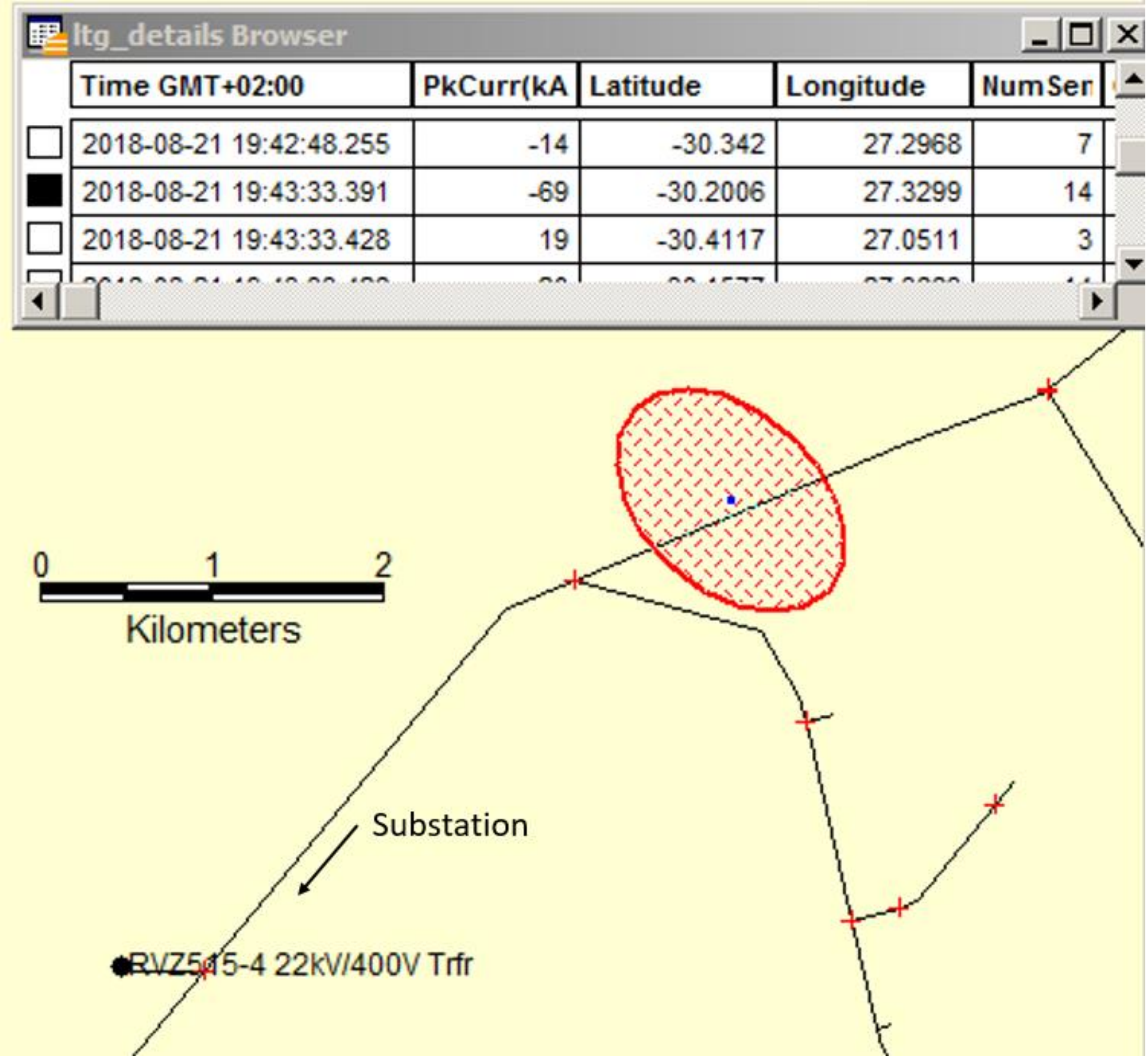

Figure 3.19 Case 5. The LDN geographical display of a -69 kA nearby lightning strike at the left side of the line 50 km from the substation.

Figure 3.20 shows a recording at the feeder substation of the negative nearby lightning strike shown in Figure 3.19. No LIOV could be seen on the voltage recording, but an LGC with a positive polarity could be seen on the current recording due to the negative nearby lightning strike.

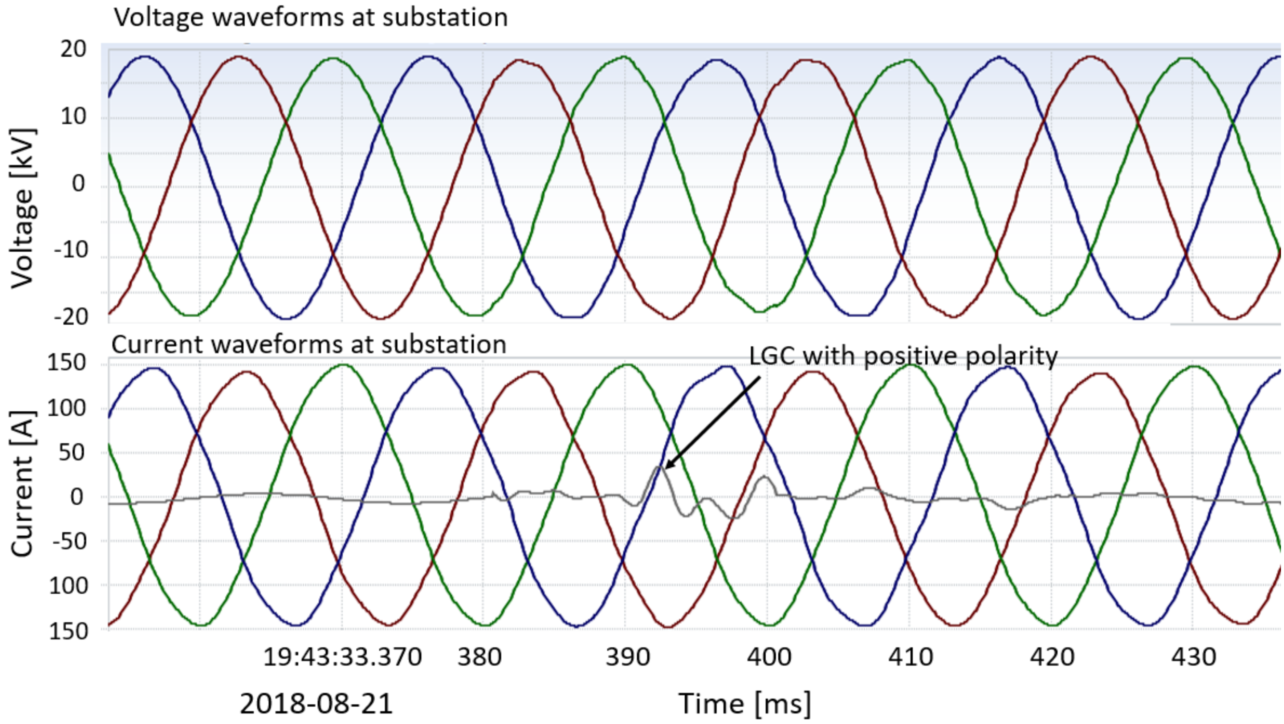

Figure 3.20 A recording of the voltage and the current at the feeder substation due to a -61 kA nearby lightning strike shown in Figure 3.19. The LGC polarity was positive which was opposite to the nearby lightning return-stroke current polarity.

Figure 3.21 shows a simulation of the nearby lightning strike in Figure 3.19. The polarity of the LGC in the recording and the simulation is positive and of opposite polarity to the negative lightning return stroke. The -61 kA nearby lightning strike in Figure 3.16 was on the right side of the line and the -69 kA nearby lightning strike in Figure 3.19 was on the left side of the line. In both cases, the LGC and LIOV were of opposite polarity to the nearby lightning strike return-stroke current polarity.

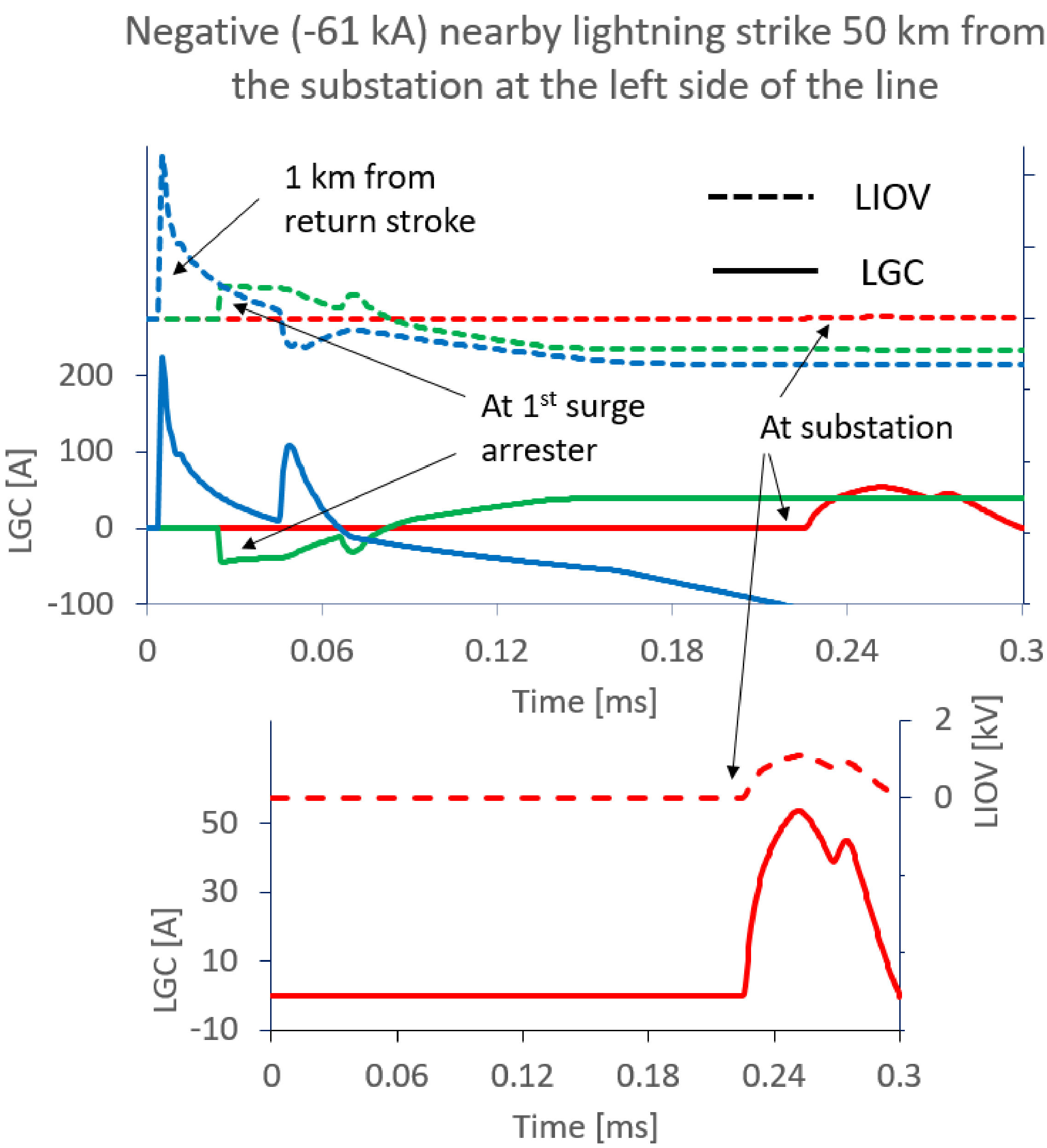

Figure 3.21 A simulation of the LIOV and LGC due to a negative nearby lightning strike shown in Figure 3.19. Both the LGC and LIOV polarity was positive and of opposite polarity of the negative nearby lightning strike.

Two positive nearby lightning strikes (Figure 3.22), one on the left side and one on the right side of the line occurred 22 ms from each other. The time difference in the LDN database and the recording were the same. In both cases, the first half cycle of the polarity of the LGC was negative (Figure 3.23) and opposite to the positive lightning return-stroke currents.

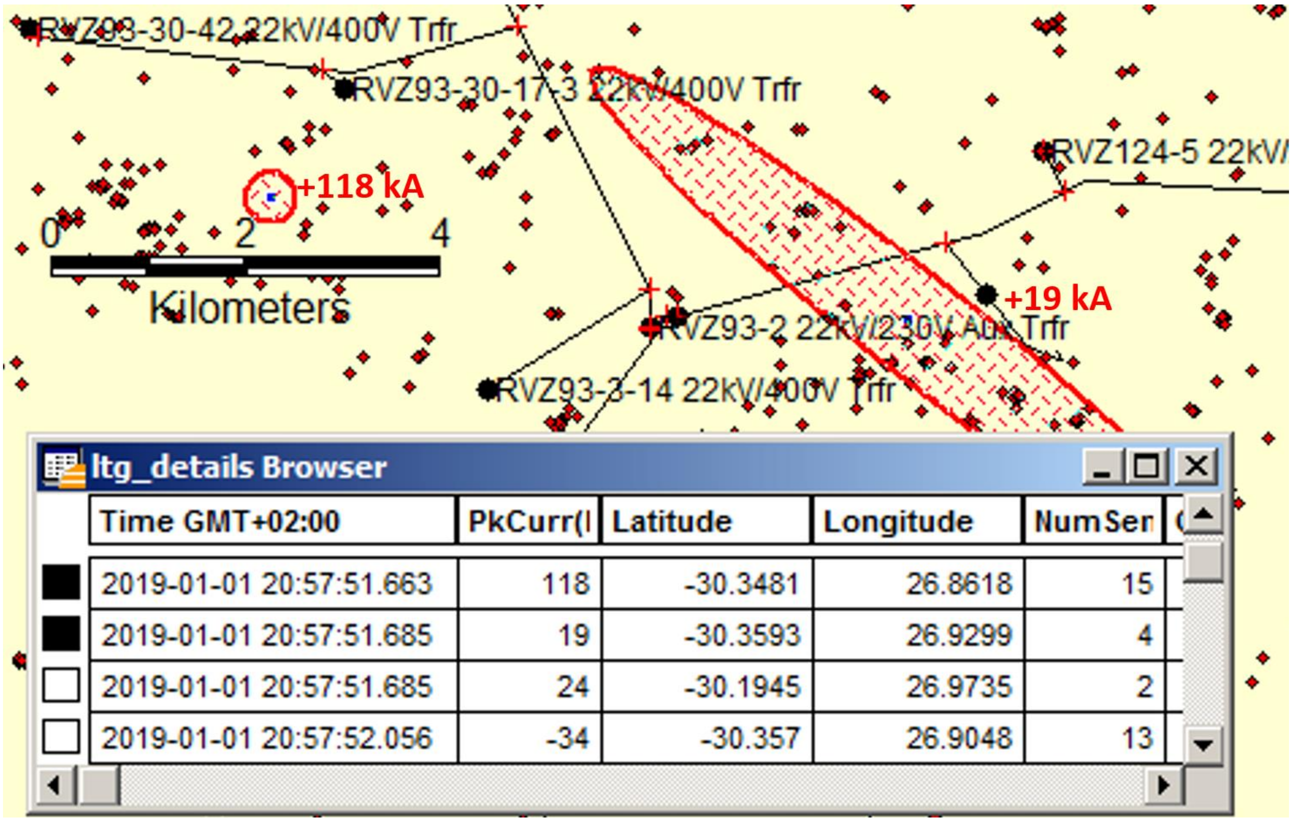

Figure 3.22 Case 6. Two nearby lightning strokes, a +118 kA with a ground termination point on the left side of the line and a +19 kA on the right side of the line. There was a time-lapse of 22 ms between the two lightning strokes.

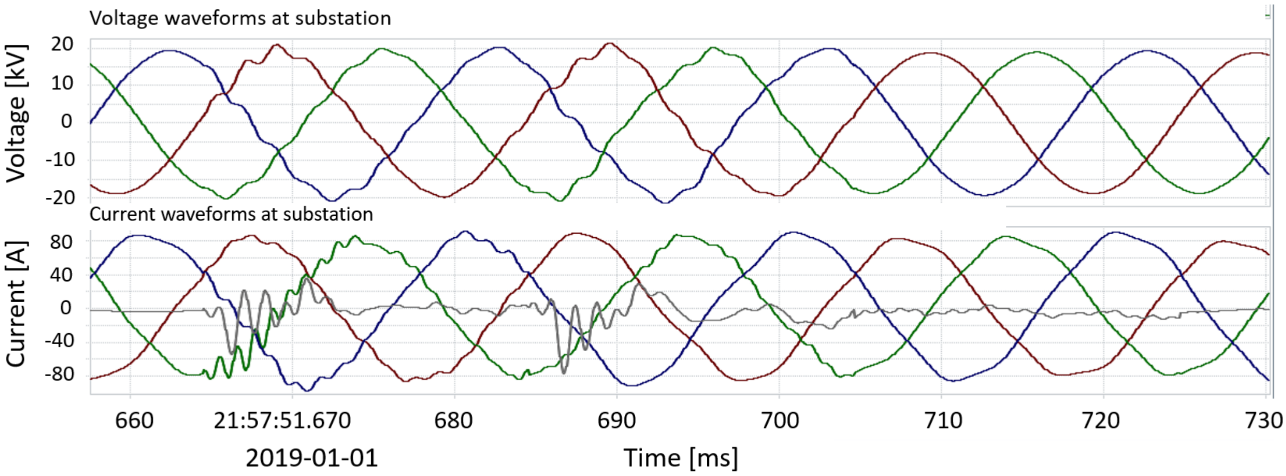

Figure 3.23 A recording at the feeder substation of the two nearby lightning events in Figure 3.22. The polarity of the first half cycle of the oscillation of both the recordings was negative while the polarity of both the lightning return-strokes was negative.

Figure 3.24 shows a positive (+101 kA) nearby lightning strike beyond the end of a branch. The polarity of the first cycle of the LGC as shown in Figure 3.25 was negative and opposite to the lightning return-stroke polarity.

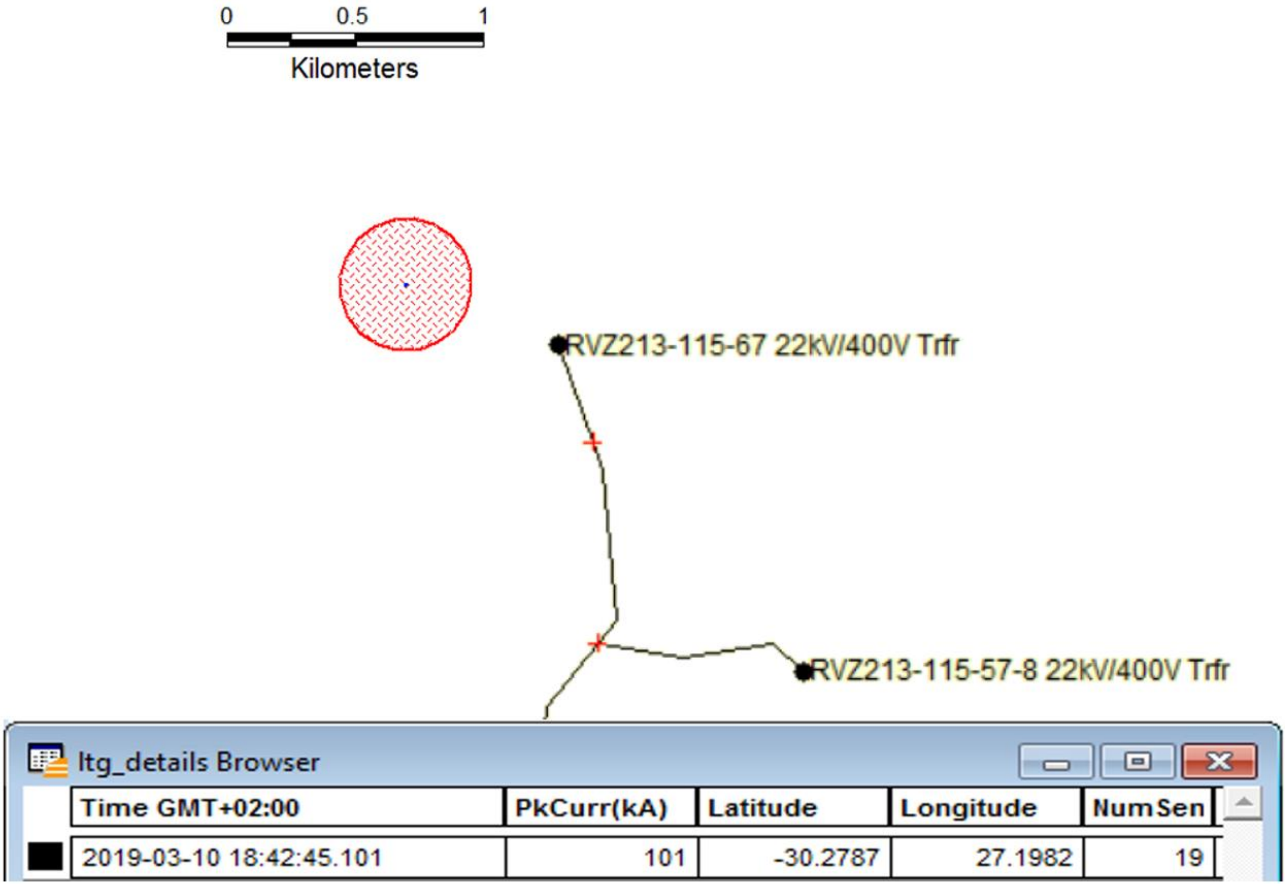

Figure 3.24 Case 7. A +101 kA nearby lightning return-stroke beyond the end of the line.

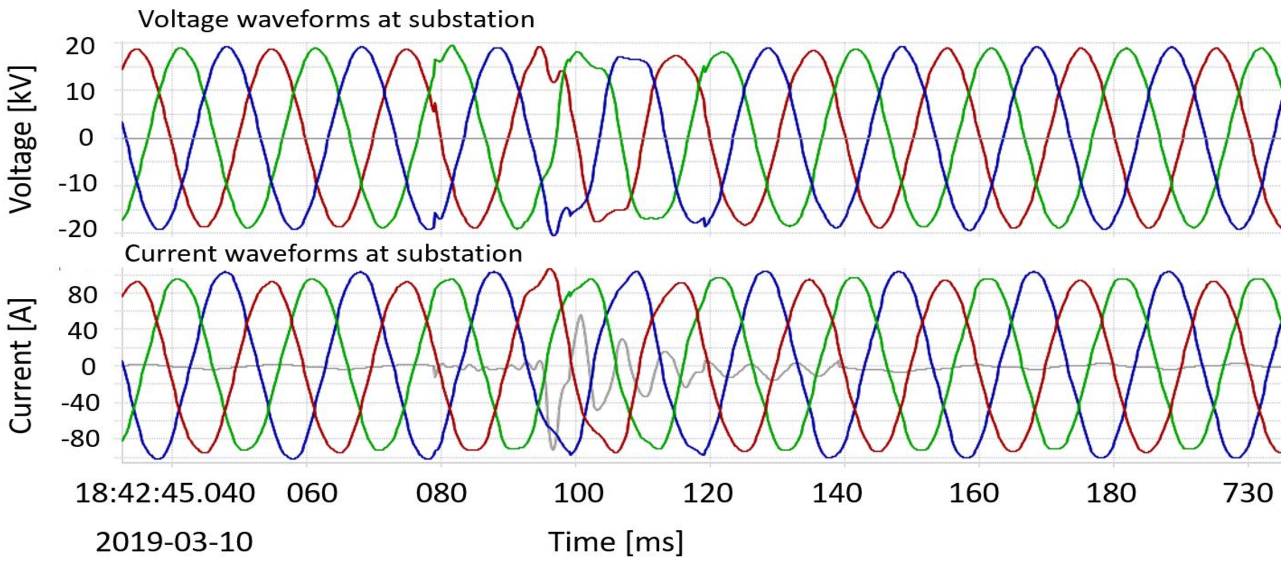

Figure 3.25 A recoding at the feeder substation shows that the first half cycle of the oscillation was of opposite polarity to the nearby lightning stroke in Figure 3.24.

All die nearby lightning strikes caused an LGC current at the substation that had an opposite polarity to the nearby lightning return-stroke polarity. It did not matter what the polarity, the amplitude, the distance from the substation was, or the position of the ground-termination point in relation to the line was. The lightning return-strokes had high amplitudes that would surely cause a LIOV that would have exceeded the line BIL. It could therefore be concluded that a nearby lightning strike to the line will have caused an LGC with a polarity that was opposite to the lightning return-stroke polarity.

Three cases where direct lightning strikes terminated to the line were modelled to verify the recordings at the feeder substation. Low amplitude lightning return-strokes were chosen for the studies. As discussed in 3.7, a nearby lightning strike 50 m from the line that exceeds 20.1 kA may cause a flashover in the worst-case scenario (no surge arresters in close proximity). A -9 kA, a -14 kA and a -13 kA direct lightning strikes were investigated. Unfortunately, positive direct lightning strikes were rare and had high amplitudes. A +81 kA direct lightning strike was used in the study. There was some wood damage at the point where the lightning strike terminated to the line which proved that the lightning strike was direct to the line.

Figure 3.26 shows that a power frequency fault current started to flow at the same time as the -9 kA lightning strike at a point that was 31 km from the feeder substation. A 9 kA nearby lightning strike 50 m from the line will induce 21 kV (39 kV if superimposed on the peak of the 50 Hz voltage waveform) at that point in the line which is far less than the 300 kV BIL of the line at this point. This meant that the LIOV exceeded the BIL of the line. Furthermore, a 9 kA nearby lightning strike (which would only induce a 60 A current in the line) would not have caused wood damage to a pole as wood damage only occurs for lightning currents larger than 7 kA [150]. It can therefore be concluded that it was a direct lightning strike to the line. Figure 3.26 shows that the LGC superimposed on the zero-sequence current recording was the same polarity as the lightning return-stroke which proved the theory used in the new methodology.

The -9 kA direct lightning strike to the line was then simulated using the extended ATP-EMTP model. Figure 3.27 shows a simulation of the LGV and LGC at the feeder substation. The polarity of both the LGV and LGC was the same as the polarity of the direct lightning return-stroke current polarity which supported the theory used in the new methodology. Although it was not important for this research, it was noted that the amplitude of the LGC was measured to be 166 A and according to the extended ATP-EMTP simulation, the LGC was 170 A. There were significant differences between the measured and simulated LGC amplitudes of the nearby lightning strikes due to many model input parameters that could not be determined reliably.

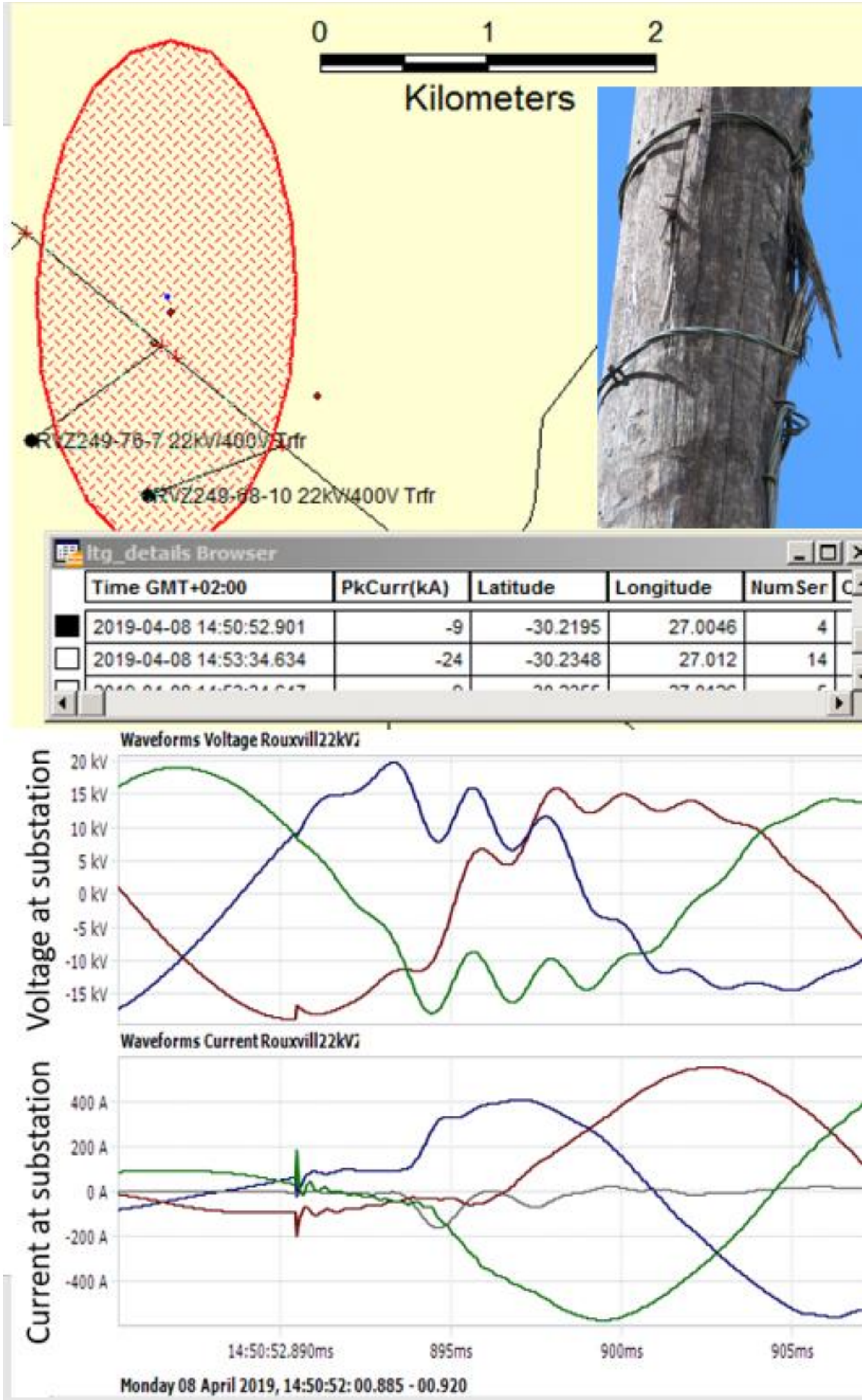

Figure 3.26 Case 8. A -9 kA direct lightning strike to a pole that was 31 km from the feeder substation resulted in a line flashover followed by a fault current. Note the similar polarities of the LGC and the return-stroke current polarity.

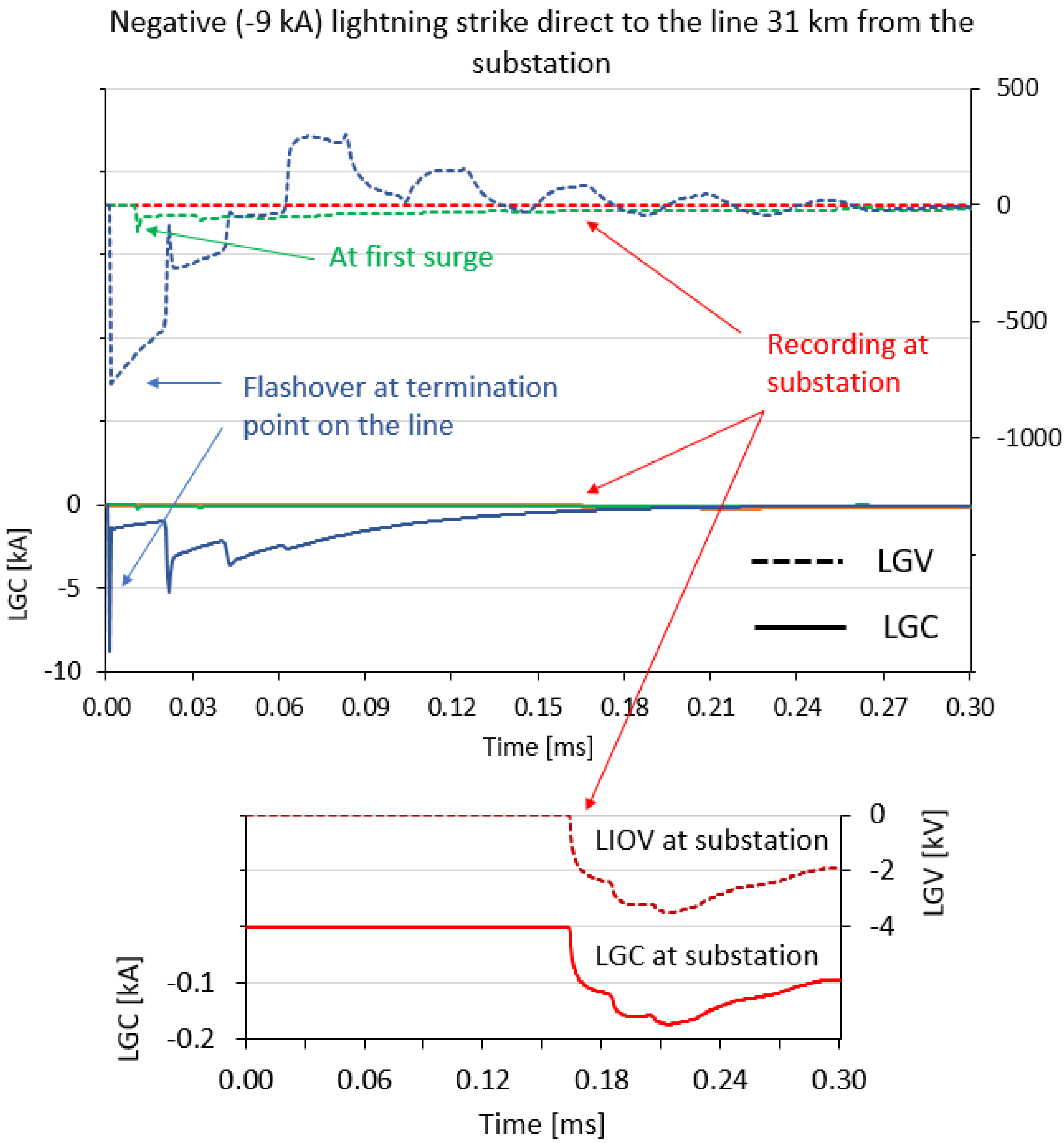

Figure 3.27 A simulation of the -9 kA lightning strike direct to the line as shown in Figure 3.26

Two strokes in the same flash as shown in Figure 3.28 terminated to the line at a point that is 18 km from the substation. The lightning return-stroke current also caused wood damage. Both the LGC and LGV measured at the feeder substation had a negative polarity which was the same polarity as the lightning strokes. The two lightning strikes were 24 ms apart and terminated most probably to the same point in the line. Figure 3.29 shows the recording of the LGC and LGV at the feeder substation.

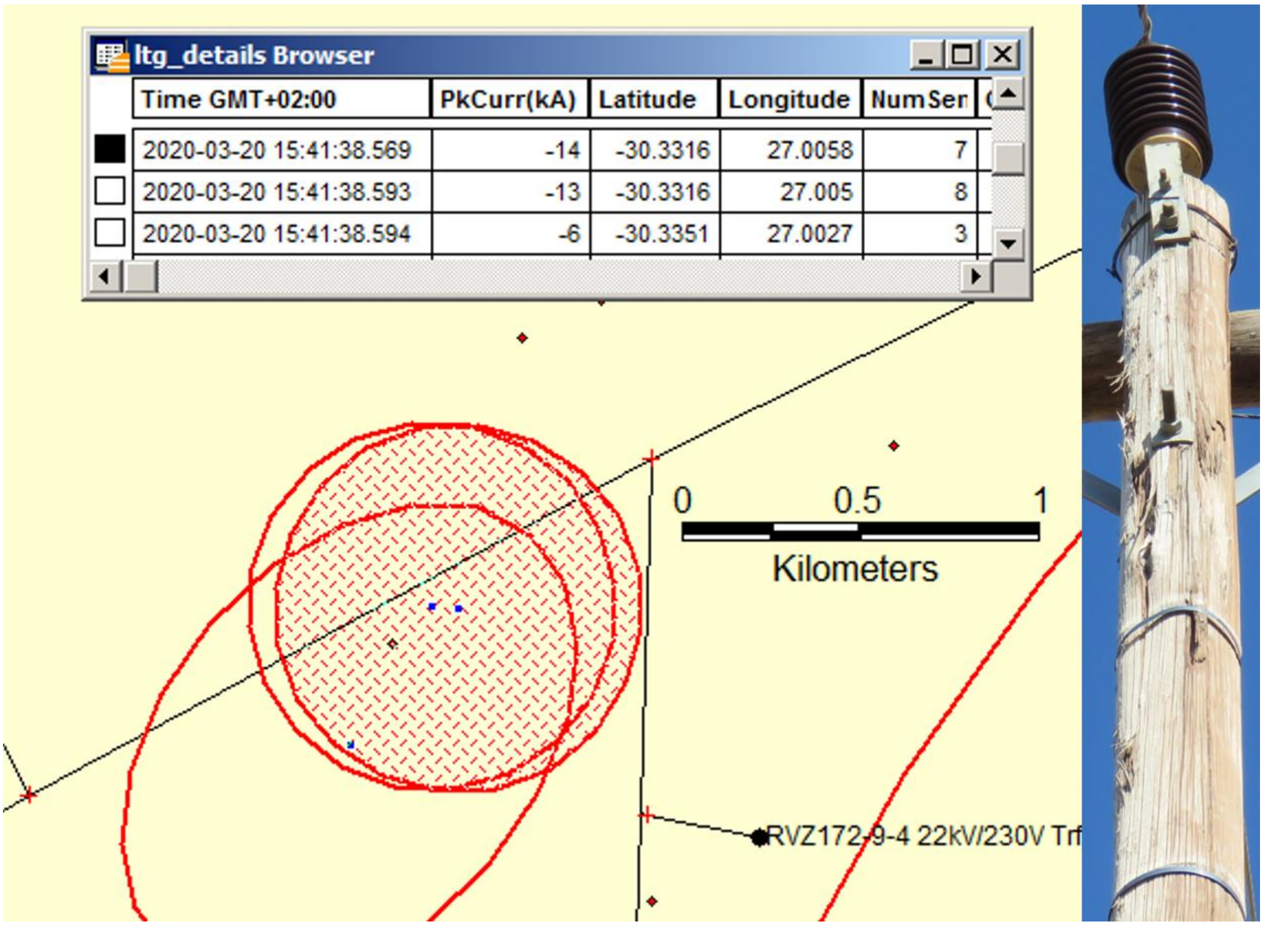

Figure 3.28 Case 9. A -14 kA and a -13 kA direct lightning strike to the line 18 km from the substation

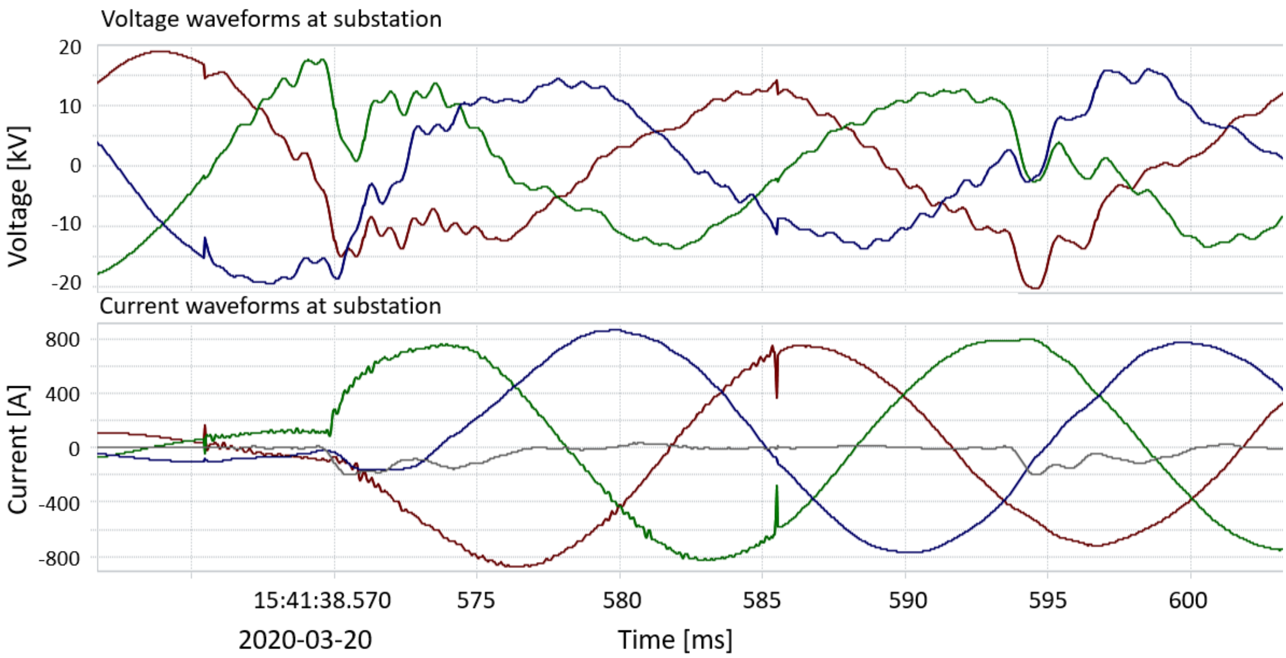

Figure 3.29 A recording at the feeder substation of a -14 kA and a -13 kA direct lightning strike to the line as shown in Figure 3.28. Both the LDN data and the current recording shows that the two lightning strikes were 24 ms apart.

Figure 3.30 shows a simulation of the -14 kA lightning strike direct to the feeder. There would have been barely any noticeable difference between a simulation of the -13 kA and the -14 kA lightning strikes and therefore only one of the cases was simulated. The simulation also shows that the polarity of the LGC and the LGV were both negative which is the same as in the recording.

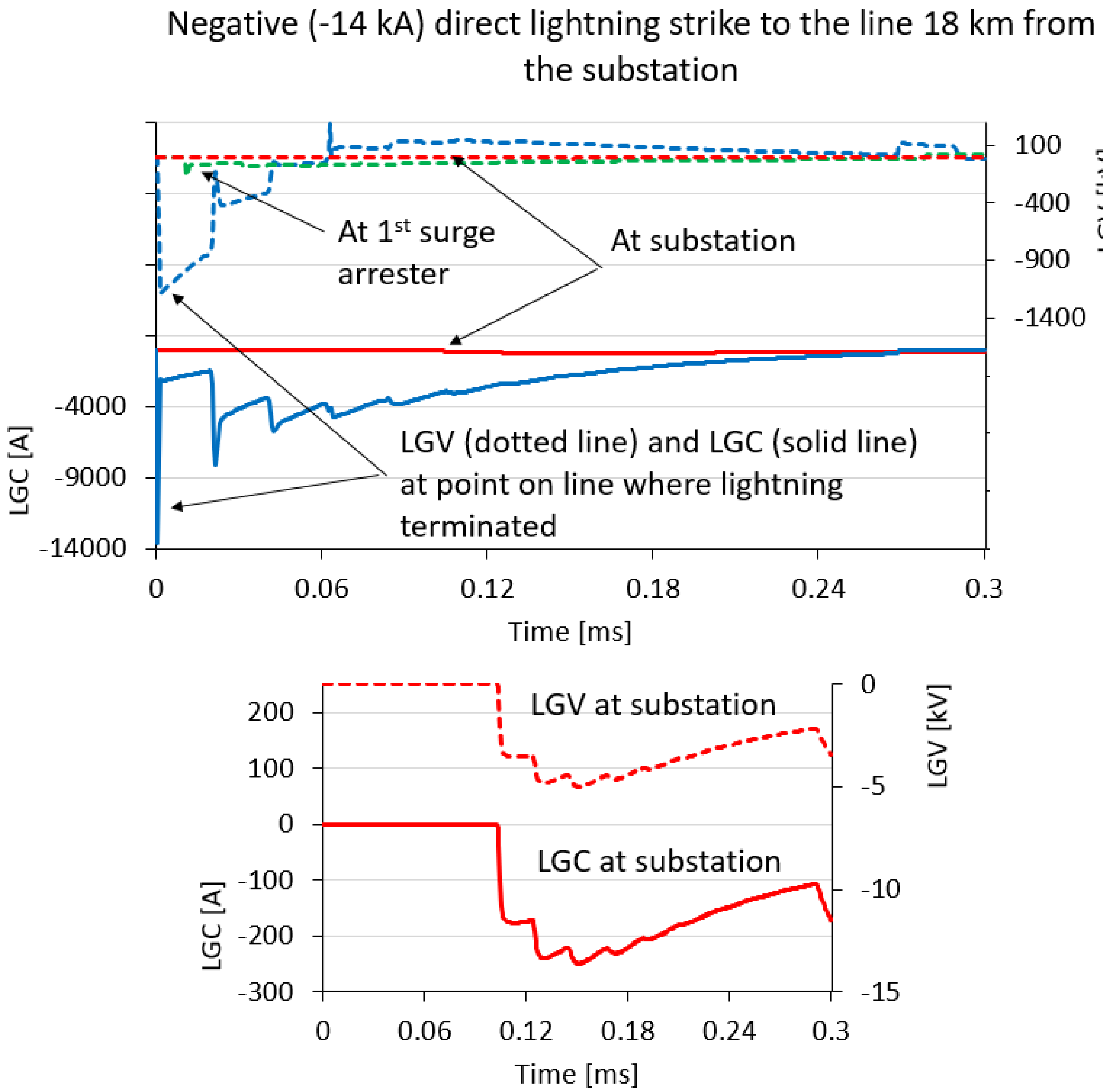

Figure 3.30 A simulation of the -14 kA direct lightning strike to the line. It confirmed that the negative lightning return stroke caused an LGC with a negative polarity.

Figure 3.31 shows an LDN geographical picture of a positive (+81 kA) direct lightning strike to the line. Some wood damage could be seen which is an indication that the lightning strike terminated direct to the line.

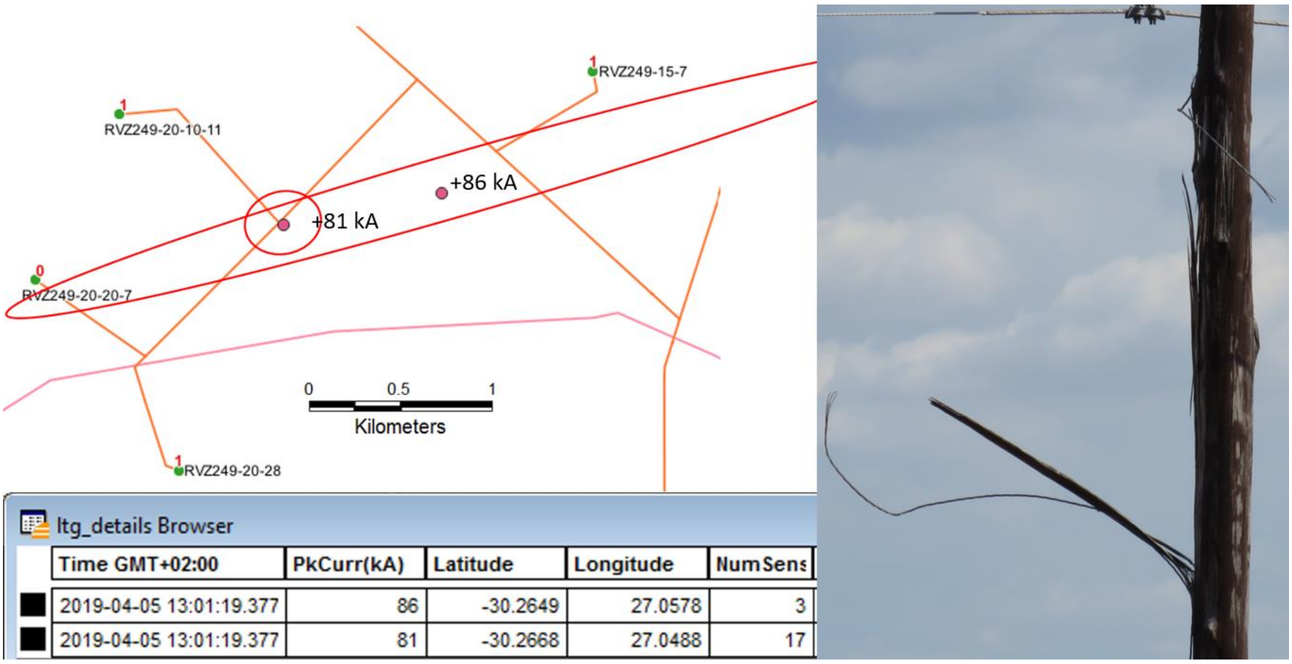

Figure 3.31. Case 10. A +81 kA lightning strike terminated direct to the line 31 km from the feeder substation. Some wood damage also occurred at the point where the lightning terminated on the pole.

Figure 3.32 shows a recording at the feeder substation of the +81 kA lightning strike. The polarity of the LGC and the LGV was positive which is the same polarity as the lightning return-stroke current polarity. Figure 3.33 shows an ATP-EMTP simulation of the direct lightning strike in Figure 3.31. Both the LGC and LGV polarity were the same as in the recording shown in Figure 3.32.

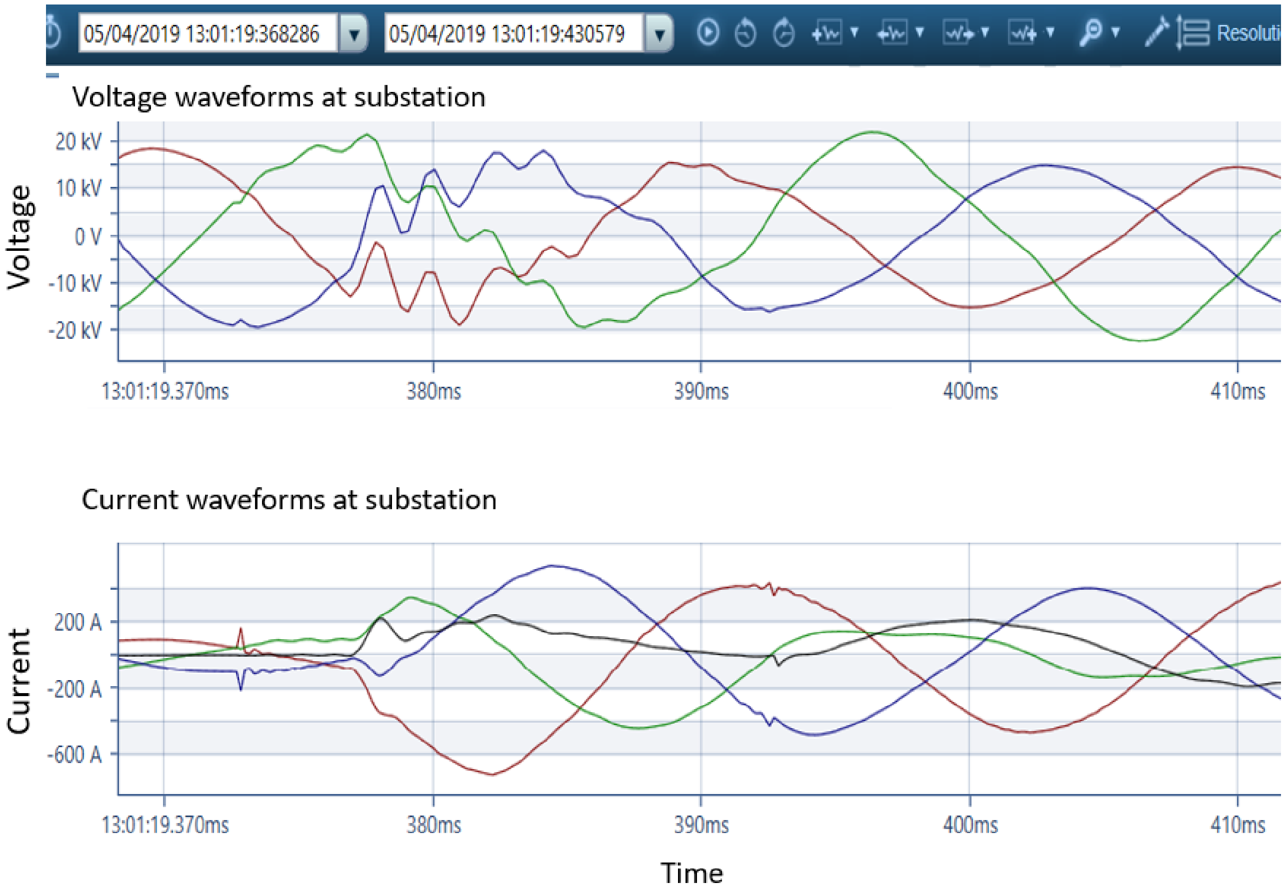

Figure 3.32. A recording at the feeder substation of the +81 kA lightning strike direct to the line

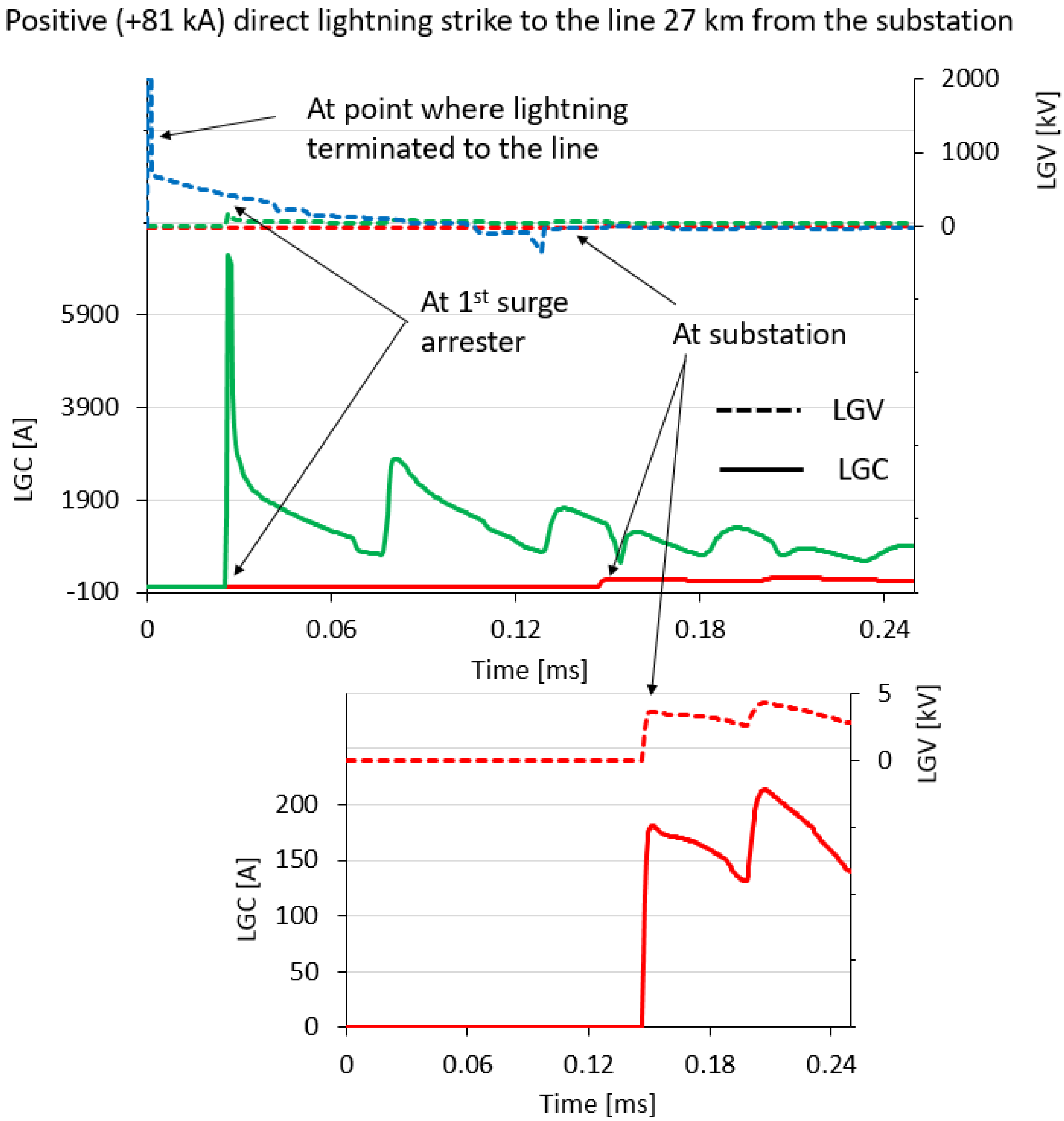

Figure 3.33. A simulation of the +81 kA lightning strike direct to line as shown in Figure 3.31.

In all four cases that were analyzed, it was found the direct lightning strikes to the line caused an LGC and an LGV that had the same polarity as the lightning return-stroke current polarity. It was concluded that nearby lightning strikes caused an LGC and a LIOV that had the opposite polarity at a point in the line further than 250 m from the point in the line closest to the nearby lightning strike. This was due to the finite soil conductivity. For direct lightning strikes, the polarity of the LGC and the LGV stayed the same from the point where the lightning return-stroke terminated to the line up to the feeder substation. This was due to the lightning strike that terminated on the conductors and there was no soil between the lightning strike termination point and the point of measurement at the feeder substation.

3.8 Data Analysis

Lightning data as from 1 July 2018 to 30 June 2020 was used to determine the line's lightning performance. It consisted of 38 675 flashes (126 311 strokes) that terminated inside a 2 km buffer around the line. The QoS loggers recorded the three-phase currents and calculated the zero-sequence current continuously at a maximum sampling rate of 400 kHz. Both QoS logger data and the LDN data were GPS timestamped and were compared within 10 ms accuracy. Each LGC and LIOV was linked to a specific lightning strike captured by the LDN. This avoided counting faults due to rain (wet insulation) and wind (conductor or tree clashing) that were part of the storm, as lightning-related faults.

Figure 3.34 shows a typical recording of a lightning flash with several lightning strikes direct to the line and that the last two lightning strikes (17 and 18) were nearby the line. The top waveform in Figure 3.34 shows a recording of the voltage in the middle of the line. The power frequency voltage in the middle of the line dropped significantly which was an indication that the fault was more towards the end of the line. The first lightning strike was direct to the line and caused a flashover on the line. Several lightning strikes within the flash were missed by the LDN. Figure 3.35 shows the recording of the first stroke in this flash. The polarity of the LGV, as well as the LGC, were negative. The sampling rate of the QoS recorder increased when high-frequency components (due to the leader activities) on the current and voltage recordings were present and decreased again after the high-frequency components vanished. This was done to save memory space. Another example of the leader activities measured by [163] [164] is shown in Figure 3.36. Figure 3.37 shows the LDN data of this lightning flash.

An insulation failure (line flashover) was visible on the 50 Hz current recording (a 50 Hz fault current started flowing at the time of the first lightning stroke in the flash). If the fault current recorded by the QoS logger decreased to normal load current, there was no breaker operation recorded and there was no inrush current at the time the breaker should have auto-reclosed, it meant that the arc independently quenched before the breaker could operate.

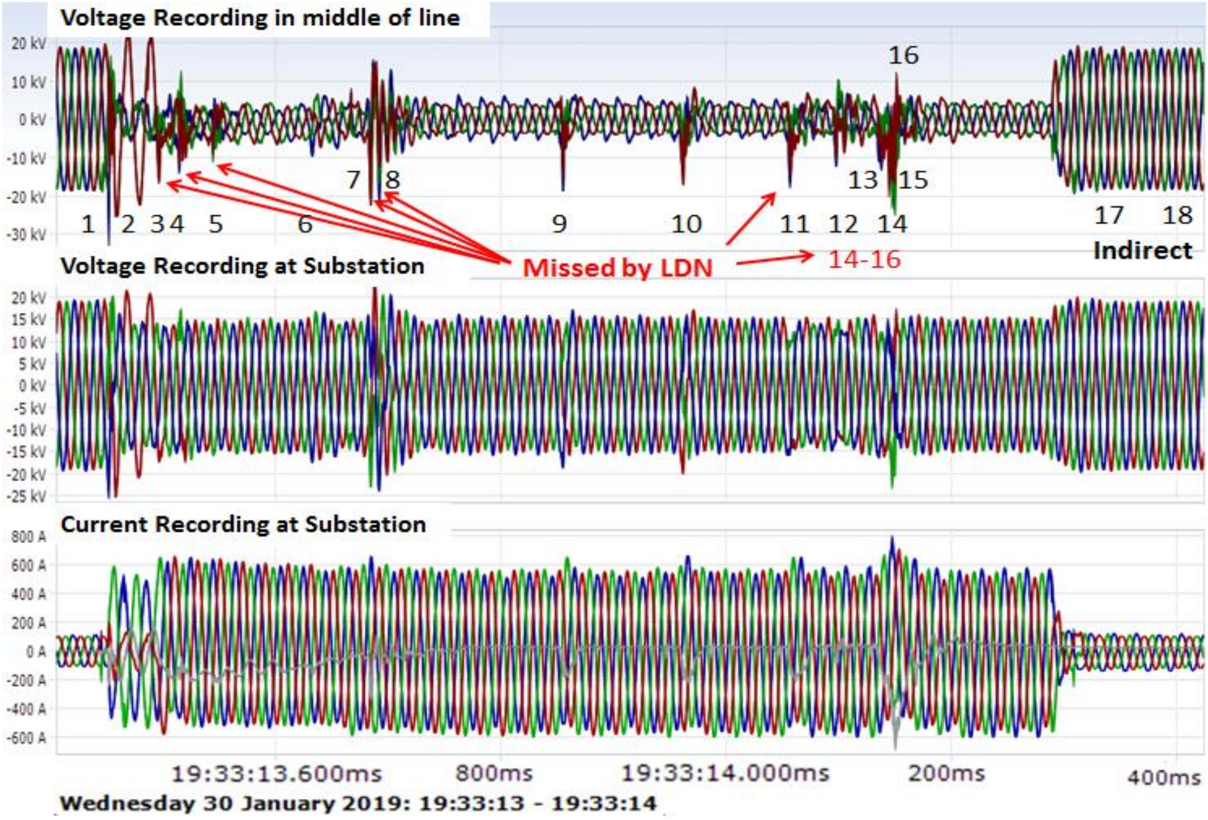

Figure 3.34 An example of a lightning flash consisting of multiple strokes of which the 1st lightning stroke terminated direct to the line causing the line to flashover while the 17th and 18th strokes terminated nearby the line. It can be seen that nine lightning strokes within the flash were missed by the LDN.

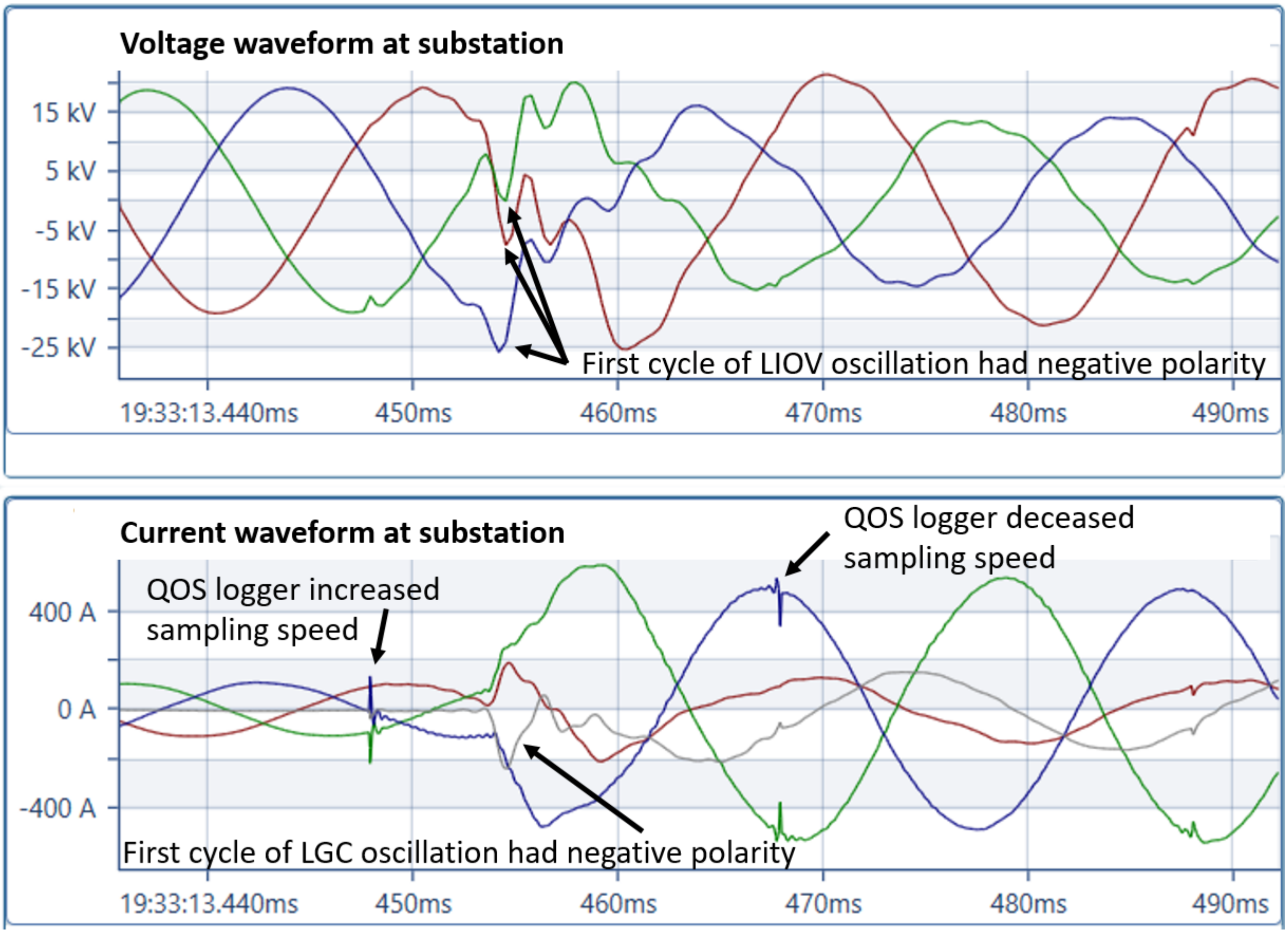

Figure 3.35 The polarity of both the LGV and LGC due to the first stroke of the flash shown in Figure 3.34 was negative. The QoS logger increased and decreased the sampling frequency during the presence and absence respectively of the higher frequency components due to the lightning activity.

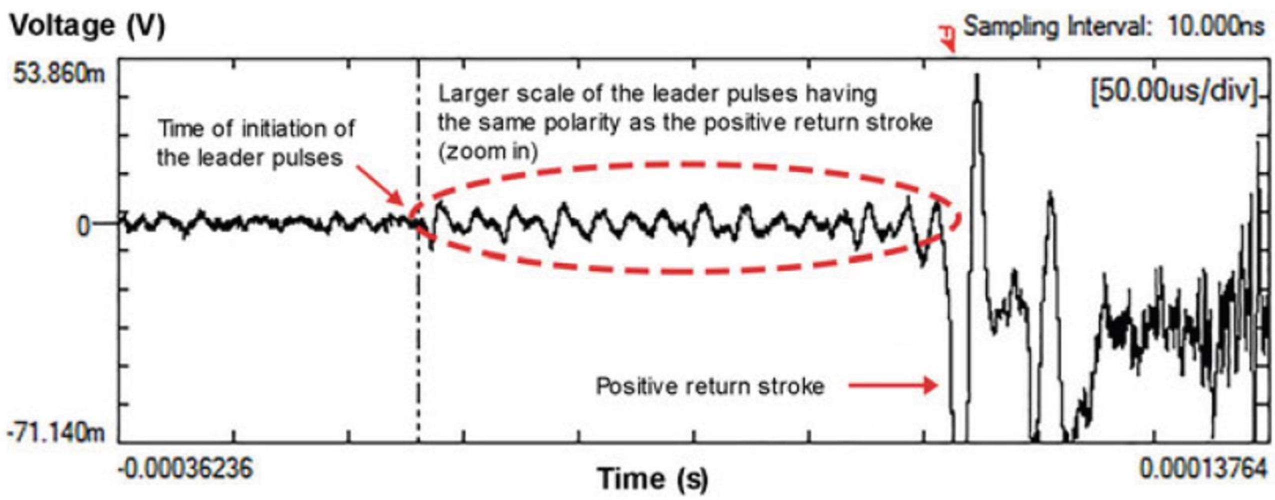

Figure 3.36 The high-frequency components due to leader activity [163]. Permission obtained from the Atmospheric Research.

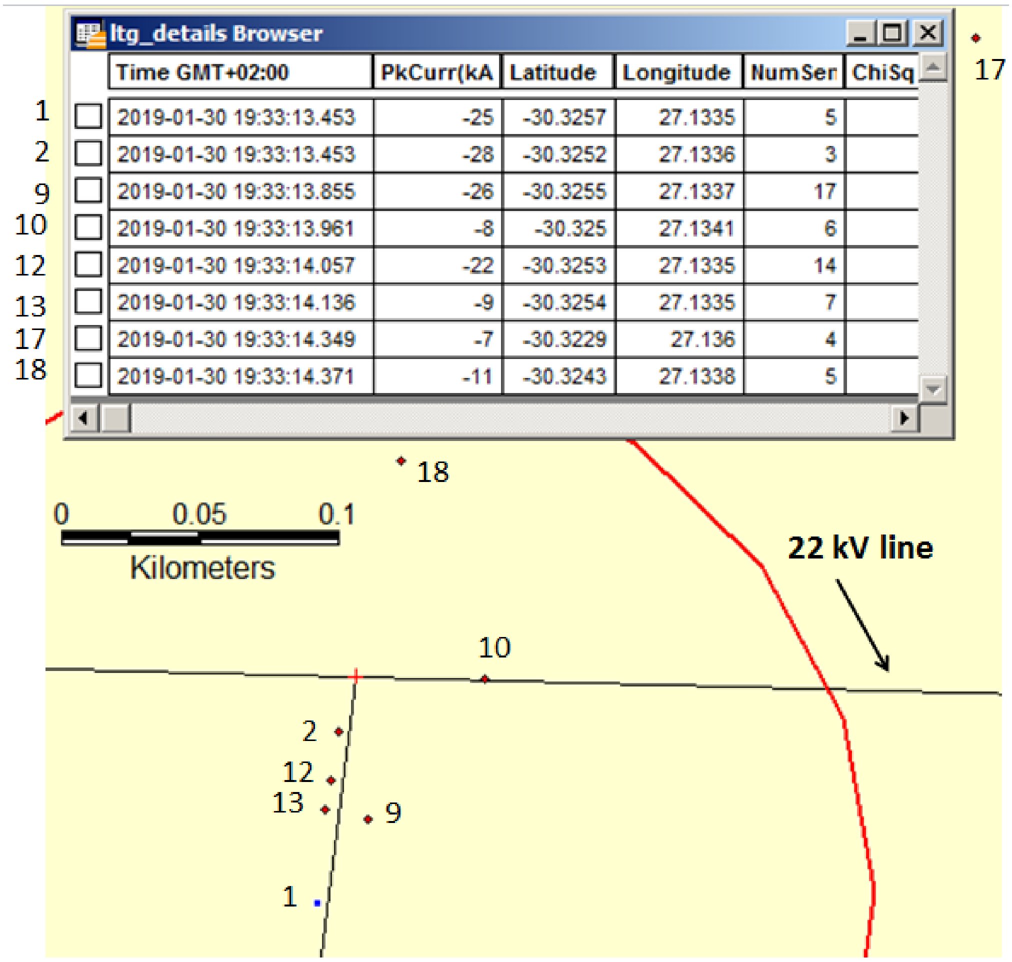

Figure 3.37 The LDN data for the incident is recorded in Figure 3.34. Strokes 17 and 18 were nearby lightning strokes and did not terminate on the line. Note the geographical inaccuracy of the LDN.

The first step in the data analysis was to analyze the recordings of the QoS logger, breaker operations and SCADA reports for possible line faults and lightning activity. Figure 3.38 shows a typical recording of a lightning storm captured on the recorder at the feeder substation. Each LGV, fault current and LGC recording was analyzed. This required zooming in several times until all the required LGC and LGV information were visible (from Figure 3.38 up to Figure 3.41). The QoS instrument recording in Figure 3.41 shows that both the LGC and the LGV had a negative polarity.

The second step was to look for lightning activity at the same time on the LDN recording. In the case, as shown in Figure 3.42, a -25 kA return-stroke caused the line flashover. The third step was to determine whether the lightning flash was nearby or direct to the line by comparing the polarity of the LGC and LGV to the lightning return-stroke data from the LDN. Similar polarities indicated that it was a direct lightning strike to the line while opposite polarities indicated that it was a nearby lightning strike to the line. In this case, it was a direct lightning strike to the line because it had the same polarity as the LGC and the LIOV as shown in Figure 3.41.

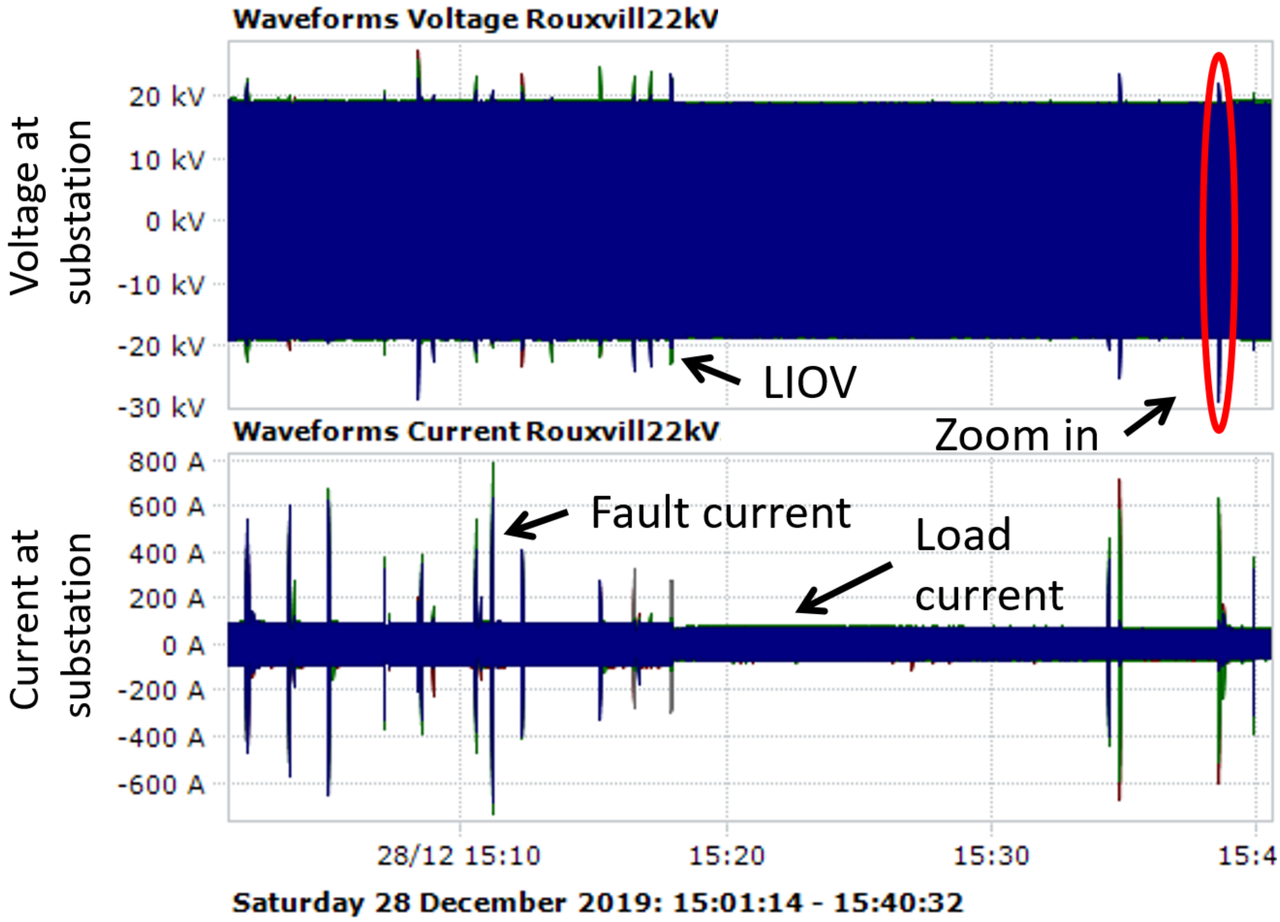

Figure 3.38 A typical voltage and current recording during a period with lightning activity in the afternoon of 28 December 2019. LGVs and fault currents were visible. Each incident had to be investigated by zooming into a smaller time period (the red ellipse) up until all the required LGV and LGC information could be seen.

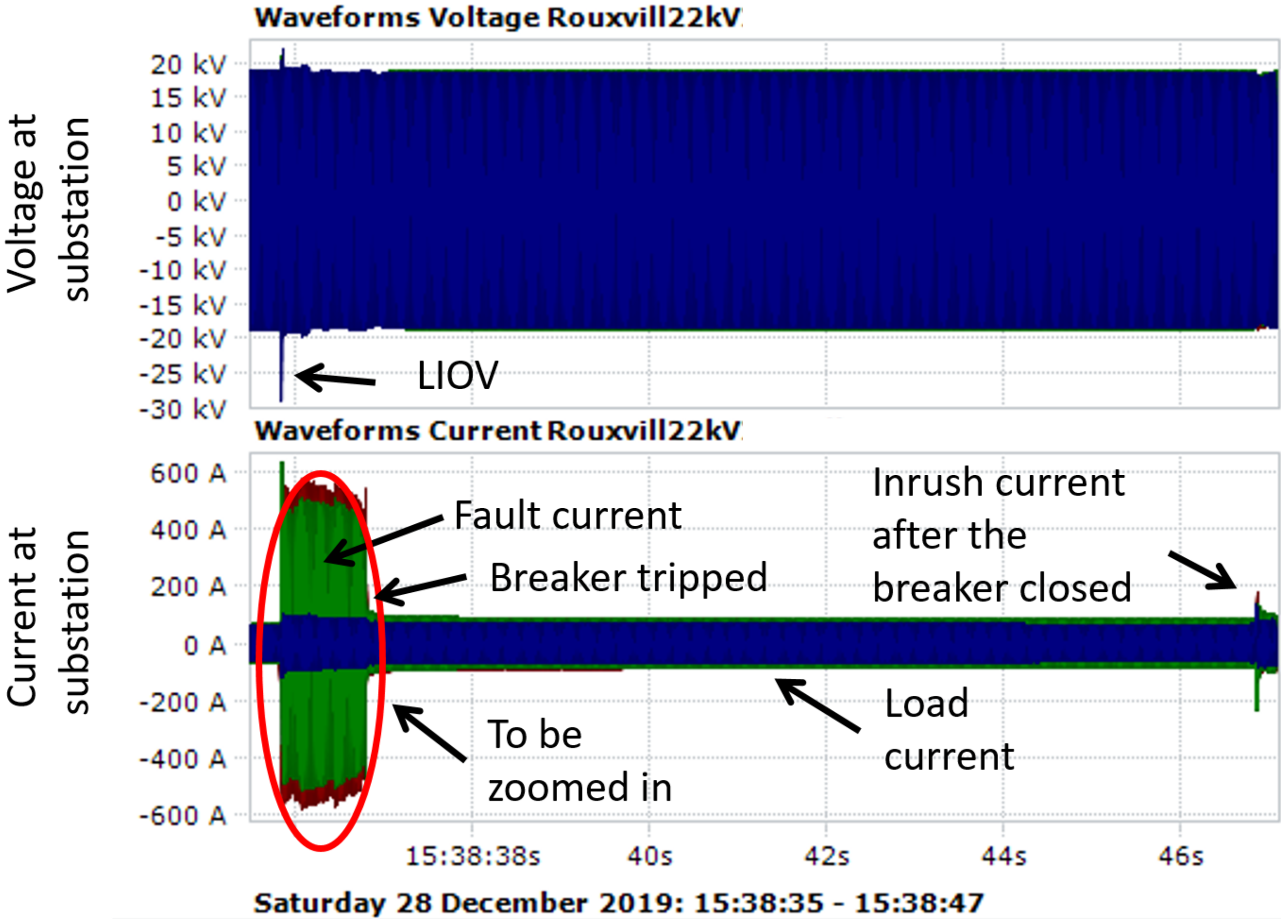

Figure 3.39 A zoomed-in picture of Figure 3.38 that shows a temporary fault caused by lightning activity. The fault current duration (within the red ellipse) and the time that the breaker auto-reclosed followed by the inrush current can be seen.

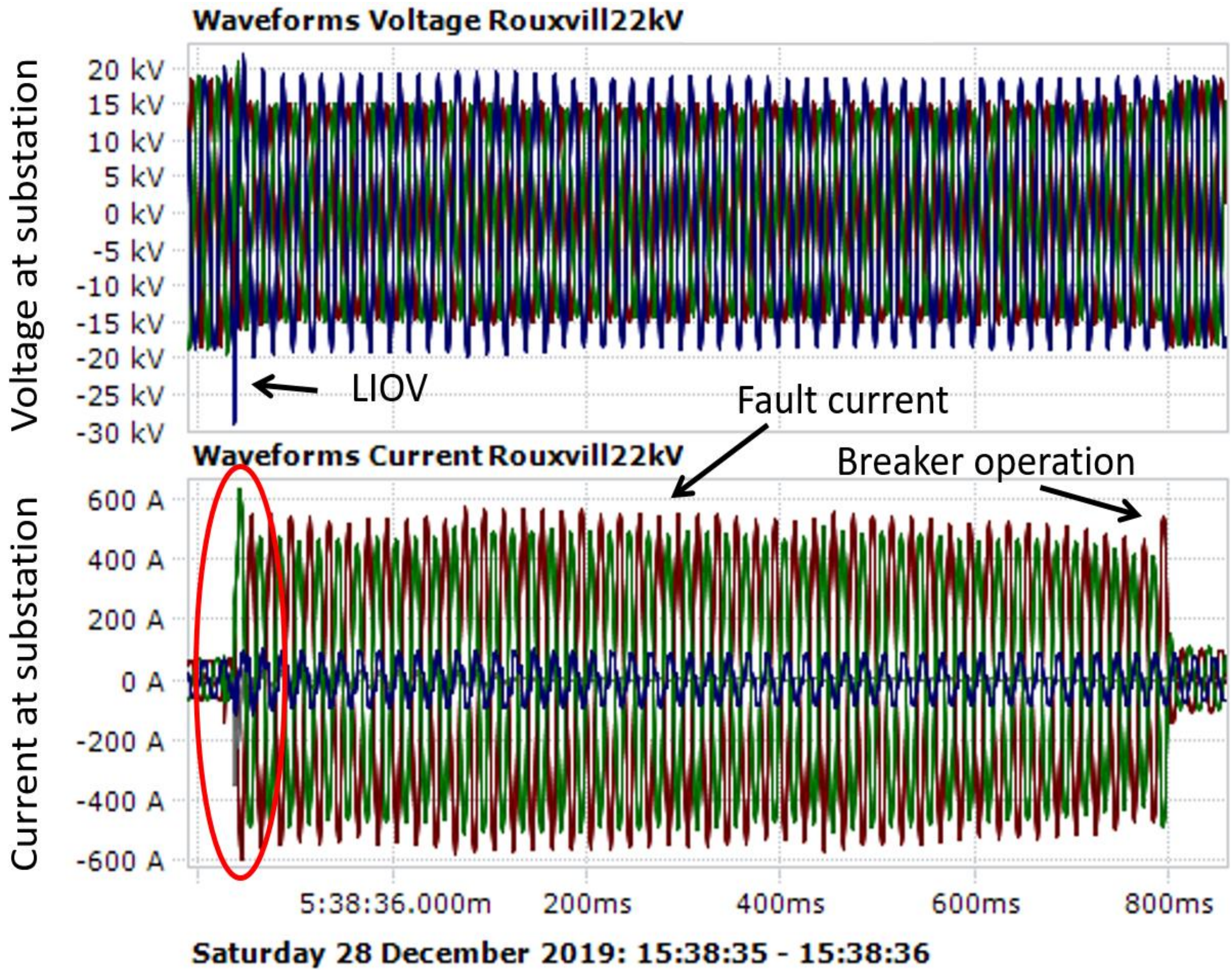

Figure 3.40 An expansion of the recording within the red ellipse in Figure 3.39 shows the duration of the fault current up to the breaker operation.

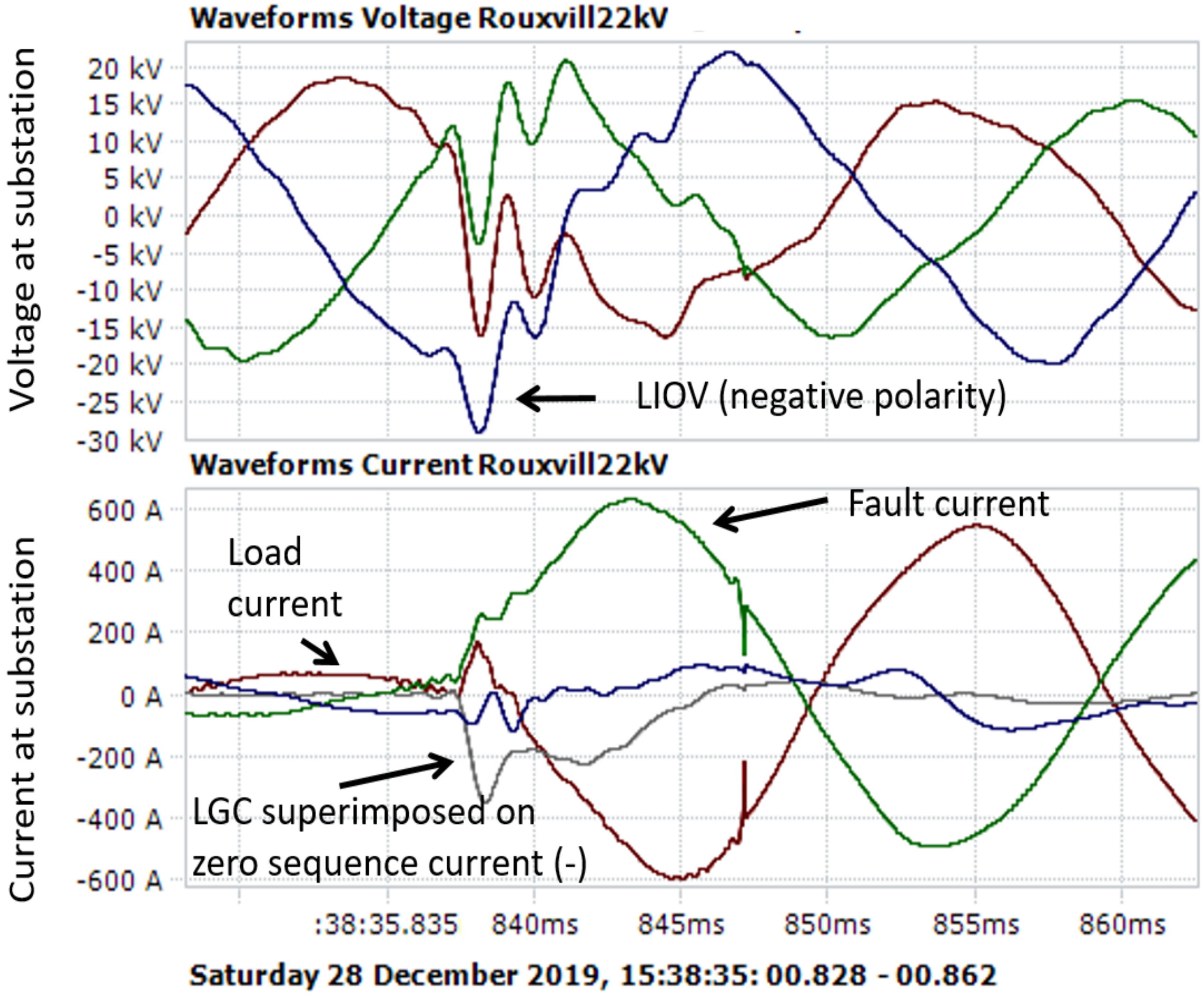

Figure 3.41 Detail showing the polarity of the LGV and the LGC. Both the LGV and the LGC had a negative polarity.

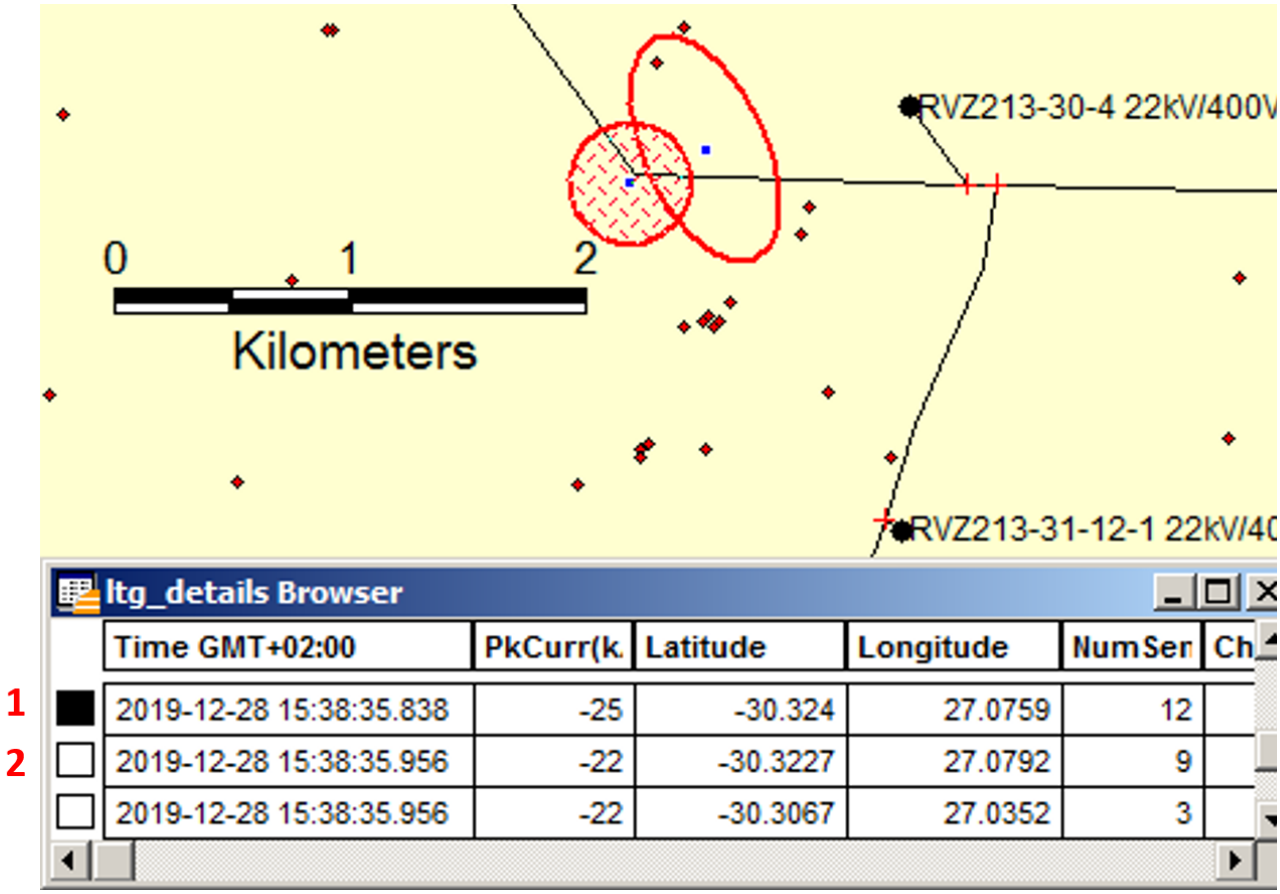

Figure 3.42 The lightning incident that caused the temporary line fault shown in Figure 3.39. The lightning strike (-25 kA) had the same polarity as the LGV and LGC and it was therefore a direct lightning strike to the line.

The next step will be to determine if there was a fault current as a result of the lightning flash and whether the 50 Hz fault current resulted in a breaker operation (Figure 3.39) or whether independent arc quenching took place as shown in Figure 3.43. These recordings were compared to the protection operation and the SCADA data.

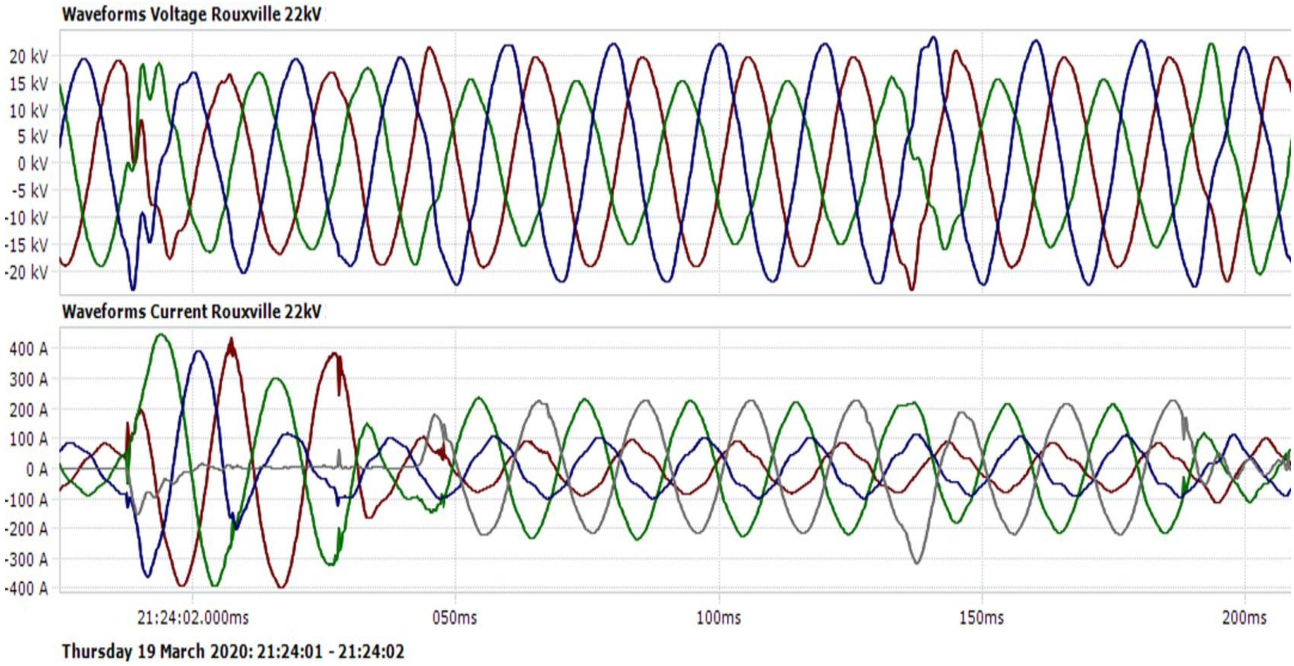

Figure 3.43 A three-phase fault that quenched independently before breaker operation.

In borderline cases or cases where additional information about the actual environment or equipment connected to the power network was needed, a site visit was done using the GPS coordinates in the LDN data to find the location. Any flash marks and damage were noted. All the locations where line flashovers due to nearby lightning strikes occurred over the two years were also visited. The BIL of the line at each of these events were verified during site visits. All the line faults were then categorized according to the number of phases involved in the fault, the root cause of the fault, and whether the fault was cleared by the breaker or quenched independently. The last step was to normalize the GFD and the lightning-related faults on the RVZ line to a format that could be compared to the IEEE standard 1410-2010 lightning performance estimations.

Appendix A shows more examples of recordings that were done in the research.

4 THE CASE STUDY EXPERIMENTAL MEASUREMENTS AND ANALYSIS

Table 4.1 and Figure 4.1 show the line fault data and the GFD respectively between July 2018 and June 2020. There were 1155 faults (flashovers) on the line of which 528 were lightning-related. A total of 38 675 flashes (126 311 strokes) that terminated inside a 2 km buffer along the line were recorded by the LDN. There were a total of 431 single-phase faults (38.2% of the faults) and 696 faults between phases which differ from [165] and [166] where it was found that between 50% and 80% of faults were single-phase faults.

Table 4.1 Recorded RVZ line faults categorized according to the involved phases, the root causes and how the faults were cleared.

<table>
<tr><td colspan="10">Total number of lightning flashes within a 2 km buffer along the line: 38 675 flashes (126 311 strokes)</td></tr>
<tr><td colspan="2">LINE FAULTS</td><td>Tripped</td><td>Quenched</td><td>No fault</td><td>Lightning related</td><td>Weather-related</td><td>Other</td><td>Total</td><td>Lightning and weather</td></tr>
<tr><td rowspan="4">Phase-to-phase faults</td><td>Direct flash</td><td>278</td><td>96</td><td rowspan="9">6</td><td rowspan="2">377</td><td rowspan="2"></td><td rowspan="3"></td><td rowspan="4">696</td><td rowspan="3">557</td></tr>
<tr><td>Nearby flash</td><td>1</td><td>2</td></tr>
<tr><td>Weather-related</td><td>99</td><td>81</td><td rowspan="2"></td><td>180</td></tr>
<tr><td>Other</td><td>78</td><td>61</td><td></td><td>139</td><td></td></tr>
<tr><td rowspan="4">Single-phase faults</td><td>Direct flash</td><td>93</td><td>51</td><td rowspan="2">151</td><td rowspan="2"></td><td rowspan="3"></td><td rowspan="4">431</td><td rowspan="3">320</td></tr>
<tr><td>Nearby flash</td><td>1</td><td>6</td></tr>
<tr><td>Weather-related</td><td>84</td><td>85</td><td rowspan="2"></td><td>169</td></tr>
<tr><td>Other</td><td>51</td><td>60</td><td></td><td>111</td><td></td></tr>
<tr><td colspan="2">Undetected by LDN</td><td>20</td><td>8</td><td>28</td><td></td><td></td><td>28</td><td></td></tr>
<tr><td colspan="2">Total</td><td>705</td><td>450</td><td>6</td><td>556</td><td>349</td><td>250</td><td>1155</td><td>877</td></tr>
</table>

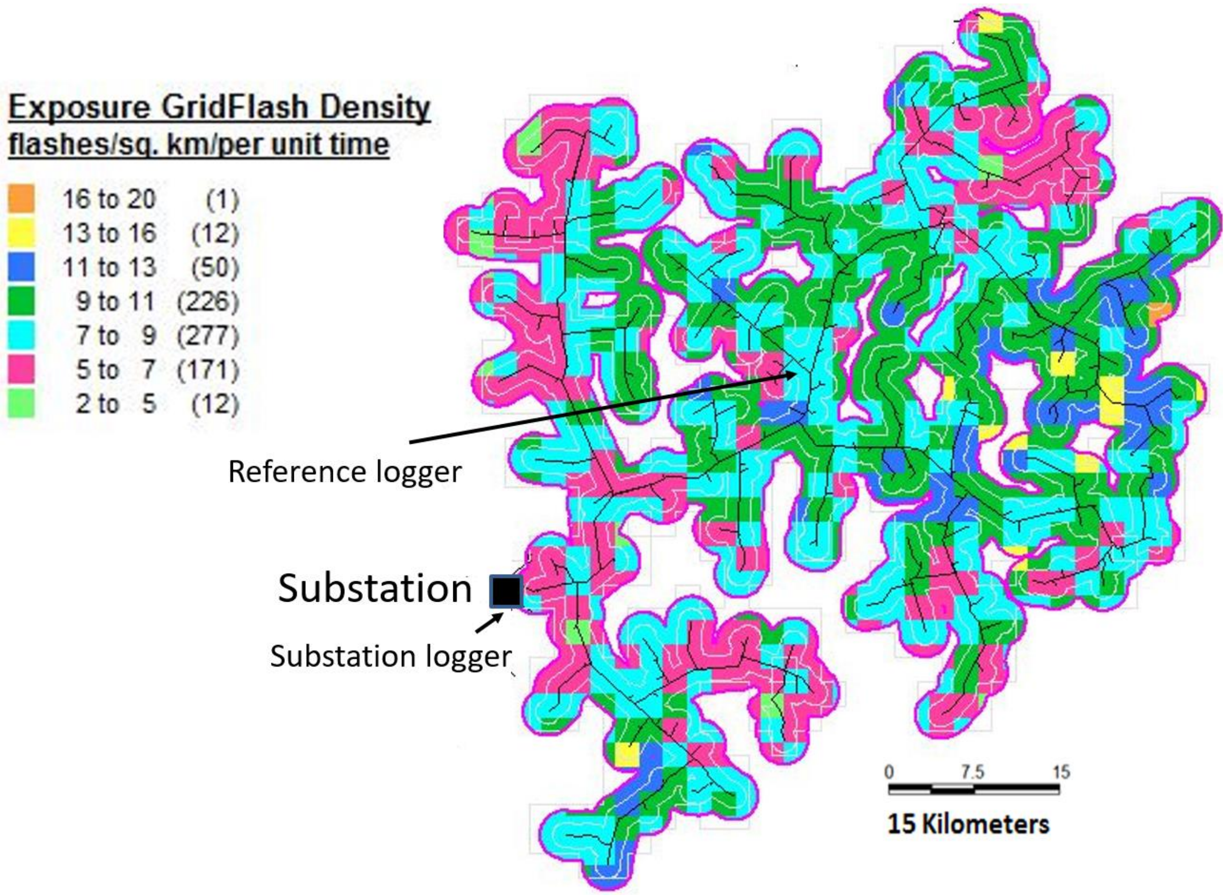

Figure 4.1 The GFD along the line between June 2018 and July 2020. The average GFD was 8.51 flashes / km² / year. An additional recorder (QoS logger) was installed for reference purposes in the middle of the line

Table 4.2 shows more detail on the lightning flashes that occurred along the RVZ line during the research period of two years.

Table 4.2 Lightning flash details along the RVZ line between 1 July 2018 and 30 June 2020.

Asset name		Count	Count -	Count +	% positive	Density	Max kA	Avg kA	Mdn kA
RVZ line		38675.8	35515.1	3160.7	8.2	8.51	180	19	16
Exp Fact	Min kA(-)	Max kA(-)	Avg kA(-)	Mdn kA(-)	Min kA(+)	Max kA(+)	Avg kA(+)	Mdn kA(+)	
319.46	1	180	19	16	6	180	18	11	

Figure 4.2 shows the lightning trend during the research period. There was much more lightning activity in the first lightning season than in the second season.

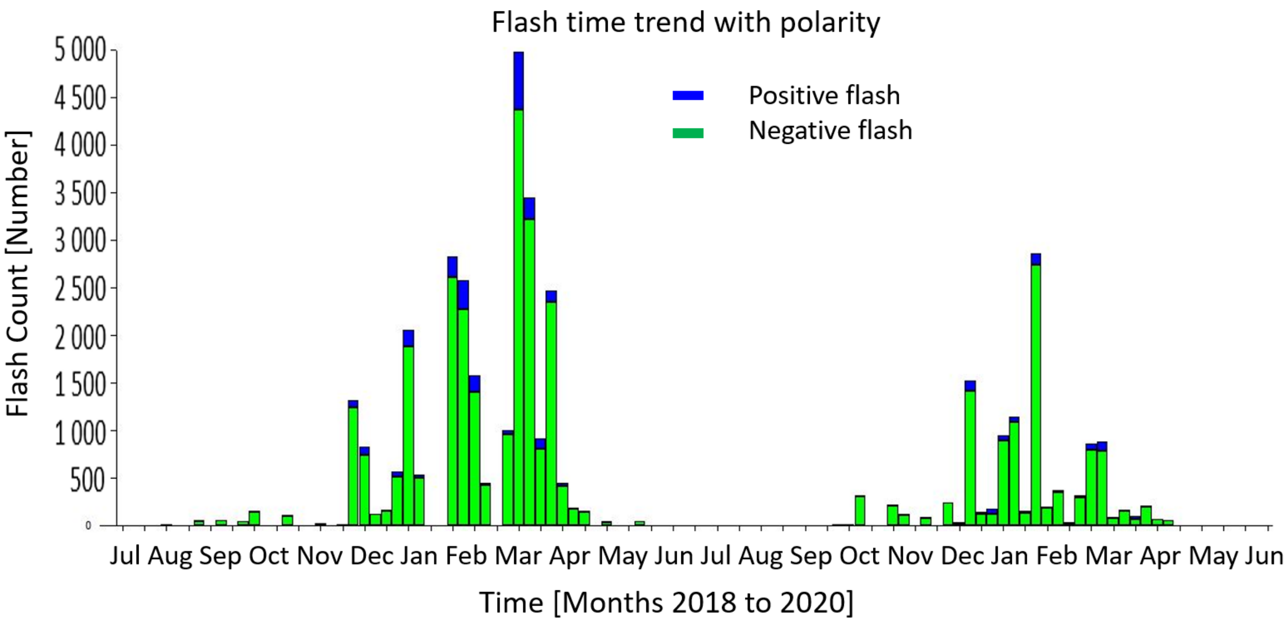

Figure 4.2 Lightning details within a 2 km buffer along the line.

4.1 Lightning flashes direct to the line

There were 524 lightning flashes direct to the line that resulted in 371 breaker operations. A total of 147 faults were quenched independently before breaker operation. A 28% error would have been made if breaker operations were used to count the number of faults due to direct lightning flashes to the line. A total of 144 faults (27.8% of the faults) were single-phase faults and 374 faults were between phases. According to the IEEE standard 1410-2010 the estimated number of direct lightning flashes/year/100 km to the line can be determined by Equation 21:

$$N = N_g \left(\frac{28h^{0.6}+b}{10}\right) \qquad (21)$$

Where

N = number of direct lightning strikes to the line per year per 100 km

N_g = lightning flash density

h = the height of the line

b = the width of the line

According to Equation 21, a total of 97 flashovers/year/100 km due to direct lightning flashes to the line were predicted in an area with a lightning GFD of 8.51 flashes/km²/year, a line-height of 10 m and a line width of 2 m. There were 524 direct lightning flashes to the 714 km line during the 2-year research period. The normalised number of direct lightning flashes to the line for one year per 100 km line was measured to be 37 flashovers/year/100 km which was lower than the 97 as calculated by using Equation 21. The IEEE Std 1410-2010 overestimated the number of direct flashes to the line. This could have been due to the environment and ESOs in the vicinity of the line.

4.1.1 Nearby lightning flashes to the line

Only 10 out of the 38157 nearby lightning flashes caused flashovers on the line over two years – an average of 5 flashovers annually. The flashover rate for a line with a BIL of 165 kV should be 218.7 flashovers/714 km/year for a GFD of 8.51 and a soil resistivity of 300 Ω-m according to the IEEE standard 1410-2010 as shown in Figure 4.3. This is much higher than the measured average of 5 flashovers/714 km/year. The main reasons for the difference were most probably due to reasons as discussed in the Literature Survey chapter. The lightning performance of the line due to nearby lightning strikes was affected by surge arresters connected to the line, a possible lower rise time and tortuosity of the lightning return-strokes, lower amplitude return-strokes, varied line-height and soil resistivity.

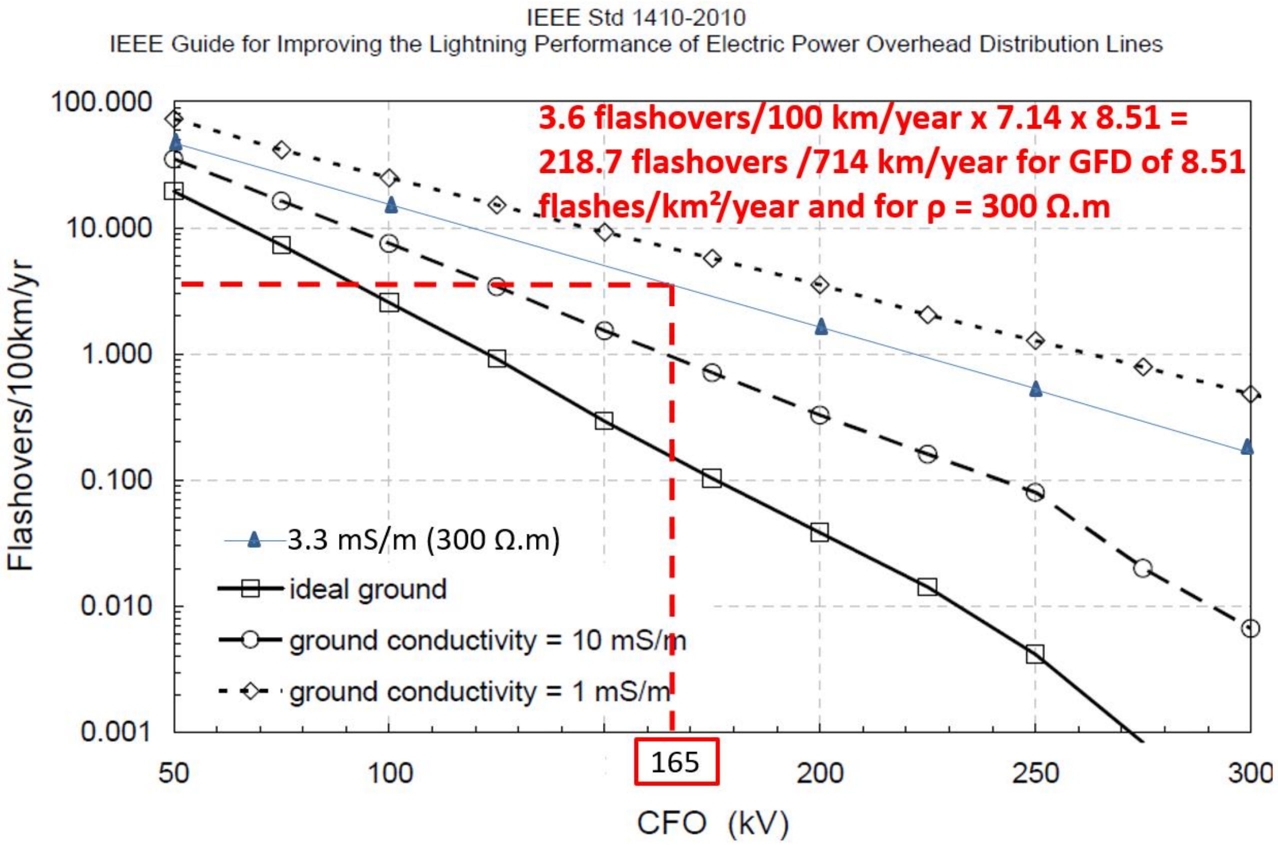

Figure 4.3 According to the IEEE Standard 1410-2010 the flashover rate due to nearby lightning flashes should be 3.6 flashovers/100 km/year for a line with a 165 kV BIL and soil conductivity of 3.3 mS/m (Permission obtained from the IEEE 2010 [12]). The flashover rate should therefore be 218.7 flashovers/714 km line/year if the GFD was 8.51 flashes/km²/year.

Only two of the ten nearby lightning strikes that caused a line flashover resulted in a breaker operation which meant that 80% of the faults in this category were independently quenched before breaker operation. This was an indication that the fault mechanism was different to fault mechanisms due to lightning events which had a lower (between 25% and 35%) independent fault current quench rate. Some badly degraded insulators (Figure 4.4), as well as damaged surge arresters (Figure 4.5), were found in the area where nearby lightning flashes caused flashovers on the line. It is possible that some of the line faults that were at the same time as nearby lightning strikes occurred could have been caused by a combination of damaged insulation and the moister content in the storm. This may explain why lightning measurements on a new line did not show any flashovers due to nearby lightning strikes [148].

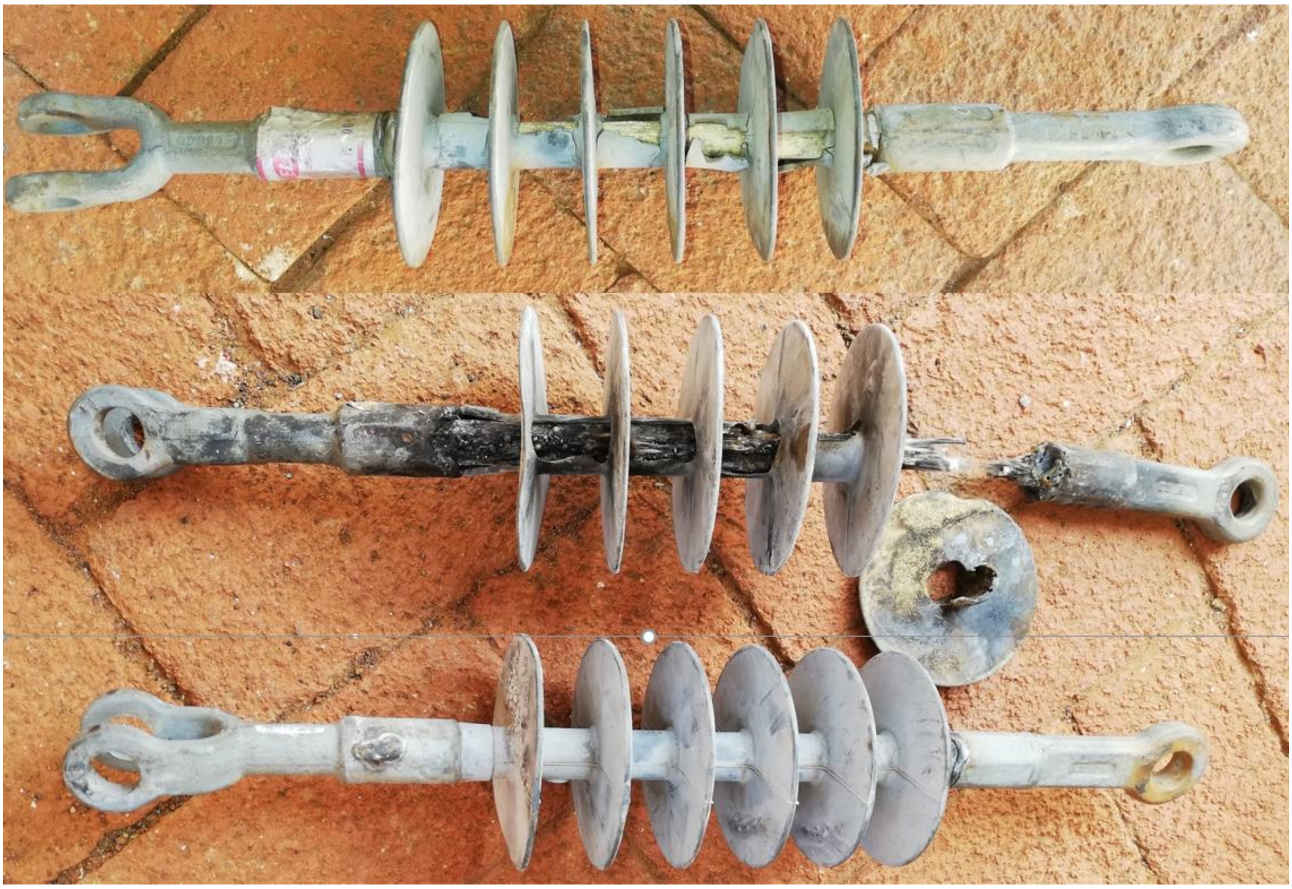

Figure 4.4 Many insulators were found to be in a degraded condition in the area where flashovers occurred due to nearby lightning flashes. The insulator at the top was still functional during normal dry weather.

Figure 4.5 A surge arrester with a failed ground lead disconnector. The surge arrester stand-off insulator had a very short creepage distance and the power frequency insulation was further compromised by moisture during thunderstorms.

4.2 Lightning flashes missed by the LDN

In some cases, the logger recorded a line fault with a visible LGC and LIOV amid a lightning storm while no lightning strike was recorded by the LDN at that specific time. Figure 4.6 and Figure 4.7 show an event where the lightning flash was not detected by the LDN. In such cases, the QoS recording was omitted from the lightning performance of the line and was logged as "not detected by the LDN" as shown in Table 4.1. It was omitted as the polarity of these lightning strikes was unknown. 28 such cases appeared to be lightning strikes that were direct to the line and caused line faults. The flash detection efficiency of the LDN was 95% if 28 out of 528 lightning flashes that caused line faults were missed by the LDN. This was within the 90% flash DE specification of the LDN.

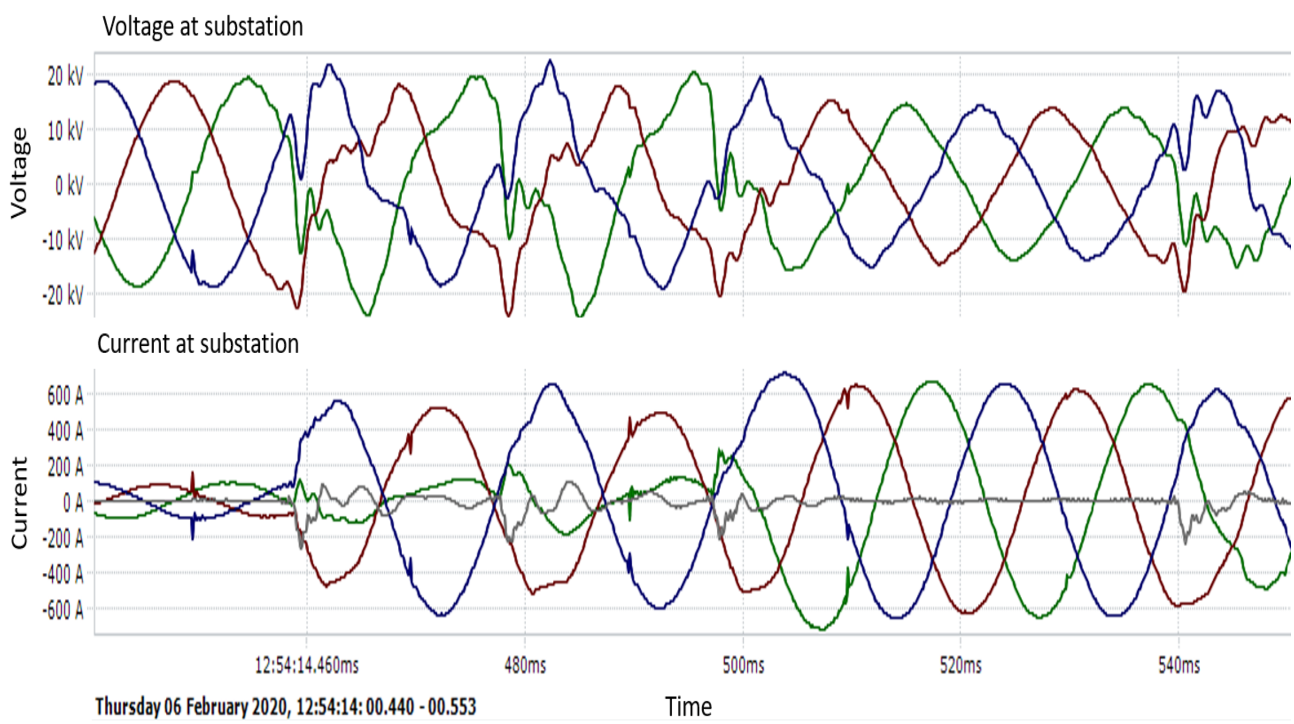

Figure 4.6 A recording at the feeder substation showed that lightning activity caused a line fault.

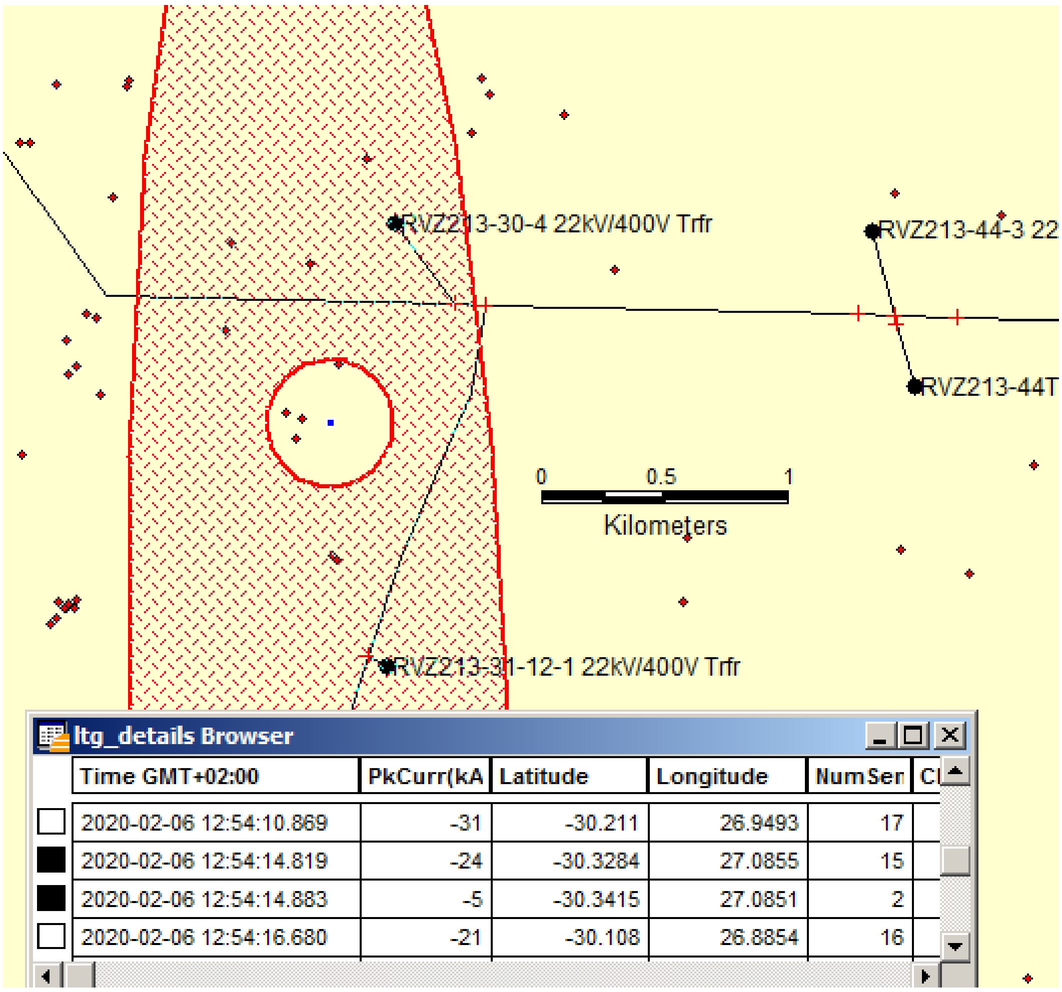

Figure 4.7 The LDN data at the time of the recording shown in Figure 4.6. There were no lightning strikes at the time of the waveform recordings.

4.3 Storm-related faults

Storm-related faults can be easily confused with lightning-related faults as they can happen during lightning activity. These faults are not directly related to the line BIL, but rather due to the power frequency creepage that is compromised by ageing insulation or other external elements. The insulation was then further compromised by moisture that caused flashovers. The BIL of an insulator is usually not compromised by more than 10% due to damaged insulation [167]. A total of 349 faults (30.2%) were found to be storm-related faults where lightning was not directly involved.

4.4 Other faults

Faults classified as "Other" occurred more than an hour before or after a storm. Only 21.7% of the faults were not storm-related. These faults were mostly caused by fatigue, birds, vandalism and overloading.

4.5 Equipment failure due to the energy component in LGVs

Equipment failure was not properly monitored in this research because the format of the maintenance and equipment failure database had some limitations. There was only one field in the database that could be populated with the equipment that failed and also only one field where the cause of the failure can be logged. All additional information had to be populated in the comments field which was not compulsory. Normally the most expensive piece of equipment (such as the transformer) that failed was logged and the other less expensive equipment (such as the fuses and surge arresters) that failed at the same time and location, were sometimes logged in the comments field. No database sorting could be done on the comments field which was also incomplete. The operating sheets of the field staff were used to count the equipment failures manually for this research. Appendix B shows all the equipment failures as well as possible remedies to prevent equipment failure due to lightning. Equipment failures and remedies to prevent it was not part of the scope of this research.

5 DISCUSSION

The methodology by using the finite soil conductivity to measure the actual lightning performance of a long MV line in operation that was not dependent on input data which was difficult to get hold of, with little logistics involved and was inexpensive proved to be rigorous. There were no previous research, measurements and models that this methodology could be compared to and verified. Actual lightning strikes of which the location was known without any doubt, were used to verify the methodology with the supporting measurement method and the model that was developed. The methodology was then used to distinguish between nearby lightning and direct lightning strikes to the line and to create a significant data set over two years. The database was used to verify the IEEE Std 1410-2010 estimate lightning performance of the long operational line.

The better than the estimated direct lightning performance of the line could be attributed to environmental conditions. The measured nearby lightning performance of the line was only 2% of the IEEE Std 1410-2010 estimation due to the RVZ line that was equipped and energized while the estimations were based on a floating line. Previous as well as this research revealed that the BIL on operational lines can be very small and still give adequate protection against nearby lightning.

This methodology was used to categorize the line faults into four root causes that could be used to distinguish between lightning-related faults, other weather-related faults and other faults happening on clear days. It could further be categorized into single-phase faults, multiphase faults, faults that independently quenched before breaker operation and faults that had to be cleared by breaker operation. This information could be used by designers to optimize the line BIL, protection against lightning damage, insulation materials, creepage distances and protection operation.

Using the LGC as the primary source of measurement instead of the traditional LIOV to determine the polarity of the charge generated on the line overcame the problems due to the LIOV attenuation along the line. There was a significant logistical saving in travelling and resources by setting the recorder to vary the sampling speed and compressing the data to save storage space (downloads were required only every second month). The research cost was low as only one recorder (and no cameras) was required.

This research proved that lightning was one of the biggest contributors to faults on this particular MV line that was used for the research. The two categories of lightning flashes namely nearby lightning and direct lightning strikes require opposite design criteria. A lower BIL result in a better line performance due to nearby lightning while a lower BIL resulted in more lightning energy directed into the earth and less energy through the equipment such as fuses and surge arresters. Fewer equipment failures resulted in fewer outages on the line. An investigation to further improve the line performance by minimising lightning-related equipment failure was a secondary contribution of this research and was attached as Appendix B.

6 ASSESSMENT

6.1 Research Question 1:

Extending the existing theoretical models of the lightning-induced voltages on MV lines, can a model be developed and verified that uses the polarity of the lightning channel current obtained from the LDN and the polarity of the measured zero-sequence current to discriminate between nearby lightning and direct lightning strikes to a long MV line?

Existing theoretical electromagnetic coupling models that include the soil resistivity were evaluated within their validated limits on short floating lines. One of the computer models, the ATP-EMTP model was chosen to be used in the studies as it could easily be extended to include the RVZ line ATP model. The extended ATP-EMTP model was then configured using the same parameters as the published results of the ERM [160]. There was a good comparison between the two models and the polarity of the first half cycle of the LIOV oscillation changed in both cases after about 250 m along the line. This verified the most important part of the research to distinguish between nearby lightning and direct lightning to the line for short lines.

The ATP-EMTP model was then extended to include the MV line to the feeder substation where the recording instrument was installed. There were no existing models that the extended ATP-EMTP model could be compared to and therefore actual measurements had to be used for verification of the new methodology. A nearby lightning strike with a high amplitude that would have certainly caused a flashover on the line if it was a direct lightning strike to the line was chosen. The recording of the LGC superimposed on the power frequency zero-sequence current due to a +59 kA nearby lightning return-stroke current, 42 km from the feeder substation was compared with a simulation using the extended ATP-EMTP model with the same parameters. The LGC polarity was negative and opposite polarity to the nearby lightning return-stroke current polarity in both the simulation and the recording. No power frequency fault current proves that it could not be a direct lightning strike to the line. This served as proof that both the measurement and the simulation determined correctly that it was a nearby lightning event and not direct lightning to the line.

Similarly, the LGC in both the recording and simulation of a -18 kA nearby lightning strike 12 km from the feeder substation had a positive polarity that was opposite to nearby lightning return-stroke current polarity. The LGC polarity (negative) in both the recording at the feeder substation and the simulation due to a -9 kA direct lightning strike to the line (31 km from the feeder substation) were the same as the polarity of the negative direct lightning strike to the line.

Three lightning strikes of which the termination point (nearby or direct to the line) could be established without using cameras or installing any measurements were chosen to verify the model and the method of recording that was used in the new methodology. The validity of the new methodology to use a polarity comparison between the LDN data and LGC recordings could be proven without any doubt. The methodology is rigorous and valid for lightning strike ground termination points that are further than 250 m from the recorder (logger) installation.

6.2 Research Question 2:

Using the measured lightning performance data and the developed theoretical model, can the deficiencies of the IEEE standard 1410-2010 estimation method applied to a given long MV line be checked?

This research showed that the worst-case scenario (a floating line) should not be used to design a line BIL as it will lead to insulation over design. The biggest differences were that there were surge arresters with an average distance of 3 km between them on the operational line and that the line was energized. As shown in the literature study [12] [17] [157], surge arresters that were more than 1.8 km apart did not make a big contribution.

There were 1 155 line faults that could be classified into faults due to nearby lightning, direct lightning strikes, weather-related and other faults over two years. Of the 528 lightning-related faults, 518 faults were due to direct lightning strikes to the line while 10 faults were due to nearby lightning. The lightning-related faults were normalized to the number of faults in one year in an area with a ground-flash density of 1 flash/km^2/year and were then compared to the IEEE Std estimation as shown in Figure 6.1. The average BIL of the 714 km line (including the branches) was 165 kV. There was a strong suspicion that on average 14 faults per year on the line were due to direct lightning strikes but were not captured by the LDN. That would decrease the percentage difference between the measured results and the IEEE Std estimations. It was also suspected that the five faults annually that occurred at the same time as nearby lightning, could be due to damaged insulation on the 30-year-old line. Should this be the case, these faults should be categorized as weather-related faults and would have resulted in a bigger discrepancy between the IEEE Std estimation and the measured results.

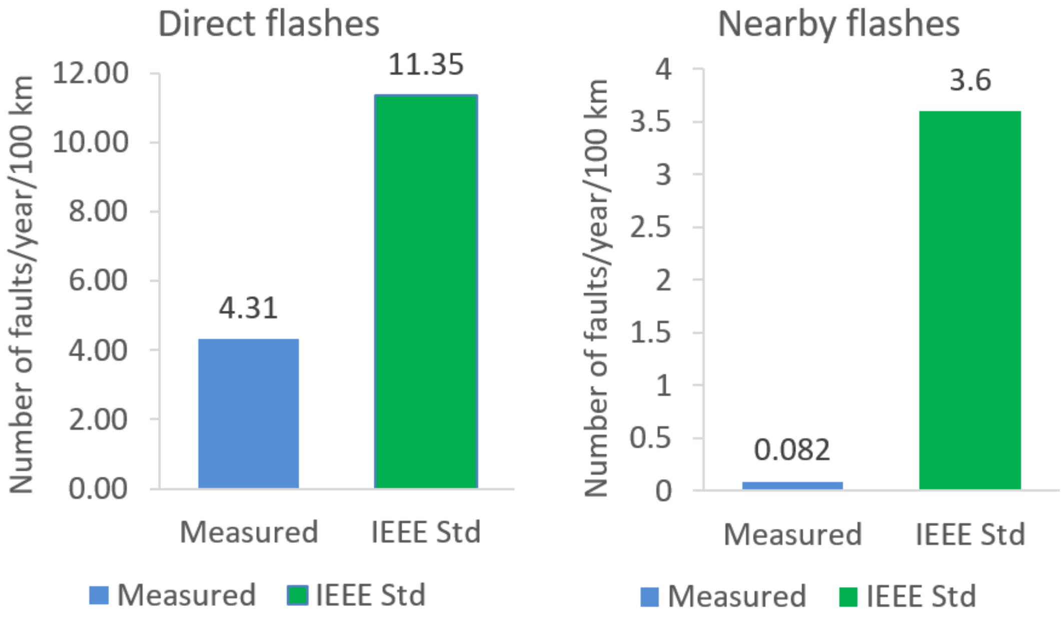

Figure 6.1 A comparison between the measured results and the IEEE Std of the annual lightning performance for a 714 km line in an area with a GFD of 8.51 and a ground resistivity of 300 Ω.m. The results were normalised to number of faults/year/100 km with a ground lightning density of 1 ground flash/km^2/year.

The theoretical model principles could be applied to the measured results that were normalized and then compared to the IEEE Std. The outcome was that the IEEE Std overestimated the number of line faults due to nearby lightning and the number of faults due to direct lightning strikes. Accurate input data parameters to the existing electromagnetic models (that are theoretical very accurate) were not available and resulted in a difference between the estimated and measured lightning performance of long MV lines in operation. A significant statistical database consisting of 1 155 line faults and 38 675 flashes (126 311 lightning strokes) within a 2 km buffer around the line over two years was used to evaluate the deficiencies of the IEEE Std estimations when applied to operational lines.

7 CONCLUSION

7.1 Contribution of the research

and it showed the IEEE Std 1410-2010 overestimated the effect of lightning on this line. There were numerous lightning channel models and electromagnetic coupling models that can accurately calculate the electric fields and lightning-induced voltages on lines provided that all the critical input data parameters to the models were accurate. The accuracy of the input data to the models became less as the line became longer and even more so when the equipment was connected to the line. The contribution of this research was that a methodology was proposed to distinguish between nearby and direct lightning strikes to the line for measuring the lightning performance of long operational lines that were only dependent on data that could easily be obtained. Other contributions made include:

- Those estimations of the line nearby lightning performance based on a floating line, resulted in a significant BIL overdesign at the cost of equipment failure.
- The new methodology was less costly, easier to obtain the equipment for measurements and simpler to be used by engineers.
- It also provided the actual lightning performance of the line in question and not the estimated lightning performance of the line.
- There was a finding that the number of faults due to nearby lightning on MV lines was negligible and therefore less effort was needed to optimize the BIL.
- It showed that the number of breaker operations was less than the number of insulation failures due to arc quenching and that protection operation alone can compromise the accuracy of lightning-related faults
- A finding that ageing insulation and mechanical fatigue on old lines can contribute (30.2% in this case) to line faults due to moisture and wind during a lightning storm.
- The LGC on the zero-sequence current could be measured to detect lightning activity instead of the traditional LIOV to solve the problem of the rapid LIOV attenuation along the line.
- The LIOV and LGC could be measured with a lower sampling rate instrument provided that there was some distance between the nearby lightning strike ground termination point and the point of measurement.
- A continuous sampling recorder could also detect lightning activity that was not detected by the LDN and could be used to determine the LDN DE.

7.2 Weaknesses of this research

The biggest weakness of the study was that the DE of the LDN was less than 100%. It resulted in 28 faults (5.3% of the lightning-related faults) during the two-year period that could not be categorized. Although some learnings from the research suggest that all the 28 flashovers were due to direct lightning strikes to the line, it was still decided to rather create a separate category for these line faults. Other weaknesses include:

- There were ten line faults (1.9% of the lightning-related faults) over the two years that were most probably due to damaged insulation rather than a case where the LIOV exceeded the line BIL. As these faults occurred at the same time as the nearby lightning strike, it was categorized as line faults due to nearby lightning.
- Lightning strikes that were closer than 250 m (0,035% of the line) from the substation might have been categorized incorrectly. There was only one lightning strike within this distance which terminated on top of the substation and it was omitted from the results.
- Only cloud-to-ground flashes were studied as data of flashes between clouds was not available. The effect of flashes between clouds if any, needs to be further investigated.
- The maintenance and equipment failure databases were not structured to keep a record of all the equipment failures which made it difficult to relate the equipment failures to lightning incidents.

There were also times that the network was without supply during a lightning storm when no measurements were done. However, this could not worsen the line lightning performance as the customers connected to the line were already without supply.

8 REFERENCES

[1] M. Izadi, M. S. Rahman, M. Z. Ab-Kadir, C. Gomes, J. Jasni and M. Hajikhani, "The influence of lightning induced voltages on the distribution power line polymer insulator," *PLOS one,* vol. DOI:10.1371, p. 2, February 2017.

[2] W. J. Dirkse van Schalkwyk and J. M. Van Coller, "An investigation into a more optimal choice of BIL on MV feeders," in *7th Southern Africa Regional Conference*, Somerset Wes, ZA, 2013.

[3] E. W. Gunther and H. Mehta, "A survey of distribution system power quality-preliminary results," *IEEE Trans. on Power Delivery,* Vols. 10-1, pp. 322 - 329, January 1995.

[4] C. Boonseng and V. Kinnares, "Analysis for 12- pulse converter under unbalanced voltages operation due to lightning voltage sags and short term interruption," *IEEE PES Winter Meeting,* vol. 3, pp. 1009 - 1014, 2001.

[5] W. J. Dirkse van Schalkwyk, "The placing of line surge arresters and fuses on 11 kV and 22 kV lines to protect equipment against lightning," *M Eng Thesis,University of Stellenbosch,* pp. 3,79, March 2001.

[6] M. Bernardi, C. Giorgi and V. Biscaglia, "Medium voltage line faults correlation with lightning events recorded with the Italian LLP system CESI SIRF," *Proc. 24th International Conference on Lightning Protection,* vol. 1, pp. 187-192, 1998.

[7] K. L. Cummins, M. D. Malone and E. P. Krider, "The U.S. National Lightning Detection Network and applications of cloud-to-ground lightning data by electric power utilities," *IEEE Trans. Electromagnetic Compatibility,* vol. 40, no. 4, pp. 465 - 480, 1998.

[8] C. A. Nucci, M. Paolone and M. Bernardi, "Use of Lightning Location Systems Data in Integrated Systems for Power Quality monitorng," *Proc. IEEE T&D Conference,* vol. 1, pp. 552 - 556, October 2002.

[9] M. H. J. Bollen, "Characterization of voltage sags experienced by three-phase adjustable-speed drives," *IEEE Trans. on Power Delivery,* Vols. 12-4, pp. 1666 - 1671, October 1997.

[10] K. J. Sadurski, "Woodpole splitting and its prevention," in *Seminar on the lightning protection of distribution lines, SAIEE,* Pretoria, 1-2 August 1989.

[11] H. J. Geldenhuys, C. T. Gaunt and A. C. Britten, "Insulation co-ordination of unshielded distribution lines from 1 kV to 36 kV," Johannesburg, SAIEE publication, 1991, pp. 4-36.

[12] IEEE Std 1410 - 2010, "IEEE Guide for Improving the Lightning Performance of Electric Power Overhead Distribution lines," IEEE, 2010.

[13] "Lightning Protection of Distribution networks," in *The Electricity Council of Britain*, London: Electricity Council, 1973, p. 49.

[14] S. Oguchi, T. Ishii, S. Okabe, Y. Sakamoto, M. Tsuji and A. Asakawa, "Observational and experimental study of lightning stroke attraction effect with ground wire system construction," *IEEE Transactions of Dielectrics and Electrical Insulation,* vol. 19, no. 1, p. 366, February 2012.

[15] H. Taniguchi, H. Sugimoto and S. Yokoyama, "Observation of lightning performance on power distribution line by still cameras," *Proc 23rd International Conference on Lightning Protection,* vol. 1, pp. 119 - 124, 1996.

[16] J. D. Schoene, Direct and Nearby Lightning Strike Interaction with Test Power Distribution Lines, Florida: University of Florida, 2007.

[17] C. A. Nucci, A. Borghetti, M. Paolone, P. Boselli, M. Bernardi, S. Malgarotti, I. Mastandrea and F. Rachidi, "Lightning-Induced Voltages on Overhead Distribution Lines: Theoretical and Experimental Investigation of related Problems and their Impact on Power Quality," *Cigre C4-303,* p. 4, 2004.

[18] H. K. Høidalen, "Calculation of Lightning-induced Voltages in MODELS Including Lossy Ground Effects," in *International Conference on Power System Transients*, New Orleans, USA, 2003.

[19] C. A. Nucci and F. Rachidi, "Lightning-Induced Overvoltages," in *IEEE Transmission and Distribution Conference*, New Orleans, 1999.

[20] A. K. Agrawal, H. J. Price and S. H. Gurbaxani, "Transient Response of a Multiconductor Transmission Line Excited by a Nonuniform Electromagnetic Field," *IEEE Transactions on Electromagnetic Compatibility,* Vols. EMC-22, pp. 119-129, May 1980.

[21] F. De la Rosa, Effects of Close Lightning on Electric Power Distribution Lines, Uppsala University, October 1985.

[22] M. J. Master and M. A. Uman, "Transient electric and magnetic fields associated with establishing a finite electrostatic dipole," *American Journal of Physics,* no. 51, pp. 118-126, 1983.

[23] C. A. Nucci, "Lightning-Induced Voltages on Overhead Power Lines, Part I: Return-Stroke Current Models with Specified Channel-Base Current for the Evaluation of the Return-Stroke Electromagnetic Fields," *Cigre Working Group 33.01 (Lightning),* no. Electra no 161, pp. 75-102, Aug 1995.

[24] C. A. Nucci, “Lightning-Induced Voltages on Overhead Power Lines, Part II: Coupling Models for the Evaluation of the Induced Voltages,” *Cigre Working Group 33.01 (Lightning),* no. Electra No 162, pp. 121-145, Oct 1995.

[25] C. Nucci, F. Rachidi, M. Ianoz and C. Mazzetti, “Lightning-induced overvoltages on overhead lines,” *IEEE Transactions on EMC,* vol. 35, pp. 75-86, 1993.

[26] D. Pavanello, F. Rachidi, W. Janischewskyj, M. Rubinstein, A. Hussein, E. Petrache, V. Shostak, I. Boev and C. A. Nucci, “On return stroke currents and remote electromagnetic fields associated with lightning strikes to tall structures: 2. Experiment and model validation,” *Journal of Geophysical Research,* vol. 112, no. D13122, p. 5, 2007.

[27] SABS Standard Division, “SANS 62305-1: Protection against lightning,” no. Edition 2, p. 29, 2011.

[28] A. Currus, E. Cinieri, A. Fumi and C. Mazzetti, “Breakdown behaviour of air-spark gaps with non-standard lightning voltages,” in *Proc. of 7th Int. Conference on Gas discharges and their Applications*, London, 1982.

[29] C. A. Nucci and F. Rachidi, “Interactions of electromagnetic fields with electrical networks generated by lightning,” in *The lightning Flash: Physical and engineering Aspects', IEE Power and Energy series 34*, IEE Press, 2003, p. 426.

[30] R. B. Anderson and A. J. Eriksson, “Lightning parameters for engineering applications,” *Electra,* no. 69, p. 65–102, 1980.

[31] D. M. Le Vine, “Review of measurements of the RF spectrum of radiation from lightning,” *Meteorology and Atmospheric Physics,* vol. 37, no. 3, pp. 195-204, September 1987.

[32] “IEEE Guide for Improving the Lightning Performance of Electric Power Overhead Distribution Lines,” *1410™-2004, IEEE Std,* no. 1, pp. 14, 23, 2004.

[33] K. Udaya, B. R. Rosy and K. P. Dileepkumar, “Direct Time Domain Modelling of First Return Stroke of Lightning,” in *29th International Conference on Lightning protection*, Uppsala, 2008.

[34] M. Shigihara, A. Piantini and J. M. Janiszewski, “Analysis of the current distribution along the lightning channel based on a current waveform recorded at the bottom of an elevated structure,” in *IX International Symposium on Lightning protection,* Foz do Iguacu, 2007.

[35] C. F. Wagner, “The relation between stroke current and velocity of the return stroke,” *IEEE Transactions on Power Apparatus and Systems,* vol. 82, pp. 609 - 617, 1963.

[36] V. A. Rakov, “Lightning Return Stroke speed,” *Journal of Lightning Research,* vol. 1, pp. 80 - 89, 2007.

[37] S. Streedhar and V. Srinivasan, “Lightning Return Stroke Models - A Critical Review Based on Comparison of Lightning Parameters,” *Scientiic and Technology Research,* vol. 9, no. 1, pp. 486-498, January 2020.

[38] S. I. Braginski, “Theory of the Development of a Spark Channel,” *Experimental and Theoretical Physics,* vol. 34, no. 34, pp. 1548 - 1557, 1958.

[39] R. D. Hill, “Channel Heating in Return-Stroke Lightning,” *Geophysical Research,* vol. 76, no. 3, p. 637, 1971.

[40] E. P. Krider, G. A. Dawson and M. A. Uman, “The Peak Power and Energy Dissapation in a Single-Stroke Lightning Flash,” *Geophysical Research,* vol. 73, pp. 3335 -3339, 1968.

[41] M. N. Plooster, “Shock Waves from Line Sources. Numerical Solutions and Experimantal Measurements,” *Physics of Fluids,* vol. 13, no. 11, pp. 2665 - 2675, 1970.

[42] J. E. Borovsky, “Lightning Energetics: Estimates of Energy Dissipation in Channels, Channel Radii, and Channel- Heating risetimes,” *Geophysical Research,* vol. 103, pp. 11537-11553, 1998.

[43] V. A. Rakov and M. A. Uman, “Review and Evaluation of Lightning Return Stroke Models including some aspects of their Application,” *IEEE Transactions on Electromagnetic Compatibility,* vol. 40, no. 4, pp. 403 - 426, November 1998.

[44] V. A. Rakov, “Characterization of lightning electromagnetic fields and their modeling,” in *14th International Zurich Symposium on EMC,* Zurich, 2001.

[45] R. Moini, V. A. Rakov, M. A. Uman and B. Kordi, “An Antenna Theory Model for the Lghtning Return Stroke,” in *Proc 12th International Zurich Symposium Electromagnetic Caompatibility,* Zurich , Switzerland, February 1997.

[46] Y. Baba and V. A. Rakov, “Electromagnetic Models of the Lightning Return Stroke,” *Geophysics of Research,* vol. 112, no. D4, pp. 1-17, 2007.

[47] K. Chen, “Transien Response of a Infinite Cylindrical Antenna,” *IEEE Transactions Antennas Propagation,* vol. 31, no. 1, pp. 170-172, 1983.

[48] Y. Baba and V. A. Rakov, “Evaluation of lightning return stroke Electromagnetic Models,” in *29th International Conference on Lightning Protection,* Uppsala, Sweden, 2008.

[49] V. Cooray, “The mechanism of the lightning flash,” in *The lightning flash,* London, The Institution of Engineering and Technology, 2003, pp. 144-147.

[50] V. A. Rakov and M. A. Uman, “Lightning Physics and effects,” New York, Cambridge University Press, 2003, pp. 160-161.

[51] N. Theethayi and V. Cooray, “On the Representation of the Lightning Return Stroke Process as a Current Pulse Propagating along a Transmission Line,” *IEEE Transactions on Power Delivery,* vol. 20, no. 2, pp. 832-837, April 2005.

[52] P. Ratnamahilam and P. Hoole, “Modeling the Lightning Earth Flash Return Stroke for Studying its Effects on Engineering Systems,” *IEEE Transactions On Magnetics,* vol. 29, no. 2, pp. 1839 - 1844, March 1993.

[53] M. A. Uman and D. K. McLain, “Magnetic field of lightning return stroke,” *Journal of Geophysical Research,* vol. 74, no. 28, pp. 6899 - 6910, 1969.

[54] V. A. Rakov and A. A. Dulzon, “A modified transmission line model for lightning return stroke field calculations,” in *Proceedings of the 9th International Symposium on Electromagnetic Compatibility*, Zurich, 1991.

[55] C. A. Nucci, C. Mazetti, F. Rachidi and M. Ianoz, “On Lightning Return Stroke Models for LEMP calculations,” in *Proceedings of the 19th International Conference on Lightning Protection*, Graz, 1988.

[56] C. Bruce and R. M. Golde, “The lightning discharge,” *J. Inst. Elec.Eng*, vol. 88, pp. 487 - 520, 1941.

[57] G. Diendorfer and M. A. Uman, “An Improved Return Stroke Model with Specified Channel-base Current,” *Journal of Geophysical Resesearch,* vol. 95, no. 1, pp. 13621-13644, 1990.

[58] C. A. Nucci, “Tutorial on Lightning-induced Effects on Transmission Lines,” in *4th International Symposium on Electromagnetic Compatibility*, Zurich, 2000.

[59] C. A. Nucci and F. Rachhidi, “Experimental Validation of a Modification to the Transmission Line Model for LEMP Calculations,” in *8th International Symposium on Electromagnetic Compatibility*, Zurich, 1989.

[60] V. A. Rakov and A. A. Dulzon, “Calculated Electromagnetic Fields of Lightning Return Strokes,” *Teknicheskaya Electrodinamika,* vol. 1, no. 1, pp. 87-89, 1987.

[61] F. Heidler, “Traveling current source model for LEMP calculation,” *Proc. 6th Int Symp. Tech. Exhibition on Electromagn. Compat.,* pp. 157 - 162, March 1985.

[62] D. E. Crawford, V. A. Rakov, M. A. Uman, G. H. Schnetzer, K. J. Rambo and M. V. Stapleton, “Multiplestation Measurements of Triggerred-Lightning Electric and Magnetic Fields,” in *Procedure 11th International Conference on Atmospheric Electricity*, Guntersville, Alabama, 1999.

[63] R. Thottappillil, R. A. Rakov and M. A. Uman, “Distribution of Charge Along the Lightning Channel: Relation to the Remote Electric and Magnetic fields and to the Return Stroke Models,” *Journal of Geophysical Research,* vol. 102, no. 1, pp. 6887-7006, 1997.

[64] A. Andreotti, C. Petrarca, V. A. Rakov and L. Verolino, “Calculation of Voltages Induced on Overhead Conductors by Nonvertical Lightning Channels,” *IEEE Transactions on Electromagnetic Compatibility,* vol. 54, no. 4, pp. 860-870, August 2012.

[65] E. A. S. Rios, “Lightning Induced Voltages Study on Overhed Distribution Networks Placed over Non-flat Terrains,” in *PhD,* Manizales, Colombia, National University of Colombia, 2014, pp. 15-77.

[66] C. A. Nucci, G. Diendorfer, M. A. Uman, F. Rachidi, M. Ianoz and C. Mazzetti, “Lightning Return Stroke Current Models with Specified Channel Base Current: A Review and Comparison,” *Journal of Geophysics Research,* vol. 95, no. 1, pp. 395-408, 1990.

[67] V. A. Rakov, “Characterization of Lightning Electromagnetic Fields and their Modeling,” in *6th International Conference on Electrical Engineering,* Cairo, Egypt, 27-29 May 2008.

[68] S. Sreedhar and V. Srinivasan, “Lightning Return Stroke Models - A Critical Review Based on Comparison of Lightning Parameters,” *International Journal of Scientific & Technology Research,* vol. 9, no. 1, pp. 486-499, January 2020.

[69] C. A. Nucci and F. Rachidi, “Panel discussion "Disribution Lightning Protection", slides 6 to 11,” in *IEE '99 T&D Conference,* New Orleans, April 1999.

[70] S. Rusck, Induced Lightning Over-voltages on Power Transmission Lines with Special Reference to the Over-voltage Protection of Low-voltage networks, Stockholm, Sweden: Royal Institute of Technology, PhD Thesis, 1957.

[71] P. Chowdhuri, “Analysis of Lightning-Induced Voltages on Overhead Lines,” *IEEE Transactions on Power Delivery,* vol. 4, no. 1, pp. 479-492, 1989.

[72] A. Piantini, “Extention of the Rusck Model for Calculating Lightning-Induced Voltages on Overhead Lines Considering the Soil Electrical Parameters,” *IEEE Trans. Electromagnetic Compatibility* , vol. 59, pp. 154-162, 2017.

[73] V. Cooray, “Calculating Lightning-Induced Overvoltages in Power Lines: A comparison of two Coupling Models,” *IEEE Transactions on Electromagnetic Compatibility,* vol. 36, no. 3, pp. 179-183, August 1994.

[74] C. A. Nucci, F. Rachidi, M. Ianoz and C. Mazzetti, “Comparison of Two Coupling Models for Lightning-Induced Overvoltage Calculations,” *IEEE Tansactions on Power Delivery,* vol. 10, no. 1, pp. 330-340, January 1995.

[75] M. Paolone, “Modeling of lightning-induced voltages on distribution networks for the solution of power quality problems, and relevant implementation in a transient program,” PhD Thesis, University of Bologna, Italy, 2002.

[76] K. M. Minja, P. V. Chombo, N. Promvichai and B. Marungsri, “Mitigation of Flashover from Multiple Lightning strokes in Overhead Catenary System by using ATPDraw,” in *IEEE PES Thailand Symposium on Advanced Technology in Power System*, Bangkok, Thailand, March 2017.

[77] F. Rachidi, S. L. Loyka, C. A. Nucci and M. Ianoz, “A New Expression for the Ground Transient Resistance Matrix Elements,” *Electric Power Systems,* vol. 65, no. 1, pp. 41-46, 2003.

[78] V. Cooray, “Some considerations on the 'Cooray-Rubenstein' approximation used in deriving the horizontal electric field over finitely conducting ground,” in *International Conference on Lightning Protection, pp. 282-286,* Birmingham, UK, September 1998.

[79] F. M. Tesche, M. V. Ianoz and T. Karlsson, EMC Analysis methods and computational models, New York: Wiley Intersience, 1997.

[80] A. Piantini and J. M. Janiszewski, “An Improved Model for Lightning Induced Voltages Calculations,” *IEEE/PES Transmission & Distribution Conference & Exposition,* p. 558, 2004.

[81] F. Rachidi, M. Ianoz and C. A. Nucci, “Transient analysis of multiconductor lines above a lossy ground,” *IEEE Transactions on Power Delivery,* Vols. 14 - 1, pp. 294 - 302, January 1999.

[82] A. L. Timotin, “Longitudinal Transient Parameters of a Unifilar lLine with Ground Return,” *Revue Roumaine des Sciences Techniques,* Vols. 12-4, pp. 523-535, 1967.

[83] E. D. Sunde, Earth Conduction Effects in Transmission Systems,, Dover, New York: Dover Publications, 2nd edition, 1968.

[84] J. P. Silva, A. E. A. Araujo and J. O. S. Paulino, “Calculation of the Lightning-Induced Voltages with Rusck's Method in EMTP - part II: Effects of Lightning Parameter Variations,” *Elsevier,* vol. 61, no. 1, pp. 133-137, 2002.

[85] J. P. Silva, E. A. E. Arauja and H. W. Dommel, “Calculation of Lightning-Induced Voltages with RUSCK’s Method in EMTP Part I: Comparison with Measurements and Agrawal"s Coupling Model,” *Elsevier,* vol. 60, no. 1, pp. 49-54, 2001.

[86] D. H. Ha, J. K. Choi and Y. B. Yoon, “Parametric Analysis of Lightning Induced Voltage on Distribution Lines using EMTP,” *Journal of the Korean Institute of Illuminating and Electrical Installation Engineers,* vol. 68, no. 3, pp. 19-26, 2019.

[87] A. Andreotti, G. Luppo and C. Petrarca, “Evaluation of EM fields from Return Stroke for Indirect — Lightning Protection of Wind Turbines,” in *International Conference on Clean Electrical Power,* Alghero, Italy, June 2013.

[88] M. Natsui, A. Ametani, J. Mahseredjian, S. Sekoika and K. Yamamoto, “FDTD Analysis of Distribution Line Voltages Induced by non-vertical lightning,” in *International Conference on Power Systems*, Perpignan, France, 2019.

[89] A. Piantini, “Lightning-Induced Overvoltages on Overhead,” in *2016 IEEE International Conference on High Voltage Engineering and Application,* Chengdu, China, 2016.

[90] A. Piantini, “Lightning Transients in MV Power Distribution Lines,” in *Russian Conference on Lightning Protection,* Saint Petersburg, Russia, May 2016.

[91] M. Darveniza, “A Practical Extension of Rusck's Formula for Maximum Lightning-Induced Voltages That Accounts for Ground Resistivity,” *IEEE Transactions on Power Delivery,* vol. 22, p. 606, January 2007.

[92] A. Borghetti, M. Paolone and C. A. Nucci, “An Improved Procedure for the Assessment of Overhead Line Indirect Lightning Performance and its Comparison with the IEEE Std. 1410 Method,” *IEEE Transactions on Power Delivery,* vol. 22, pp. 684-692, Jan 2007.

[93] S. Guerrieri, M. Ianoz, C. Mazzetti, F. Rachidi and C. A. Nucci, “Lightning-induced voltages on an overhead line above lossy ground: a sensitivity analysis,” *Proc. of 23rd International Conference on Lightning Protection, Florence, Italy,* pp. 328 - 333, September 1996.

[94] R. L. Holle, “Policy Development in Lightning Hazard Mitigation Strategies in Countries with High Ground Flash Density,” in *International Roundtable,* 11-12 May 2021.

[95] R. Said and M. Murphy, “GLD360 Upgrade: Performance Analysis and Applications,” in *24th International Lightning Detection Conference & 6th International Lightning Meteorology Conference*, San Diego, California, USA, 18-21 April 2016.

[96] L. Schwalt, S. Pack and W. Schulz, “Ground truth data of atmospheric discharges in correlation with LLS detections,” *Elsevier,* vol. 180, no. 10.1016, pp. 1-8, 2019.

[97] C. T. Mata, A. G. Mata, A. Nag, V. A. Rakov and J. Saul, “Evaluation of the performance characteristics of CGLSS II and U.S. NLDN Using Ground Truth Data from Launch Complex 39B, Kenedy Space Centre, Florida,” in *International Conference on Lightning Protection* , Vienna, Austria, 2012.

[98] J. Cosmac, G. Milev and Z. Toros, “Evaluation of lightning parameters correlated with distribution line faults,” in *16th International symposium on high voltage engineering*, Capetown, 2009.

[99] J. Jerauld, V. A. Rakov, M. A. Uman, K. J. Rambo, D. M. Jordan, K. L. Cummins and J. A. Cramer, “An evaluation of the performance characteristics of the U.S. National Lightning Detection Network in Florida using triggered lightning,” J Geophys, Florida, 2005.

[100] H. G. P. Hunt, Y. C. Liu and K. J. Nixon, “Evaluation of the South African Lightning Detection Network using Photographed Tall Tower Lightning Events from 2009 - 2013,” in *International Conference on Lightning Protection (ICLP)*, Shanghai , China, 2014.

[101] H. G. P. Hunt, “Dataset of Photographed Lightning Events Attaching to and Around the Brixton Tower, Johannesburg, South Africa for the 2015-2016 thunderstorm season,” *Elsevier,* vol. doi.org/10.1016/j.dib.2020.105630, pp. 1-11, 2020.

[102] H. G. P. Hunt, K. J. Nixon and I. R. Jandrell, “Establishing a methodology to investigate LDN median error ellipses used as corroborating evidence for a lightning event at a specific geographic locations,” *Elsevier,* vol. dx.doi.org/10.1016/j.epsr.2014.02.033, pp. 104-114, 2014.

[103] H. G. P. Hunt, K. J. Nixon and I. R. Jandrell, “Can LDN Data Provide Corroborating Evidence for a Lightning Event at a Specific Geographic Location,” in *International Conference on Lightning Protection (ICLP)*, Vienna, Austria, 2012.

[104] C. Schumann, H. G. P. Hunt, J. Tasman, H. Fensham, K. J. Nixon, T. A. Warner and M. M. f. Saba, “High-Speed Video Observation of Lightning Flashes over Johannesburg, South Africa 2017 - 2018,” in *34th International Conference on Lightning Protection*, Rzeszow, Poland, 2018.

[105] H. G. P. Hunt, K. J. Nixon, I. R. Jandrell and W. Schulz, “Can we model the statistical distribution of lightning location system errors,” *Elsevier,* vol. doi.org/10.1016/j.epsr.2019.106042, p. Electric Power Systems Research 178 (2020) 106042, 2019.

[106] H. G. P. Hunt, “Matching lightning detection network data with real lightning events,” *WhatNow,* p. 36, May 2012.

[107] H. G. Fensham, C. Schumann, H. G. P. Hunt, K. J. Nixon, T. A. Warner and M. Gijben, “Performance evaluation of the SALDN using highspeed camera footage of ground truth lightning events over Johannesburg, South Africa,” in *International Conference on Lightning Protection*, Rzeszow, Poland, 2018.

[108] F. J. Jooste, W. J. Dirkse van Schalkwyk and A. C. Britten, “The influence of lightning on 11 kV and 22 kV lines with varying BIL, Evaluation of lightning parameters correlated with distribution line faults,” in *16th International Symposium on High Voltage Engineering,* Cape Town, 2009.

[109] C. Gomes, “Science, Engineering, and Economic Implications for Developing Countries,” in *Lightning,* Johannesburg, South Africa, Springer, 2021, pp. 10-65.

[110] A. Piantini, J. M. Janiszewski, A. Borghetti, C. A. Nucci and M. Paolone, “A scale model for the Study of the LEMP Response of Complex Power Distribution Networks,” *IEEE Transactions on Power Delivery,* vol. 22, no. 1, pp. 710 - 720, 2007.

[111] A. F. Zalhaf, M. Abdel -Salam, D. A. Mansour, M. Ahmed and S. Ookawara, “An Experimental Study of Lightning Overvoltages on a Small-Scale Wind Turbine Model,” in *5th International Conference on Power and Energy Systems Engineering,* Nagoya, Japan, 2018.

[112] N. H. Halim, A. Azmi, Y. Yahya, F. Abdullah, M. Othman and M. S. Laili, “Development of A Small Scale Standard Lightning Impulse Current Generator,” in *5th International Power Engineering and Optimization Conference,* Shah Alam, Selangor, Malaysia, 6-7 June 2011.

[113] J. S. Zheng, G. F. Li, Z. N. Ji, F. W. Liao, L. Lan, J. Hu, W. W. Huang and X. S. Wen, “Small Scale Model Experimental Study on Lightning Screening Performance of 500 kV Transmission Lines in Mountain Area,” *Corpus,* vol. 45, no. 1, pp. 119-122, January 2009.

[114] J. Wang, S. Wang, L. Cai, D. Lu, Q. Li, M. Zhou and Y. Fan, “Observation of Induced Voltage at the Terminal of a 10 kV Distribution Line by Nearby Triggered Lightning,” *IEEE Transactions on Power Delivery,* vol. 35, no. 4, pp. 1968 - 1976, 2020.

[115] J. Schoene, M. A. Uman and V. A. Rakov, “Return Stroke Peak Current Versus Charge Transfer in Rocket-Triggered Lightning,” *Journal of Geophysical Research,* vol. 115, no. D12, p. D12107, 2010.

[116] M. Rubinstein, M. A. Uman, P. J. Medelius and E. M. Thomson, “Measurement of the Voltage Induced on an Overhead Power Line 20 m from Triggered Lightning,” *IEEE Transactions Electromagnetic Compatibility,* vol. 36, no. 1, pp. 134-140, May 1994.

[117] F. Rachidi, M. Rubinstein, S. Guerrieri and C. A. Nucci, “Voltages Induced on Overhead Line by Dart Leaders and Subsequent Return Strokes in Natural and Rocket-Triggered Lightning,” *IEEE Transactions Electromagnetic Compatibility,* vol. 39, no. 1, pp. 160-166, May 1997.

[118] M. Rubenstein, F. Rachidi, M. A. Uman, R. Thottappillil and V. A. Rakov, “Characterization of Vertical Electric Fields 500 m and 30 m from Triggered Lightning,” *Journal of Geophysical Research,* vol. 100, no. D5, pp. 8863-8872, May 1995.

[119] Y. Baba and M. Ishii, “Numerical Electromagnetic Field Analysis of Lightning Current in Tall Structures,” *IEEE Transactions on Power Delivery,* vol. 16, no. 2, pp. 324-328, April 2001.

[120] S. Yokoyama, K. Miyake, H. Mitani and N. Yamazaki, “Advanced observation of lightning induced voltage on power distribution lines,” *IEEE Trans. Power Del.,* Vols. PWRD-1, no. 2, pp. 129 - 139, January 1986.

[121] V. Cooray and F. de la Rosa, “Shapes and amplitudes of the Initial Peaks of Lightning-Induced Voltages in Power Lines Over Finitely Conducting Earth: Theory and Comparison with Experiment,” *IEEE Transactions on Antennas and Propagation,* Vols. AP-34, no. 1, pp. 88-93, January 1986.

[122] P. Barker and C. W. Burns, “Photography helps solve distribution lightning problems,” *IEEE power Eng. Rev.,* vol. 13, pp. 23 - 26, 6 June 1993.

[123] T. Miyazaki and S. Okabe, “A detailed field study of lightning stroke effects on distribution lines,” *IEEE Transactions on Power Delivery,* vol. 24, no. 1, pp. 352 - 359, 2009.

[124] T. Miyazaki, S. Okabe and S. Sekioka, “An experimental validation of lightning performance in distribution lines,” *IEEE Trans. Power Delivery,* vol. 23, no. 4, pp. 2182 - 2190, 2008.

[125] H. J. Geldenhuys, “MV test line lightning recording CSIR 1983-1984 report,” Pretoria, South Africa, CSIR, 1984, p. 28.

[126] M. N. N. Santos and A. Piantini, “Characteristics of lightning-induced voltages based on experimental data,” *The Institute of engineering and Technology,* vol. DOI: 10.1049/hve2.12055, no. High Voltage 2020, pp. 1-7, December 2020.

[127] A. J. Eriksson and D. V. Meal, “Lightning Overvoltages in Rural Distribution Line - Prelimary Results,” *South African Institution of Electrical Engineers Transactions,* vol. 71, no. 1, pp. 158-163, June 1980.

[128] A. J. Eriksson, M. F. Stringfellow and D. V. Meal, “Lightning Induced Overvoltages on Overhead Distribution Lines,” *IEEE Power Application System,* Vols. PAS-101, no. 4, pp. 980-968, 1982.

[129] A. J. Eriksson and D. V. Meal, “Lightning Performance and Overvoltage Surge Studies on a Rural Distribution Line,” *Proceedings of the Institution of Electrical Engineers,* vol. 129, no. 23, pp. 59-69, 1982.

[130] A. J. Eriksson, “Studies on the lightning performance of distribution lines,” in *AMEU technical meeting,* George, May 1982, pp. 8-21.

[131] W. J. Dirkse van Schalkwyk, C. Gomes, J. M. van Coller and A. A. Beutel, “Discrimination between Nearby and Direct Lightning Strikes to a Long Operational Medium Voltage line to

Assist in the Determination of the Basic Insulation Level (BIL)," in *The 8th EPPEI Annual Student Workshop Vitrual Conference*, Durban, South Africa, 11 - 12 November 2021.

[132] M. Bernardi and D. Ferrari, "The Italian lightning detection system (CESI-SIRF): main statistical results on the first five years of collected data and a first evaluation of the improved system behaviour due to a major network upgrade," in *Proc. 25th International Conference on Lightning Protection*, Rhodes, Greece, September 2000.

[133] R. Iorio and D. Ferrari, "1995 descriptive statistics on lightning activity over Italy, obtained by means of the Italian lightning detection system 'CESI-SIRF," *Proc. 23rd International Conference on Lightning Protection,* vol. 1, pp. 191-196, September 1996.

[134] C. A. Nucci, F. Rachidi, M. Ianoz and C. and Mazzetti, "Lightning Induced Voltages on Overhead Lines," *IEEE Transactions on Electromagnetic Compatibility,* vol. 35, no. 1, pp. 75-86, Feb 1993.

[135] A. Borghetti, M. Paolone, E. Petrache, F. Rachidi, J. A. Gutierrez and C. A. Nucci, "Lightning-induced voltages on complex distribution systems: models, advanced software tools and experimental validation," *Journal of Electrostatics,* Vols. 60/2-4, pp. 163-174, 2004.

[136] A. Borghetti, M. Paolone and C. A. Nucci, "Effect of tall instrumented towers on the statistical distributions of lightning current parameters and its influence on the power system lightning performance assessment," *European Transactions on Electrical Power,* Vols. 13-6, pp. 365 - 272, November/December 2003.

[137] F. Rachidi, M. Mazzetti, C. Ianoz and C. A. Nucci, "Influence of a lossy ground on lightning-induced voltages on overhead lines," *IEEE Transactions on EMC,* Vols. 38-3, pp. 250-264, 1996.

[138] M. Paolone, E. Petrache, F. Rachidi and C. A. Nucci, "Mitigation of lightning-induced overvoltages in medium voltage distribution lines by means of periodical grounding of shielding wires and of surge arrester modeling and experimental validation," *IEEE Trans. on Power Delivery,* Vols. 19-1, pp. 423 - 431, January 2004.

[139] M. Paolone, C. Nucci and F. Rachidi, "A New Finite Difference Time Domain Scheme for the Evaluation of Lightning Induced Overvoltages on Multiconductor Overhead Lines," *Proc. 5th Int. Conf. on Power System Transient,* vol. 2, pp. 596 - 602, 2001.

[140] Electromagnetic Transient Program (EMTP), Portland, Oregon: Bonneville Power Administration, 1984.

[141] EMTP, Electromagnetic Transient Program Rule Books, Oregon: Vol. 1 and 2, EPRI-EMTP DCG, 1996.

[142] J. G. Kapperman, M. E. Gordon and T. W. Guttormson, "High-precision location of lightning-caused distribution faults," in *Proc. IEEE Transmission and Distribution Conference and Exposition*, Atlanta, 2001.

[143] S. M. Chen, Y. Du, L. M. Fan, H. M. He and D. Z. Zhong, "Evaluation of the Gaung Dong lightning location system with transmission line fault data," *IEE Proc-Sci. Meas. Technol.*, vol. 149, no. 1, pp. 9 - 16, 2002.

[144] G. Diendorfer and W. Schulz, "Ground flash density and lightning exposure of power transmission lines," in *Proc. IEEE Bologna Power Tech Conference*, Bologna, 2003.

[145] G. Diendorfer, "Correlation of power line failures and lightning location failure data," in *5th International Workshop on physics of lightning*, Nagoya, 2001.

[146] F. Napolitano, A. Borghetti, M. Paolone and M. Bernardi, "Voltage transient measurements in a distribution network correlated with data from lightning location system and from sequence of event recorders," *Electric Power Systems Research*, vol. 81, pp. 237 - 253, 2011.

[147] S. Rusck, "Protection of distribution systems in lightning," *R.H. Golde, Ed.*, vol. 2, pp. 747 - 771, 1977.

[148] W. J. Dirkse van Schalkwyk and J. M. Van Coller, "A feeder BIL to benefit Quality of Supply and Network Performance in high lightning areas," in *CIGRE International Colloquium on Lightning and Power Systems*, Bologne, 2016.

[149] S. Yokoyama, "Designing concept on lightning protection of overhead power distribution line," in *IX International Symposium on Lightning Protection*, Foz do Iguacu, Brazil, 2007.

[150] M. Darveniza, Electrical properties of wood and line design, St. Lucia: University of Queensland Press, 1980.

[151] M. J. Master, W. Beasley, M. Darveniza and M. A. Uman, "Lightning induced voltages on power lines: Experiment," *IEEE Trans. Power Apparatus and System*, vol. 103, pp. 2519 - 2529, September 1984.

[152] S. Yokoyama and A. Asakawa, "Experimental study of response of power distribution lines to direct lightning hits," *IEEE Power Del.*, vol. 4, no. 4, pp. 2242 - 2248, October 1989.

[153] F. J. Jooste and W. J. Dirkse van Schalkwyk, "Earthing for 50Hz and lightning frequencies," in *SAUPEC*, Pretoria, 2003.

[154] N. Mafatle and W. J. Dirkse van Schalkwyk, "Screening wire and earthing concept," in *SAUPEC*, Stellenbosch, 2004.

[155] S. Yokoyama, H. Mitani, K. Miyake and N. Yamazaki, “Corroboration of Induced Lightning voltage Suppressing Effect of Overhead Ground Wire Using Natural Lightning,” *Trans. IEEE,* Vols. 105-B, no. 2, pp. 125 - 132, 1985.

[156] S. Yokoyama, K. Yamamoto and H. Kinoshita, “Analogue Simulation of Lightning Induced Voltages and its Application for Analysis of Overhead-Ground-Wire Effect,” *IEEE, Proc.,* vol. 132, no. 4, pp. 208 - 216, 1985.

[157] A. Piantini and J. M. Janiszewski, “The effectiveness of surge arresters on the mitigation of lightning induced voltages on Distribution lines,” in *VIII International Symposium on Lightning Protection*, Sao Paulo, 2005.

[158] A. Piantini and J. M. Janiszewski, “Use of surge arresters for protection of overhead lines against nearby lightning,” in *Proceedings of the 10th International Symposium on High Voltage Engineering*, Montreal, 1997.

[159] A. Borghetti, A. Morched, F. Napolitano and C. A. Nucci, “Lightning-Induced Overvoltages Transferred Through Distribution Power Transformers,” *IEEE Trans. on Power Delivery*, vol. 24, no. 1, January 2009.

[160] A. Piantini, “Lightning-IInduced Overvoltages on Overhead Medium-Voltage lines,” in *IEEE International Conference on Hogh Voltage Engineering and Application (ICHVE)*, Chengdu, China, September 2016.

[161] H. K. Høidalen, “Lightning induced voltages in low voltage systems with Emphasis on lossy ground effects,” in *IPST 97 - Inernational Conference on Power System Transients*, Seattle, June 1997.

[162] W. J. Dirkse van Schalkwyk, C. Gomes and J. Van Coller, “A New Method to Measure the Lightning Performance of a Long Medium Voltage Line,” in *Proceedings of IEEE Africon 2021*, Arusha, Tanzania, September 2021.

[163] M. M. Ismail, M. Rahman, V. Cooray and S. Sharma, “Electric Field Signatures in Wideband, 3 MHz and 30 MHz of Negative Ground Flashes Pertinent to Swedish Thunderstorms,” *Atmosphere*, vol. 6, no. 12, pp. 1904-1925, December 2015.

[164] D. Johari, “Features of the Electric Fields Generated by Lightning with Special Attention to Positive Ground Flashes,” Digital Comprehensive Summaries of Uppsala Dissertations from the Faculty of Science and Technology 1588, Uppsala, 2017.

[165] R. Smeets and P. Knol, “Verification of Lifetime arcing stress withstand of circuit breakers for testing,” in *Cigre 6th South Africa conference Paper no. P402*, Cape Town, August 2009.

[166] A. M. Dan, Z. S. Czira and D. Raize, “Comparison of Different Methods to Decrease the Harmonic Content of the Fault Current during Single-Phase to Ground Faults in Compensated Networks,” in *Power Tech, 2005 IEEE*, Russia, July 2005.

[167] W. L. Vosloo, *Outdoor High Voltage Insulator Course,* Cape Town, South Africa: Eskom Academy of Learning, 18-20 May 2021.

[168] B. Richter, “Overvoltage protection Metal oxide surge arresters on Medium Voltage lines,” Wettingen, ABB Switzerland, May 2011, p. 23.

[169] M. F. Stringfellow, “The Operating Duty of Distribution Surge Arresters Due to Indirect Lightning Strikes,” *Transactions of SAIEE,* vol. 72 part 5, pp. 102 - 122, May 1981.

[170] SABS Standards Division, “SANS 780: Distribution Transformers,” vol. Edition 4, 2009.

[171] ABB Switzerland Ltd, “Surge arrester POLIM-D datasheet,” *High voltage products,* p. 2, 2013.

[172] M. Du Preez and W. J. Dirkse van Schalkwyk, “Lightning and Power Frequency Performance of MV Pole Mounted Transformers,” in *Cigre 7th Southern Africa Regional Conference & Joint Colloquium,* Somerset West, 2013.

[173] P. Sewkumar and W. J. Dirkse van Schalkwyk, “Fusing Philosophy for Eskom Distribution’s North West Region,” in *SAUPEC,* Stellenbosch, 2004.

[174] M. Du Preez and W. J. Dirkse van Schalkwyk, “Lightning protection for Equipment on MV feeders,” in *IDC Technology, Earthing , Lightning and Surge Protection.*, Johannesburg, July 2011.

[175] F. J. Jooste and W. J. Dirkse van Schalkwyk, “Lightning Resistant Fuses With Enhanced 50 Hz Applications,” in *SAUPEC,* Stellenbosh, 2004.

[176] M. S. Naidu and V. Kamaraju, High Voltage Engineering, New Delhi: Tata McGraw-Hill, 2009, 4 th Edition, pp. 239 - 243.

[177] R. C. Weast, The CRC Handbook of Chemistry and Physics 62nd Edition, CRC Press, 1981.

[178] A. Bouwers, Elektrische Höchstspannungen, Berlin: Springer, 1939.

[179] H. J. Geldenhuys, “Design of a spark gap to achieve a 300 kV BIL to avoid wood pole shattering,” University of the Witwatersrand, Johannesburg, March 2002.

[180] A. Beutel, “MV & LV Network Safety project stream 5,” Eskom RT&D , Johannesburg, 20 November 2020.

[181] R. G. Moore, “Impulse test report ERI200-34,” Eskom Rotek Industries, Johannesburg, 5 December 2018.

9 Appendix A

9.1 More examples of recordings during the research

Figure 9.1 shows a recording of the RMS voltage, the voltage waveform, the RMS current and the current waveforms that were measured at the feeder substation. The lightning activity lasted for 10 hours. Two feeders are connected to the substation. The first and the last faults due to lightning were on the adjacent feeder as the voltage disturbances were significant while the current deviations were small. However, each voltage and current disturbance was investigated.

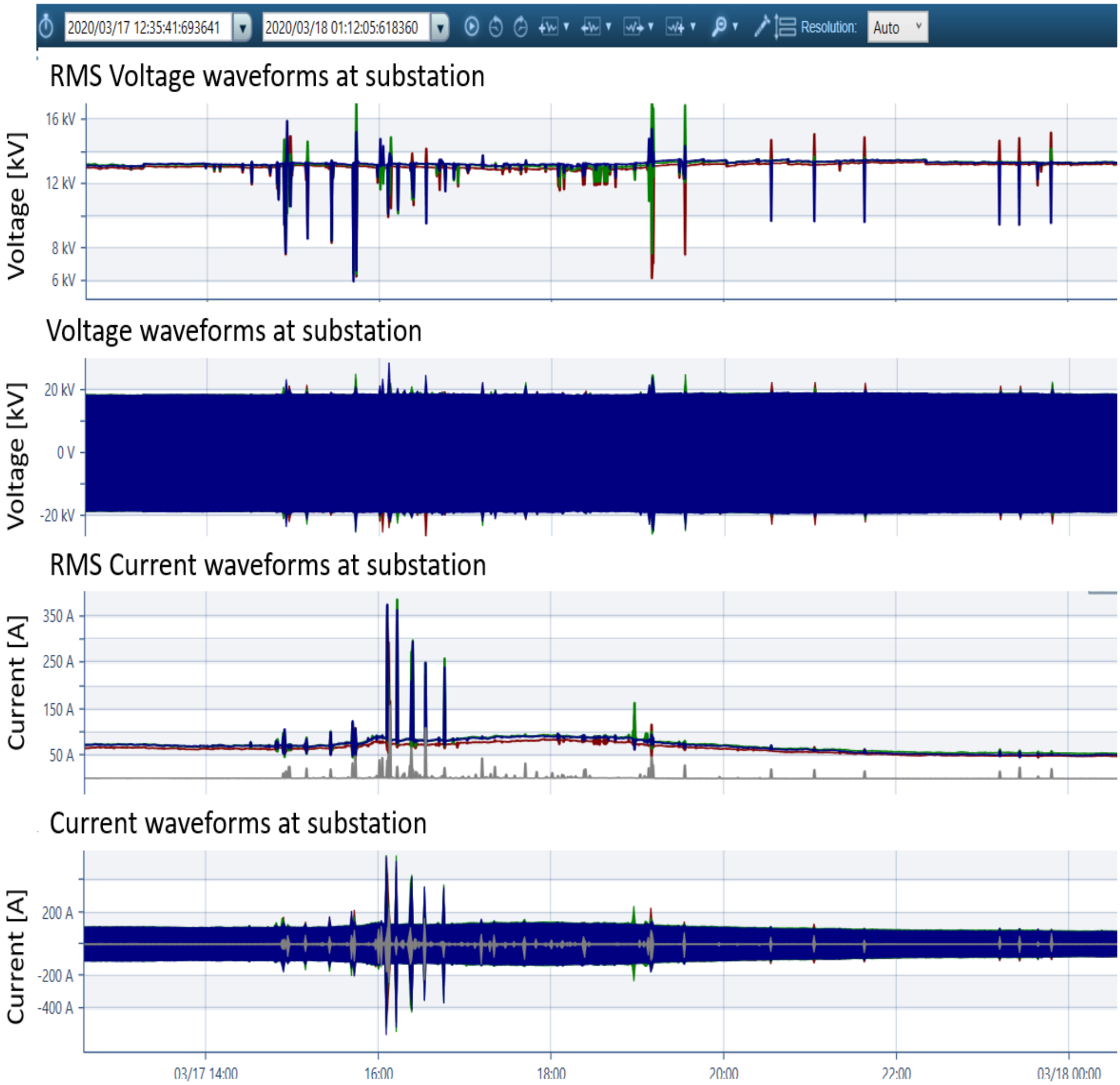

Figure 9.1 A recording of a typical lightning storm. Lightning caused several fault currents or disturbances in the voltage and current recordings.

Figure 9.2 shows an example of a flashover between the red and white phases due to a direct lightning strike captured by the LDN (shown in Figure 9.4). A flashover to the blue phase also occurred after a while which quenched again. Figure 9.3 shows that there was an LGC with a negative polarity that was the same polarity (negative) as the lightning return-stroke current captured by the LDN. This indicated that it was a direct lightning strike to the line.

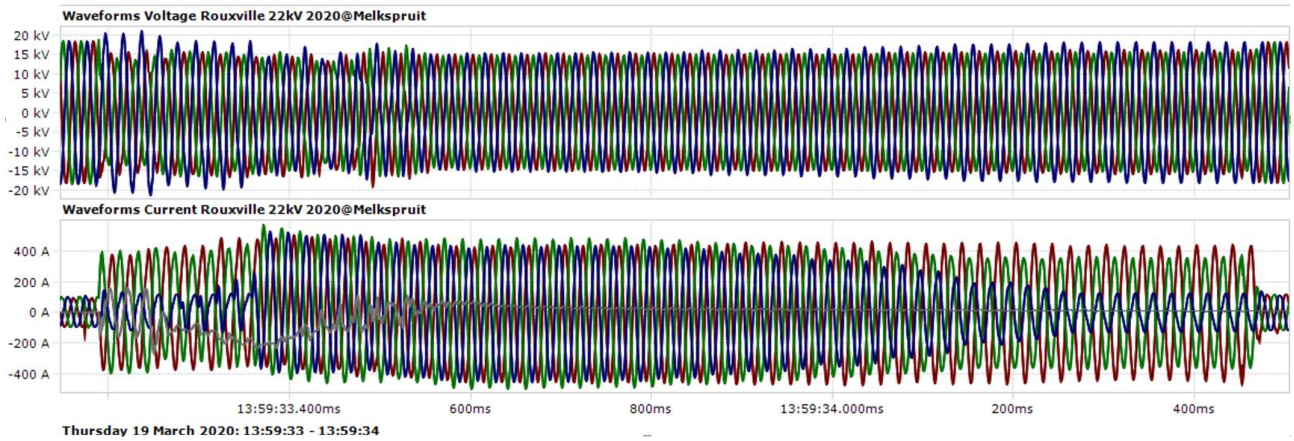

Figure 9.2 An example of a "Phase to Phase fault" due to a direct lightning strike to the line. The fault was cleared by a breaker further down the line.

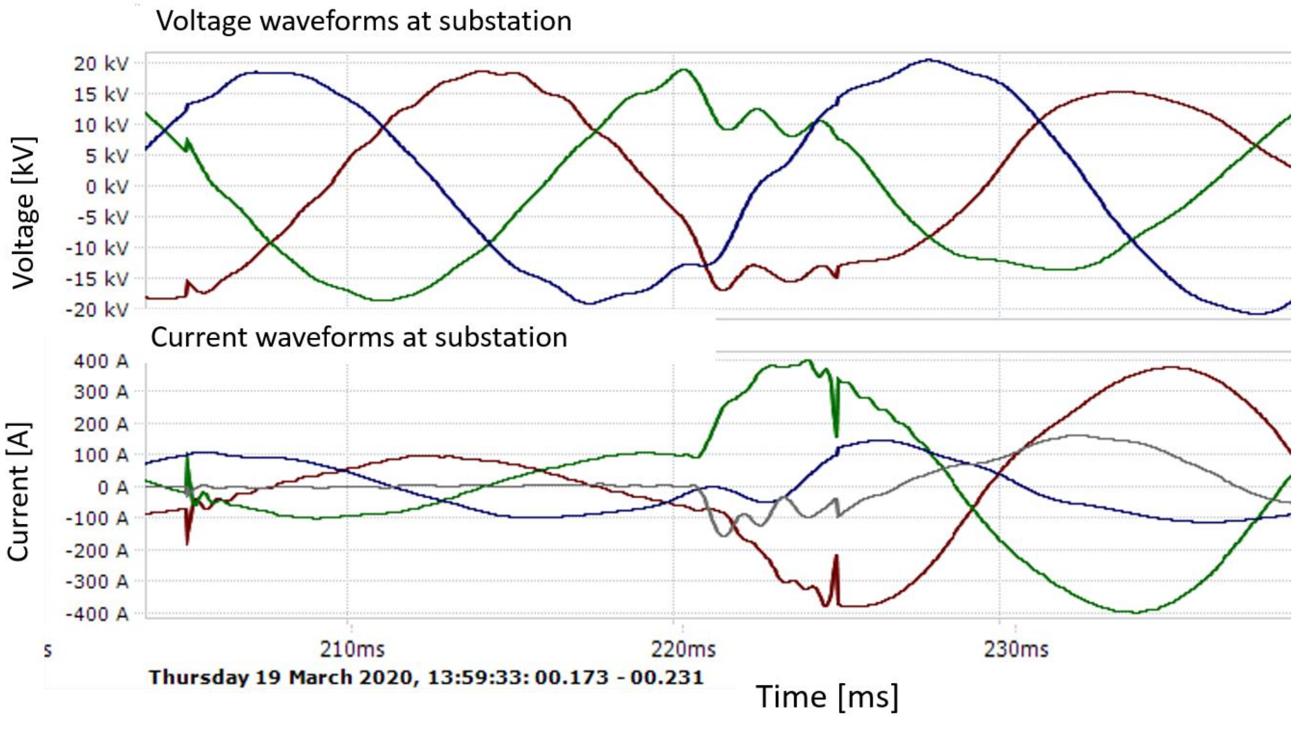

Figure 9.3 A zoomed-in picture of the fault in Figure 9.2 showing an LGC with a negative polarity.

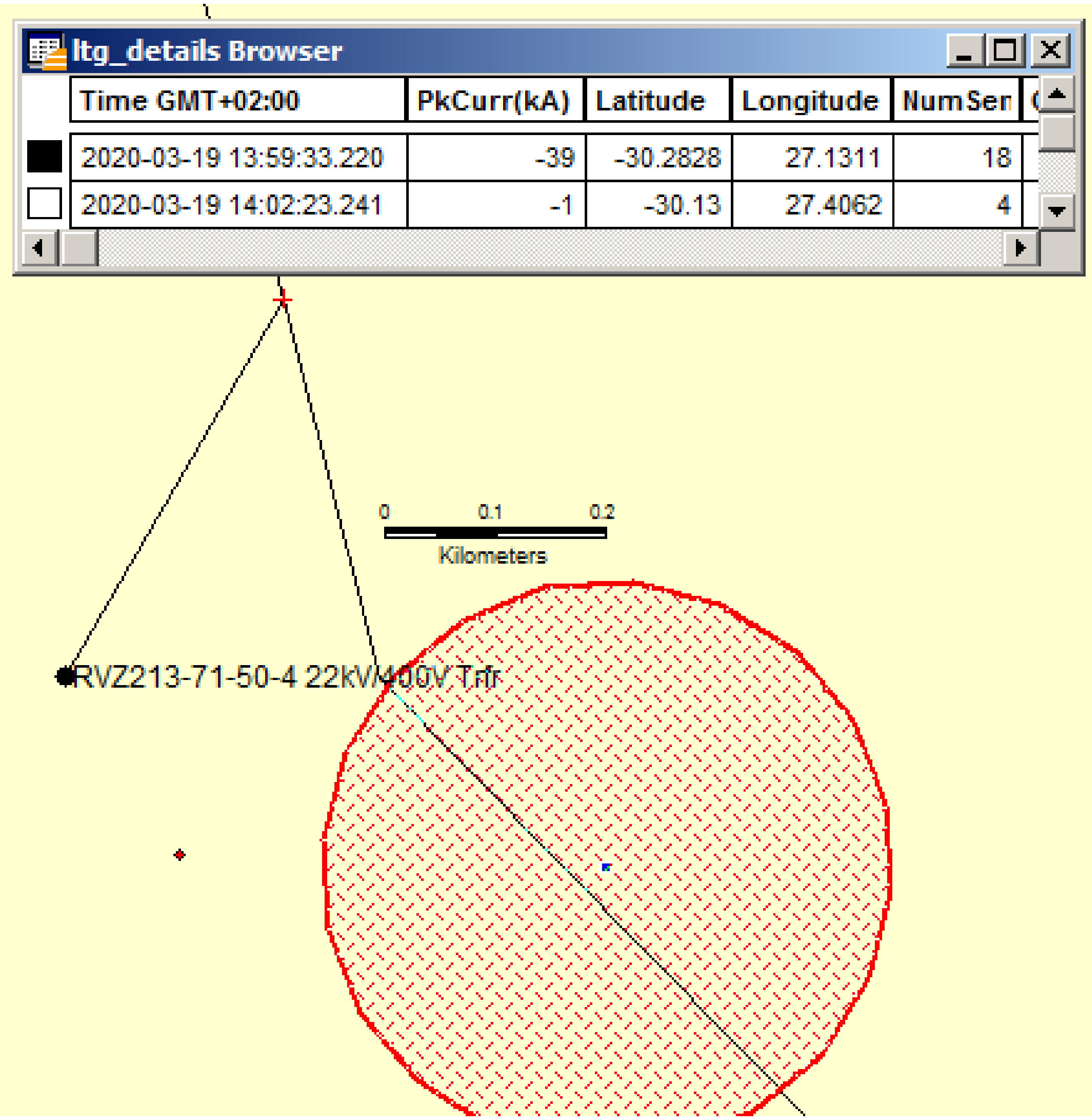

Figure 9.4 A -39 kA direct lightning strike to the line causing a fault between the phases shown in Figure 9.3.

Figure 9.5 shows a recording of a +140 kA nearby lightning strike that did not cause a line flashover. If it was a direct strike to the line, a flashover would have occurred. As this lightning strike was 42 km from the feeder substation, the LIOV did not give any indication of the polarity of the lightning strike. The polarity of the LGC was negative which was opposite to the polarity (positive) of the nearby lightning strike shown in Figure 9.6.

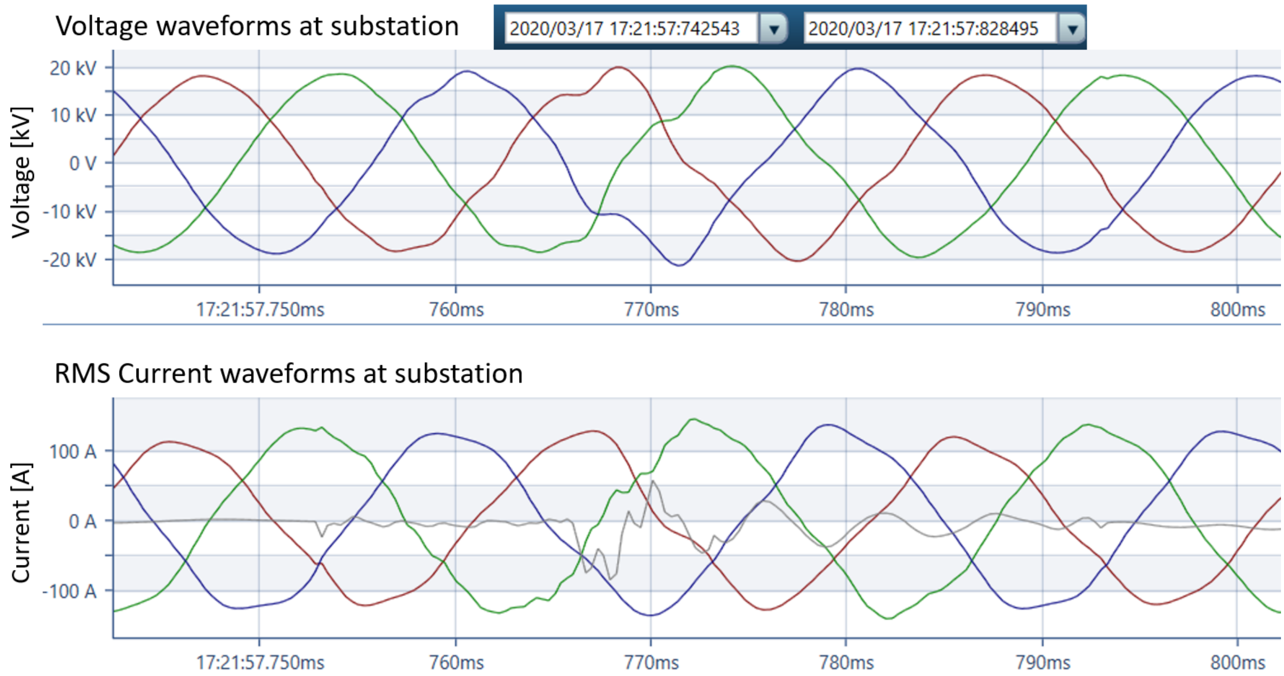

Figure 9.5 A recording of a nearby lightning strike. The lightning strike captured by the LDN is shown in Figure 9.6.

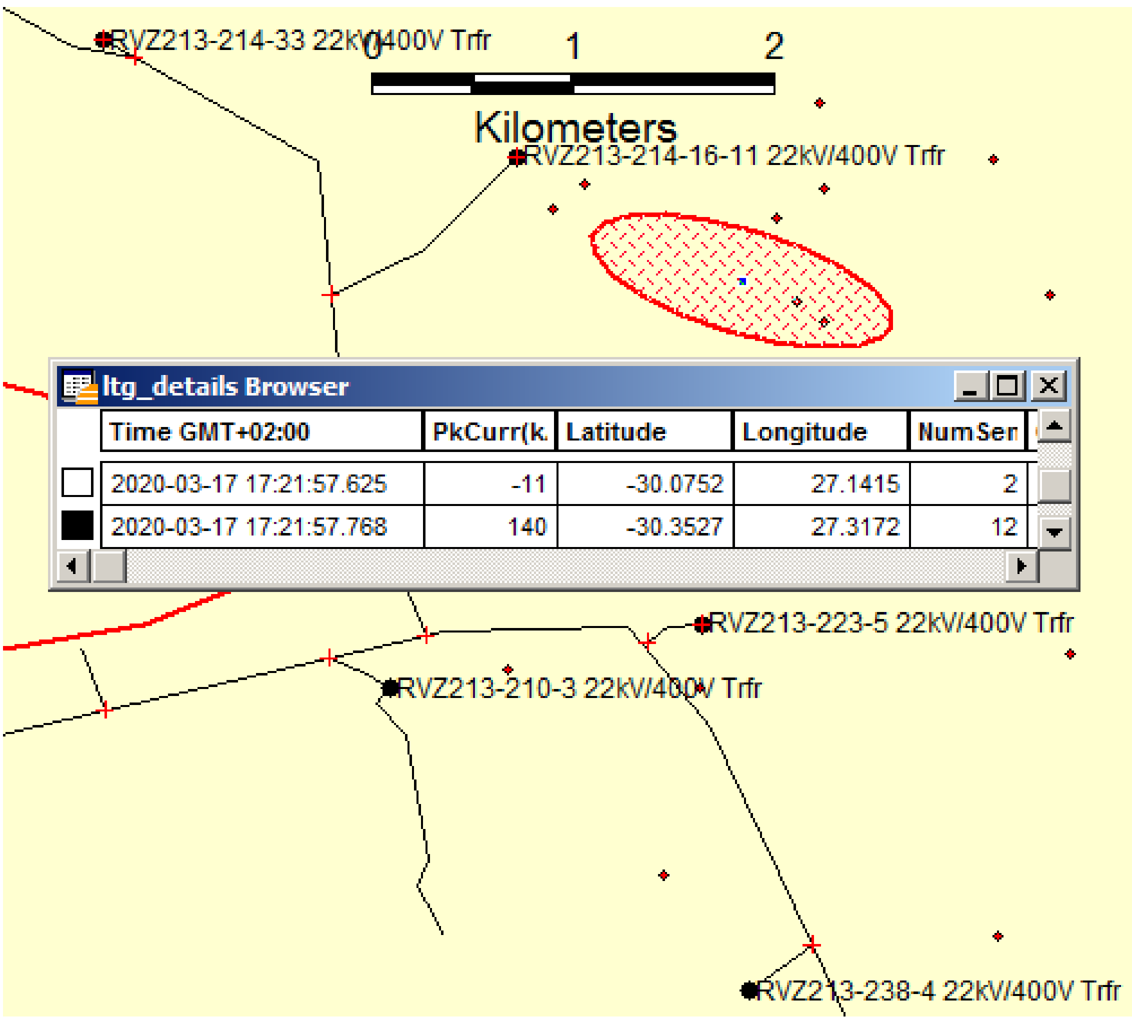

Figure 9.6 The LDN data for the nearby lightning strike that was recorded in Figure 9.5.

Figure 9.7 is an example of a lightning flash that caused a flashover on the line. The disturbances of the lightning strokes within the flash were clearly visible in the recording. However, none of the strokes within the flash was captured by the LDN. Figure 9.8 shows the LDN data before and after the time of the recording.

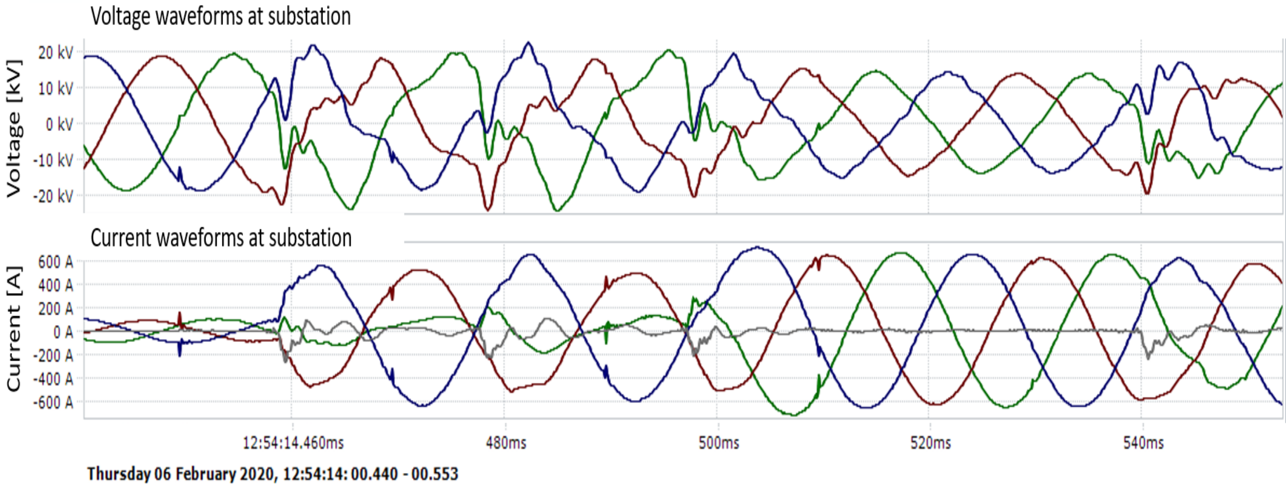

Figure 9.7 An example of a lightning flash that was not detected by the LDN.

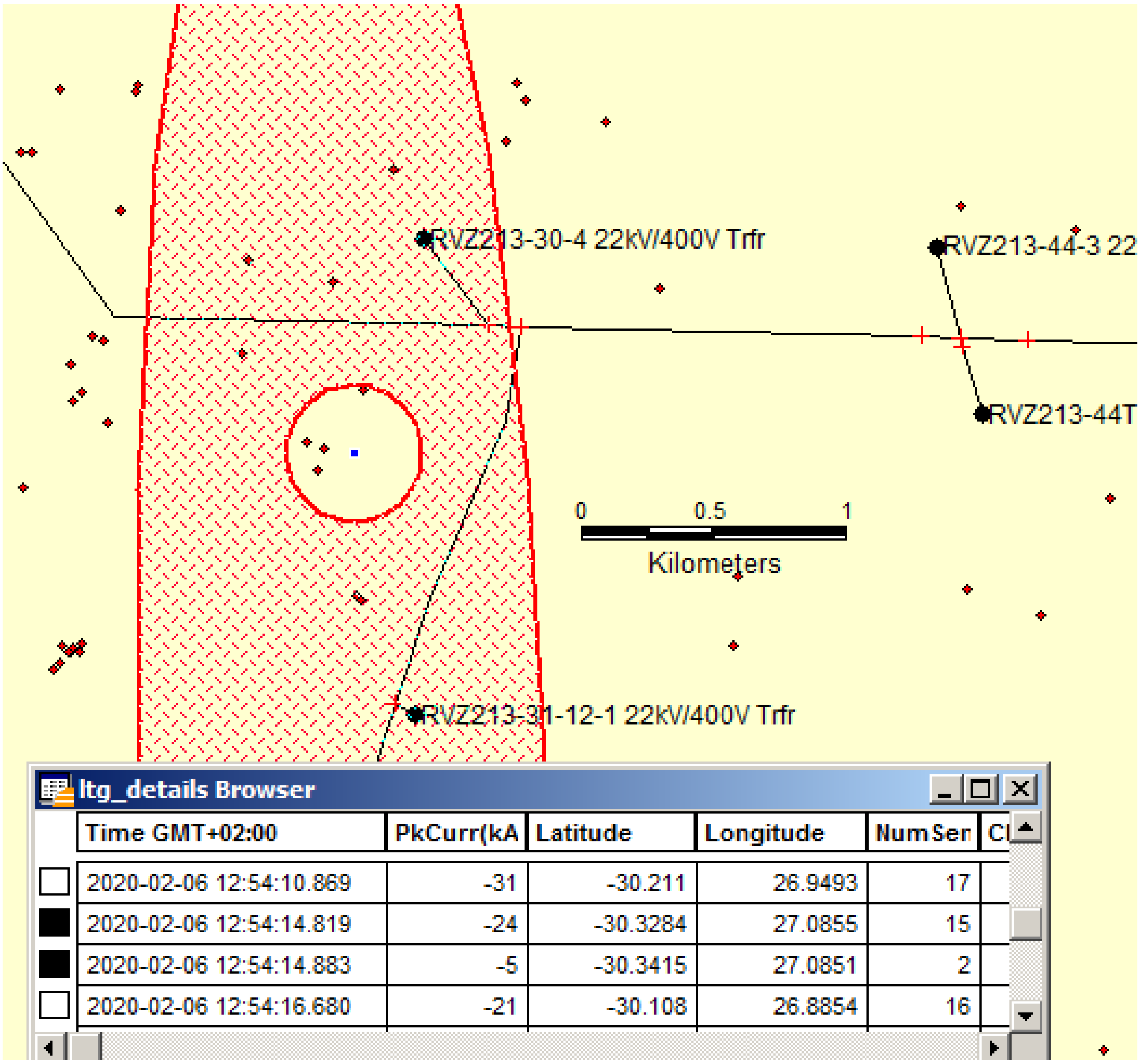

Figure 9.8 The LDN data before and after the lightning flash in Figure 9.7.

Figure 9.9 and Figure 9.10 show a flashover between the blue phase and the earth during a lightning storm. However, no disturbance due to lightning activity could be seen in the voltage or current recordings. There was also no lightning strike captured by the LDN at the time of the recording as shown in Figure 10.11.

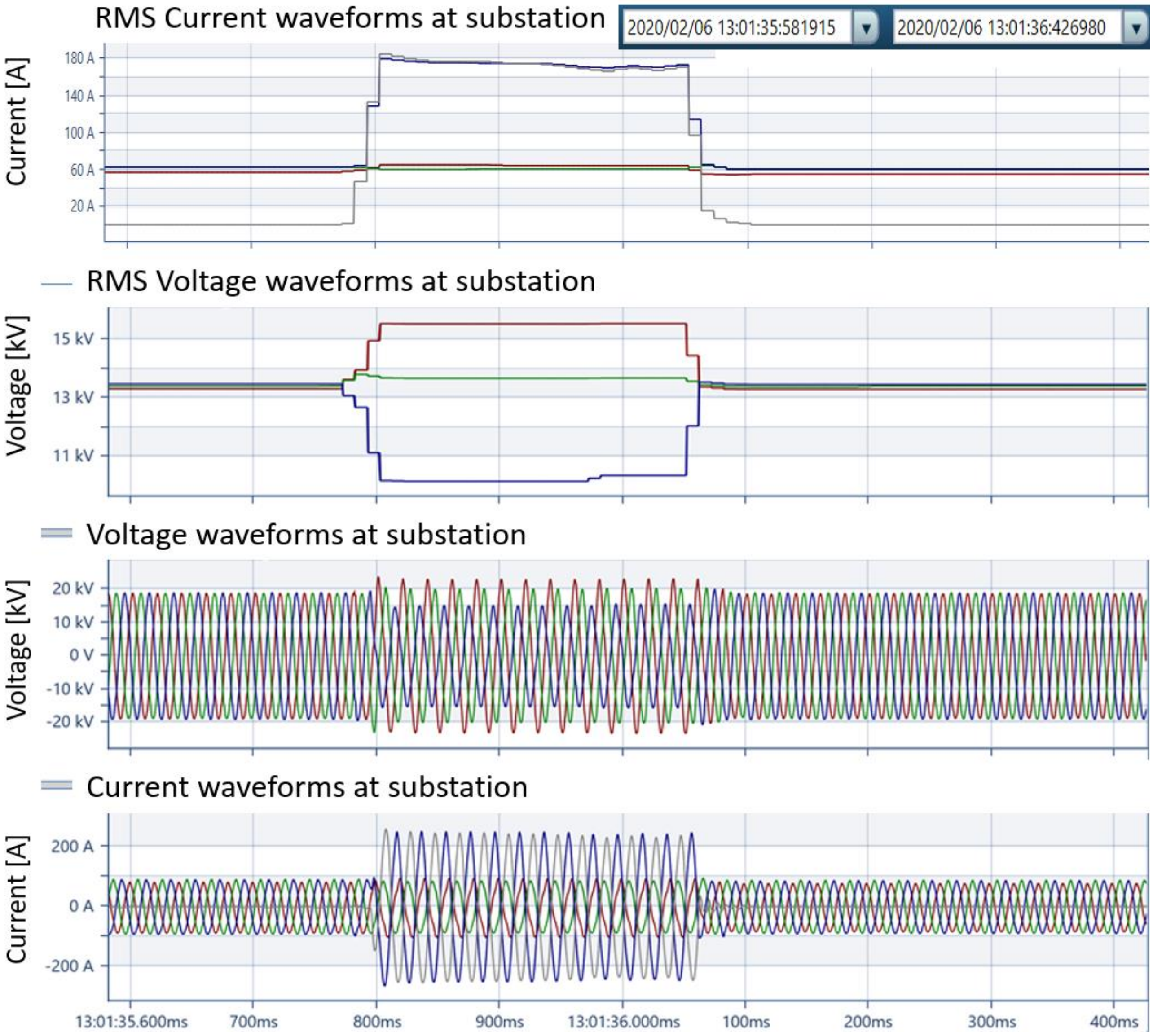

Figure 9.9 An example of a "Weather-related fault" Although the fault occurred during a storm, no lightning activity could be seen on the recordings.

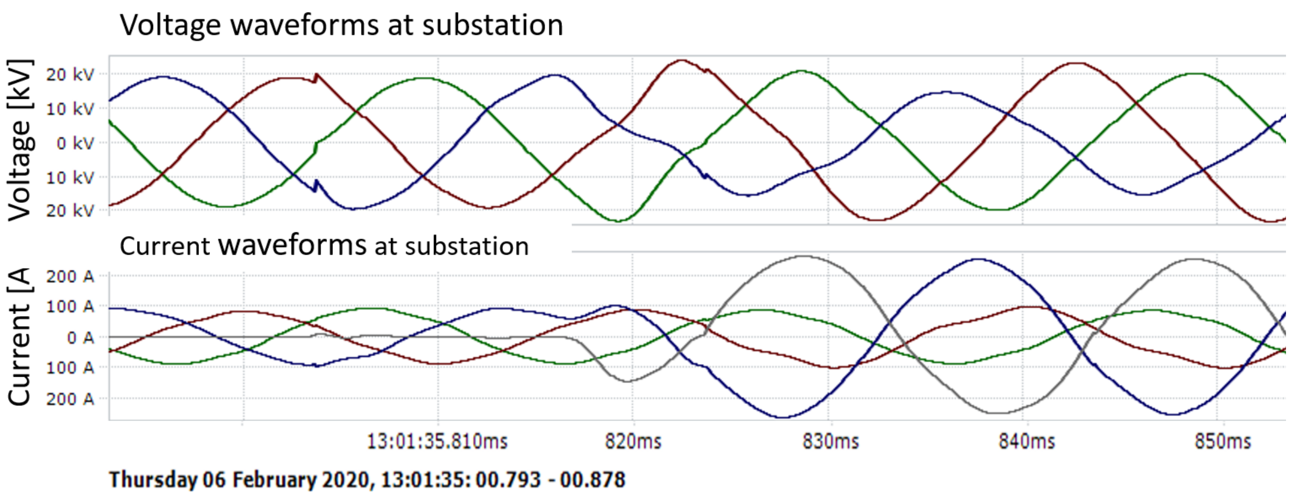

Figure 9.10 The time when the fault in Figure 9.9 started. No lightning activity can be seen in the recordings.

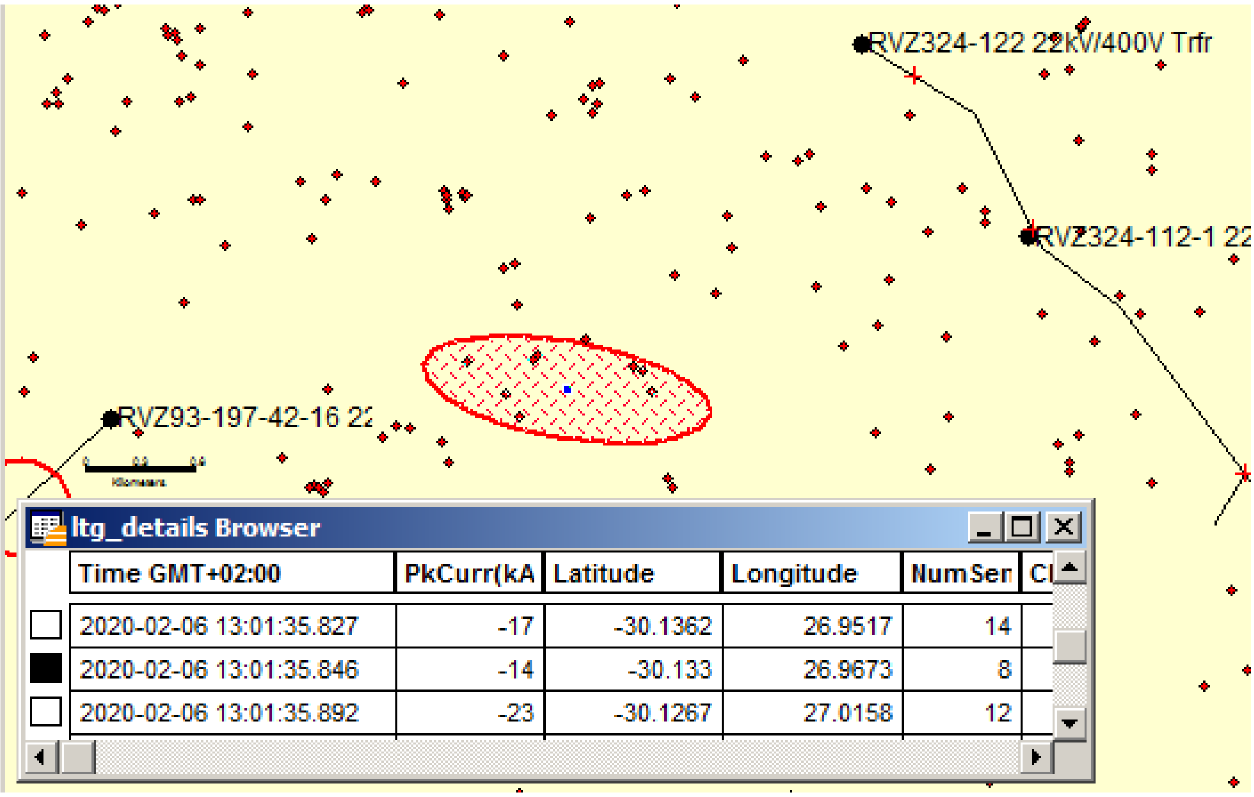

Figure 9.11 Lightning activity at the time that the fault in Figure 9.9 occurred.

Figure 10.12 and Figure 10.13 show a line fault that occurred at a time when there was no lightning. There was lightning 6 hours before and 12 hours after this incident.

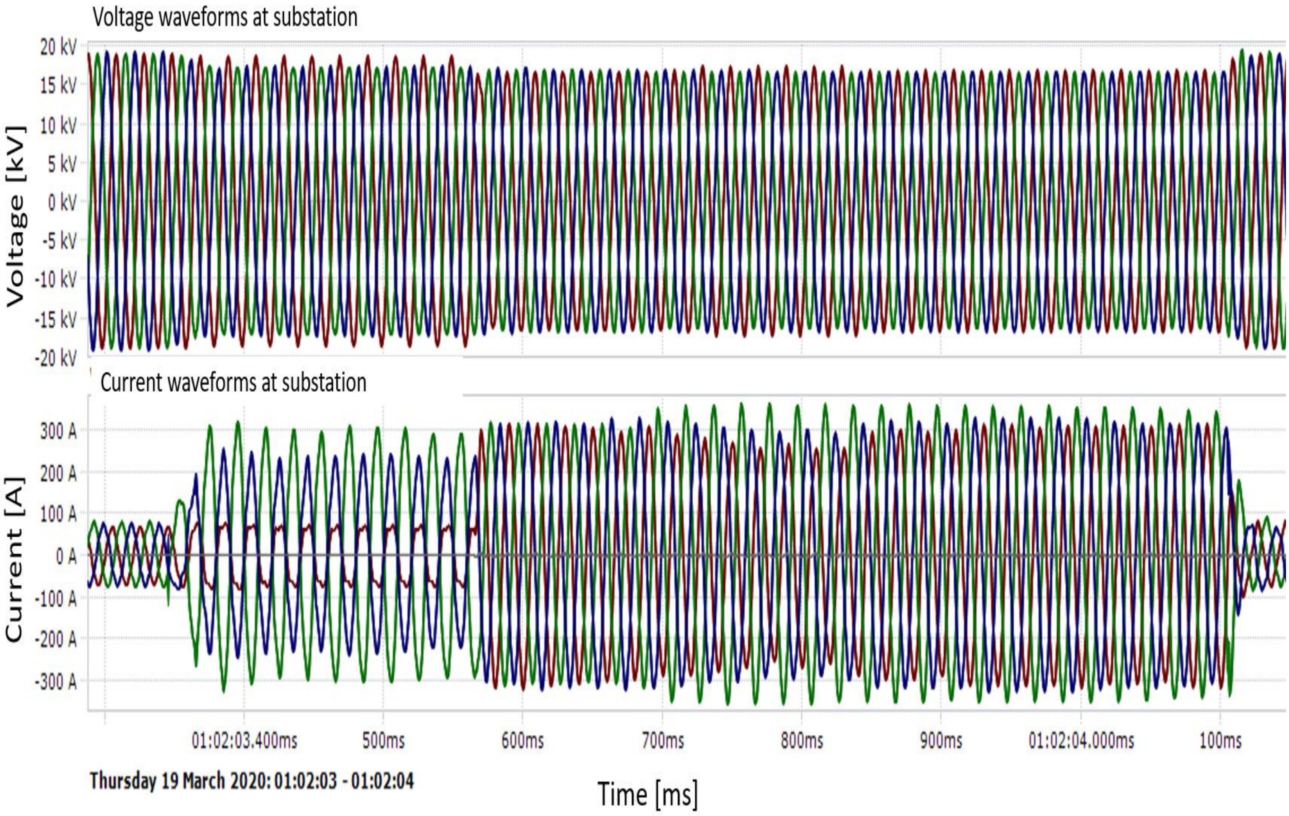

Figure 9.12 A typical "other" fault that happened on a clear day.

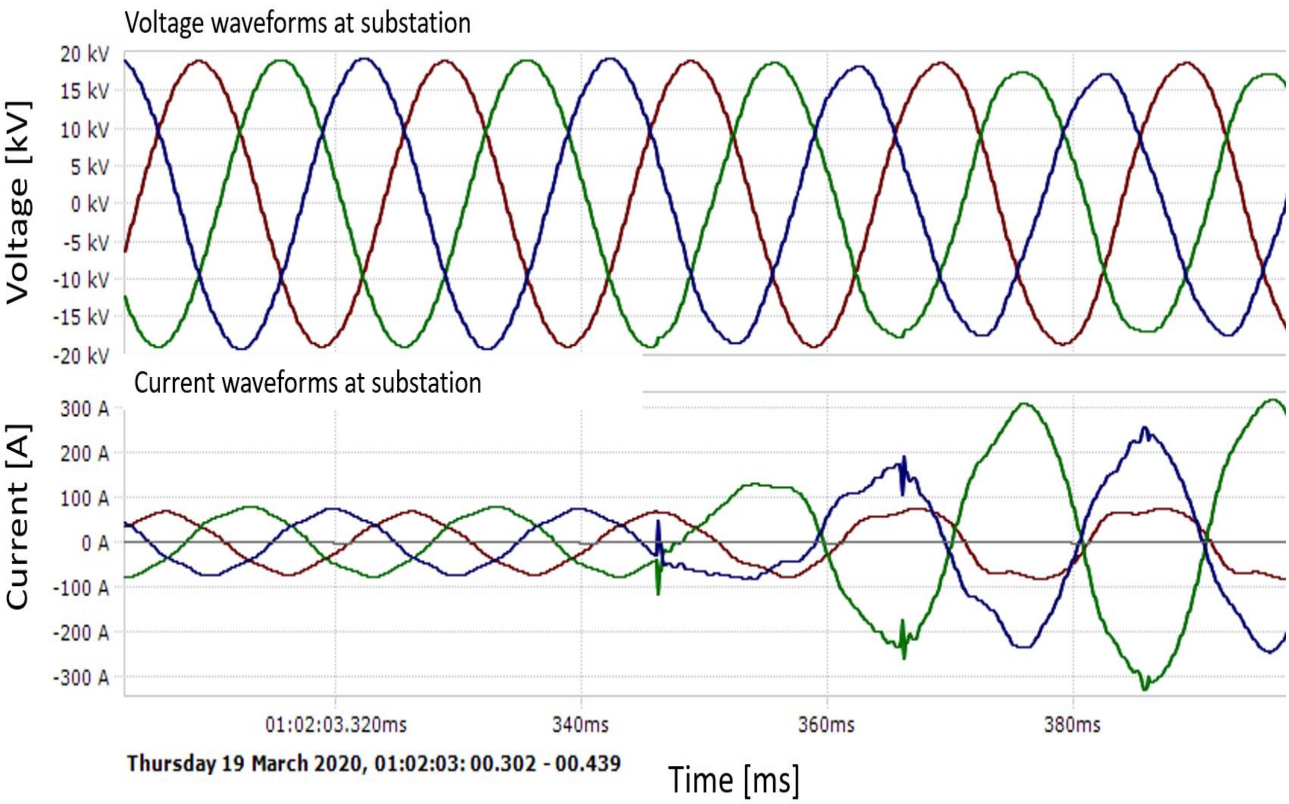

Figure 9.13 An "Other" fault that happened on a clear day.

10 Appendix B

10.1 Mitigation measures to minimize lightning-related equipment failure

Figure 10.1 shows the equipment that failed on the RVZ line during the research period. It can be noted that the fuses were most vulnerable to lightning. Although the fuse elements were very cheap, the travelling (the average distance that had to be travelled was 60 km per fuse) and overtime made it expensive to replace the blown fuses. Most of the lightning activity was in the afternoon and as a result, overtime was booked in 42% of the incidents.

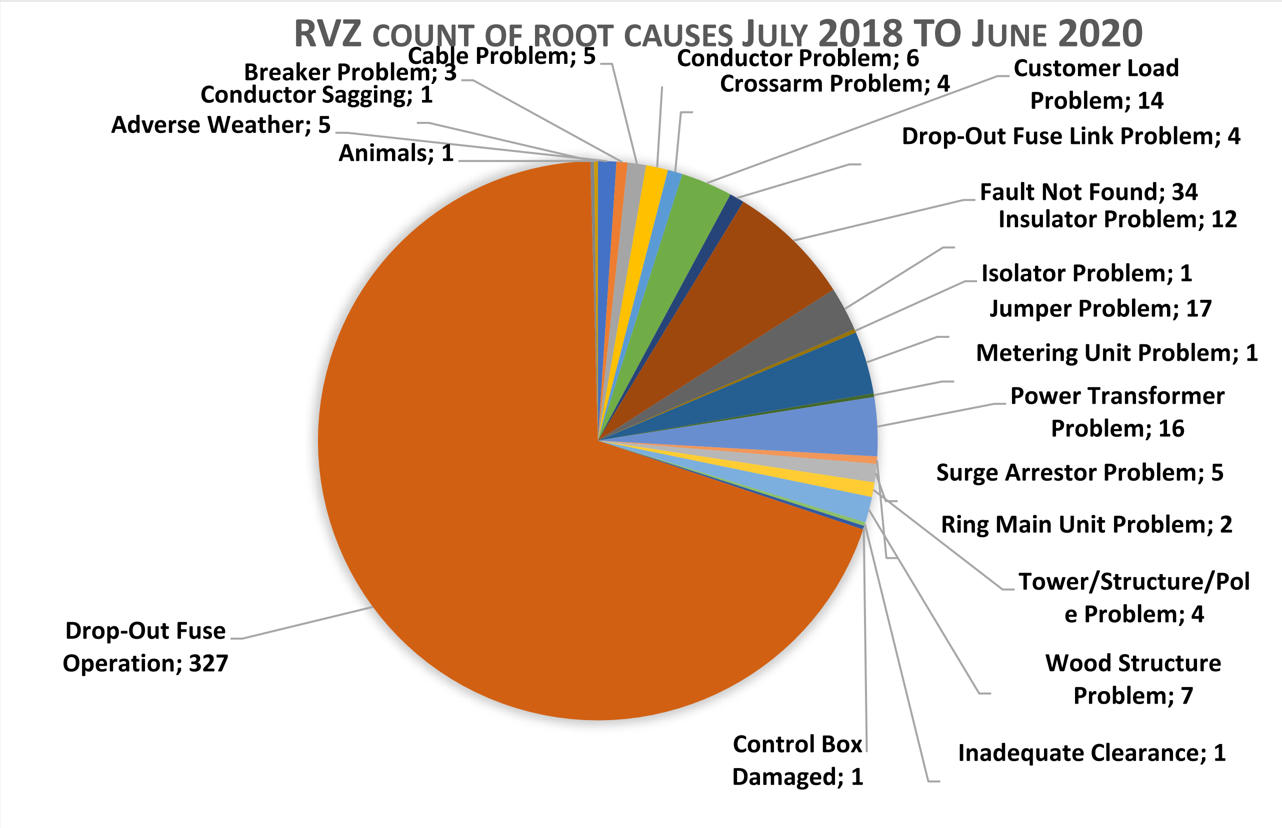

Figure 10.1 The equipment that failed on the RVZ line during the research period. The Field Operators mention that about 80% of the equipment failed during lightning activity. It can be noted that the fuse elements were the most vulnerable equipment.

The surge arresters on the MV line are the primary protection of the pole-mounted transformers against direct lightning strikes. It is therefore important to preserve the surge arrester's life expectancy. Numerous studies were done to determine what the energy absorption in the surge arresters will be with different lightning surges and at different distances from the surge arresters. Figure 10.2 shows the ATP model that was used for the studies to determine the energy absorption in a surge arrester due to a -18 kA 3/70 µs direct lightning strike to the line. A study was performed whereby this direct lightning strike on the phase conductors of a 150 kV, 180 kV, 300 kV BIL as well as a fully insulated line configuration was simulated. Lastly, another study was also performed where the lightning strike terminated on the pole's "earth" conductor. The lightning strike to the line was set to terminate more than 2 km from where the surge arrester was installed. The pole closest to the surge arrester installation where no flashover occurred due to the surge voltage was modelled to be 2 km away. At this point, the LIOV amplitude was just less than the line's BIL.

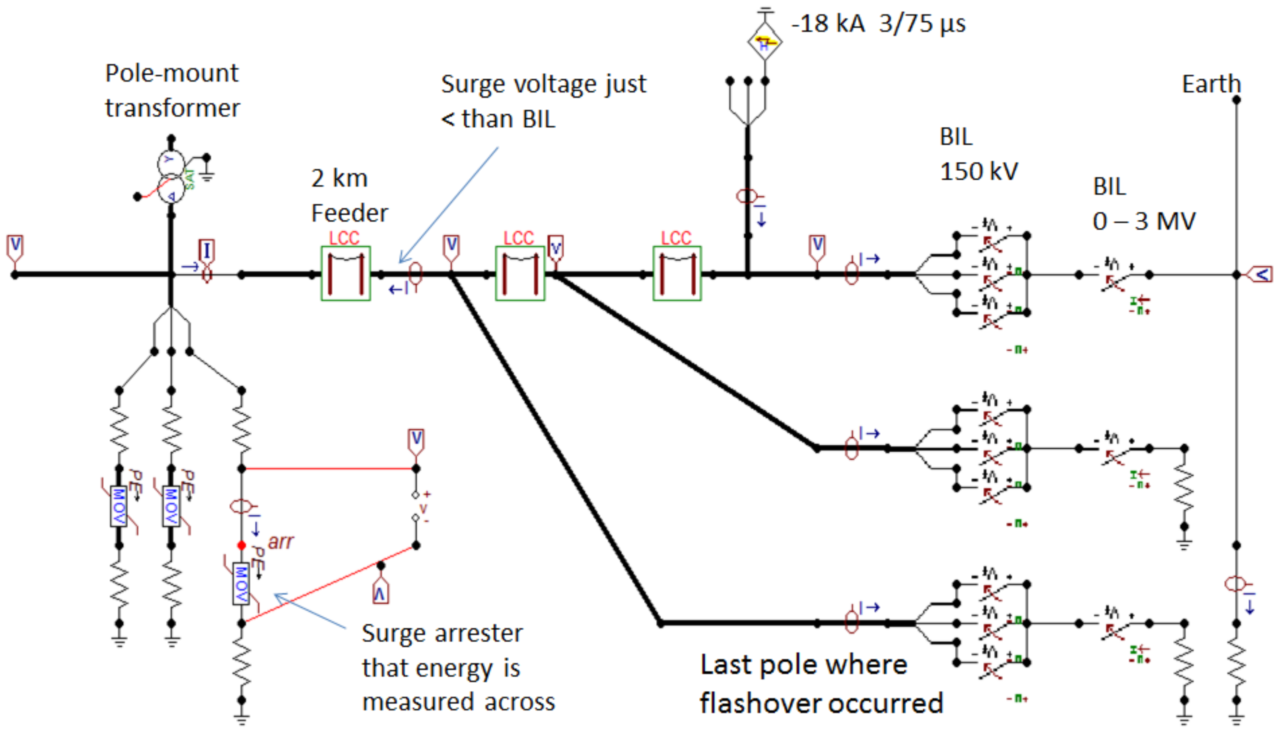

Figure 10.2 The ATP model that was used to simulate the energy absorption in a surge arrester using different line BIL options.

A comparison of the energy absorption in a surge arrester at different line BIL configurations is shown in Figure 10.3. The simulation revealed that a lower line BIL results in less energy absorption in the surge arresters. A BIL of 150 kV was used during the simulation where a lightning strike to the pole's earth wire was simulated. As predicted, a flashover occurred between the earth conductor and the phases and therefore very little difference between the 150 kV BIL and the earth curve could be seen. All the parameters except for the BIL were kept the same for all the simulations. The energy absorption in the surge arresters will change significantly should simulations be done with other wave-shaped surges.

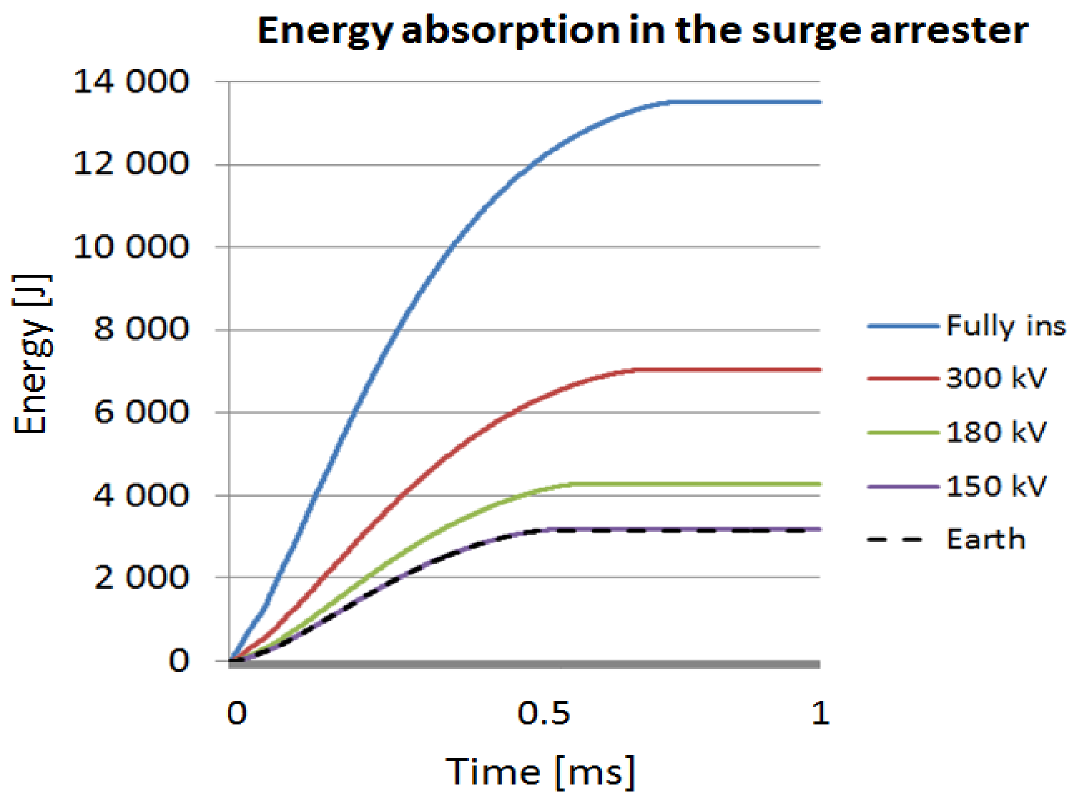

Figure 10.3 Energy absorption in the surge arrester for different line BILs due to a lightning strike direct to the line. Note that the higher the BIL, the more energy had to be absorbed by the surge arrester.

A surge arrester takes between 45 and 60 minutes to cool down [168]. During this time the combination of several lightning surges might exceed the surge arrester energy rating. The transformer was unprotected after a surge arrester failure against voltage surges that could result in transformer failure. According to Stringfellow [169], surge arresters fail very rarely due to nearby lightning. For direct lightning strikes, the lower the BIL, the more flashovers would occur simultaneously at several poles on the line, which in turn resulted in more parallel paths for the lightning current to flow to earth and less energy needs to be absorbed in a surge arrester.

According to [150], a wood path can also quench a power frequency arc caused by a lightning strike. However, these tests were only done for currents up to 3500 A. Independent arc quenching was found to be very inconsistent and could not be confirmed in this research.

10.2 Pole-mounted substation equipment reliability

A pole-mounted transformer installation consisted mainly of a transformer, a distribution type surge arrester per phase and a fuse per phase. The BILs of the 11 kV and 22 kV transformers were 95 kV and 150 kV [170] respectively. The fuse base insulator had a BIL of 150 kV for both 11 kV and 22 kV installations. Due to the earth wire and soil impedance, a 22 kV surge arrester lowered the peak surge voltage to between 57 kV and 87 kV depending on the surge current. These values are between 31 kV and 47 kV for an 11 kV surge arrester [171]. The pole-mounted transformer configuration is shown in Figure 10.4.

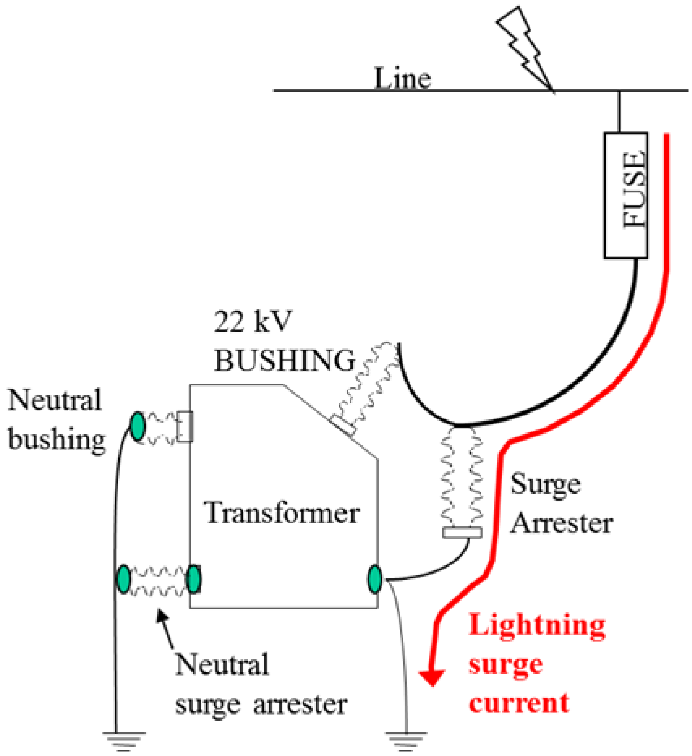

Figure 10.4 A typical pole-mounted transformer installation configuration in South Africa. A lightning surge current flows through the fuse and surge arrester to earth at the pole-mounted installation.

The equipment on a pole-mounted installation was exposed to lightning surges on the line and needs to be protected accordingly. Incorrect isolation of faulty equipment leads to line outages. The network performance was strongly related to the pole-mounted installation performance. During the investigation, it was also found that some of the surge arresters were not serviceable (GLD operate) due to the long periods between line inspection [5].

It was also found that the surge arrester placement was not always adequate (surge arresters too far from the transformer) and differs from transformer to transformer. Most transformers did not have any lightning protection on the secondary side (400 V) and it was possible that the transformer can be damaged from the secondary side. According to Yokoyama [149] on average 28% of the outages were due to transformer failures.

10.3 Alternatives to minimize MV pole-mounted transformer failures.

The network performance was greatly influenced by equipment failures on the pole-mounted installations. Part of the aim of the research was to minimize the surge amplitude and surge energy to reduce pole-mounted equipment failures. However, the line BIL did not influence the LGV when lightning terminates directly to a pole-mounted installation. Nearly all direct lightning strikes to the pole-mounted installations caused equipment failure. In most cases, the fuses failed and in several cases, the surge arresters failed. Failed surge arresters that were not replaced in time, led to transformer failures.

Combi-Units [172] [173] [174] and Lightning Proof Fuses [175] were alternatives to protect pole-mounted installations against lightning damage. The Lightning Proof Fuse (shown in Figure 10.5) was designed in such a way that lightning current flows around the fuse element. The fuse element can now be graded with the power frequency protection without the necessity to take lightning surges into account. The Combi Unit (combination of a fuse and surge arrester as shown in Figure 10.8) was designed to ensure that a pole-mounted transformer as well as the fuse, will still be protected against lightning even after the surge arrester had failed.

10.3.1 Lightning Proof Fuse (LPF)

A spark gap was introduced in parallel with an MV drop-out expulsion fuse which is in series with an inductor. The inductor had a low impedance at 50 Hz and a high impedance at lightning frequencies (causing the spark gap to spark over and hence causing the surge current to bypass the fuse). During 50 Hz operation, the inductor dissipated 500 mW at 5 A. Figure 10.5 and Figure 10.6 show a schematic and a photograph of the LPF respectively.

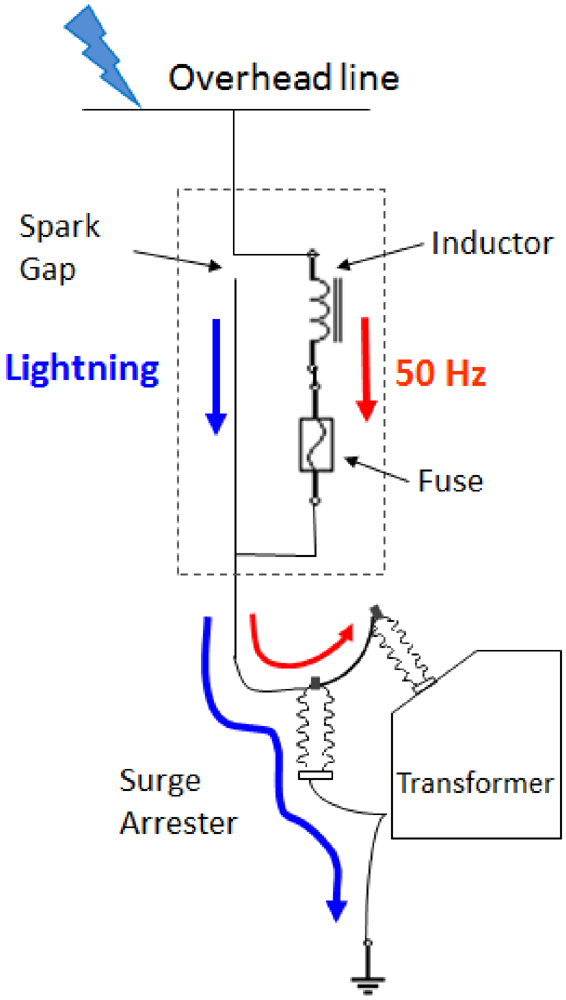

Figure 10.5 The Lightning Proof Fuse layout.

All current impulse tests on the LPF were performed at NETFA using 8/20 μs current impulses. The 8/20 μs current impulse test was done to determine the breakdown currents of the 3 A and 5 A fuses. The 3 A fuse lasted for 5 tests in succession (without operating during the last test) with current varying from 20 kA to 70 kA.

The advantages of the Lightning Proof Fuse were:

- No nuisance fuse operation.
- No permanent line faults due to incorrect fuse operation.
- Reduction in Call Centre, Work Management Centre, Network Management Centre and Field Services workload peaks.
- Reductions on overtime since 42% of the incidents were after hours.
- Large reduction in vehicle mileage and safety risks.
- Improvement in customer satisfaction and relations with the utility.

- Fewer circuit breaker operations and thus less frequent circuit breaker maintenance.
- Improvement of the network performance due to correct protection operation.

The disadvantages of the LPF are:

- It did not protect the pole-mounted transformer against lightning.
- Whenever the fuse operated for a 50 Hz fault at the transformer, a flashover would occur across the spark gap while the fuse was falling open. The arc would be cleared by the upstream circuit breaker. The circuit breaker would auto reclose in about 3 s and the faulty transformer would have been isolated from the network.
- The LPF was more costly than a standard fuse.
- The LPF could not be used as a line fuse (coil heats up for load current greater than 15 A).
- If one phase operates, the customer is left with an unbalanced supply

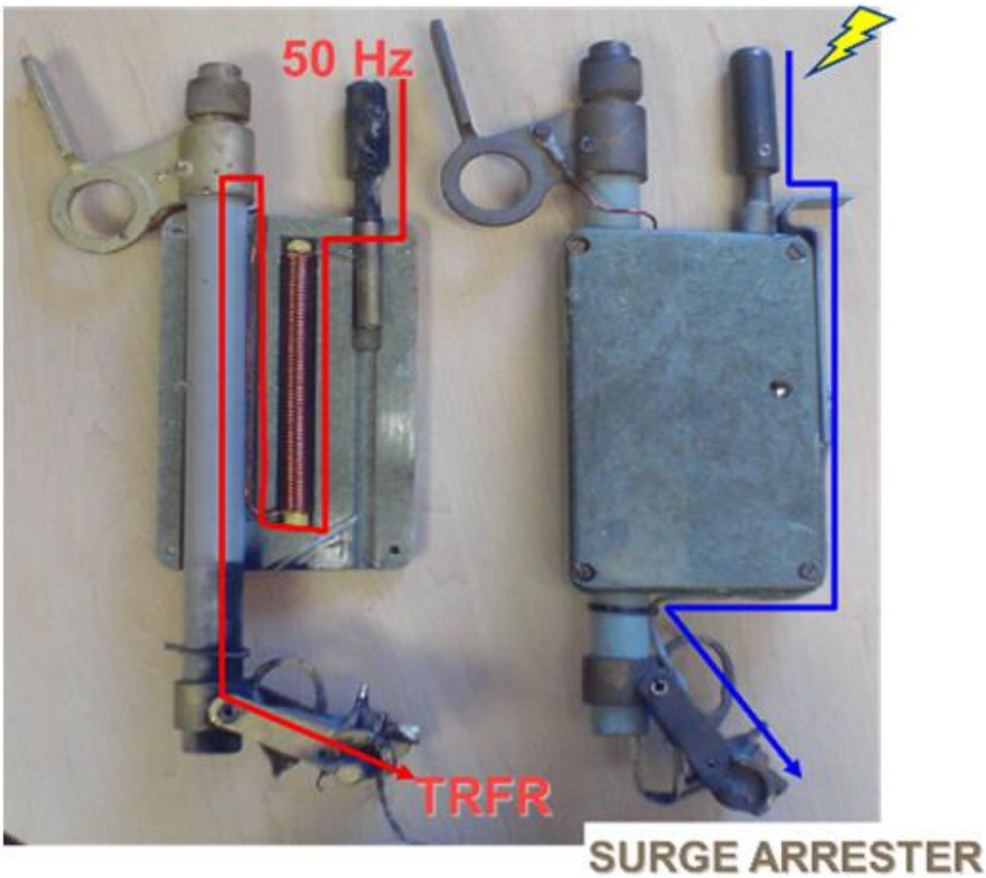

Figure 10.6 The Lightning Proof Fuse. The power frequency current flows through the inductor (0.15 V drop at 5 A) while the lightning current flashes across the spark gap and flows around the fuse.

Eight hundred LPFs were installed at points where numerous fuse failures were experienced due to lightning. No lightning-related fuse failures were recorded after the installation of the LPFs. Up to date three LPFs failed - one due to birds causing a short circuit, one was incorrectly installed and operated due to a line fault and the last one was that the transformer was equipped with arcing horns instead of surge arresters and the fuse failed due to the flashover of the arcing horns.

10.3.2 The Combi Unit

In the standard configuration, the MV fuses were exposed to lightning as they are installed on the line side of the surge arrester. Therefore, an alternative configuration was proposed where the surge arrester was connected in parallel with the fuse and transformer to provide lightning protection to both, as can be seen in Figure 10.7.

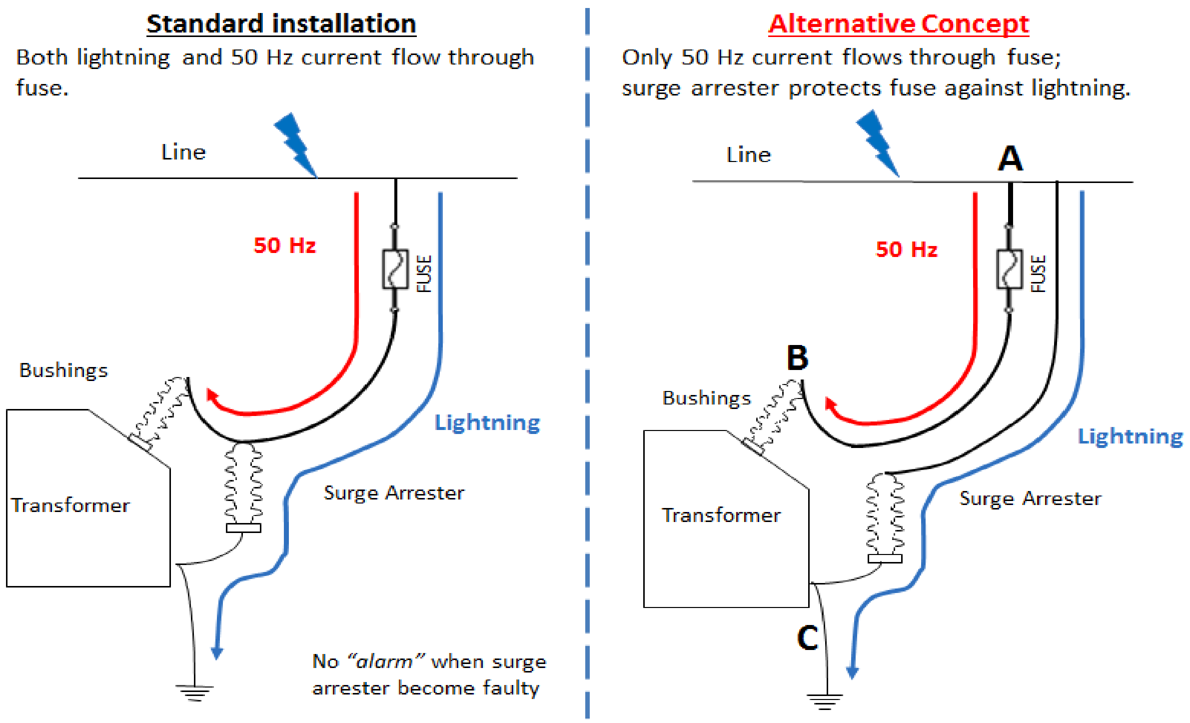

Figure 10.7 The standard pole-mounted transformer configuration on the left and the proposed configuration on the right.

The Combi Unit consisted of a post insulator in the middle with a drop-out type surge arrester on the one side and a drop-out expulsion fuse on the other side (see Figure 10.8). The Combi Unit was primarily developed to minimize the MV drop-out expulsion fuse and MV pole-mounted transformer failures during lightning activity.

If the fuse blew, only the fuse would fall open while the surge arrester remained connected. In the case where the surge arrester GLD operated, both the fuse holder (fuse element still healthy) and the surge arrester fell open. Figure 10.8 The Combi Unit. Should the fuse fail due to overcurrent, only the fuse will fall open. If the surge arrester fails due to excessive lightning current, the surge arrester as well as the fuse will fall open. shows a photograph of the Combi Unit.

Operating on the Combi Unit could be done safely. The only challenge was the weight of the surge arrester when it had to be picked up from ground level with a fully extended link stick. However, should the operator use the correct method (use the telescopic function of the link stick) the installation of the drop-out surge arrester should not be more challenging than the installation of an MV drop-out expulsion fuse.

The Combi Unit had the following advantages:

- Replacing drop-out fuses and surge arresters from ground level.
    - No slip and fall from a step ladder
    - No risk of electric contact
- Both the transformer and fuses were protected against lightning.
- No nuisance fuse operations due to lightning.
- A maximum size of 15 A fuses was used in the Combi Units to ensure correct protection grading.
- The transformer and fuse were always protected against lightning.
- A faulty fuse or surge arrester fell open and was easily noticeable.
- The Combi Unit could be used as an isolation point.
- Standard utility fuses and fuse holders were used.
- No outage booking was necessary for the replacement of a fuse or surge arrester.
- The replacement time of a Combi Unit surge arrester was much faster than replacing a surge arrester in the standard installation.

The disadvantages of the Combi Unit were:

- Cost of installation: it costs more to install a Combi Unit than a normal fuse and surge arrester arrangement.
- Should the surge arrester fail, the customer was without supply. A new surge arrester was therefore installed as soon as possible. However, a surge large enough to damage a surge

arrester would have blown the fuse in the standard configuration and there would have been an outage anyway.

- In the Combi Unit, the surge arrester is further away from the transformer, resulting in a 137 kV surge amplitude instead of a 122 kV surge amplitude across the transformer. However, the transformer was specified to have a BIL of 150 kV.

A total of 1064 pole-mounted installations were fitted with Combi Units over the 6 years. At all these installations at least one transformer failure had occurred bi-annually. After the installation of Combi Units, only 6 transformers were recorded to have failed within the 6 years, as compared to the predicted 3000 transformer failures in 6 years. Four transformers failed due to an incorrect earthing configuration. One transformer failed due to a lightning flash which consisted of 18 strokes, terminating on the pole-mounted installation. The last transformer failed under normal operating conditions. Based on the six-year transformer failure trends it could be assumed that if the Combi Units were not installed on these 1064 transformer points, these transformers would have continued to fail at least every second year.

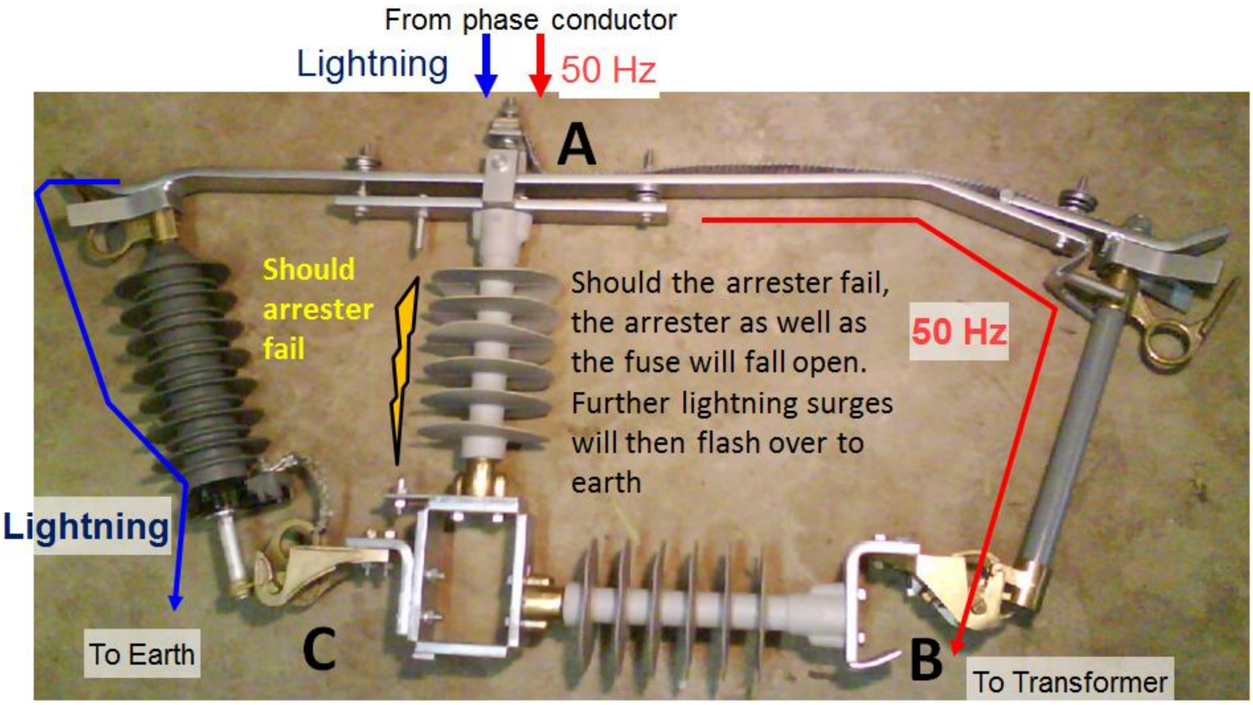

Figure 10.8 The Combi Unit. Should the fuse fail due to overcurrent, only the fuse will fall open. If the surge arrester fails due to excessive lightning current, the surge arrester as well as the fuse will fall open.

10.4 The earth configuration at the pole-mounted installation.

Significant electric stresses can be reduced within the fuses and surge arresters on the pole-mounted installation by only changing the earthing configuration. The phase conductors are normally the highest point on the pole-mounted installation. There is therefore a high probability that lightning will terminate to one of the phase conductors. In this case, the current surge will split into a small portion which will travel along the line and a larger portion which will travel through the fuse and surge arrester to earth. Should the earth conductor be extended to the highest point on the pole-mounted installation, the probability of lightning terminating on the earth wire becomes very large. This will result in only a small portion of the current surge passing through the surge arrester and the fuse to the phase conductors if the earth resistance is too high. Figure 10.9 is a schematic illustration of a pole-mounted installation with all the relevant components and shows where the lightning surge current flows.

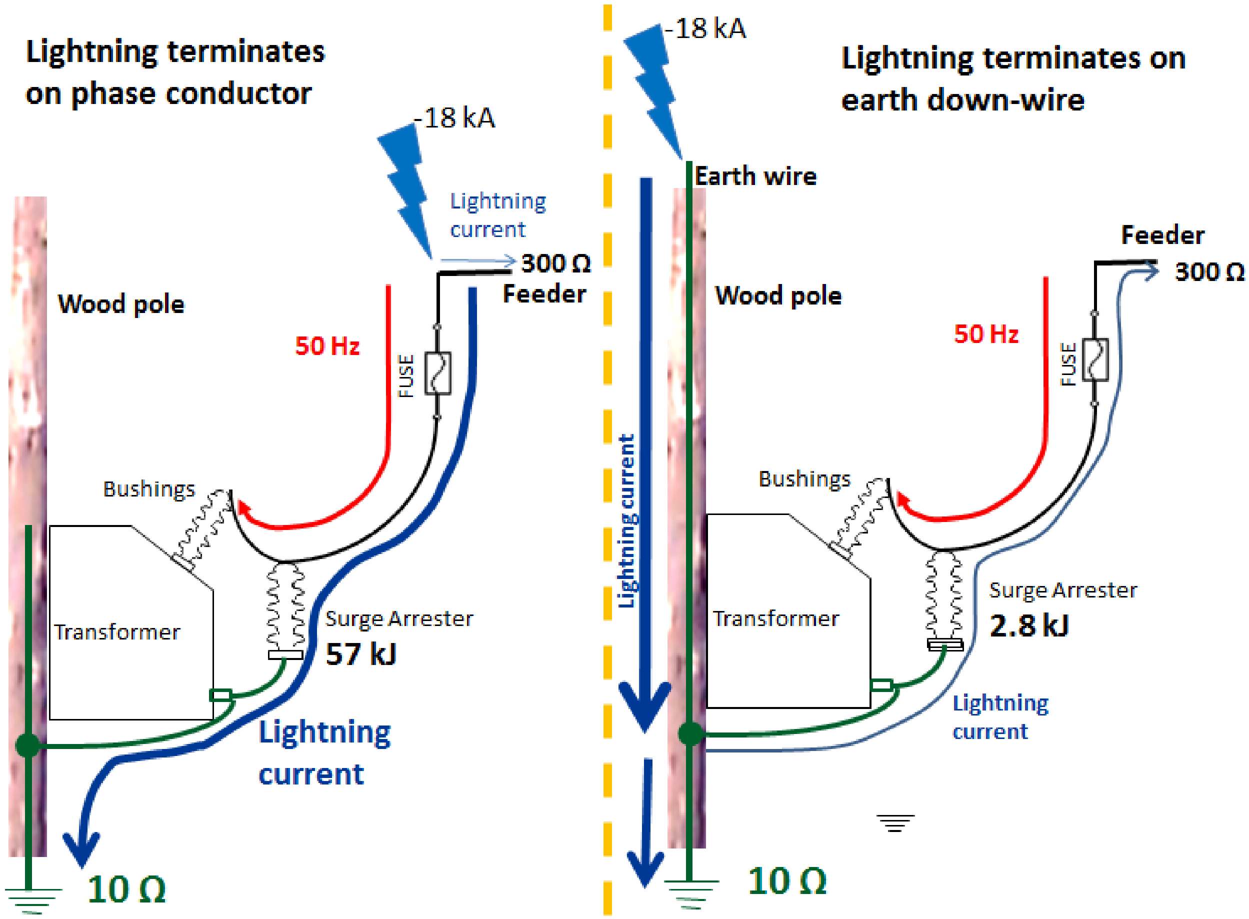

Figure 10.9 A schematic illustration of lightning terminating on the phase conductor and flowing down the earth conductor.

Figure 10.10 shows the ATP model that was used to calculate the energy dissipated in the surge arrester due to a -18 kA 3/70 μs lightning strike that terminates at the pole-mounted installation. Figure 10.11 shows that the energy dissipated in the surge arrester is 20 times less if the lightning strike terminates on the earth conductor instead of on the phase conductor.

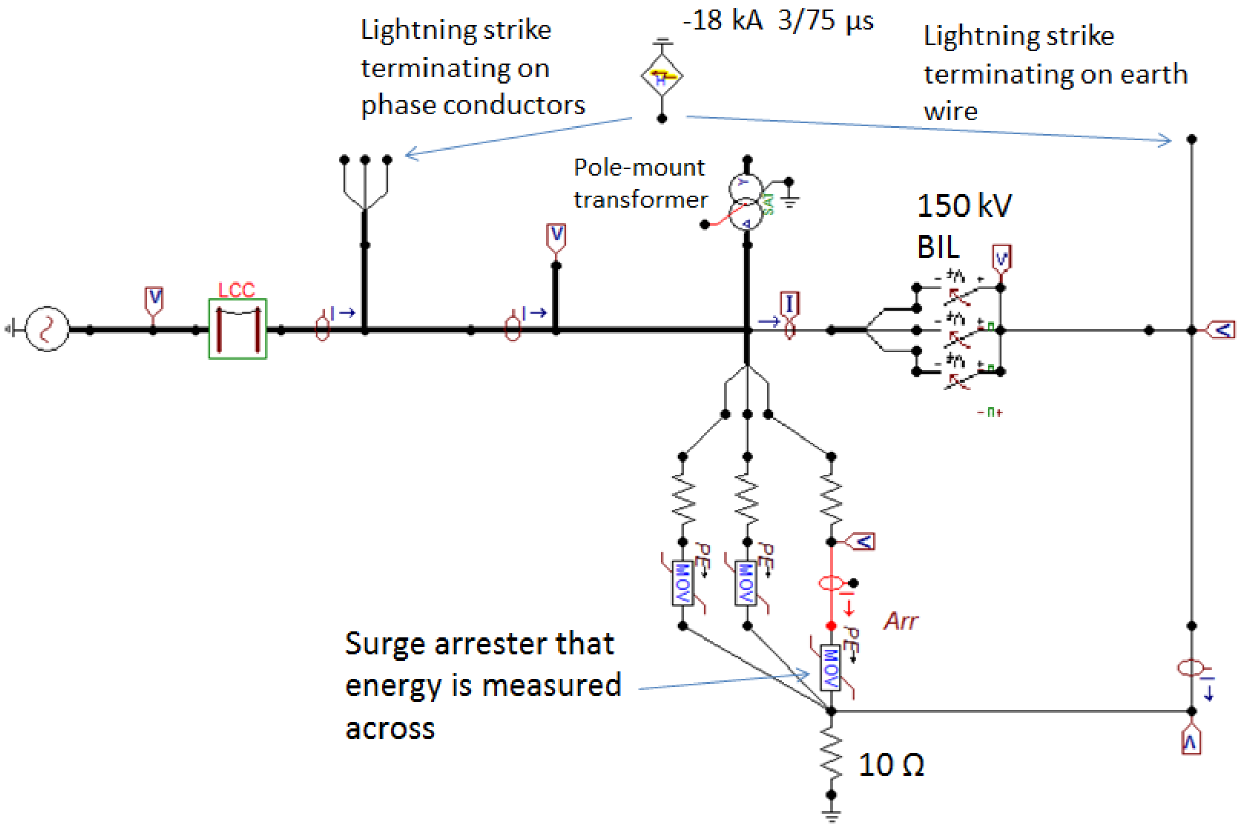

Figure 10.10 The ATP model that was used to calculate the energy absorption in the surge arrester.

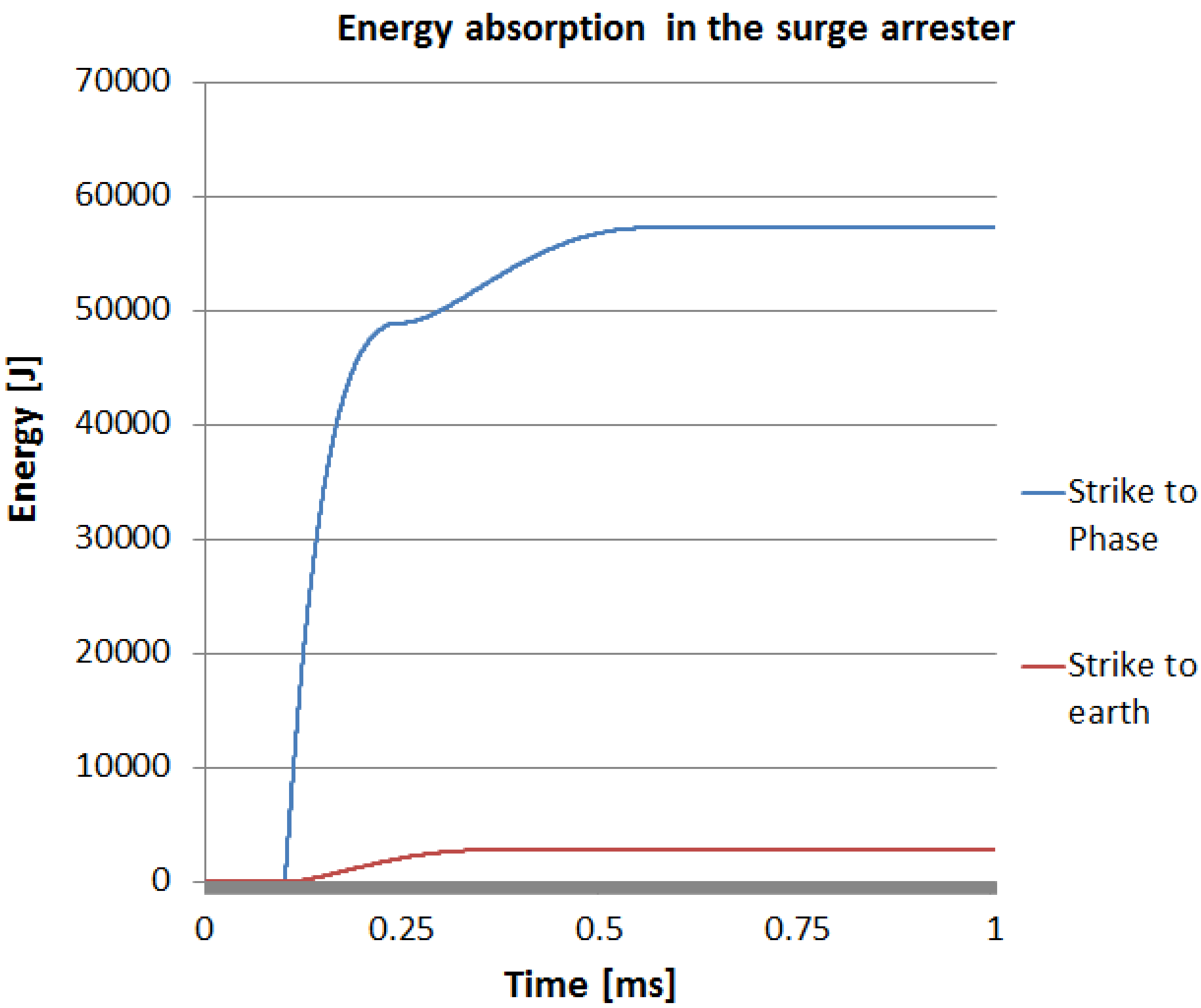

Figure 10.11 A graph showing the energy absorption in the surge arrester as 2.8 kJ and 57 kJ when the lightning strike terminated to the earth and phase conductor respectively.

10.5 The line configuration

Several requirements had to be met with the wood-pole configuration. Firstly, the pole-top of the line had to be bird-friendly and therefore a wood-gap had to be inserted on the earth wire along the pole to the earth point. According to several researchers [176] [177] [178], a 27 mm gap between two rods would result in a 30 kV BIL (and 33 kV AC insulation) that would have been sufficient for the pole to be bird-friendly. However, a 27 mm gap did not have enough tolerance for error during construction and a bigger wood-gap had to be investigated.

Work was done by [179] to configure a wood gap with a length of 260 mm in such a way that the ends of the bonding wires were 200 mm away from the wood. As shown in Figure 10.12, the wood will not be damaged as the arc will then follow the path labelled “1”. However, this configuration will result in a BIL of 194 kV [179] between the bonding wire gaps and a total line BIL of 303 kV (at high altitude) was measured at the University of the Witwatersrand HV laboratory [180]. This BIL would result in a high equipment failure rate due to direct lightning strikes to the line.

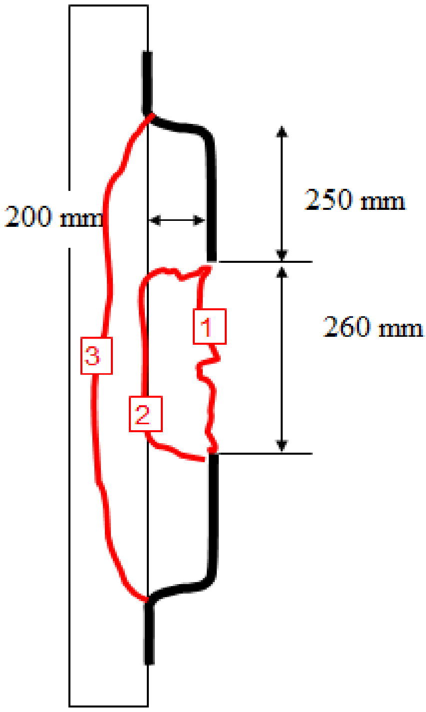

Figure 10.12 The bonding wire ends were bent away from the wood in such a way that the arc will follow the number 1 route.

A further test was done at the Eskom Rotek Industries HV laboratory [181] with different wood gaps. It was found that the BIL of the insulator was 193.5 kV and increased to 201.3 kV with a 100 mm wood gap in series with the insulator as shown in Figure 10.13. A 100 mm wood gap in series with an insulator resulted in a small increase in the total BIL. Figure 10.14 shows a suggested configuration of the wood gap as well as an impulse test on the wood-gap configuration that verified that a flashover due to lightning took place across the wood gap and not through the wood.

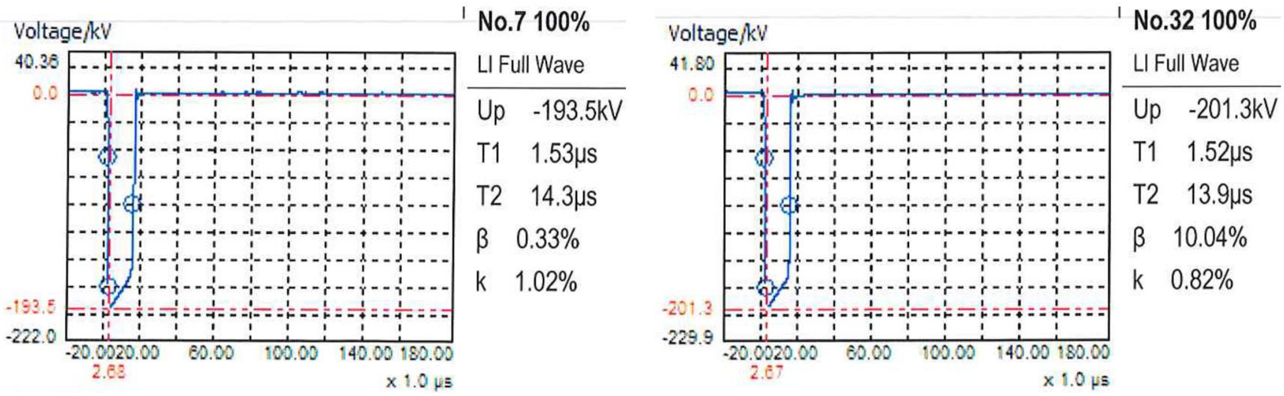

Figure 10.13 The BIL of an insulator alone (left) was 193.5 kV and it increased to 201.3 kV with a 100 mm wood gap in series with the insulator.

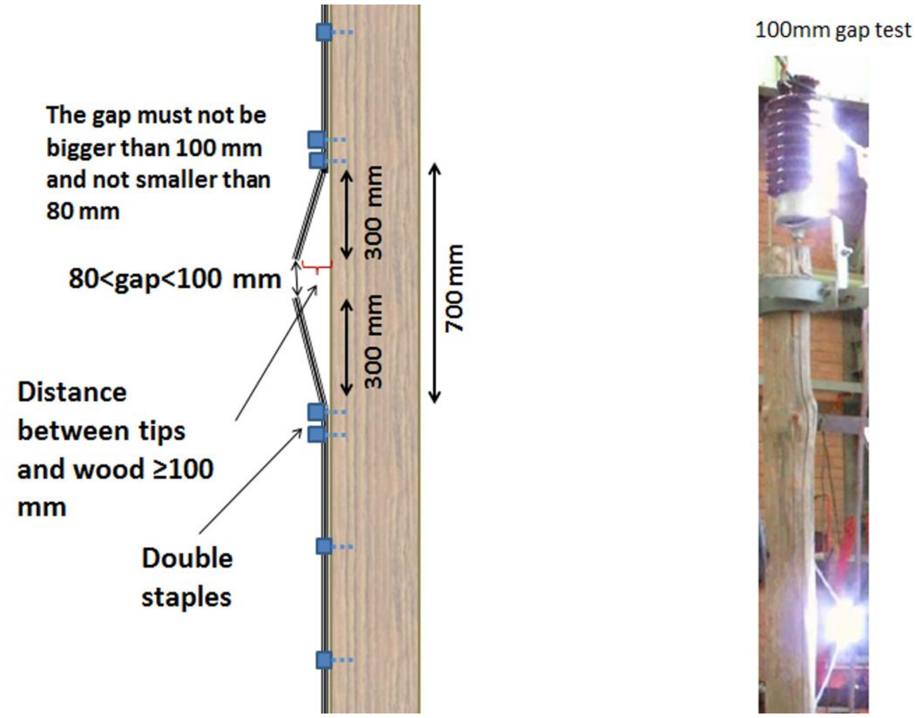

Figure 10.14 The suggested configuration of the wood gap (left) and a test in the HV laboratory verifying that the flashover occurred across the wire ends and not through the wood (right).